

c.1

PHOTOCHEMISTRY OF TETRAHYDRO-1,4-
NAPHTHOQUINONES IN THE SOLID STATE

by

ALICE AFI DZAKPASU

B.Sc., Stanford University, 1969

M.Sc., University of California, Los Angeles, 1971

Lecturer in Chemistry, University of Cape Coast, Ghana, 1971-74

A THESIS SUBMITTED IN PARTIAL FULFILLMENT OF
THE REQUIREMENTS FOR THE DEGREE OF
DOCTOR OF PHILOSOPHY

in the Department of
CHEMISTRY

We accept this thesis as conforming
to the required standard

THE UNIVERSITY OF BRITISH COLUMBIA
April, 1977

© Alice Afi Dzakpasu, 1977

In presenting this thesis in partial fulfilment of the requirements for an advanced degree at the University of British Columbia, I agree that the Library shall make it freely available for reference and study.

I further agree that permission for extensive copying of this thesis for scholarly purposes may be granted by the Head of my Department or by his representatives. It is understood that copying or publication of this thesis for financial gain shall not be allowed without my written permission.

Department of Chemistry

The University of British Columbia
2075 Wesbrook Place
Vancouver, Canada
V6T 1W5

Date 2nd May 1977

To Professor John I. Brauman
who taught and introduced
me to the fascinating
world of organic
Chemistry.

Abstract

Previous investigations involving the behaviour of cis-4a,5,8,8a-tetrahydro-1,4-naphthoquinone and its derivatives in solution under UV irradiation raised the question of what role, if any, the ground state conformations of these molecules play in a) the type of photochemical behaviour the substrate exhibits and b) the product distribution in cases where more than one product is formed. In addition, it has never been established experimentally just what the geometric requirements for the various reactions encountered in this series are. Such requirements usually provide insights into the geometry of the transition state itself. In the solid state, the initial conformation of molecules of any given substrate can be accurately determined by single crystal X-ray diffraction methods. Furthermore, since the crystal lattice usually resists any gross changes in conformation during the course of a reaction, it follows that most reactions in the crystalline state will occur from the ground state conformation of the substrate. By studying these reactions in the solid state and correlating the results with the X-ray data, it was hoped that the questions raised as well as others e.g. concentration effects could be answered.

Eleven substrates were chosen for the investigation. They were all prepared by the Diels Alder addition of a diene to a quinone. By slow crystallization all substrates with the exception of 6,7-dimethyl-4a β ,5,8,8a β -tetrahydro-1,4-naphthoquinone, 2 and 2,3,4a β ,5 α ,8 α ,8a β -hexamethyl-4a β ,5,8,8a β -tetrahydro-1,4-naphthoquinone, 10, gave crystals suitable for single crystal X-ray structure determination.

Relevant X-ray data of nine of these substrates and five of the solid state photoproducts are reported.

In the solid state, 5 α ,8 α -dimethyl-4a β ,5,8,8a β -tetrahydro-1,4-naphthoquinone, 1, 6,7-dimethyl-4a β ,5,8,8a β -tetrahydro-1,4-naphthoquinone, 2, and the parent compound 4a β ,5,8,8a β -tetrahydro-1,4-naphthoquinone, 3, did not undergo the photochemical intramolecular hydrogen abstraction they undergo in solution. Instead, they dimerized stereospecifically to their respective centrosymmetric dimers when irradiated with UV light below their respective eutectic temperatures. This is rationalized in terms of a parallel alignment of the C(2), C(3) double bonds of adjacent monomers and short intermolecular centre-to-centre separation ($\leq 4.040\text{\AA}$) of these double bonds.

Five of the substrates, namely, 6,7-diphenyl-4a β ,5,8,8a β -tetrahydro-1,4-naphthoquinone, 4, 2,3-dimethyl-1,4-4a β ,9a β -tetrahydro-9,10-anthraquinone, 6, 4a β ,8a β -dicyano-6,7-dimethyl-4a β ,5,8,8a β -tetrahydro-1,4-naphthoquinone, 7, 2,3,4a β ,6,7,8a β -hexamethyl-4a β ,5,8,8a β -tetrahydro-1,4-naphthoquinone, 9 and 2,3,4a β ,5 β ,8 β ,8a β -

hexamethyl-4a β ,5,8,8a β -tetrahydro-1,4-naphthoquinone, 11 have intermolecular double bond contacts exceeding 4.1Å and did not undergo dimerization in the solid state. Instead, upon UV irradiation, they formed tricyclic enone alcohols derived from intramolecular abstraction by oxygen of the C(8) hydrogen which lies in the plane of the C(1)=O(1) carbonyl group. Substrates 9 and 11, in addition, each gave a tricyclic diketone resulting from the abstraction of one of the C5 hydrogens by C2. The geometric requirements, the geometries of the transition states and intermediates and the factors governing the modes of closure of the biradical intermediates in both of these hydrogen abstraction reactions and their implications for other hydrogen abstractions such as the Norrish Type II are discussed.

One substrate, namely, 4a β ,8a β -dicyano-5 α ,8 α -dimethyl-4a β ,5,8,8a β -tetrahydro-1,4-naphthoquinone, 8, which lacks short intermolecular double bond contacts and has its C(8) hydrogen out of plane and far removed from the C(1)=O(1) group neither dimerized nor gave hydrogen abstraction products when irradiated in the solid state. Instead, it gave an oxetane resulting from an intramolecular [$\pi_2 + \pi_2$] addition of C(1)=O(1) to the C(6)=C(7) double bond. The intermolecular double bond contact here was 3.20Å.

Lastly, 2,3,6,7-tetramethyl-4a β ,5,8,8a β -tetrahydro-1,4-naphthoquinone, 5, and 2,3,4a β ,5 α ,8 α ,8a β -hexamethyl-4a β ,5,8,8a β -tetrahydro-1,4-naphthoquinone, 10, failed to react when irradiated in the solid state.

The reason for this is not clear but the possibility of deexcitation via excimer formation and subsequent dissociation is raised.

Table of Contents

	<u>Page</u>
INTRODUCTION	1
1. General	1
X-ray Diffraction Methods	2
Defects in Crystals and Their Effects on Chemical Reactivity	3
Energy Transfer in Organic Solids	17
2. Photochemistry of Tetrahydro-1,4-naphthoquinone and Its Derivatives	19
Biradical vs Charge-Transfer Mechanisms	26
Characteristics of the β - and γ -Hydrogen Abstraction Reactions in the Tetrahydro-1,4-naphthoquinone Series:	
Substituent Effects	34
Solvent Effects	37
Quantum Yield and Quenching Studies	39
Stereoelectronic Requirements	40
Other Reactions	41
3. Objectives of Present Research	41
RESULTS AND DISCUSSION	47
Preparation of Substrates	47
1. Intermolecular [$\pi 2 + \pi 2$] Dimerization:	
5 α ,8 α -Dimethyl-4 $\alpha\beta$,5,8,8 $\alpha\beta$ -tetrahydro-1,4- naphthoquinone, <u>1</u>	54
6,7-Dimethyl-4 $\alpha\beta$,5,8,8 $\alpha\beta$ -tetrahydro-1,4-naphthoquinone, <u>2</u>	60
4 $\alpha\beta$,5,8,8 $\alpha\beta$ -Tetrahydro-1,4-naphthoquinone, <u>3</u>	64

	<u>Page</u>
Irradiation of <u>3</u> in Solution	80
Reactive State and Mechanism for Photodimerization	81
2. Intramolecular Hydrogen Abstraction:	
6,7-Diphenyl-4a β ,5,8,8a β -tetrahydro-1,4-naphthoquinone, <u>4</u>	85
2,3-Dimethyl-1,4,4a β ,9a β -tetrahydro-9,10-anthraquinone, <u>6</u>	96
6,7-Dimethyl-4a β ,8a β -dicyano-4a β ,5,8,8a β -tetrahydro- 1,4-naphthoquinone, <u>7</u>	99
2,3,4a β ,6,7,8a β -Hexamethyl-4a β ,5,8,8a β -tetrahydro- 1,4-naphthoquinone, <u>9</u>	107
2,3,4a β ,5 β ,8 β ,8a β -Hexamethyl-4a β ,5,8,8a β -tetrahydro- 1,4-naphthoquinone, <u>11</u>	114
The Geometry of the Transition State for β - and γ^c - Hydrogen Abstractions	121
3. Intramolecular Oxetane Formation:	
4a β ,8a β -Dicyano-5 α ,8 α -dimethyl-4a β ,5,8,8a β -tetrahydro- 1,4-naphthoquinone, <u>8</u>	134
4. Unreactive Substrates:	
2,3,6,7-Tetramethyl-4a β ,5,8,8a β -tetrahydro-1,4- naphthoquinone, <u>5</u>	143
2,3,4a β ,5 α ,8 α ,8a β -Hexamethyl-4a β ,5,8,8a β -tetrahydro- 1,4-naphthoquinone, <u>10</u>	149
EXPERIMENTAL	156
BIBLIOGRAPHY	211
APPENDIX	221

List of Tables

<u>Table #</u>	<u>Caption</u>	<u>Page</u>
I	UV Absorptions	25
II	Product Ratios Obtained in Benzene and tert-Butyl Alcohol	38
III	Substrates and Reaction Types Observed in Solution	45
IV	Product Yields for the <u>1</u> → <u>1A</u> Conversion	59
V	Product Yields for the <u>2</u> → <u>2A</u> Conversion	63
VI	Product Yields for the <u>3</u> → <u>3A</u> Conversion	64
VII	Product Yields for the <u>4(s)</u> → <u>4A</u> + <u>4B</u> Conversion	88
VIII	Product Yields for the <u>4_{solution}</u> → <u>4A</u> + <u>4B</u> Conversion ..	91
IX	Specific Rotation of Solutions of Crystals of <u>7A</u>	105
X	Product Ratios and Combined Yields for the <u>9</u> → <u>9A</u> + <u>9B</u> Conversion in the Solid State	108
XI	Product Ratios for the <u>9</u> → <u>9A</u> + <u>9B</u> Conversion in Solution	109
XII	Product Yields and Ratios for the <u>11</u> → <u>11A</u> + <u>11B</u> Conversion	115
XIII	Effects of Structure on the McLafferty Rearrangement ...	123
XIV	Interatomic Distances, Å, and Approach Angles for Hydrogen Abstraction	129
XV	Intramolecular C(1)=O(1)···C(6)=C(7) Bond Contacts and Orientation	139
XVI	UV Absorption Spectra of Substrates <u>1-11</u>	235

List of Schemes

<u>Scheme #</u>		<u>Page</u>
1	12
2	13
3	14
4	15
5	21
6	23
7	29
8	32
9	33
10	35
11	36
12	40
13	87
14	95
15	98
16	102
17	111
18	113
19	119
20	131
21	147
22	149

List of Figures

<u>Figure #</u>	<u>Caption</u>	<u>Page</u>
1	Vacancy; Interstitial Atom	4
2	Model of a simple cubic lattice and dislocations	5
3	Voids and Diffusion	8
4	Ground state, n, π^* and π, π^* states	28
5	Operational Definition of the Angle τ	42
6	Uncorrected Endothermic Transition for <u>1</u> + <u>1A</u> Eutectic Mixture	52
7	Stereo diagram of an adjacent pair of molecules of 5 α ,8 α -dimethyl-4 $\alpha\beta$,5,8,8 $\alpha\beta$ -tetrahydro-1,4- naphthoquinone, <u>1</u>	55
8	Stereo diagram of dimer <u>1A</u> in an orientation analogous to that of the monomer, <u>1</u>	57
9	Stereo diagram of dimer <u>2A</u>	62
10	Infrared spectra of KBr pellets containing 4-5% by weight of dimer <u>3A</u> (Top) and dimer <u>3B</u> (Bottom)	67
11	Stereo diagram of the <u>3B</u> molecule	69
12	Part of the absorption spectrum of benzene	73
13	Stereo diagram of the contents of the unit cell for compound <u>3</u>	76
14	Stereo diagram of molecule type A and its nearest neighbour related by a simple cell translation	77
15	Stereo diagram of a type B molecule and its nearest neighbour related by a centre of symmetry, X	77
16	Stereo diagram of compound <u>4</u>	86
17	(a) A 100 MHz PMR Spectrum of 2,3-Diphenyltricyclo- [5.3.0.0 ^{5,10}]deca-2-ene-6,9-dione, <u>4B</u>	90
	(b) A 100 MHz PMR Spectrum of 2,3-Dimethyltricyclo- [5.3.0.0 ^{5,10}]deca-2-ene-6,9-dione, <u>2C</u>	90

<u>Figure #</u>	<u>Caption</u>	<u>Page</u>
18	Stereo diagram of compound <u>6</u>	98
19	Stereo diagram of compound <u>7</u>	100
20	Stereo diagram of enone-alcohol, <u>7A</u>	104
21	Neighbouring ene-dione systems of a pair of molecules of <u>7</u>	106
22	Stereo diagram of substrate <u>9</u>	110
23	Stereo diagram of substrate <u>11</u>	118
24	(a) Ground state geometry of substrate <u>9</u> (b) The proposed transition state geometry for the <u>9</u> → <u>9B</u> conversion	132 132
25	Stereo diagram of substrate <u>8</u>	136
26	Approach geometry of the C(1)=O and C(6)=C(7) π bonds...	136
27	Stereo diagram of oxetane <u>8A</u>	137
28	Stereo diagram of substrate <u>5</u>	143
29	Two adjacent molecules of <u>5</u> within a crystallographic cell	145
30	The reaction cavity before reaction	152
31	Apparatus for irradiations in the solid state	165,166
32	Apparatus for low temperature irradiations in solutions	170
33	A 60 MHz PMR spectrum of 5α,8α-dimethyl-4αβ,5,8,8αβ-tetrahydro-1,4-naphthoquinone, <u>1</u>	221
34	Fourier transform 100 MHz PMR spectrum of 5,8,15,18-tetramethylpentacyclo[10.8.0.0 ^{2,11} .0 ^{4,9} .0 ^{14,19}]eicosa-6,16-dien-3,10,13,20-tetrone, <u>1A</u>	221
35	A 60 MHz PMR spectrum of 6,7-dimethyl-4αβ,5,8,8αβ-tetrahydro-1,4-naphthoquinone, <u>2</u>	222
36	Fourier transform 100 MHz PMR spectrum of 6,7,16,17-tetramethylpentacyclo[10.8.0.0 ^{2,11} .0 ^{4,9} .0 ^{14,19}]eicosa-6,16-dien-3,10,13,20-tetrone, <u>2A</u>	222

<u>Figure #</u>	<u>Caption</u>	<u>Page</u>
37	A 60 MHz PMR spectrum of 4a β ,5,8,8a β -tetrahydro-1,4-naphthoquinone, <u>3</u>	223
38	Fourier transform 100 MHz PMR spectrum of pentacyclo-[10.8.0.0 ^{2,11} .0 ^{4,9} .0 ^{14,19}]eicosa-6,16-diene-3,10,13,20-tetrone, <u>3A</u>	223
39	A 60 MHz PMR spectrum of 6,7-diphenyl-4a β ,5,8,8a β -tetrahydro-1,4-naphthoquinone, <u>4</u>	224
40	A 100 MHz PMR Spectrum of 1-hydroxy-7,8-diphenyltricyclo[5.3.0.0 ^{5,10}]deca-2,8-dien-4-one, <u>4A</u>	224
41	A 60 MHz PMR spectrum of 2,3,6,7-tetramethyl-4a β ,5,8,8a β -tetrahydro-1,4-naphthoquinone, <u>5</u>	225
42	A 60 MHz PMR spectrum of 2,3-dimethyl-1,4,4a β ,9a β -tetrahydro-9,10-anthraquinone, <u>6</u>	226
43	A 100 MHz PMR spectrum of 1-hydroxy-2,3-benzo-7,8-dimethyltricyclo[5.3.0.0 ^{5,10}]deca-8-ene-4-one, <u>6A</u>	226
44	A 60 MHz PMR spectrum of 4a β ,8a β -dicyano-6,7-dimethyl-4a β ,5,8,8a β -tetrahydro-1,4-naphthoquinone, <u>7</u>	227
45	A 100 MHz PMR spectrum of 1-hydroxy-5,10-dicyano-7,8-dimethyltricyclo[5.3.0.0 ^{5,10}]deca-2,8-dien-4-one, <u>7A</u> ...	227
46	A 60 MHz PMR spectrum of 4a β ,8a β -dicyano-5 α ,8 α -dimethyl-4a β ,5,8,8a β -tetrahydro-1,4-naphthoquinone, <u>8</u> ..	228
47	A 100 MHz PMR spectrum of 5,10-dicyano-6,9-dimethyl-11-oxatetracyclo[6.2.1.0 ^{1,7} .0 ^{5,10}]undec-2-ene-4-one, <u>8A</u>	228
48	A 60 MHz PMR spectrum of 2,3,4a β ,6,7,8a β -hexamethyl-4a β ,5,8,8a β -tetrahydro-1,4-naphthoquinone, <u>9</u>	229
49	A 100 MHz PMR spectrum of 1-hydroxy-2,3,5,7,8,10-hexamethyltricyclo[5.3.0.0 ^{5,10}]deca-2,8-dien-4-one, <u>9A</u>	229
50	A 100 MHz PMR spectrum of 2,3,5,7,8,10-hexamethyltricyclo[6.2.0.0 ^{5,10}]deca-2-en-6,9-dione, <u>9B</u>	230
51	A 60 MHz PMR spectrum of 2,3,4a β ,5 α ,8 α ,8a β -hexamethyl-4a β ,5,8,8a β -tetrahydro-1,4-naphthoquinone, <u>10</u>	231

<u>Figure #</u>	<u>Caption</u>	<u>Page</u>
52	A 60 MHz PMR spectrum of 2,3,4a β ,5 β ,8 β ,8a β -hexamethyl-4a β ,5,8,8a β -tetrahydro-1,4-naphthoquinone, <u>11</u>	232
53	A 100 MHz PMR spectrum of 1-hydroxy-2,3,5,6,9,10-hexamethyltricyclo[5.3.0.0 ^{5,10}]deca-2,8-dien-4-one, <u>11A</u>	232
54	A 100 MHz PMR spectrum of 1,4,5,7,8,10-hexamethyltricyclo[6.2.0.0 ^{5,10}]deca-2-en-6,9-dione, <u>11B</u> ; (a) 1000 Hz sweep width; (b) 250 Hz sweep width of the 6.5-5.25 δ region with amplitude magnification of x10; (c) 250 Hz sweep width of the 3.05-0.8 δ region	233
55	Fourier transform 100 MHz PMR spectrum of CDCl ₃ from Merck Sharp & Dohme	234

Acknowledgement

My sincere thanks to my research director, Dr. J.R. Scheffer, for arousing and sustaining my interest in this area of research through many invaluable discussions and for his helpful suggestions during the preparation of this manuscript.

I am greatly indebted to Dr. James Trotter and Dr. Simon E.V. Phillips who carried out all the X-ray structure determinations reported in this work. It really was a pleasure collaborating with such a fine, zealous team. I also thank Dr. Steve J. Rettig who, with Dr. Trotter, helped me with some of the calculations involved.

I am also indebted to other members of the teaching staff of this department especially Dr. R.E. Pincock and Dr. E.A. Ogryzlo for their helpful suggestions during the initial stages of this research and for being so generous with some of their instruments.

My thanks to the mechanical team of the technical staff of this department especially Mr. B. Powell and Mr. M. Symonds who helped design and build the photochemical reactor which was used for the solid state reactions.

I would also like to thank my former and present colleagues of laboratory 346 for their friendliness and cooperation.

My thanks to the Canadian Commonwealth Scholarship and Fellowship Association for their award (1974-77) and to the University of Cape Coast, Ghana for granting me study leave from my teaching duties to undertake this project.

Last, but not least, my special thanks to Louise Hon who typed this manuscript.

Introduction

General

Organic solids, being generally low melting and complex as compared to metals, are more prone to crystal imperfections than the latter. It is, therefore, not surprising that the Journal of Solid State Chemistry is exclusively inorganic. While this attitude of solid state chemists and physicists is, perhaps, understandable, the aloofness of organic chemists themselves from this area of research is surprising since most organic compounds are solids. For, although it is true that limited diffusion of reactants in the solid state places restrictions on the type of reactions which can occur, it is, nevertheless, also true that many unimolecular and polymerization reactions occur via mechanisms which require no assistance from solvents. The elimination of the use of solvents from such systems is not only beneficial in terms of cost but also in minimizing secondary reactions and in reducing the number of factors which need to be considered in proposing mechanisms.

Organic solid state reactions have occasionally appeared in the literature since 1880 but the correlation of reactivity with structure of organic compounds became possible only after improved methods in

X-ray crystallography became available.

X-ray Diffraction Methods¹

When X-rays are passed through matter, some of the rays are scattered or diffracted, some are absorbed. X-ray crystal structure analysis relies on the recording and analyses of accurate values of the intensities of the diffracted rays. The intensity determinations can be made on a single crystal or on a fine powder composed of small grains. The powder method has serious drawbacks the greatest of which is the inherent lack of resolving power which causes reflections originating from different points in the crystal and which are not symmetrically related to fall together or coincide as a single spot. This makes the interpretation of intensity data from this method more difficult. Powder diffraction methods are, therefore, unsuitable for crystals having large cells and are hardly ever used for complex structure analyses. Organic crystals are invariably investigated by the single-crystal method. In this method, a single crystal measuring 0.1 - 1.0 mm on a side is mounted on a goniometer head and several photographs are taken at varying angles using Weissenberg and precession cameras. From these photographs the dimensions of the unit cell and also the space group to which the crystal structure belongs are determined. Next, diffraction intensities are recorded using an automatic diffractometer. Using these intensities, the structure factors are derived and their respective phases determined by statistical methods. These latter quantities allow for the calculation of electron

density maps from which the positions and nature of the atoms may be determined. Because of the uncertainties involved in pinpointing an atom from electron density maps, the resulting structure is only approximate. This approximate structure is subsequently used to calculate intensities which are then compared with the observed intensities. Usually, the structure is deemed satisfactory only when the average percent difference between the observed and calculated intensities, the R factor, falls below 10%. Otherwise, the structure is successively refined using a least-squares refinement method until the R factor is minimal and satisfactory. All computations involved in X-ray structure determinations are carried out using a digital computer.

Thus used, this method yields the structure, conformation, stereochemistry, intramolecular bond distances, the packing arrangement in the crystal as well as the intermolecular geometries and distances.

The next step in establishing structure-reactivity correlations is to study the reactions or the lack thereof of the crystalline compound.

Since, all real crystals contain imperfections and since defects in crystals have been shown to play an important role in chemical reactivity², a brief discussion of these defects is desirable.

Defects in Crystals and Their Effects on Chemical Reactivity²⁻¹⁶

Imperfections in non-metallic solids, of which organic solids are an example, are complex and diverse and have not been as systematically and thoroughly studied as those found in metals. Furthermore, the study

of crystal defects has been the specialty of solid state physicists. The result has been a mathematical and highly technical treatment of the subject. Only a qualitative and simplistic discussion of crystal defects will be attempted in this text.

Possible defects in solids can be classified into four categories:

A. Zero-dimensional or point defects e.g. vacancies and interstitials.

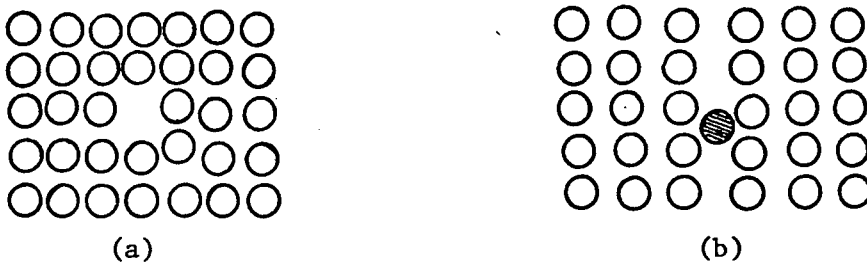


Figure 1. (a) Vacancy; (b) Interstitial atom

A vacancy is formed by the absence of an atom from an atomic site while an interstitial is what results when an atom is present at a non-atomic site. These two defects are illustrated in Figure 1.

B. One-dimensional or line defects commonly referred to as dislocations.

A dislocation is a boundary between two parts of a crystal which are displaced with respect to one another. There are two types of dislocations viz., edge and screw dislocations. The first type is exemplified in Figure 2b in which an extra half plane of atoms has been inserted into the top half of the crystal lattice giving rise to a severe distortion of the atomic layers in the vicinity of the dislocation. An edge dislocation may begin and end anywhere in the crystal and so may not

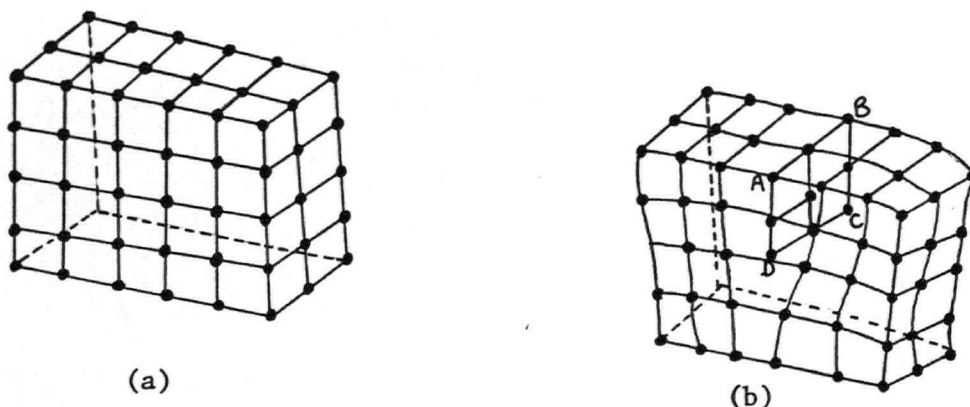


Figure 2. Model of a simple cubic lattice; (a) the perfect crystal, (b) a view of an edge dislocation caused by the insertion of an extra half plane of atoms, ABCD.

always be perceptible externally. A screw dislocation, on the other hand, manifests itself on the crystal surface. Figure 2c illustrates a screw dislocation caused by the displacement of the two faces of the ABCD plane

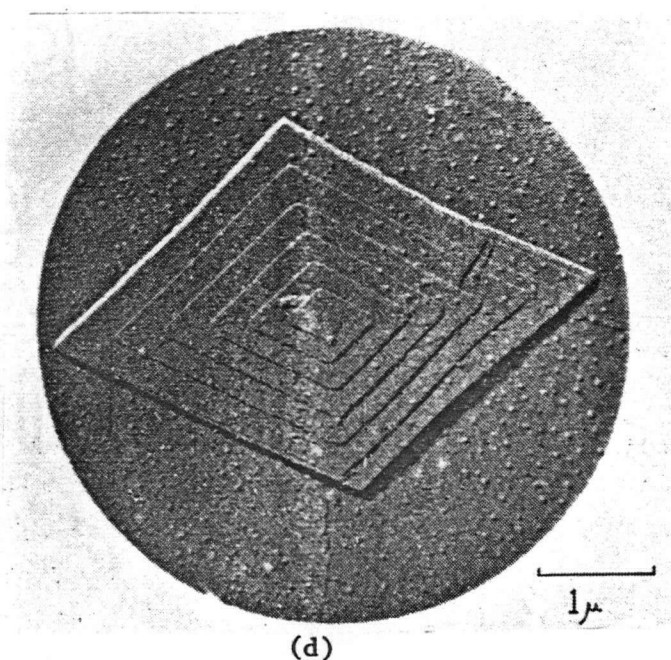
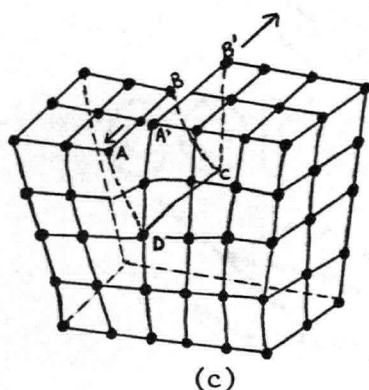


Figure 2. (c) a screw dislocation; (d) growth spiral on the face of an n-paraffin ($C_{36}H_{74}$) crystal resulting from a screw dislocation (reproduced from reference 6).

in the directions shown. When such a slip occurs during crystallization, it usually gives rise to a growth spiral which is not uncommon in long chain hydrocarbons grown from solution by cooling. Figure 2d is a photograph of one such crystal reproduced from reference 6.

C. Two dimensional or surface defects include boundary dislocations of one kind or another. We shall concern ourselves with three kinds of boundary imperfections, viz., defects of surface atoms, phase boundary dislocations and grain boundary dislocations. The atoms in a single crystal are held together by a cohesive force which may be of the metallic, ionic, covalent, or van der Waals type. Regardless of which type of cohesive force is involved, the atoms on the surface of the crystal experience only a fraction of the total force felt by the atoms in the interior of the crystal. This, plus the fact that they are exposed to an environment different from the environment of their interior counterparts, makes surface atoms different from those of the bulk crystal. They are usually distorted and have properties unlike those of the bulk crystal. This deviation is classified as a defect inasmuch as it may be the initiator or inhibitor of a physical or chemical process. The second type of boundary defect is caused by the presence of one or more phases within the crystal e.g. the presence of an impurity or the formation of product(s) may give rise to new phases on the surface or inside of the crystal. The reactant-product interface may then serve as a defect site. Lastly, grain boundaries may act as defect

sites. Most solids crystallize out, not as single crystals, but as aggregates of crystals. Any two grains represent two single crystals and a misorientation between them constitutes a grain boundary dislocation. The atoms at such sites are distorted. In addition, such locations are the sites of other defects such as interstitials and holes.

D. Three-dimensional or volume defects refer to voids and inclusions. In the perfect lattice, all atoms are in minimum energy positions and only vibrational motion about these positions occurs. When the atoms are displaced from their minimum energy positions, as is the case at the site of dislocations, then the atoms are subjected to forces that tend to move them back to their equilibrium positions. The movement of atoms in the vicinity of the dislocation to correct the defect often results in the formation of clusters of vacancies or voids. These channels of empty space and vacancies, in general, provide a mechanism of diffusion in solids. Figure 3 is a diagrammatic representation of movement in the lattice facilitated by a void. As can be seen from this illustration, the departure of the designated atom from an atomic site to the site of the void leaves behind a vacancy. This mechanism of diffusion, therefore, results in the creation of a new defect site. The multiplication of defect sites, in this fashion, can be an effective method of propagating reactions permissible only at defect sites. A second example of volume defect is the presence of impurities or inclusions, in general. An inclusion in the crystal lattice can be an impurity, an entrapped molecule of the solvent of crystallization or in the case of

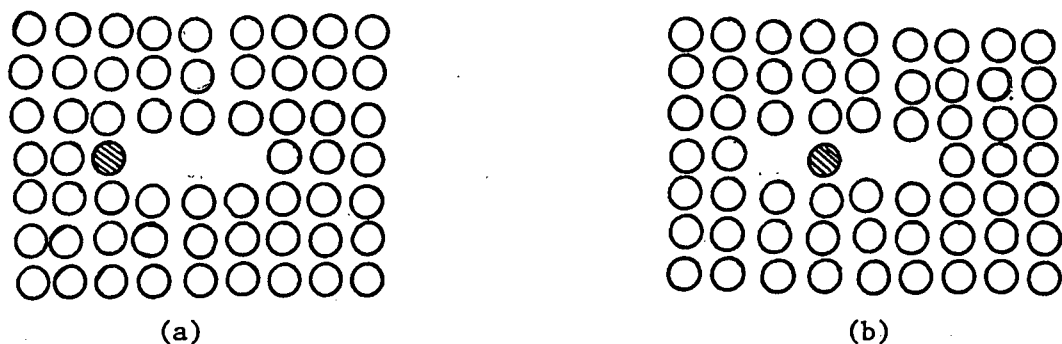


Figure 3. (a) a void formed from a cluster of vacancies; (b) the diffusion of an atom (⊗) to a new atomic site and the creation of a vacancy at the original atomic site.

solid state reactions, a product molecule. There are two major effects of these inclusions namely (i) they, generally, lower the melting point of the host and (ii) they may initiate or terminate a physical and/or chemical process within the crystal.

For simplicity in illustrations, only monatomic molecules have so far been used in defining structural faults. Although, all of the above discussion applies equally well to polyatomic molecules such as organic solids, the sheer bulk and complexity of these molecules give rise to other considerations which will now be discussed.

One of the major differences between solids of small molecules such as metals and those of large organic entities is the rate of diffusion through the solid. As mentioned earlier, one mechanism of diffusion in solids entails the movement of an atom from an atomic site to an empty space (a void or vacancy). The energy required to move a

small atom or ion from one location to another is quite small compared to that necessary to effect the movement of a complex molecule such as an organic one. The calculated coefficient of diffusion in a single crystal of anthracene is of the order of $10^{-10} \text{ cm}^2 \text{ sec}^{-1}$ at 40° below its melting point and the activation energy for diffusion is calculated to be 42 kcal per mole⁷. Diffusion in organic solids can therefore be assumed to be negligible. One manifestation of this, is the inability of radicals formed during decomposition of organic crystals to combine to products, a phenomenon termed a cage effect^{6,9}. Not only are molecules confined to the same location in a crystal but other molecular motions such as tumbling seem to be absent as well. Proof of this comes from the persistence, over periods up to months, of the anisotropy (electron spin-nuclear spin magnetic interaction) exemplified by proton hyperfine splittings in the electron spin resonance spectra of various organic compounds which have been exposed to ionizing radiation^{6,8}. Restrictions such as this on molecular movements form the basis of the topochemical postulate which will be discussed later.

A second feature of complex molecules such as organic compounds is their potential to crystallize out in more than one polymorphic form. Polymorphism may be associated with variations in conformation of the molecules and/or with the packing arrangement of molecules in the crystal lattice. Polymorphs of the same substance differ not only in their physical properties but may react differently. Although, this multiplicity of form is not a defect as such, the contamination of one

crystal form by the presence of a second form is undesirable in the study of such solids. There are two types of polymorphism namely enantiotropic and monotropic. When each of two polymorphs is stable at a given temperature range and pressure, then the two are said to be enantiotropic. This means that a substance A will exist in polymorphic modification A_1 at T_1° and a pressure of P_1 . At T_2° and P_2 , it is transformed into polymorphic modification A_2 . In the second type of polymorphism, one of the pair is unstable at all temperatures below the melting point. Such a pair is said to be monotropic. This latter form of polymorphism presents less problem in organic reactions than the former since the metastable form can only be prepared by quenching the melt and is, therefore, unlikely to form during crystallization or reaction. Enantiotropic forms, on the otherhand, may interfere in reactions in the following manner: (i) where one form interconverts to the other during the course of a reaction, it becomes difficult to determine from which modification the reaction is occurring. One such compound is cis-decahydronaphthalene which undergoes enantiotropic change at about 14° below its melting point¹⁰; (ii) when a reaction sample containing predominantly one polymorph is contaminated by a second polymorph. Although, it is possible to check single crystals grown for X-ray crystallographic purposes, the sensitivity of this method is only about 5%. Furthermore, checking bulk samples used in organic solid state reactions is impractical. Fortunately, this type of contamination can be treated much like defects. Since there are very few of the unwanted forms as compared to the bulk of the crystals,

the properties and reactivity of the crystal will approach that of the pure form.

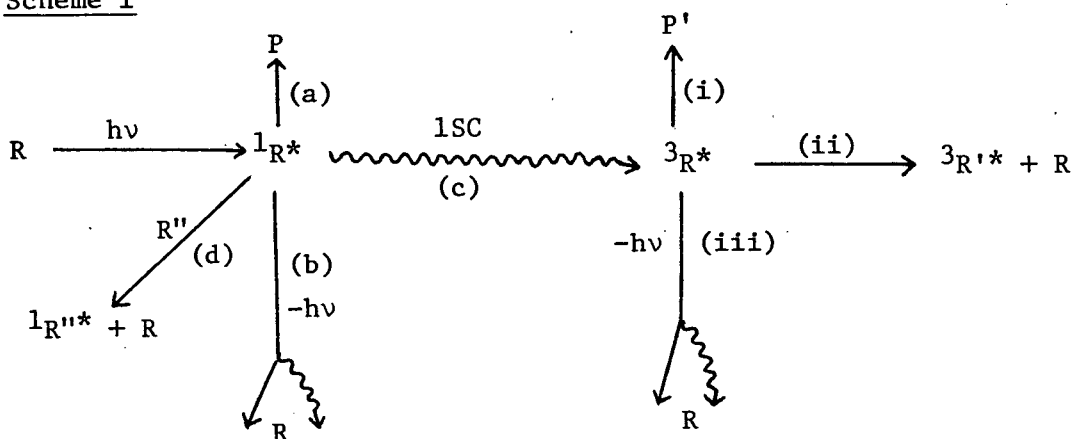
As mentioned earlier, organic solids are generally lower melting and more prone to contamination than the inorganic ones. One consequence of this is that, unless reaction temperatures are chosen so as to be many degrees below the melting point, an apparent solid-phase reaction may actually be occurring in a molten region of the crystal. Moreover, as reaction proceeds, product molecules will further depress the melting point of the host sample so that not only should reaction temperatures be below the melting point of the starting material but must be below the eutectic temperature of the mixture comprising reactant and product(s).

We have so far defined some of the possible defects which can be present in a crystalline solid. Experimentally, the defects most often implicated in organic solid reactions are dislocations of one kind or another. To understand their role in such reactions, an examination of the stages involved in transforming reactant molecules to product within the crystal lattice of the reactant will be useful. To be pertinent, the discussion will be limited to photochemical transformations in the solid state.

Let R denote a reactant molecule in the crystal lattice. Following the absorption of light by R, it is promoted to the first excited singlet state, $^1R^*$. It may then (a) react to give product, P, or (b) deactivate (i) radiatively (fluoresce) or (ii) non-radiatively to the

ground state, or (c) intersystem-cross into the excited triplet manifold, $^3R^*$, from which it can (i) react, (ii) transfer its excitation energy to a second molecule, (iii) deactivate radiatively (phosphoresce) or non-radiatively to the ground state or (d) transfer its excitation energy to another molecule R'' . This entire sequence of events, schematically represented in Scheme 1, is crystal structure dependent. The only processes which may directly or eventually lead to product formation are (a) and (d)

Scheme 1

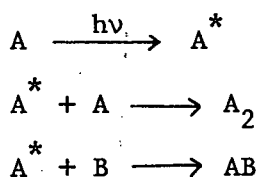


from the excited singlet manifold and (c) (i) and (ii) from the excited triplet state. Attention will, therefore, be focused on the effects of structural imperfections on these processes. In a reaction in which the absorption of energy leads directly to reaction i.e. energy transfer does not occur, molecules situated at or near lattice defects play no significant role since their concentration is negligible compared to the concentration of molecules in ordered arrays. The photodimerization of trans-cinnamic acid and its derivatives^{11,12} affords an example of this

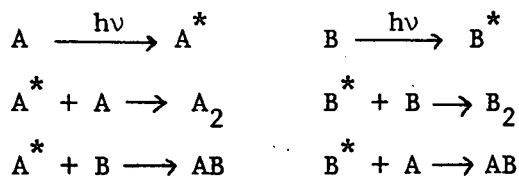
type of reaction. In one such reaction, Cohen and coworkers¹¹ irradiated mixed crystals of p-methoxycinnamic acid and p-methylcinnamic acid with both filtered and unfiltered light. With filtered light, only p-methoxycinnamic acid monomers absorbed the light. Analyses of the resulting products showed them to be the homodimer formed by the combination of an excited p-methoxycinnamic acid with a non-excited p-methoxycinnamic acid together with the heterodimer formed by the reaction of excited p-methoxycinnamic acid with a non-excited p-methylcinnamic acid. Hardly any homodimer of p-methylcinnamic acid was formed. When unfiltered light was used, however, the products comprised both homodimers and also the heterodimer. These results, summarised in Scheme 2 below, show that only molecules which initially absorb the irradiation react i.e. no energy transfer occurs in this system. Schmidt and coworkers¹² have

Scheme 2

For filtered light



For unfiltered light



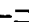




A = p-methoxycinnamic acid; B = p-methylcinnamic acid

studied the crystal structures and dimerization reactions of these and other cinnamic acids and in all cases found only the products predicted

from the orientation of the monomers in the crystal lattice. Thus, the α -type crystal (Scheme 3 below) in which monomer pairs are related by a centre of symmetry give the centrosymmetric dimer. The second type of crystal, the β -type, in which monomer pairs are related by simple translation along a crystallographic axis dimerize to the mirrorsymmetric dimer. And lastly, the γ -type crystal in which the double bonds of adjacent monomers are offset in such a way that they do not overlap and

Scheme 3

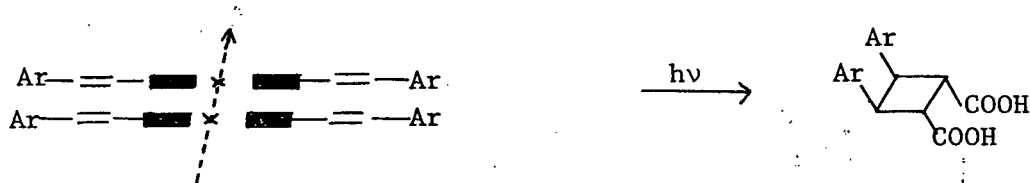
Ar—— × ——Ar edge-on view of carboxylic acid pair

 = COOH × = centre of symmetry

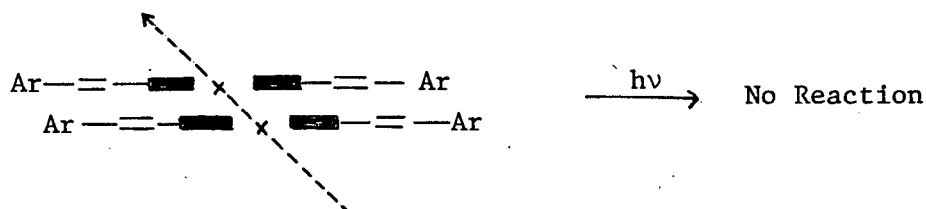
α -type. Separation of double bonds $\approx 4\text{\AA}$



β -type. Separation of double bonds $\approx 3.8\text{--}4.1\text{\AA}$



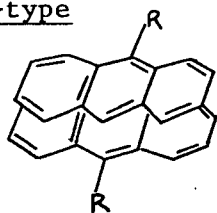
γ -type. Separation of double bonds $\approx 4.8\text{--}5.2\text{\AA}$



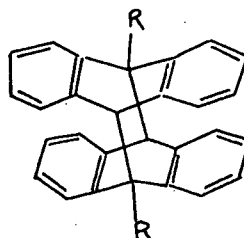
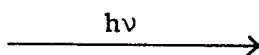
the distance between them is 4.8\AA or greater are found to be photochemically inert. In contrast to these photodimerizations which are topochemically controlled, there are solid state reactions which are best understood in terms of the geometry of molecules situated at or near defective sites such as dislocations. The opportunity for molecules at dislocations to control reactivity arises when steric or other factors make reaction in the perfect parts of the crystal energetically unfavorable and that at dislocations comparatively desirable and a mechanism exists for excitation energy to reach such defective sites. An example of this is provided by the photodimerization of 9-substituted anthracenes in the solid state^{13b,16}. As in the cinnamic acids, there are three crystal forms, α , β and γ . The α type is predicted on the basis of the monomer arrangements in the crystal to give the centrosymmetric dimer and it does, Scheme 4; the γ -type is photoinert as expected but the β -type which on the basis of the crystal structure should give the mirrorsymmetric dimer reacts to give the centrosymmetric dimer. The formation of this non-topochemical dimer is now fairly well understood. Dimerization here involves bonding the C9, C10 positions of one monomer to the C10, C9

Scheme 4

α -type

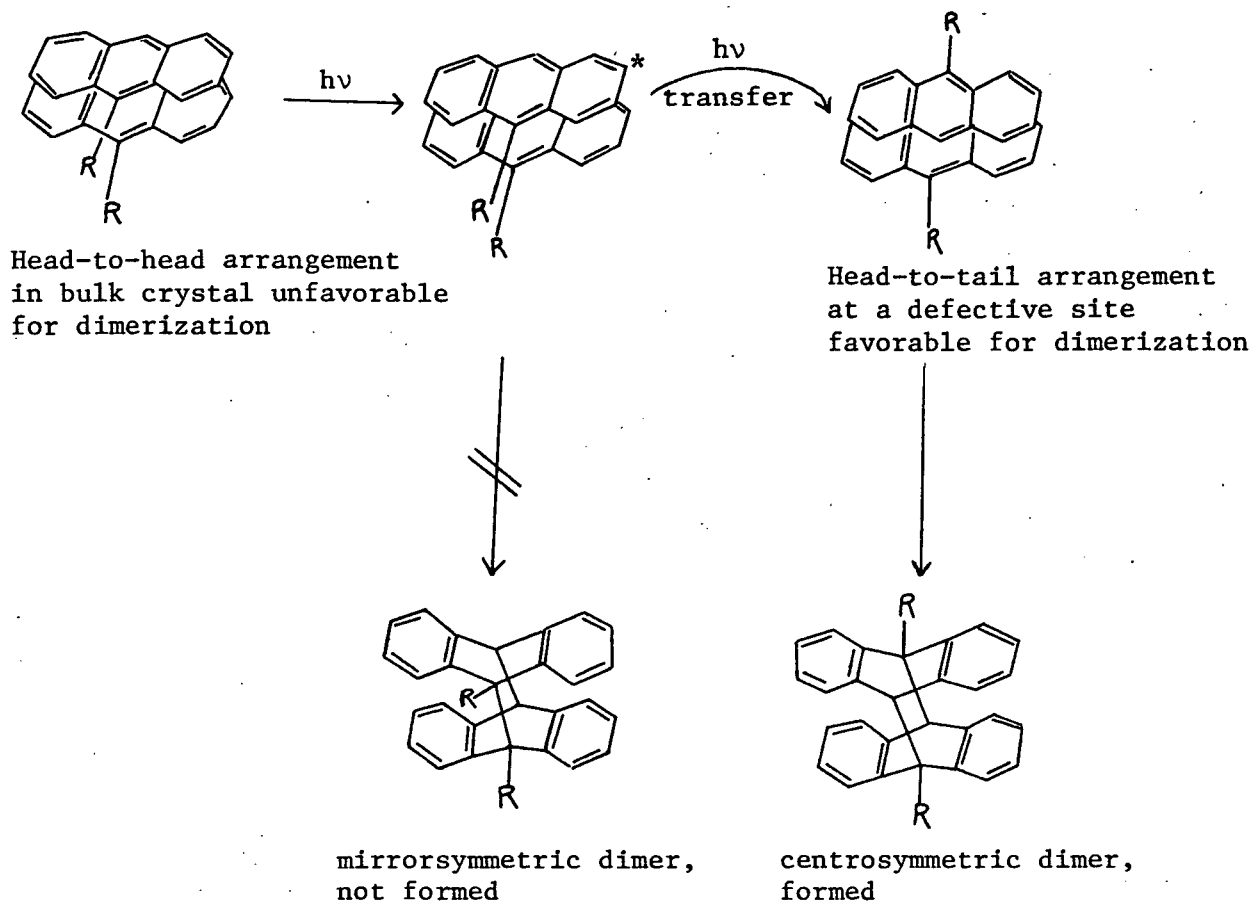


Head-to-tail
arrangement

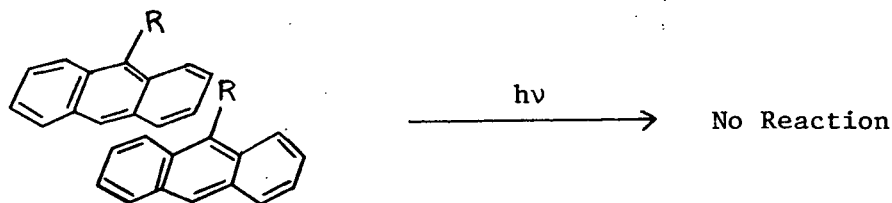


centrosymmetric dimer

β -type



γ -type



positions, respectively, of its nearest neighbour. When any of these positions is substituted, the β -arrangement becomes energetically unfavourable for dimerization presumably because of steric hindrance. So that one would expect such crystals to be photoinert. This is found true for some of the 9-substituted and 9,10-disubstituted anthracenes^{13b,16}. But in others linear defects i.e. dislocations have made possible the head-to-tail approach of two monomers so that reaction begins only at these defective sites and is propagated through multiplication of the defect as reaction proceeds. In these anthracene-derived compounds, it has also been shown that the initial absorption of irradiation need not be by the molecules at these defective sites in order to have the reaction to occur. Both impurities¹³ and displaced molecules at defective sites¹⁴ have been shown to act as effective exciton traps in anthracene crystals. So that energy absorbed by the bulk of 9-substituted anthracene crystals is passed on from one pair of molecules to the next until it reaches a defective site where monomer pair arrangements favor reaction. The formation of the unexpected dimer in such cases is, therefore, not a violation of the topochemical postulate since the reaction is not occurring within the "perfect" regions of the crystal lattice but is due to favorable reaction conditions at dislocations in the crystal as suggested and shown by Thomas and Williams¹⁵.

Energy Transfer in Organic Solids¹⁷⁻²¹

It will be useful to define the term "exciton" as it is used in the photochemical literature on organic solids. In solids, excitation

energy absorbed by a chromophore in a molecule may be immediately passed on to a neighboring molecule in the same crystal. Thus, the excitation energy can be thought of as being shared between the molecules within that particular crystal. This delocalized excitation energy is termed an exciton. The migration of an exciton from molecule to molecule which has been variously described as tunnelling¹⁸, a hop¹⁹, a jump²⁰ and a random-walk^{17,18a} by different investigators occurs through long range interaction between traps in contrast to the mechanism of triplet-triplet energy transfer in solution which occurs largely through molecular collisions. As mentioned earlier, energy transfer occurs in some systems and not in others depending on the types and magnitude of the interaction between the donor and recipient molecules. In cases where the probability of transfer is large ($\geq 10^{11} \text{ sec}^{-1}$) it is estimated that the jump time, T , for a migrating exciton can be as short as or shorter than lattice relaxation times²¹ (10^{-13} sec) so that in these cases the excited state molecule S^* and its surrounding unexcited molecules S_0 have the same geometry. This keeps the probability of transfer high and promotes extensive exciton migration. When, on the other hand, lattice relaxation precedes the transfer, considerable energy is expended thermally and exciton migration is curtailed. Examples of solid systems which have been shown to exhibit substantial exciton migration are those of benzene¹⁷, naphthalene¹⁸, and anthracene²⁰. Several important conclusions can be drawn from these works:

(i) Since the average number of jumps or transfers is τ/T where τ is the lifetime of the exciton and T is the time within which a single transfer occurs^{20a}, and since a triplet exciton is longer-lived than a singlet exciton, it follows that migration of a triplet exciton through a crystal is more extensive than that of a singlet exciton. Nieman and Robinson¹⁷ estimated that in pure organic crystals, $\sim 10^{11}$ triplet energy migrations are possible per radiative lifetime as compared to $10^4 - 10^6$ for the lowest singlet.

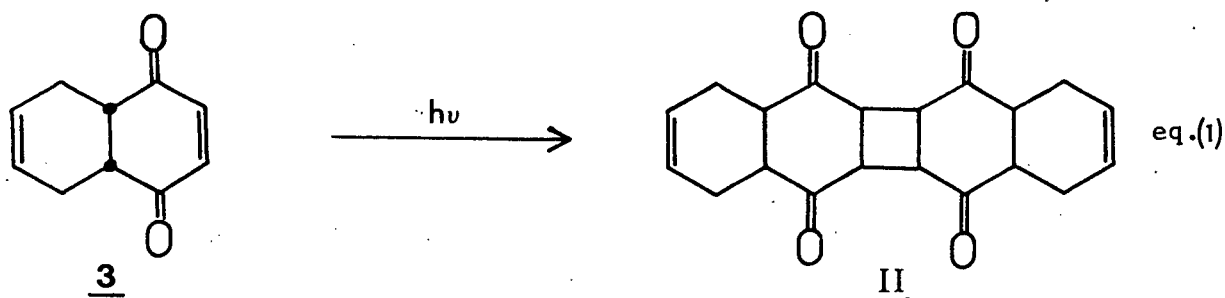
(ii) The more extensive wandering of the triplet increases the probability of its annihilation at defective sites and also through triplet-triplet quenching. This is borne out by the fact that many organic crystals having long-lived triplet states do not phosphoresce.

(iii) Structural faults and/or chemical impurities can act as exciton traps to terminate the transfer process. These energy sinks may then become the sites of physical processes such as phosphorescence and/or the reaction centres within the crystal.

2. Photochemistry of Tetrahydro-1,4-naphthoquinone and Its Derivatives

Diels and Alder²² reported the formation of a polymeric material of unknown molecular weight when they exposed crystals of the parent compound, 4a,5,8,8a-tetrahydro-1,4-naphthoquinone, 3, to sunlight. Over three decades later, Cookson and coworkers²³ reinvestigated this and similar reactions. In both ethyl acetate solution and as crystalline material, UV irradiation through Pyrex of compound 3 was reported to

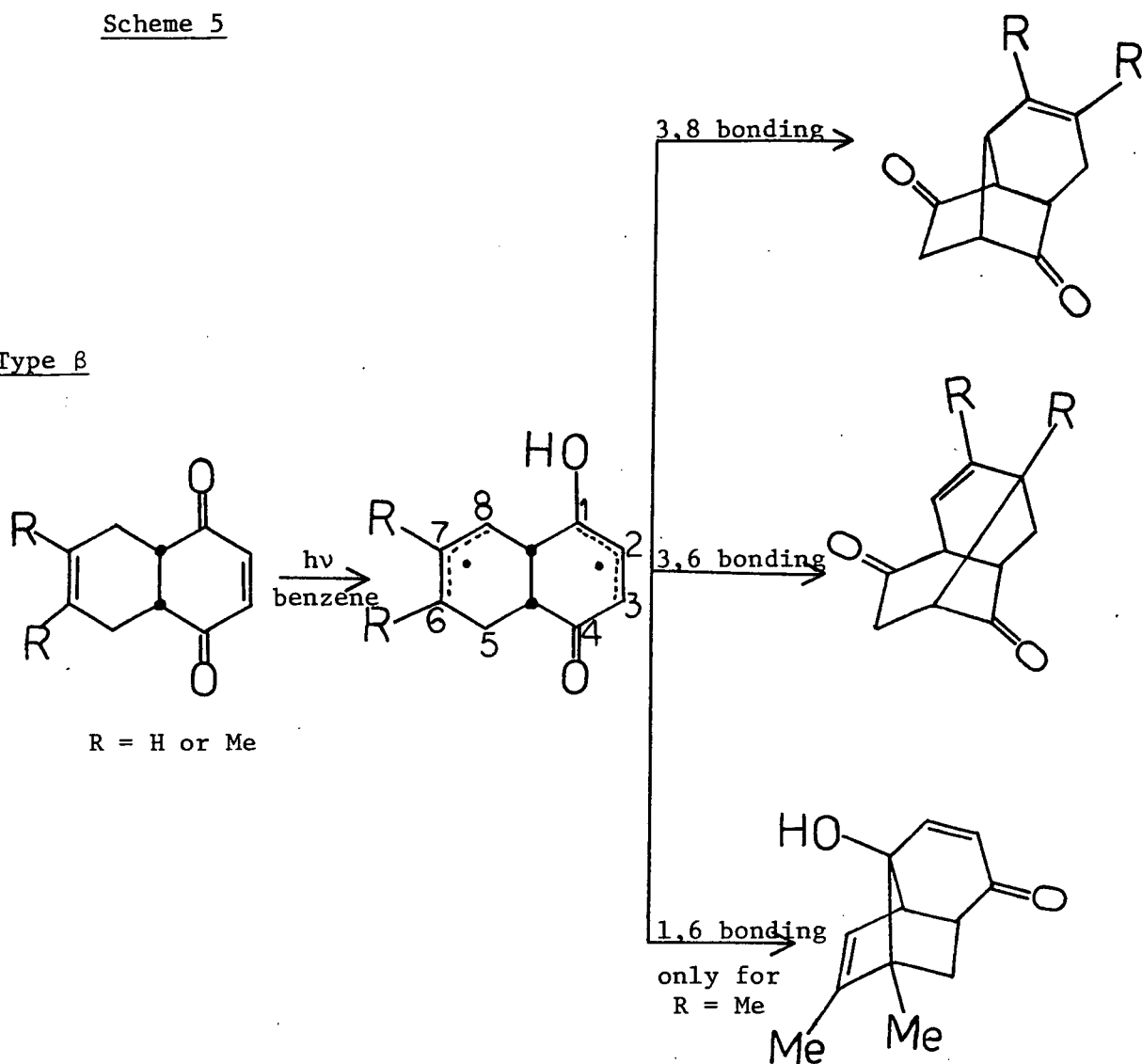
give mainly tar. Although, their attempts at characterisation met with little success, they tentatively assigned it the dimeric structure, II, of unknown stereochemistry, (eq. 1).



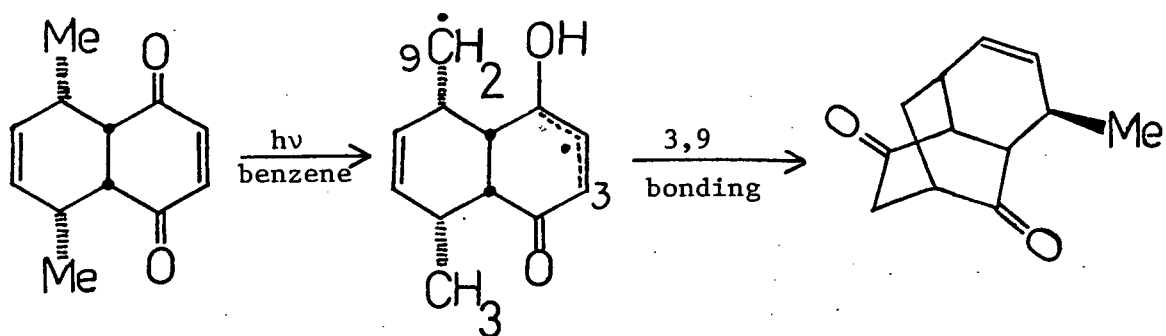
More recently, Scheffer and coworkers²⁴ have shown that selective irradiation, ($\lambda > 340$ nm) of 3 and its derivatives in solution gave tricyclic and tetracyclic products in moderate to quantitative yields. Their results are summarized in Scheme 5. The type β process has only recently appeared in the literature²⁵ and formally involves the abstraction of a hydrogen via a five-membered transition state. On the other hand, the abstraction of a γ -hydrogen by a carbonyl oxygen through a six-membered cyclic transition state is commonplace and has been widely referred to as the Norrish Type II process²⁶. The third reaction type, denoted as γ^c to differentiate it from the previous γ -process involves the abstraction of a γ -hydrogen by carbon 2 of the ene-dione system. This process is analogous to that reported in the photochemistry of some substituted cyclopentenones and cyclohexenones²⁷. The fourth reaction type i.e., intramolecular oxetane formation, is formally a 2+2 cycloaddition of a carbonyl group to an olefinic double bond. Such a reaction is well documented in the literature²⁸. The last reaction type leading to a caged

Scheme 5

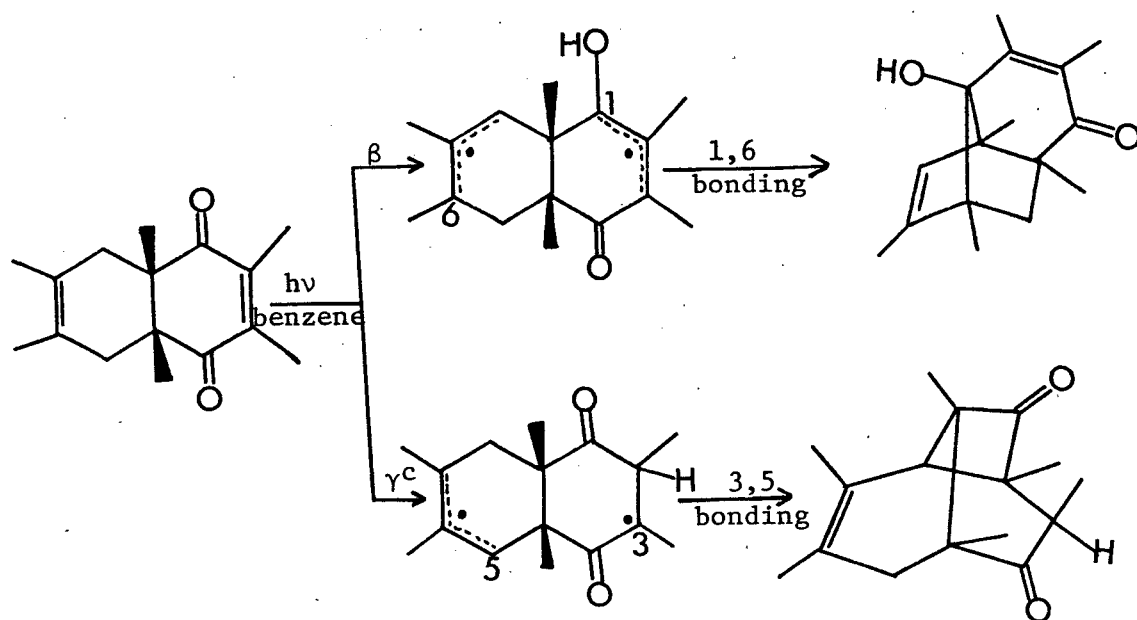
Type β



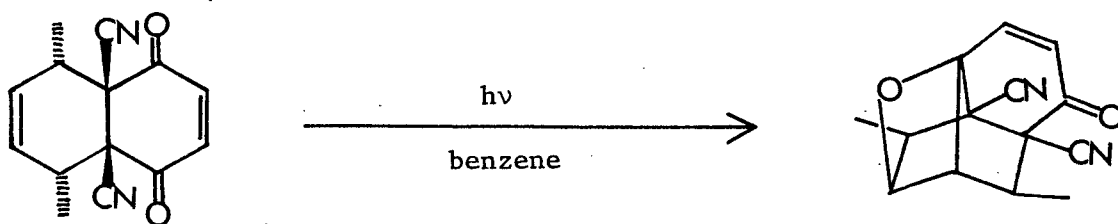
Type γ



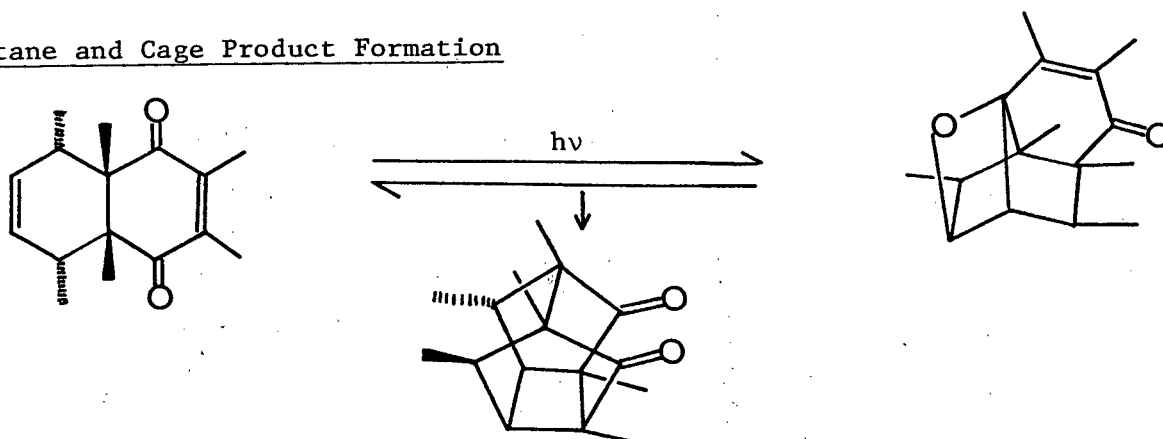
Type β and γ^c



Oxetane Formation

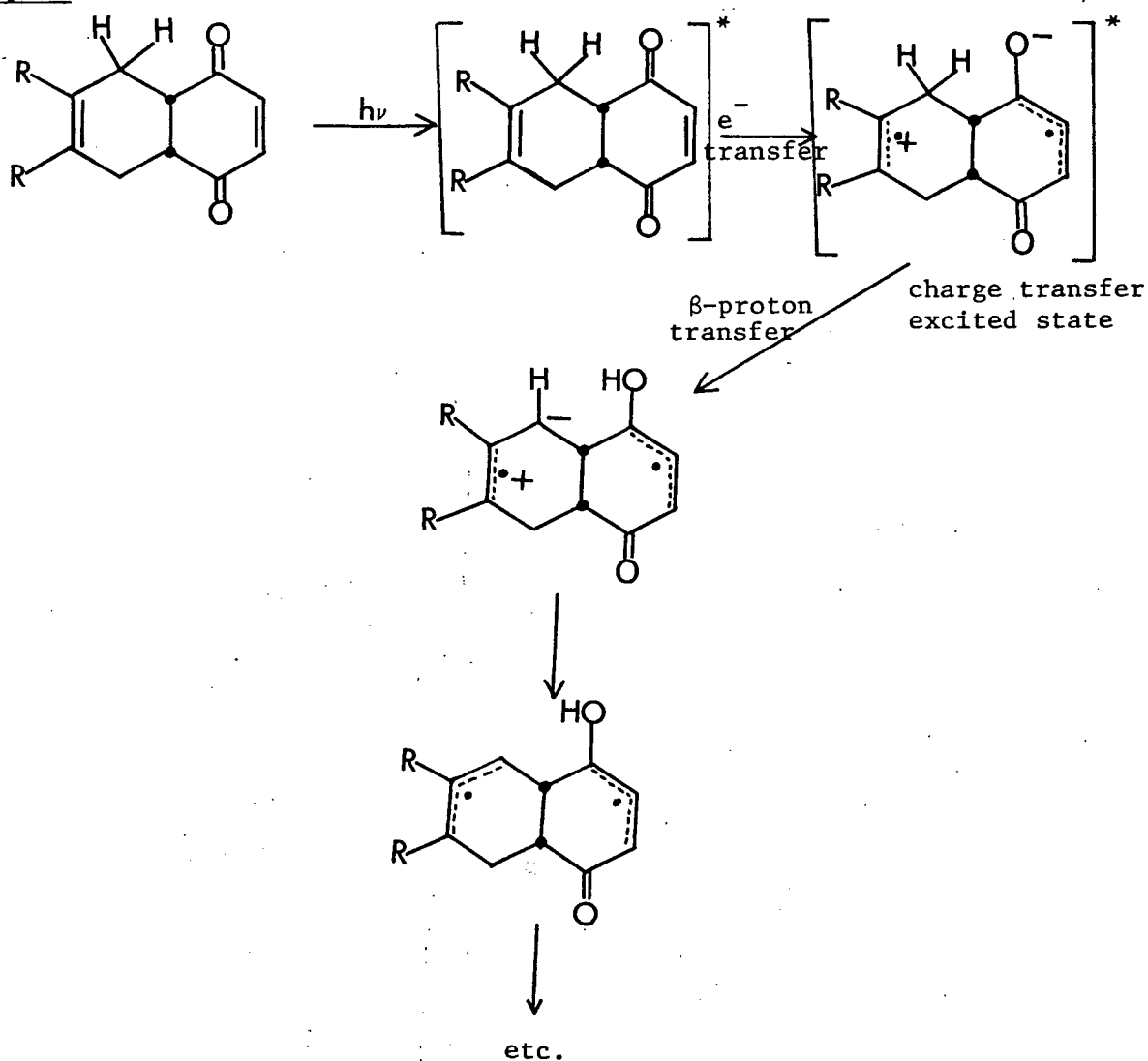


Oxetane and Cage Product Formation

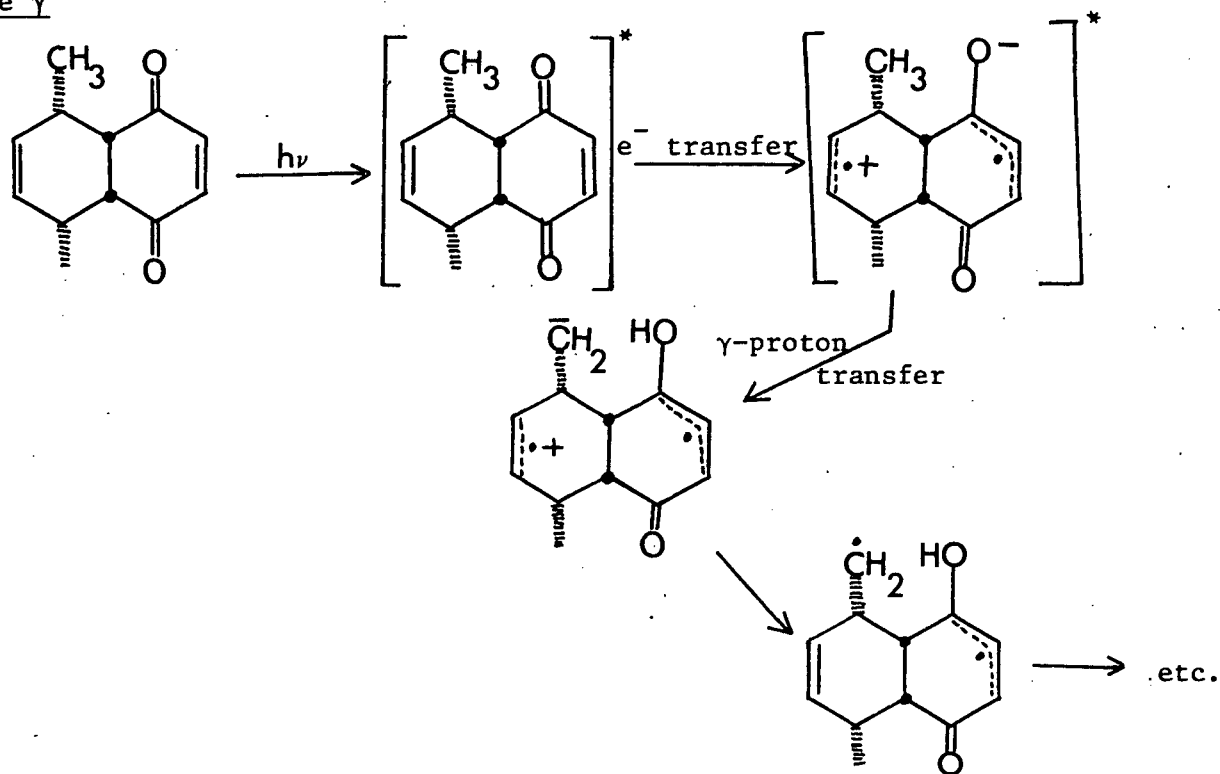


structure (Scheme 5) is also an intramolecular 2+2 cycloaddition. This time, however, the addition is between the two olefinic double bonds. This reaction is also not without precedent²⁹. There are two simple mechanisms which can explain the formation of the various products arising from hydrogen abstraction. One of these is the biradical mechanism shown in Scheme 5 and the other is the charge-transfer or ion pair mechanism shown in Scheme 6. The latter mechanism involves the

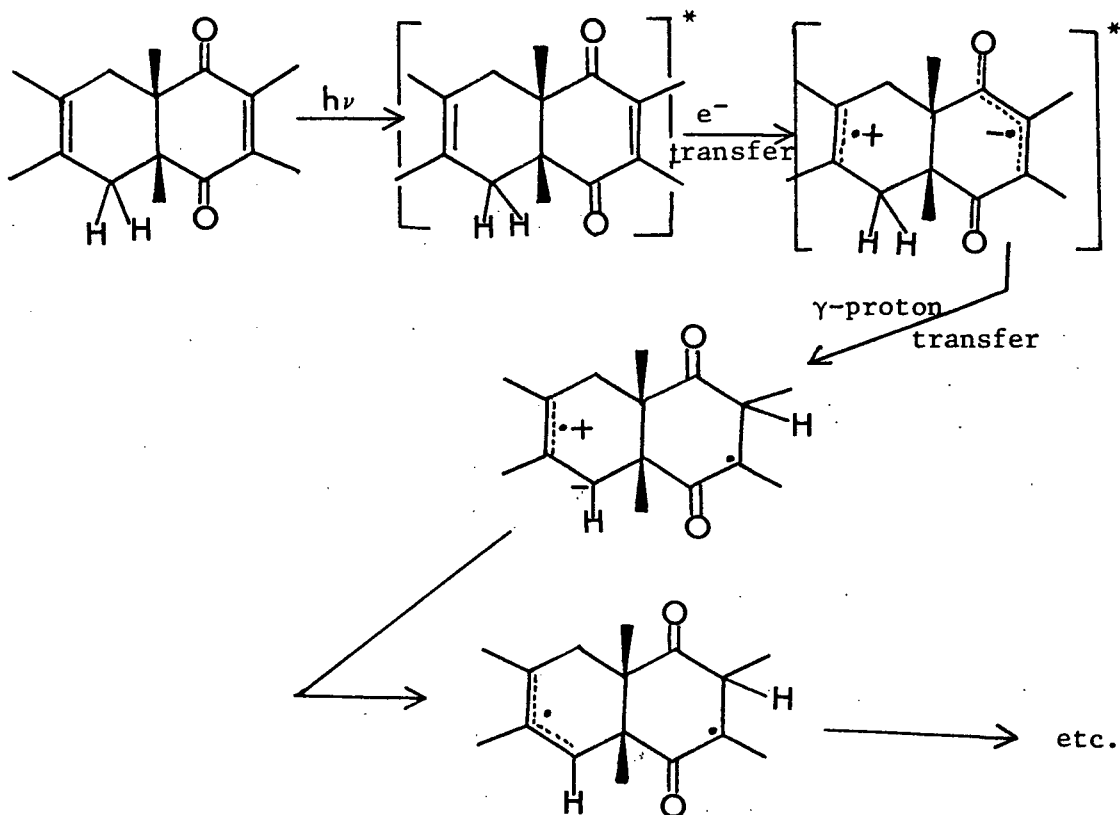
Scheme 6
Type β

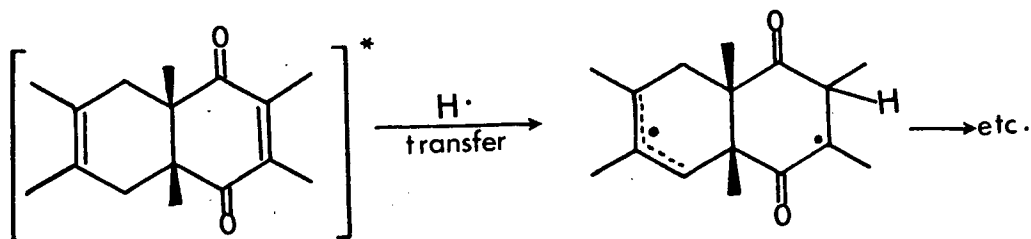


Type γ



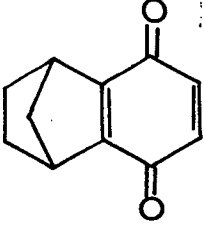
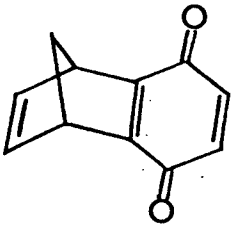
Type γ^c





transfer of an electron from the olefinic π system to the excited enedione chromophore followed by the abstraction of a proton by the oxygen. Electron reorganization in the resulting dipolar intermediate would then give rise to the same biradical intermediate formed from the direct abstraction of a hydrogen atom by the oxygen. The biradical pathway follows from that generally accepted for the Norrish Type II and related processes. On the other hand, charge transfer bands have been detected in the UV absorption spectra of some p-benzoquinone derivatives similar to those studied by Scheffer and coworkers²⁴. For example, compound IV (Table 1) has an absorption at 307 nm with a higher extinction

Table 1

Compound	UV absorptions, $\lambda_{\text{nm}}(\epsilon)$			
	$\pi \rightarrow \pi^*$ (allowed)	charge-transfer	$\pi \rightarrow \pi^*$ (forbidden)	$n \rightarrow \pi^*$
 III	255 (15,500)	-	355 (800)	435 (26)
 IV	257 (14,500)	307 (260)	385 (520)	448 (50)

coefficient than its n, π^* absorption. There was no corresponding absorption in the 300-350 nm region, however, for compound III. Cookson and coworkers³⁰ ascribed the 307 nm absorption to a charge-transfer state arising from overlap of the remote double bond with the carbonyl of the p-benzoquinone chromophore. This is not unreasonable since p-quinones are good electron acceptors and may accept an electron from the remote double bond if the geometry of the molecule allows for overlap of the two chromophores. So that, although the biradical mechanism accounts for the products observed in the investigations of Scheffer and coworkers²⁴, the possibility of a charge-transfer mechanism needs to be explored.

Biradical vs Charge-transfer Mechanisms:

Throughout this discussion it will be important to bear in mind that both of these mechanistic pathways involve a biradical intermediate. Such an intermediate is necessary to explain the different products formed in these hydrogen abstraction reactions. So that in considering these two pathways, one is solely concerned with the step(s) leading to the formation of the biradical.

The first event in the chain is surely the absorption of light. This promotes the molecule from its ground state energy level to an excited state. What is the nature of this excited state? As will be shown later, like the Norrish Type II reaction, the reactions of these tetrahydronaphthoquinones proceed from both the singlet and triplet excited states.

Since deactivation from higher excitation levels is quite rapid in solution ($k \approx 10^{12}-10^{13} \text{ sec}^{-1}$), one assumes that only first excited states are involved. In the Norrish reaction, it is found that in acyclic ketones the percentage of singlet reaction depends on the strength of the $\gamma\text{C-H}$ bond - as the bond becomes weaker, the proportion of reaction occurring from the singlet state increases^{26a}. On the other hand, ketones with high intersystem crossing efficiency e.g. aromatic ketones, may be expected to react mostly from their triplet states. A second question to be settled about the nature of the excited state(s) involved in these reactions has to do with the fact that in some ketones there are two low-lying triplet states namely, $^3n,\pi^*$ and $^3\pi,\pi^*$. Triplet lifetimes obtained from phosphorescence studies show that, of the two triplets, the $^3n,\pi^*$ is the shorter lived, its lifetime being generally of the order of 10^{-3} to 10^{-2} sec.^{26b}. Using these lifetimes it has been established that ketones with low-lying pure n,π^* triplets undergo the Norrish Type II reaction while those with pure π,π^* lowest triplets are, generally, unreactive. The reactivities of these two triplets in intramolecular hydrogen abstraction reactions have been estimated^{26b} to differ by at least a factor of 10^6 . This is not surprising, if, as is generally assumed, the reaction involves the abstraction of a hydrogen atom by an electron-deficient oxygen. For the n,π^* state has a configuration in which an electron deficiency has been created at the oxygen due to the promotion of one of its non-bonding pair of electrons into an antibonding (π^*) orbital. The n,π^* excited state of

carbonyl compounds, therefore, closely resembles and acts like an alkoxy radical^{26b}. The π, π^* state, on the other hand, has an electron-rich rather than an electron deficient oxygen as depicted in Figure 4 making it less reactive in Type II reactions. Unfortunately, some

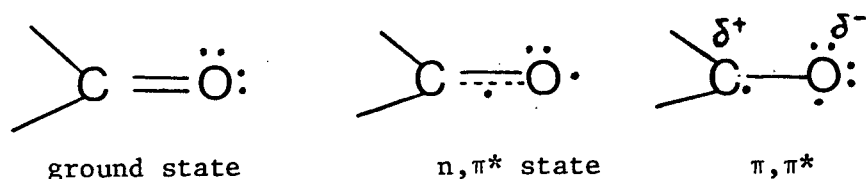


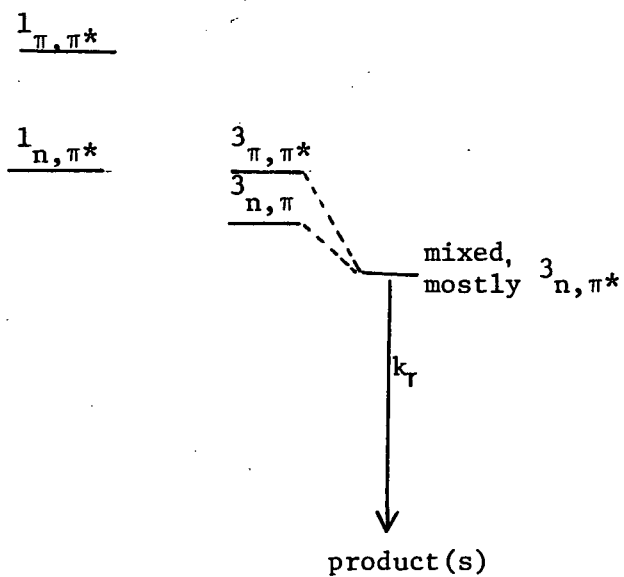
Figure 4:

ketones react via excited states which are neither pure $^3n, \pi^*$ nor $^3\pi, \pi^*$, thus making the above generalization incomplete. Investigators differ in their interpretations of results in this area. To assume that only $^3n, \pi^*$ states undergo the hydrogen abstraction reaction would lead to the inevitable conclusion that ketones having their π, π^* states below their $^3n, \pi^*$ react because (A) there is vibronic mixing of the two states, thus conferring some n, π^* character on the excited state which reacts or, alternatively, that (B) the π, π^* thermally equilibrates with the n, π^* and it is this latter triplet which reacts. Since neither of these two possibilities shown in Scheme 7 seems satisfactory in explaining all of the available experimental data³¹, the earlier view^{26a} that either or both mechanisms may operate in a given ketone seems the safest interpretation to date.

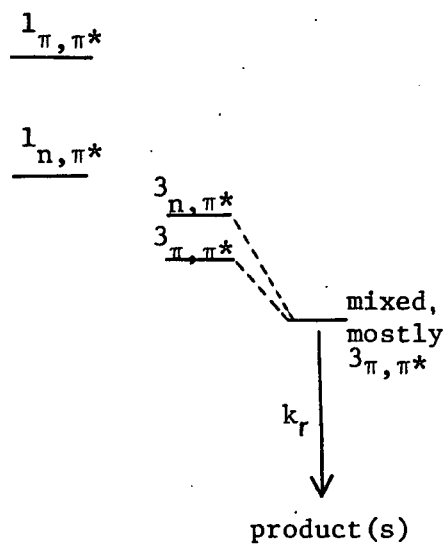
Whatever the nature of the excited state in these reactions, it is ultimately tied in with the question of whether or not the next

Scheme 7^{26b,31}

A

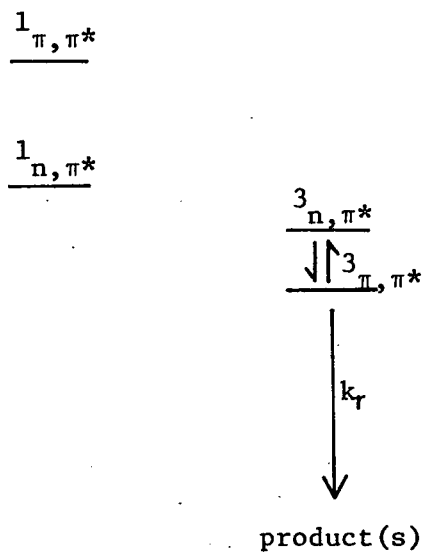


Phenyl ketones

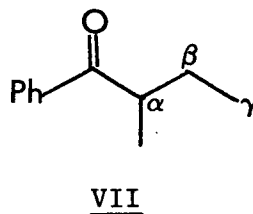
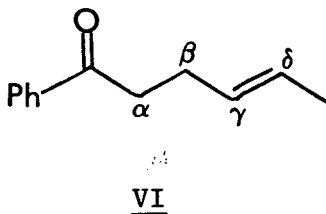
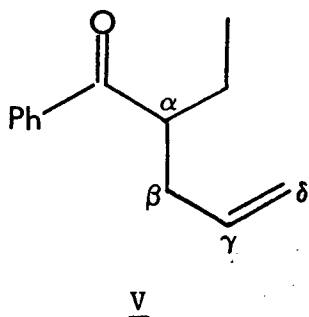


Naphthyl or biphenyl
ketones

B

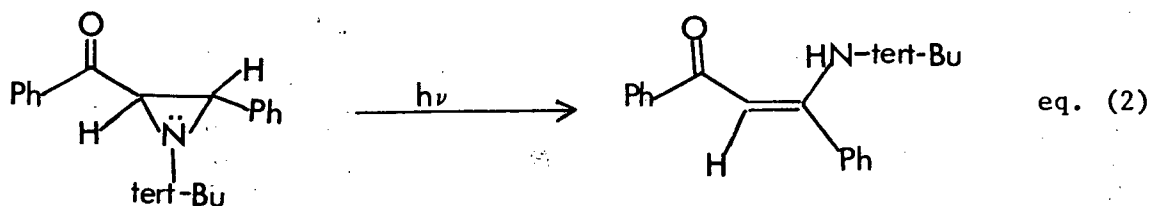


event in the sequence involves the abstraction of a hydrogen atom or the transfer of an electron because, as mentioned earlier, the electron density at the oxygen differs markedly for the n,π^* and π,π^* states. The charge-transfer (CT) state resembles the π,π^* state in its electron distribution. The oxygen is nucleophilic and subsequently can only be reactive in hydrogen abstraction reactions if the transfer involves a proton rather than a hydrogen atom. Porter and Suppan³² have studied the spectral and photochemical behaviour of a variety of substituted benzophenones. Their results showed that derivatives having charge-transfer lowest triplets were even less reactive in hydrogen abstraction reactions than substrates having pure π,π^* lowest triplets. Thus the order of reactivity of these three excited states is $n,\pi^* > \pi,\pi^* > CT^*$. This order reflects the order of electrophilicity of the oxygen in these three states thus strongly implying that it is an electron deficient oxygen which abstracts a hydrogen. This has recently been borne out by the photochemical behaviour of β -vinyl phenyl ketones³³. The interaction of the γ - δ double bond of ketones V and VI with the excited carbonyl chromophore in their photochemical transformations was evidenced by the isomerization about the double bond in VI. Comparison of their UV spectra with that of valerophenone showed that the

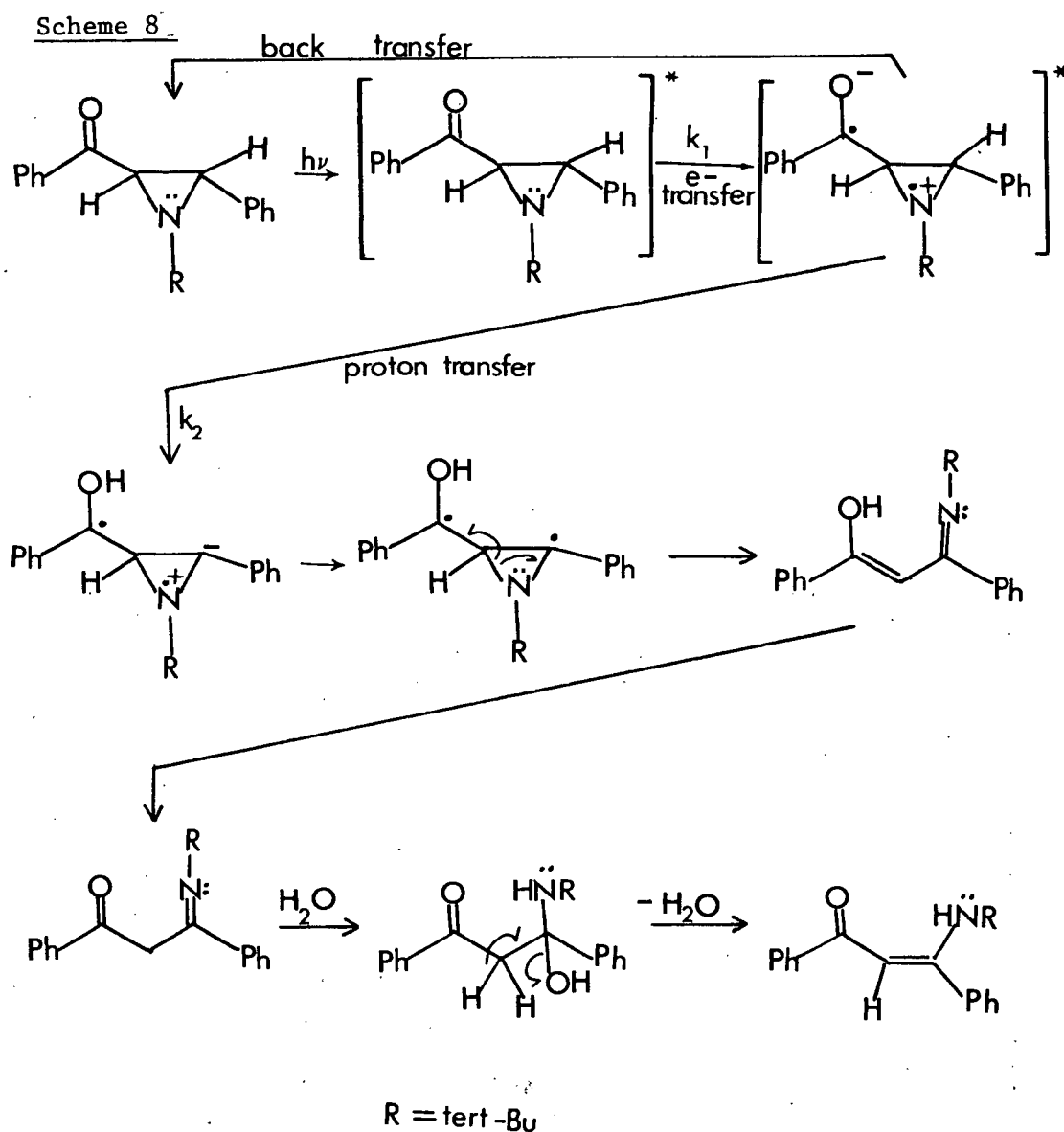


interaction is not a ground state phenomenon. Since ketones have triplet energies which fall below those of olefins, an energy transfer which excites the olefin partner in a Franck-Condon fashion has to be endothermic. Such endothermic energy transfers are now believed to involve charge transfer (CT) complexes^{33,34}. In V where the potential exists for γ -hydrogen abstraction, it was found that it competed poorly with triplet decay via intramolecular quenching by the double bond. The latter process was favored 100:1 over abstraction. Furthermore, the total quantum yield of Type II products from compound V was only 1% of the value reported for compound VII for which the reactive state was clearly n,π^* . These results would seem to indicate that the abstraction of a γ -hydrogen via a charge-transfer excited state occurs very inefficiently, if at all.

One example where a charge-transfer mechanism has been suggested is the photochemical hydrogen abstraction process in small ring nitrogen heterocycles studied by Padwa and coworkers^{25a,b}. The transformation, an example of which is given in equation 2, was found to have, generally, low quantum yield (≤ 0.02) in spite of the fact that the n,π^* triplet responsible for the transformation was too reactive to be quenched efficiently. The usual explanation for such low quantum yields in certain hydrogen abstraction reactions has been the back

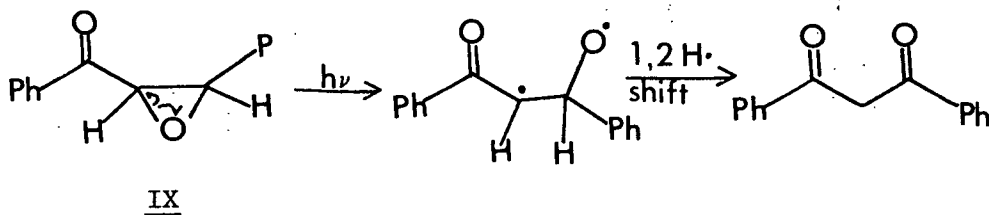


transfer of the abstracted hydrogen. The kinetic data on this particular system, however, showed that the abstraction of the hydrogen was irreversible. A charge-transfer mechanism (Scheme 8) as proposed by the authors^{25a,b} provides an explanation which is consistent with both the low quantum efficiency and the high triplet reactivity. The donation



of an electron by the heteroatom is thought to occur at a rate k_1 which exceeds diffusion-controlled rates thus making the triplet unquenchable. The low quantum efficiency for product formation is explained by competitive back-transfer of the electron in the radical ion pair accompanied by deactivation to the original ketone. This mechanism in which hydrogen abstraction involves electron transfer followed by proton transfer has, so far, been convincingly demonstrated only in amino systems. For example, photoreduction of carbonyl compounds by amines are well documented and have been shown in a few cases to involve a charge-transfer (CT) complex formed by the interaction of the electron donor with the acceptor³⁵. In some cases, such complexes have been detected by their emission spectra and/or by their e.s.r. spectra. Nevertheless, the fact that the oxygen analog of amine VIII i.e. compound IX reacts by a different mechanism^{25b} (Scheme 9) should caution against the extension of this mechanism to other related systems. Since the CT

Scheme 9



mechanism relies on both the availability of electrons on the donor atom or group and the ease of reducing the acceptor, both the ionization

potential (IP) and the nature of the excited carbonyl chromophore will determine whether or not this mechanism is feasible in any given system. Thus, the difference in the behaviour of substrates VIII and IX, for example, is likely due to the higher IP of the non-bonding electrons on oxygen relative to those on nitrogen as Padwa and Eisenhardt have suggested^{25b}. In the tetrahydro-1,4-naphthoquinone series, the possibility exists for a CT complex formation preceding a biradical intermediate since cyclohexene and its methyl substituted derivatives have IP's ranging from 8.3 to 8.9 eV³⁶ which are comparable to the reported IP values for some primary and secondary aliphatic amines³⁷ which are known to photoreduce carbonyl compounds by a CT mechanism.

Characteristics of the β - and γ -Hydrogen Abstraction Reactions in the Tetrahydro-1,4-naphthoquinone Series:

Substituent Effects

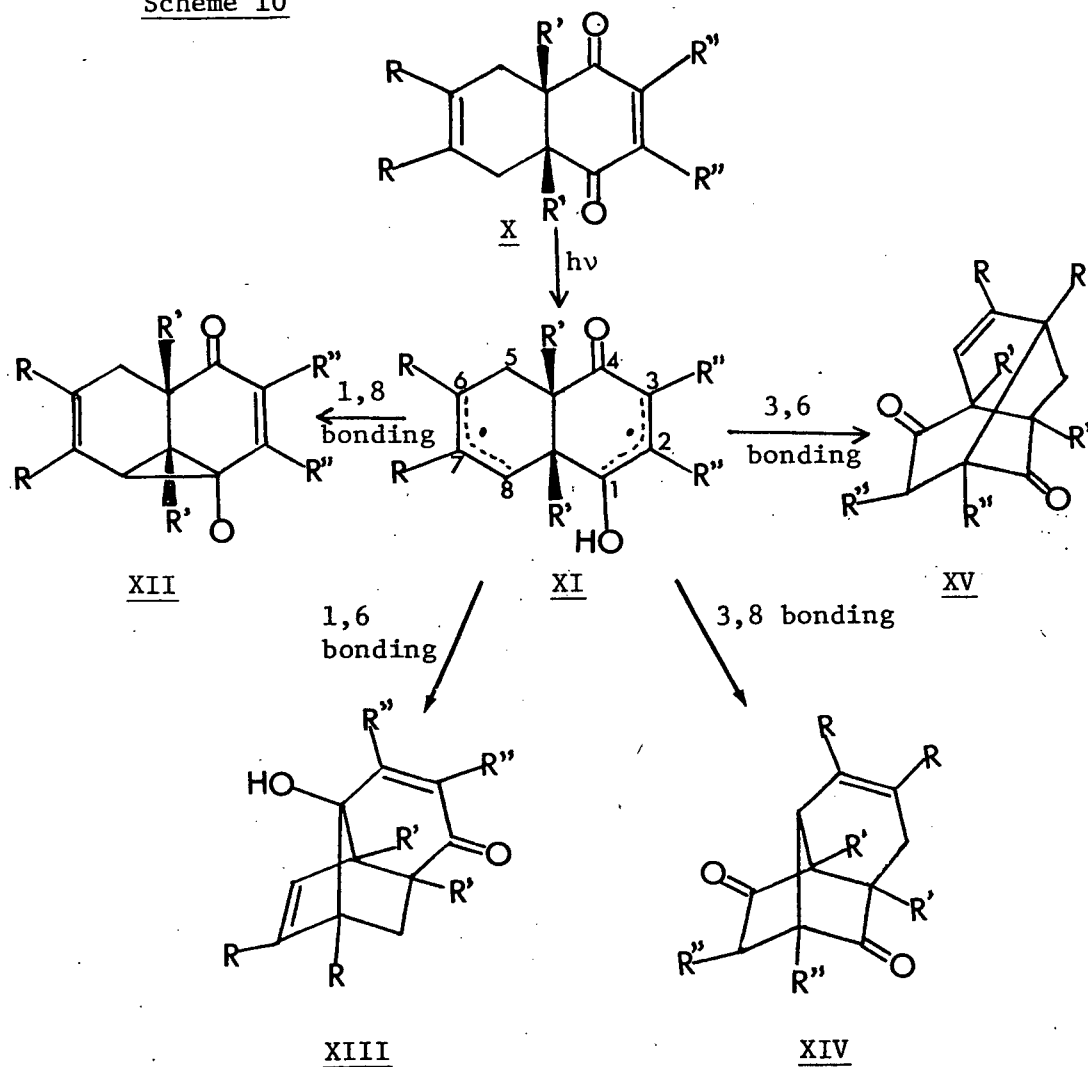
There are two effects caused by substitution:

(i) in two substrates where both the ene-dione double bond and the bridgehead positions bear methyl groups, both β - and γ^c -hydrogen abstraction products were isolated, the latter process being absent in all other substrates so far studied. The abstraction of a hydrogen by enone carbon has been reported in the literature as resulting from a $^3_{\pi,\pi^*}$ state^{27,38}. This leads one to conclude that in the tetrahydro-naphthoquinone series, only when both the bridgehead positions and the ene-dione double bond are substituted with alkyl groups does the π,π^*

triplet energy level become sufficiently lowered to favor reaction from it. This is a tenable supposition in the light of the findings of other workers³⁹ that alkyl substitution on an enone double bond causes a lowering of the $(\pi, \pi^*)^3$ energy level

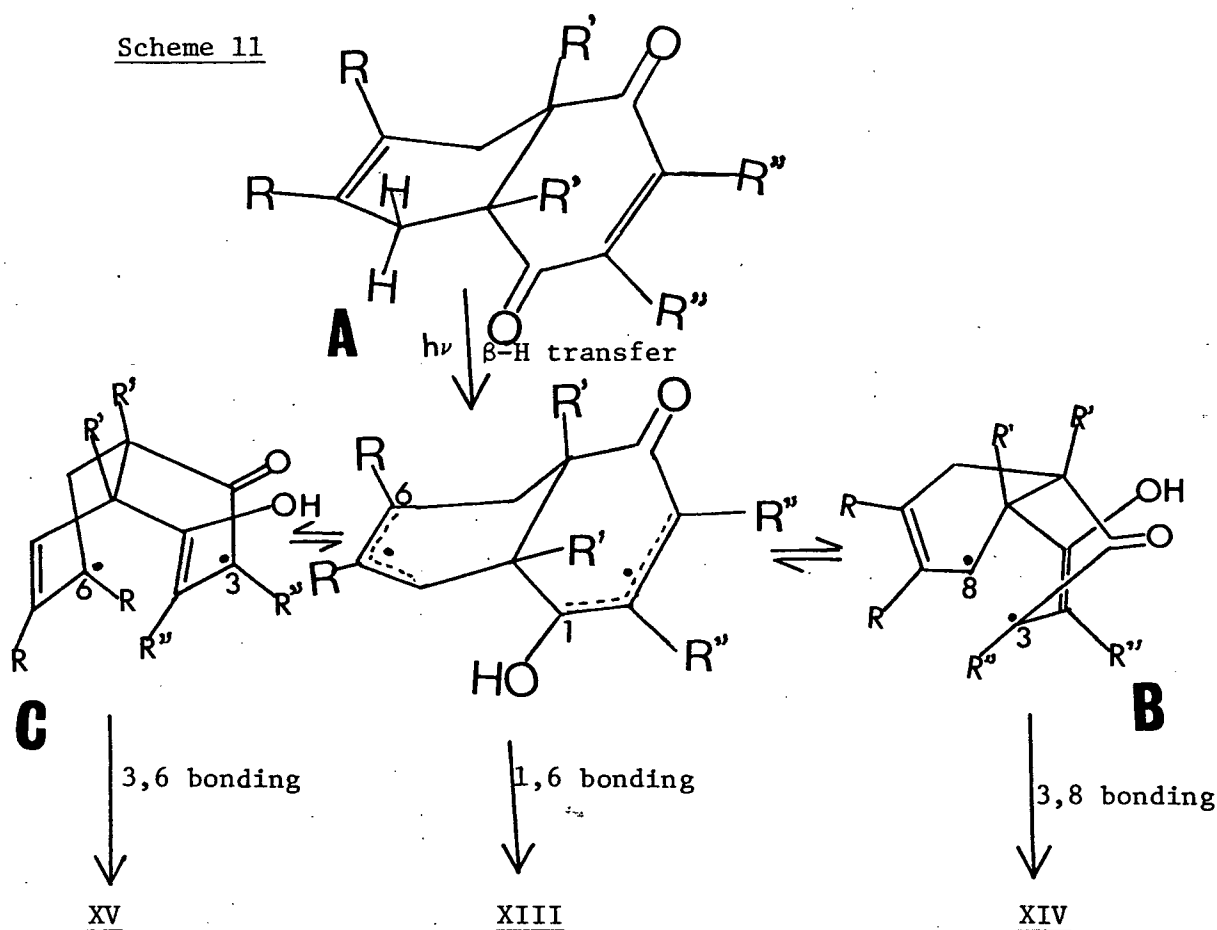
(ii) the second effect caused by substitution seems to involve the modes of closure of the intermediate biradical in the β -hydrogen abstraction reactions. As shown in the generalized scheme (Scheme 10) for such a process, there are four modes of closure open to such a

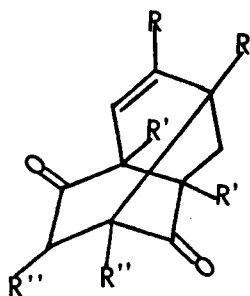
Scheme 10



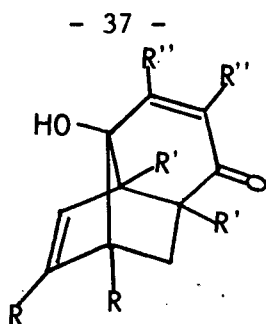
biradical. The formation of a strained cyclopropane ring in a tricyclic structure is on steric grounds alone unfavorable and so the complete absence of product type XII in the series is understandable. Product XIII, formed by bonding C-1 to C-6 is formed by all substrates except the parent compound i.e. $R=R'=R''=H$. In some cases, it is the exclusive product from a β -hydrogen abstraction process. Scheffer and coworkers²⁴ have explained the product types encountered in this series by proposing that the reactions are conformationally controlled. In this proposal, the assumption is made that these tetrahydro-1,4-naphthoquinones exist in solution mainly in the twist conformation A, Scheme 11, and that the

Scheme 11

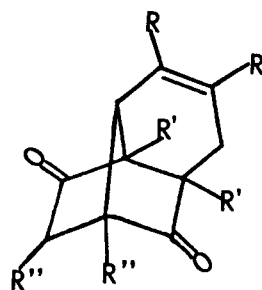




XV



XIII



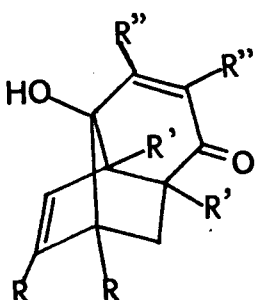
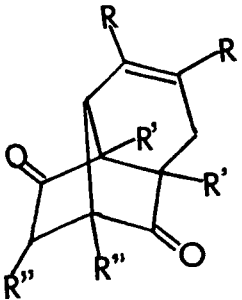
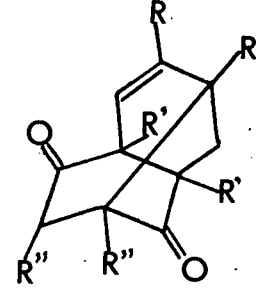
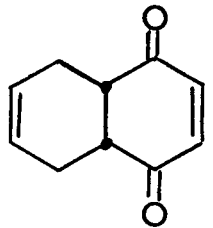
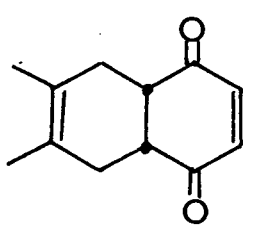
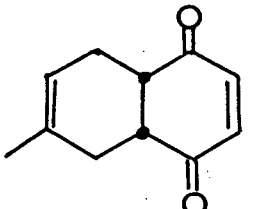
XIV

diradical intermediate XI, when formed at first has this same conformation. From this conformation, the only feasible form of ring closure is between carbons 1 and 6. The other possible bonding centres are either too far apart or would lead to the sterically unfavored cyclopropyl derivative. Thus, biradical intermediates which are immobilised, say, by bulky bridgehead substituents collapse only to enone-alcohol product XIII. On the other hand, biradicals which are not restricted to this conformation can adopt other conformations such as B and C from which C3 to C8 and C3 to C6 bonding modes are possible giving, ultimately, products XIV and XV, respectively.

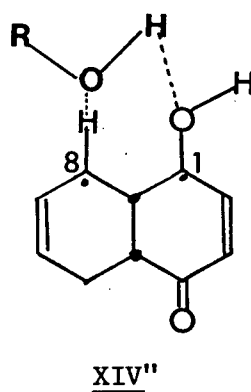
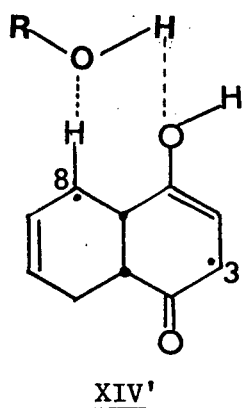
Solvent Effects

The one general solvent effect observed in this series is shown in Table II. It would seem, therefore, that ring closure of biradical intermediate XI occurs preferentially between carbons 3 and 6 in benzene. In a hydroxylic solvent, it has been suggested^{24a} that hydrogen bonding between biradical and solvent might lead to localization of the electrons at carbons 3 and 8 (XIV'). Closure between these centres

Table II. Product Ratios Obtained in Benzene (unparenthesised) and tert-Butyl Alcohol

<u>Substrate</u>	 <u>XIII</u>	 <u>XIV</u>	 <u>XV</u>
	None	1 (5)	7 (1)
	2 (trace)	trace (major)	3 (trace)
	None	3 (7)	7 (1)

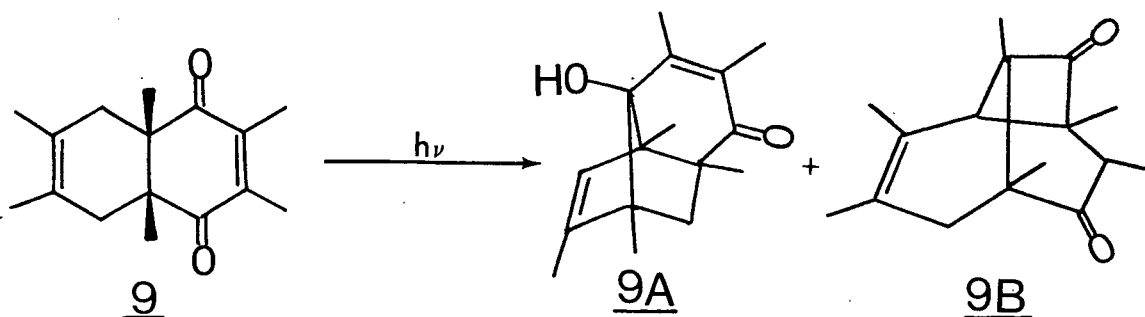
would then explain the preferential formation of product type XIV in tert-butyl alcohol. The alternative structure, XIV'', for such a



solvated species would be a 1,3 biradical which can only collapse to the sterically unfavored cyclopropyl derivative.

Quantum Yield and Quenching Studies^{24b}

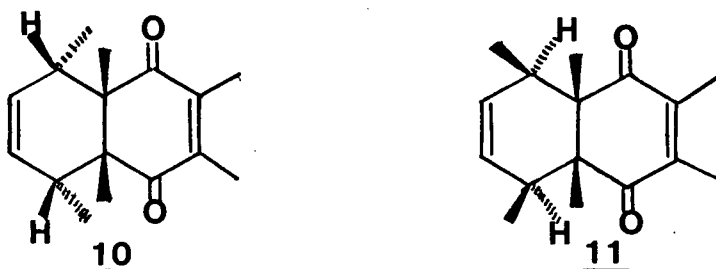
The substrate chosen for study was compound 9 which had been shown to give tricyclic products 9A and 9B in combined yields of 80%^{24a}. The quantum yields for appearances of enone-alcohol, 9A and diketone 9B



were 0.066 and 0.089 respectively^{24b}. These low quantum yields may reflect, among other possibilities, reaction from an inherently less reactive state than a pure n, π^* excited state or reversible hydrogen transfer. Quenching studies^{24b} showed that product 9B arising from γ -hydrogen abstraction by carbon is formed from a triplet excited state. The formation of 9A, a β -hydrogen abstraction product, could not be quenched, however, showing that this process occurs from a very short-lived triplet or a singlet state, a result in accord with the finding of Agosta and Cormier^{25d} in the β -hydrogen abstraction reaction of α -methylene ketones. As mentioned earlier, hydrogen abstraction by enone carbon is associated with a $^3_{\pi, \pi^*}$ state.

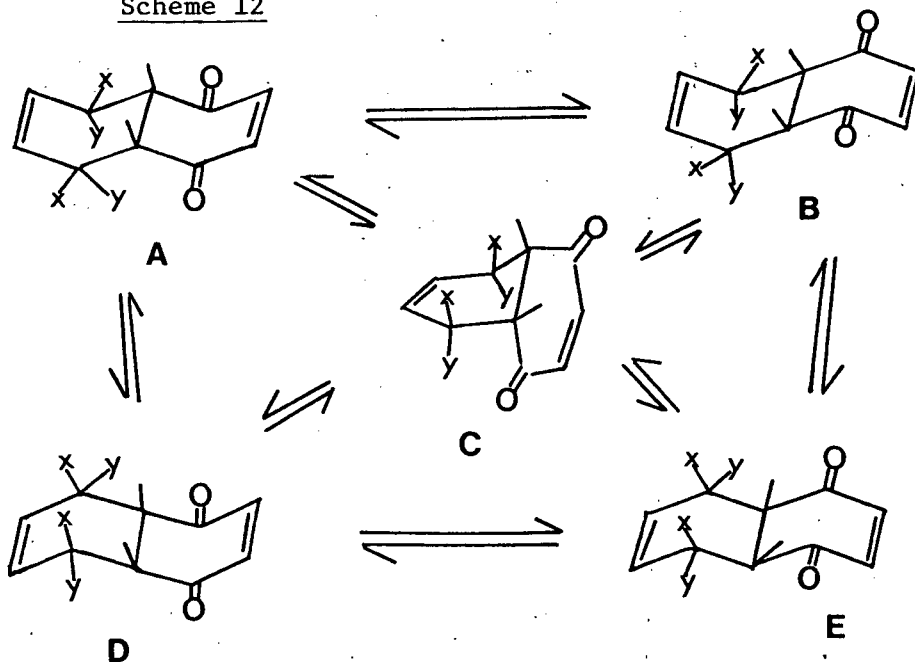
Stereoelectronic Requirements

Both β - and γ^C -hydrogen abstraction reactions seem to require that the hydrogen to be abstracted be trans to the bridgehead hydrogens or substituents. Thus, compound 11 undergoes both processes while no hydrogen abstraction occurs on irradiating 10^{24b}. This is best



understood by examining the possible conformations which these substrates can adopt in solution. These are shown in Scheme 12 where C5 and C8 hydrogens cis to the bridgehead substituents are shown by X and those trans are represented by Y. It is only in conformations A and B, that the cis hydrogen (X) comes within less than 3.5Å of the oxygen, and

Scheme 12



it is in these same conformations that the C-H bond to be broken is orthogonal to the adjacent π -system so that the developing radical centre is denied stabilization through delocalization^{24a}. The abstraction of only hydrogens in position Y is also in agreement with the observation made by Turro and coworkers⁴⁰ that only the γ -hydrogen which is in the plane of the carbonyl group (i.e. the position of the localized half-vacant n orbital of the $n-\pi^*$ state) is abstracted.

Other Reactions

The preceding discussions have been concerned with only hydrogen abstraction processes. Intramolecular cycloaddition reactions leading to oxetane and cage products have been found to occur only in substrates which have no abstractable hydrogen which leads one to conclude that these reactions compete poorly with intramolecular hydrogen abstraction in tetrahydro-1,4-naphthoquinones.

3. Objectives of Present Research

During the course of the previous discussion the possibility of the variation in product types being due to the conformational mobility or the lack thereof of the biradical intermediate was raised. Most important, there seems no doubt as in other hydrogen abstraction reactions, reactivity in this series also requires that the substrates fulfill some geometric requirements. What are these requirements? Is the partitioning of the biradical conformationally controlled? In the first published works^{22,23} on the parent compound, extensive

polymerization was observed both in the solid and in solution. Since the later work of Scheffer and coworkers^{24a} was carried out using selective irradiation, the question of whether the change from intermolecular to intramolecular reaction was due to the intrinsic properties of two different excited states needs to be answered. Djerassi and coworkers, in a series of papers⁴¹, have established that the γ -hydrogen abstraction observed in the mass spectrometer when carbonyl compounds are bombarded with electrons i.e. the McLafferty rearrangement, does not occur if the γ -hydrogen is further than 1.8\AA from the abstracting oxygen. Recent work by Henion and Kingston⁴² has revealed that, contrary to earlier calculations⁴³, the hydrogen to be abstracted need not be in the plane of the carbonyl group. Specifically they found that, the angle τ between the itinerant hydrogen atom and the plane of the carbonyl group (Figure 5) has an operational limit, namely, $80^\circ > \tau^\circ \geq 0^\circ$. Although,

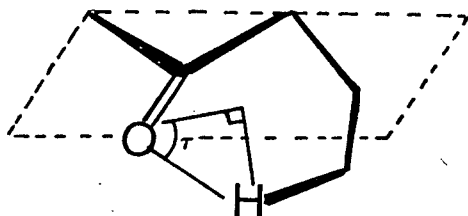
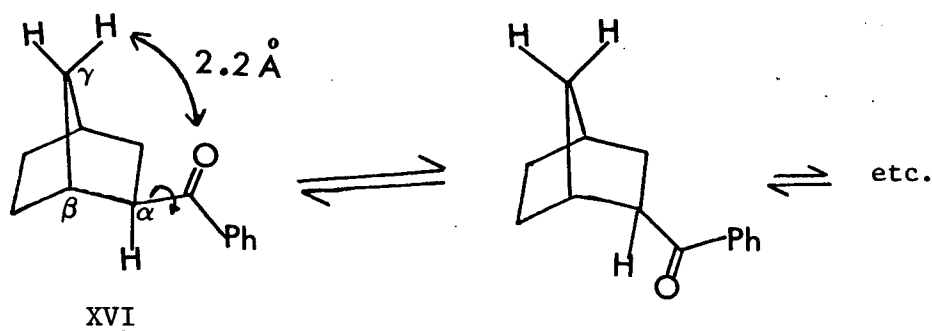


Figure 5. Operational Definition of the Angle τ .

the Norrish Type II reaction is analogous to the McLafferty rearrangement, one would not expect it to have the same geometric requirements as the McLafferty rearrangement because, unlike the latter, the Type II reaction occurs from electronically-excited states and the geometry of this state need not be the same as those of ground state or vibrationally-excited molecules.

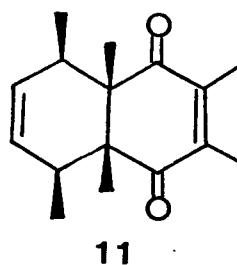
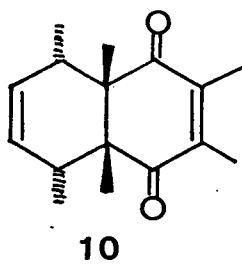
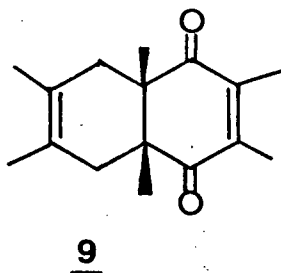
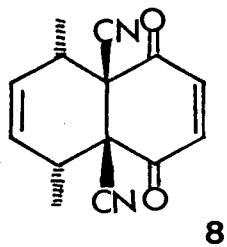
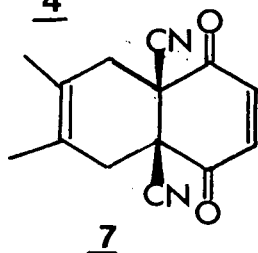
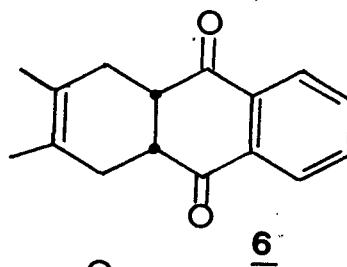
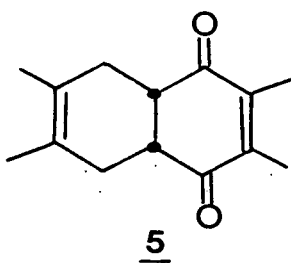
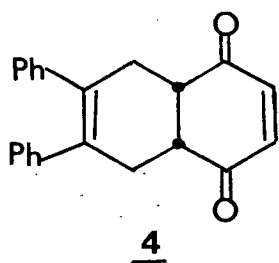
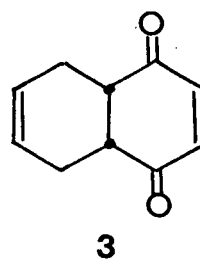
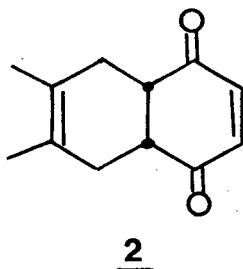
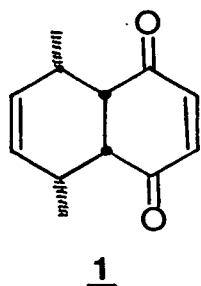
Not surprisingly, Lewis and coworkers⁴⁴ found that compound XVI, in which the geometry of closest approach of the γ -hydrogen to the oxygen does not allow these two atoms to come any closer than 2.2\AA (as measured by Dreiding models), still undergoes the Norrish Type II



reaction. Over what distances can these hydrogen abstractions occur then? In photochemical hydrogen abstraction, is the hydrogen required to lie in the plane of the carbonyl group as earlier proposed⁴³? As mentioned earlier, most compounds which are conformationally mobile in fluid media, crystallize out in just one conformation which can be accurately determined by X-ray diffraction methods. Also obtainable from the X-ray data are useful parameters such as bond distances, angles and intermolecular distances. So, the initial geometry of a starting material can be accurately determined provided it is crystalline. Furthermore, due to the restrictions of atomic and molecular movements imposed by the crystal lattice, most solid reactions are topochemically controlled^{12,45} i.e. they occur with minimum atomic and molecular movement. This means that a substrate, S, will react within the crystal lattice without gross changes in conformation. It also means that an

intermediate such as the one postulated in the photochemical hydrogen abstraction reactions of tetrahydro-1,4-naphthoquinones would, most likely, have the same conformation as the substrate and close to product(s) from that conformation.

Thus, the study of these reactions in the solid state, when used in conjunction with the X-ray structural data, promises to shed light on the geometric requirements for these reactions. To do this, eleven compounds were chosen for study. Their structures are shown below.



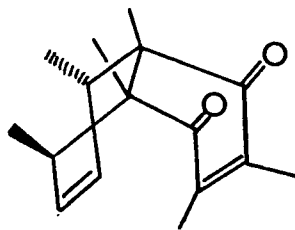
These substrates, taken as a whole, exhibited β , γ , γ^c , oxetane, and cage compound formation reactions in solution²⁴ as the table below shows.

Table III

Substrate	Reaction Type Observed in Solution				
	β	γ	γ^c	Oxetane	Cage Compound
<u>1</u>	Yes	No	No	No	No
<u>2</u>	Yes	No	No	No	No
<u>3</u>	No	Yes	No	No	No
<u>4</u>	-	-	-	-	-
<u>5</u>	Yes	No	No	No	No
<u>6</u>	Yes	No	No	No	No
<u>7</u>	Yes	No	No	No	No
<u>8</u>	No	No	No	Yes	No
<u>9</u>	Yes	No	Yes	No	No
<u>10</u>	No	No	No	Yes	Yes
<u>11</u>	Yes	No	Yes	No	No

Although compounds 8 and 10 do not undergo hydrogen abstraction reactions, it was of interest to find out if their cycloaddition reactions also occur from the same conformation as the hydrogen abstraction reactions of the other compounds. In particular, it has been suggested^{24c} that cage compound formation might be occurring from the same conformation as the hydrogen abstraction

reactions, since an alternative conformation such as C which brings the two π -systems closer together is disfavored by bridgehead methyl eclipsing.



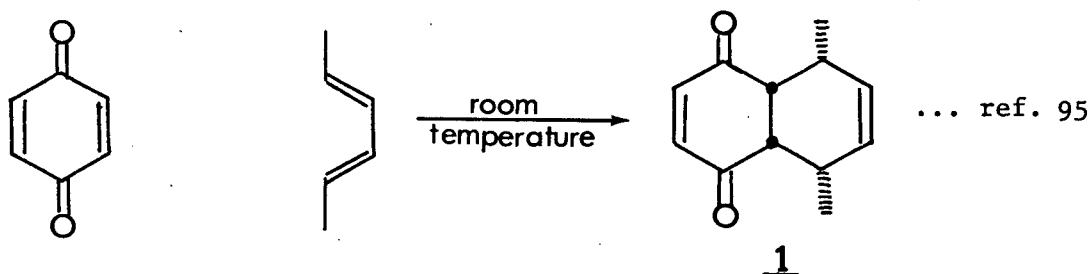
C

Results and Discussion

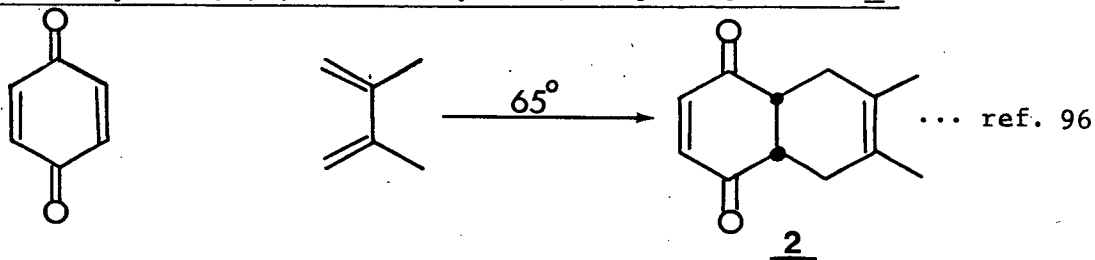
Preparation of Substrates

Without exception all of the substrates investigated were made by the Diels-Alder addition of a quinone to a diene. Most of the quinones and dienes used were readily available from commercial sources. Below is a summary of the synthetic schemes used to obtain substrates 1-11.

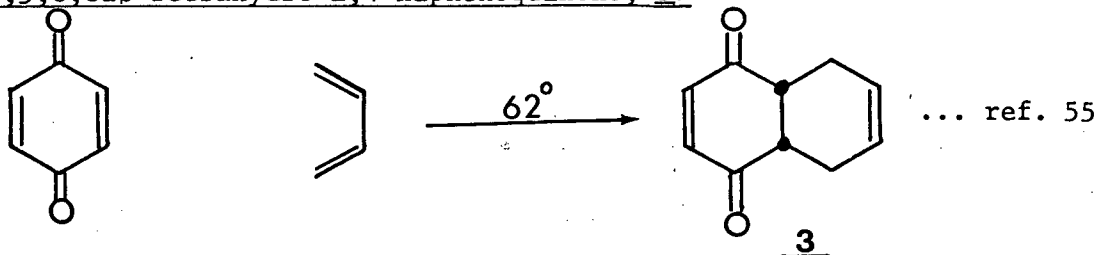
5 β ,8 β -Dimethyl-4a β ,5,8,8a β -tetrahydro-1,4-naphthoquinone, 1.



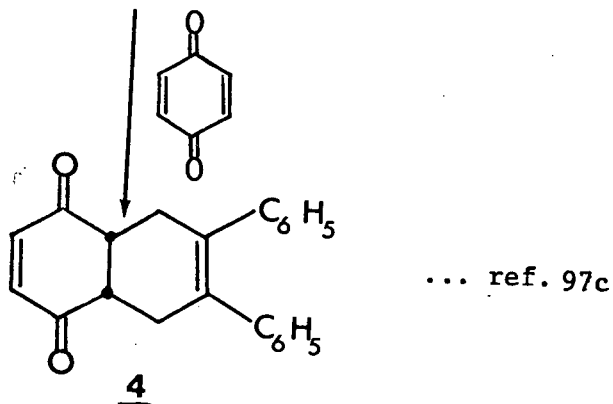
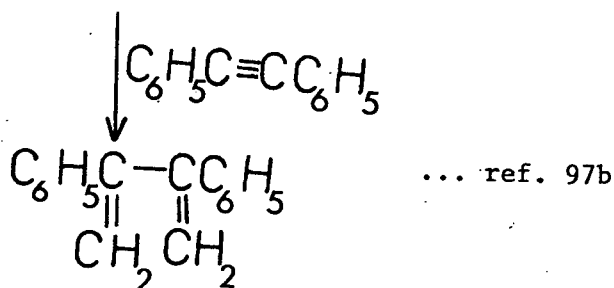
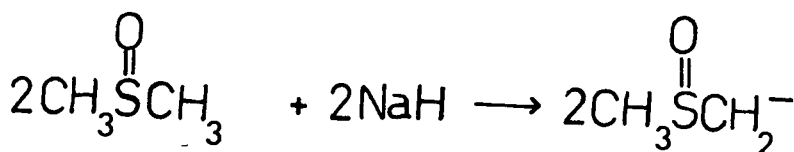
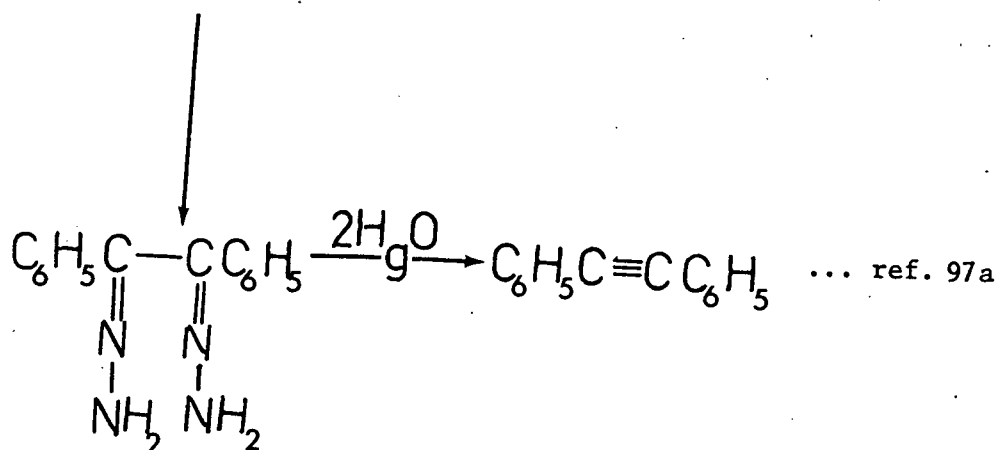
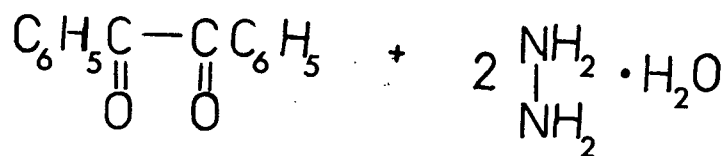
6,7-Dimethyl-4a β ,5,8,8a β -tetrahydro-1,4-naphthoquinone, 2.



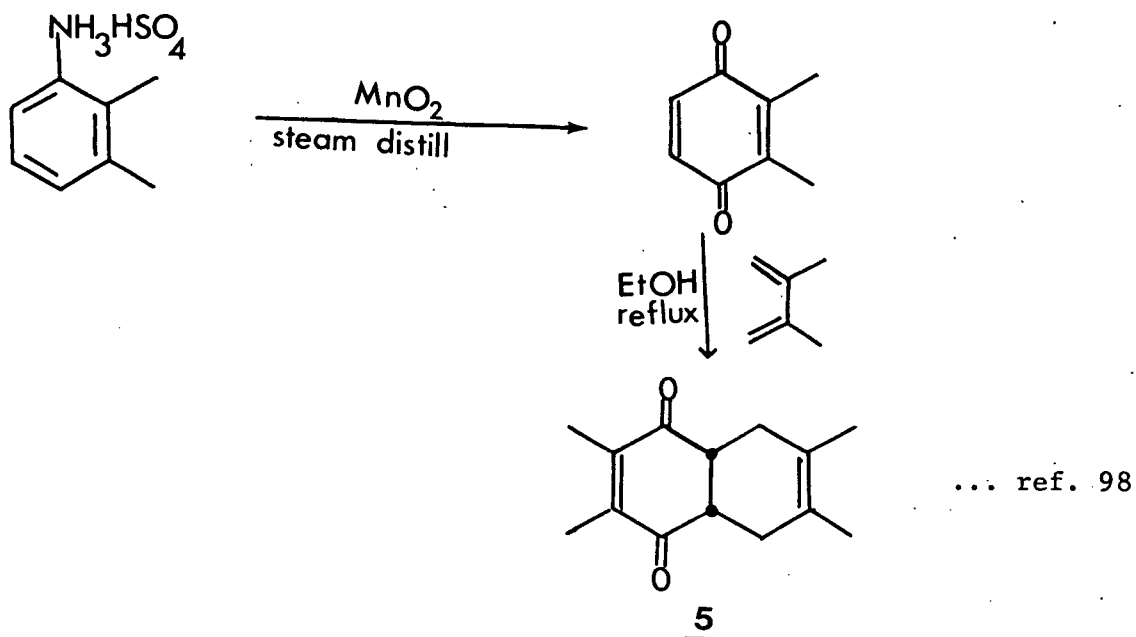
4a β ,5,8,8a β -Tetrahydro-1,4-naphthoquinone, 3.



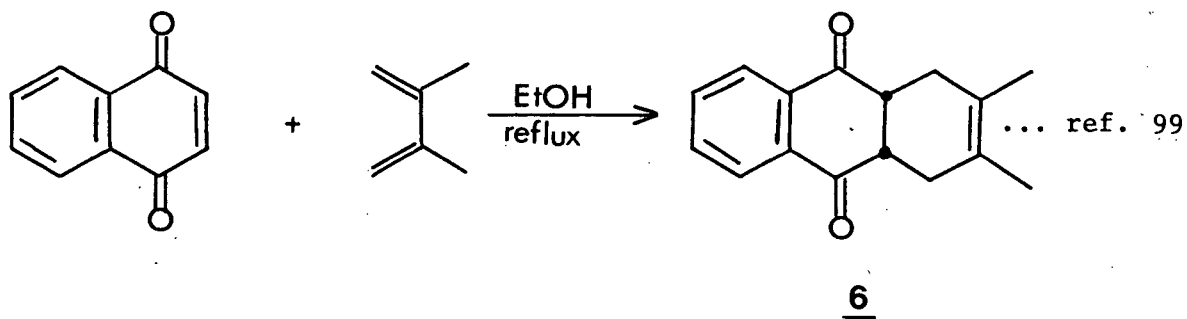
6,7-Diphenyl-4a β ,5,8,8a β -tetrahydro-1,4-naphthoquinone, 4.



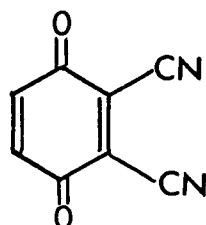
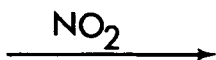
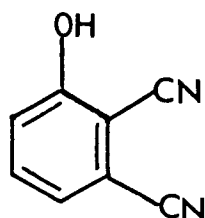
2,3,6,7-Tetramethyl-4a β -5,8,8a β -tetrahydro-1,4-naphthoquinone, 5.



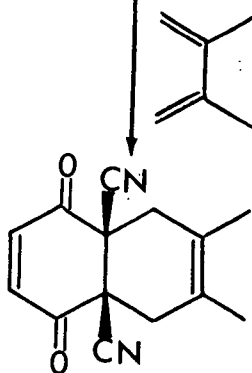
2,3-Dimethyl-1,4,4a β ,9a β -tetrahydro-9,10-anthraquinone, 6.



4 α ,8 α -Dicyano-6,7-dimethyl-4 α ,5,8,8 α -tetrahydro-1,4-naphthoquinone, 7.



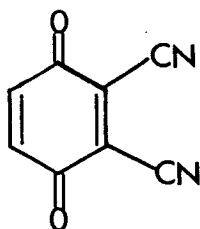
... ref. 100



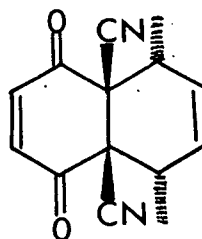
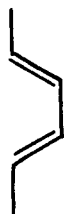
... ref. 101

7

4 α ,8 α -Dicyano-5 α ,8 α -dimethyl-4 α ,5,8,8 α -tetrahydro-1,4-naphthoquinone, 8



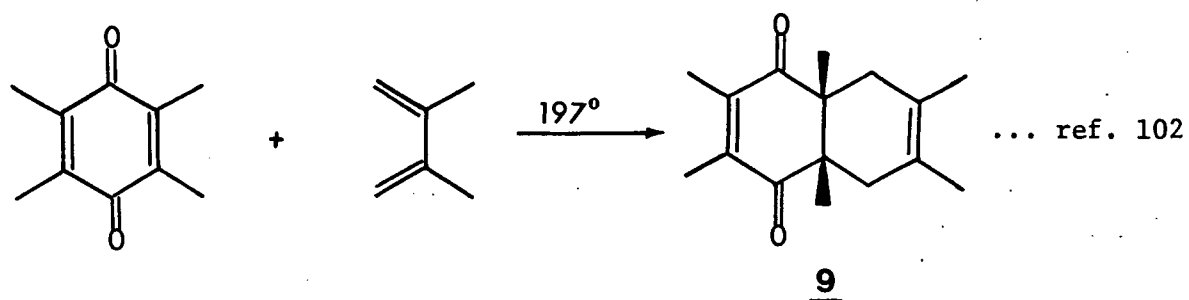
+



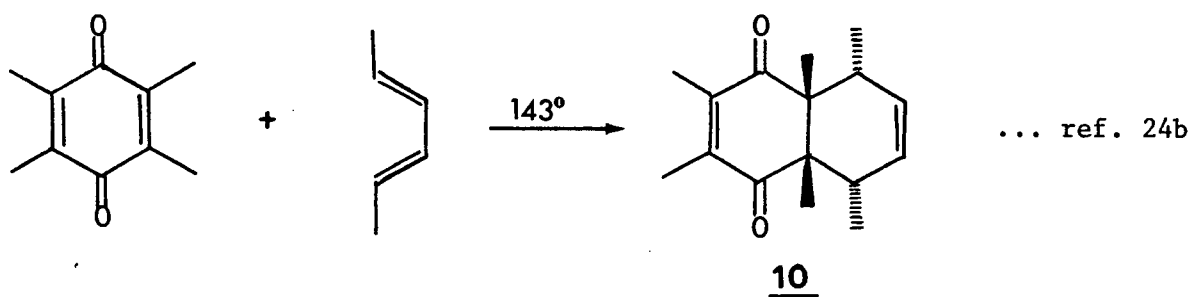
... ref. 24b

8

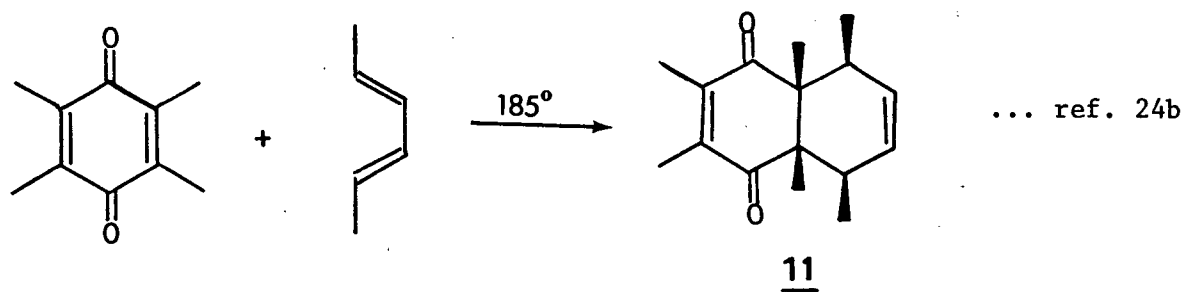
2,3,4a β ,6,7,8a β -Hexamethyl-4a β ,5,8,8a β -tetrahydro-1,4-naphthoquinone, 9.



2,3,4a β ,5 α ,8 α ,8a β -Hexamethyl-4a β ,5,8,8a β -tetrahydro-1,4-naphthoquinone, 10



2,3,4a β ,5 β ,8 β ,8a β -Hexamethyl-4a β ,5,8,8a β -tetrahydro-1,4-naphthoquinone, 11



All substrates were meticulously purified by two or more recrystallizations before use. The melting points and spectral data of all were in good agreement with the literature values. The NMR spectra of these compounds and of the products obtained by irradiating them in the solid state are given in the Appendix.

Unless otherwise stated, the apparatus for the solid state reactions was a specially designed photochemical reactor which allowed for evacuation of the reaction chamber to ≤ 0.05 torr. Reaction temperatures were chosen so as to be below the eutectic temperature of the reaction mixture comprising product(s) and starting material. The eutectic temperature was determined by differential scanning calorimetry using varying compositions of crude reaction mixture and starting material. One such scan is shown in Figure 6.

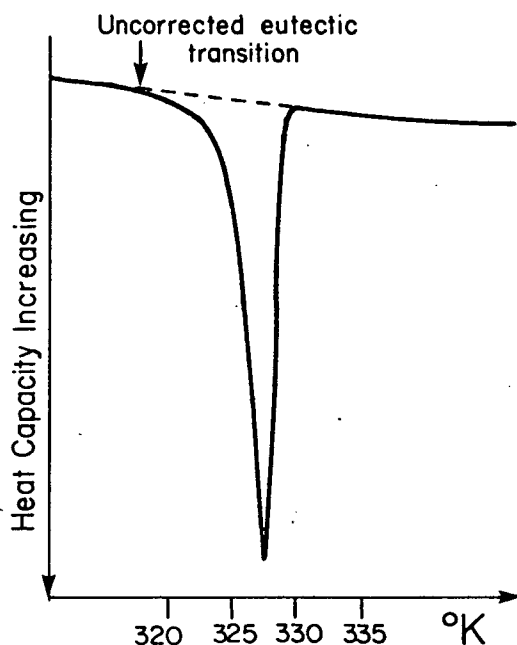
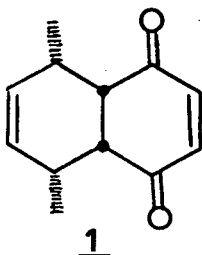


Figure 6. Uncorrected Endothermic Transition for 1 + 1A Eutectic Mixture.

Reaction temperatures were maintained within $\leq \pm 5^\circ$ by a circulating coolant from an Ultra Kryomat. The temperature at the reaction site was monitored by a copper-constantine thermocouple and read on a digital millivoltmeter. Details on the apparatus and method of use are given in the Experimental section.

1. Intermolecular [π 2 + π 2] Dimerization

5 α ,8 α -Dimethyl-4 α β ,5,8,8 α β -tetrahydro-1,4-naphthoquinone, 1



Large yellow crystals of 1 were obtained by crystallization from a solvent mixture comprising petroleum ether and diethyl ether. A large, well-formed crystal of 1 measuring 0.40 x 0.70 x 1.0 mm was used for X-ray data collection.

The X-ray structure determinations of this and other compounds discussed in this manuscript were carried out by Dr. James Trotter and Dr. Simon E.V. Phillips of this department and have been published as a series of papers in *Acta Crystallographica B*. Reference for the individual structures are given with the crystal data.

Unit cell and intensity data on 1 were measured using a Datex automated G.E. XRD 6 diffractometer with Cu K α radiation and the θ - 2θ scan technique. Accurate unit cell constants were obtained by a least-squares refinement method using 2 θ values of 18 manually centred reflections. The structure was solved by direct methods⁴⁶ using intensity data from 1557 independent reflections and refined by the full-matrix least-squares procedure to an R value of 0.048.

Crystal Data^{47a}

$C_{12}H_{14}O_2$, monoclinic, space group $P2_1/c$ with $a=7.189(1)$, $b=22.241(4)$, $c=6.843(1)$ Å, $\beta=106.51^\circ$ and $Z=4$. The molecules occur in pairs related by centres of symmetry, X (Figure 7).

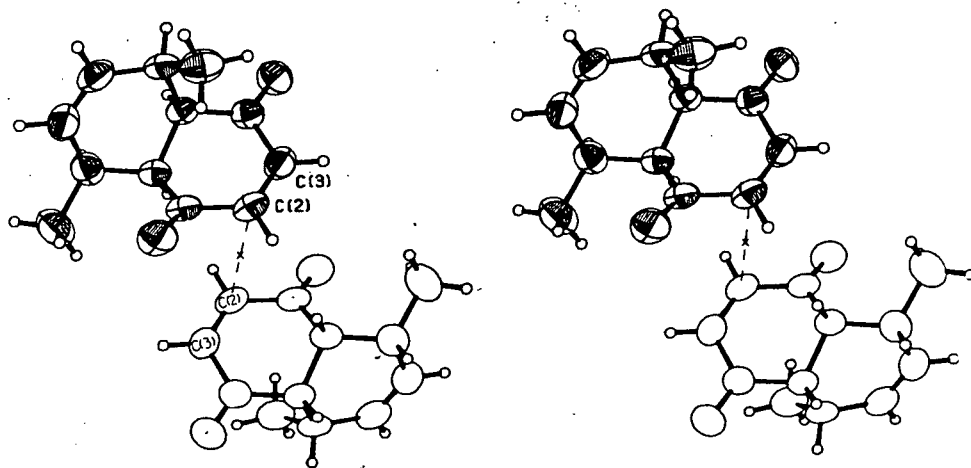
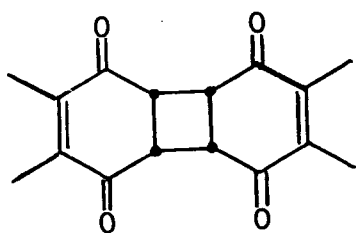


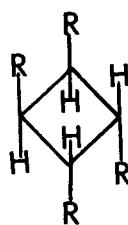
Figure 7. Stereo diagram of an adjacent pair of molecules of 5α,8α-dimethyl-4aβ,5,8,8aβ-tetrahydro-1,4-naphthoquinone, 1, with 50% probability vibration ellipsoids for non-hydrogen atoms. The centre of symmetry is indicated by X. Ellipsoids are shaded for one molecule and unshaded for its centre of symmetry related neighbour for clarity.

Irradiation of crystals of 1 in vacuo at temperatures below the eutectic temperature (52.5°) through a Corning glass filter transmitting $\lambda \geq 340$ nm gave only one product. The latter crystallized from a solvent mixture comprising chloroform and hexane as small, colorless, sparkling plates.

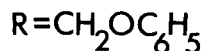
The product correctly analyzed for the dimer $C_{24}H_{28}O_4$. In the infrared, the crystallized and the crude product had identical spectra. Both had carbonyl absorptions at 5.82 and 5.90 μ . The nuclear magnetic resonance spectrum had a singlet at $\delta 3.47$ which was indicative of cyclobutane ring protons. For comparison, the cyclobutane ring protons of compounds XVII and XVIII have been reported at $\delta 3.90$ and $\delta 2.90$ respectively^{48,49}. The lack of coupling between the



XVII



XVIII



cyclobutane ring protons is due to the symmetry of the molecule.

In order to determine the stereochemistry of the dimer, one of the crystals measuring 0.40 x 0.25 x 0.10 mm was used for X-ray structure determination. Cell constants were determined and refined using 2 θ values from 17 reflections. Intensity data were collected as for the monomer from 1458 independent reflections. The R value

after refinements was 0.050.

Crystal Data^{47a}

$C_{24}H_{28}O_4$, monoclinic, space group $P2_1/c$ with $a=11.393(1)$, $b=8.029(1)$, $c=10.771(5)$ Å, $\beta=91.04(1)^\circ$ and $Z=2$. The molecule is centrosymmetric and has a planar four-membered ring (Figure 8).

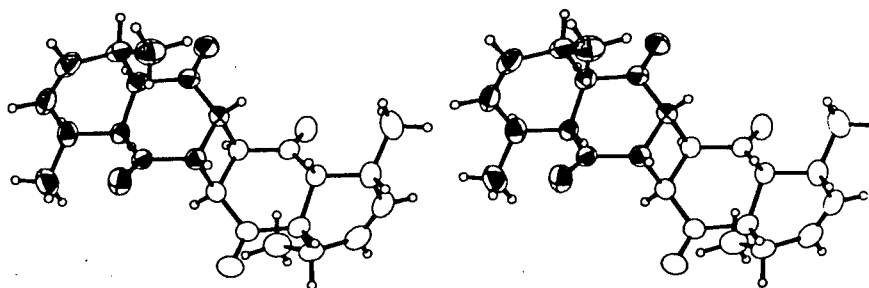
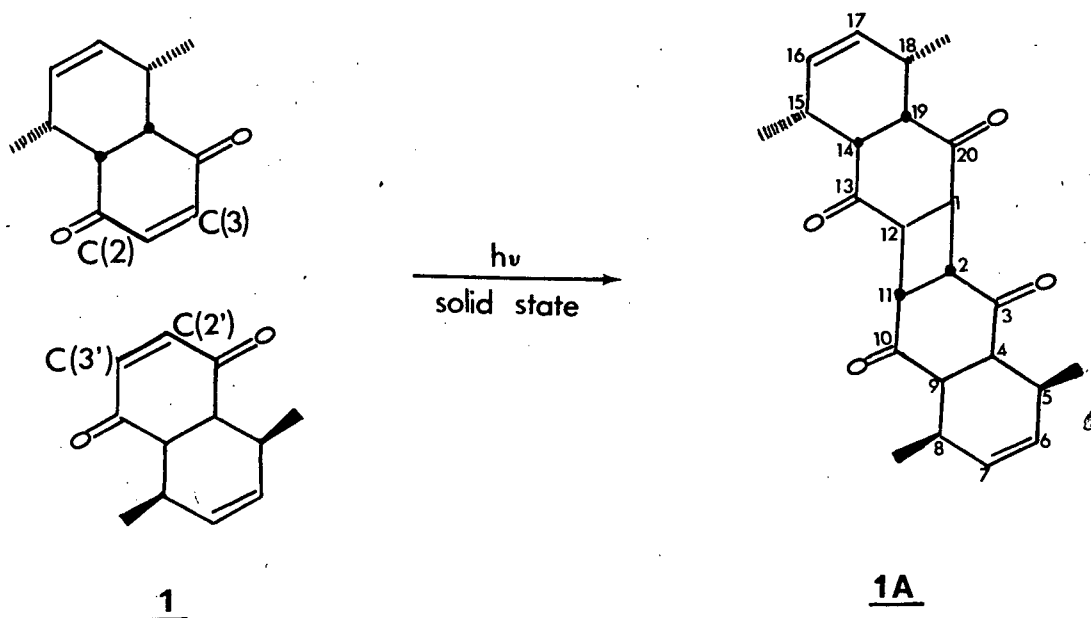


Figure 8. Stereo diagram of dimer 1A in an orientation analogous to that of the monomer 1.

The formation of 5,8,15,18-tetramethylpentacyclo-[10.8.0.0^{2,11}.0^{4,9}.0^{14,19}]eicosa-6,16-dien-3,10,13,20-tetrone, 1A, from the monomer 1 formally involves bond formation between carbons 3 and 2' and between carbons 2 and 3' of adjacent monomer pairs related by a centre of symmetry. The reaction is depicted diagrammatically below:



With the aid of a stereo viewer, it can be seen from the arrangement of monomer pairs (Figure 7) that the C3, C2 double bond of one partner is aligned parallel to the C2', C3' double bond of its adjacent partner. Such an arrangement coupled with a short centre-to-centre double bond contact of 4.040 Å between these two π systems allows for good overlap of the p orbitals. The separation, d, between the two double

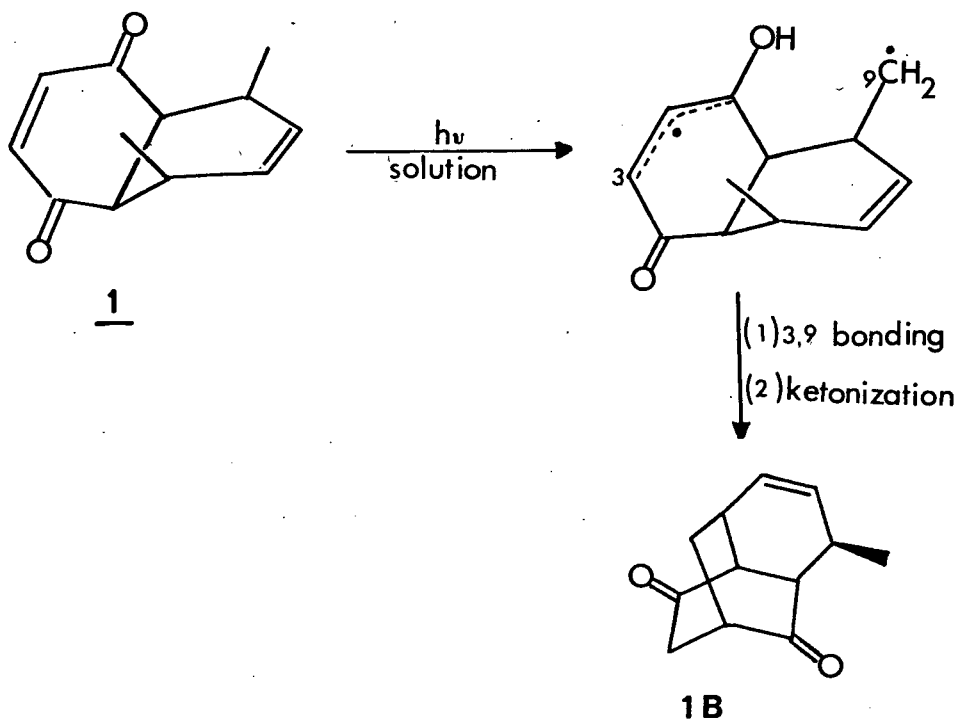
bonds is within the limit $4.2 > d > 3.5 \text{ \AA}$ established experimentally by Schmidt and coworkers^{12b,61} for photodimerizations in the solid state. As Table IV shows, the chemical yield for the 1 → 1A conversion was nearly quantitative both at low and high conversions of the monomer.

Table IV. Product Yields for the 1 → 1A Conversion

<u>Reaction Temperature</u>	<u>% Conversion</u>	<u>% Yield</u>
Room Temperature (uncontrolled)	17	91
-1.2° to -0.7°	37	87
-1.2° to -0.5°	56	94
-2.0° to -1.3°	79	96
-1.5° to -1.0°	79	96
-3.0° to -2.0°	100	89

In contrast to the above solid state dimerization, compound 1 undergoes intramolecular γ -hydrogen abstraction when irradiated in solution^{24a}. The product of this reaction, 1B, arises from the abstraction of one of the C9 hydrogens by O(1) followed by bonding between carbons 3 and 9 and subsequent ketonization. Although the nearness of one of the C(9) hydrogens to O(1) in the crystal ($H \cdots O$ distance = 2.38 \AA) makes the abstraction conceivable in the solid state, the subsequent collapse of the biradical intermediate to 1B is

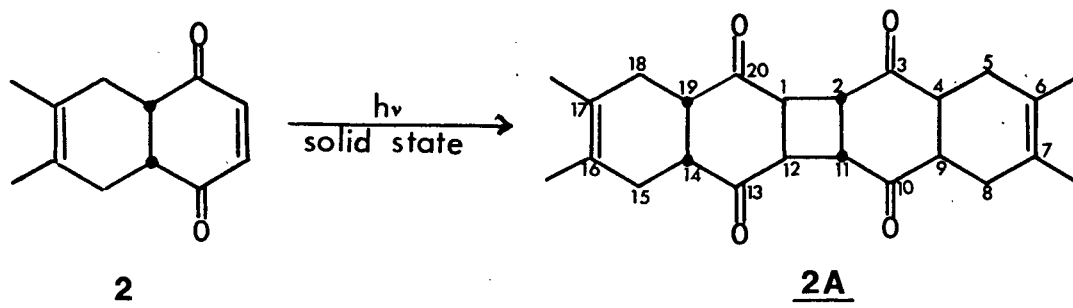
not likely to be permissible within the crystal lattice since C3 and C9 are quite remote from each other in the crystal of the substrate.



6,7-Dimethyl-4a β , 5,8,8a β - tetrahydro-1,4-naphthoquinone, 2

A second example of photodimerization in the solid state was provided when crystals of compound 2 were irradiated at long wavelength ($\lambda \geq 340$ nm) below the eutectic temperature (109.5°). The sole product of the reaction, 2A, crystallized from acetonitrile solution as colorless, sparkling plates. The infrared spectrum of these crystals was identical to that of the crude product.

Product 2A correctly analyzed for the dimer C₂₄H₂₈O₄. It had carbonyl absorption at 5.85 μ in the infrared. In the nuclear



magnetic resonance spectrum, there were no signals in the $\delta 6.0 - 7.0$ region indicating the absence of conjugated vinyl hydrogens. A singlet sited at $\delta 3.64$ was assigned to cyclobutane ring protons by analogy to previous cited examples. The positions of all other protons were comparable to the positions of the corresponding protons of monomer 2.

The ultimate proof of the assigned structure came from X-ray crystal structure determination. Data collection was carried out on a piece of crystal measuring $0.07 \times 0.25 \times 0.75$ mm which was cut from a larger crystal. Cell parameters were determined and refined from 10 reflections. The structure was solved as for compound 1 using intensity data of 1443 independent reflections. The final R value was 0.065.

Crystal Data^{47b}

$C_{24}H_{28}O_4$, monoclinic, space group $P2_1/c$ with $a=15.247(1)$, $b=6.2776(6)$, $c=10.1949(7)$ Å, $\beta=93.19(1)^\circ$ and $Z=2$.

As the stereo diagram of the dimer shows, Figure 9, this dimer like 1A has a planar cyclobutane ring and is centrosymmetric.

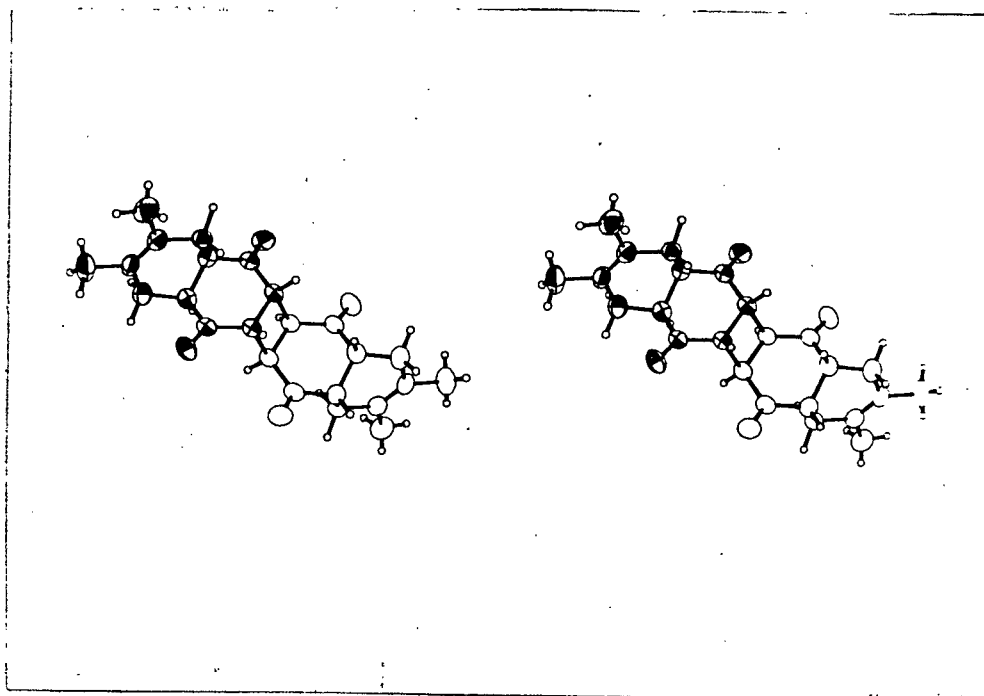


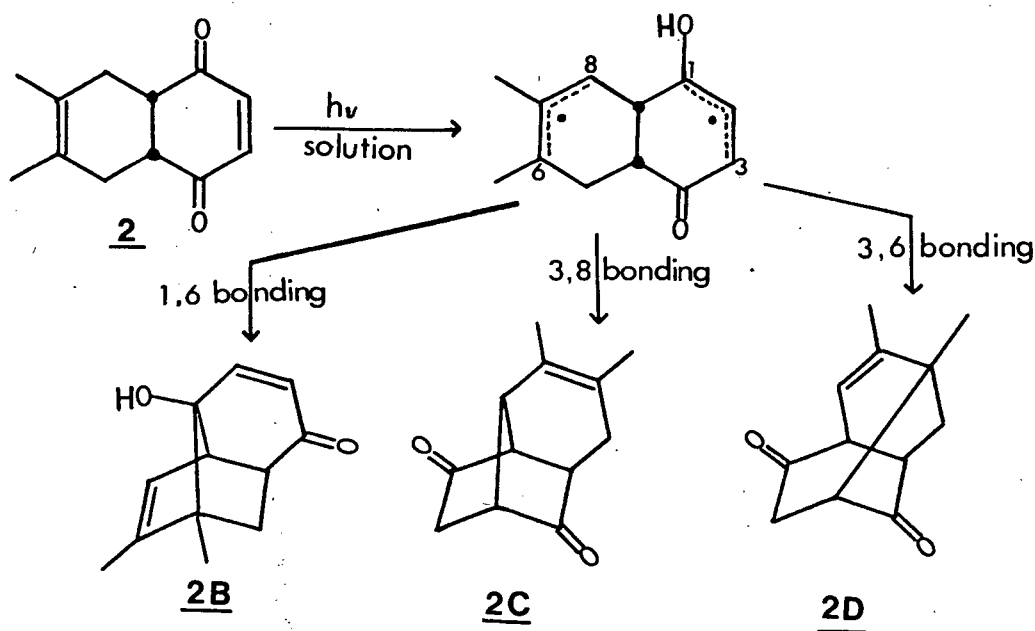
Figure 9. Stereo diagram of 2A. Non-hydrogen atoms are shaded for one of the monomer units of the union and open for the other for clarity.

As in the case of monomer 1, the 2 → 2A conversion is quantitative both at low and high conversions (Table V).

Table V. Product Yields for the 2 → 2A Conversion

<u>Reaction Temperature</u>	<u>% Conversion</u>	<u>% Yield</u>
Ambient	25	99
Ambient	40	97
Ambient	61	96

In contrast to its dimerization in the solid state, compound 2 undergoes intramolecular β -hydrogen abstraction to give photoproducts 2B, 2C and 2D in solution. The relative yields of these products were found to be solvent dependent^{24a}.



4a β , 5, 8, 8a β -Tetrahydro-1,4-naphthoquinone, 3

The parent compound of this series of tetrahydro-1,4-naphthoquinones, 3, provided a further example of photodimerization in the solid state.

Irradiation of crystals of 3 at long wavelength, $\lambda \geq 340$ nm, below the eutectic temperature (49.4°) afforded photodimer 3A in quantitative yield (Table VI).

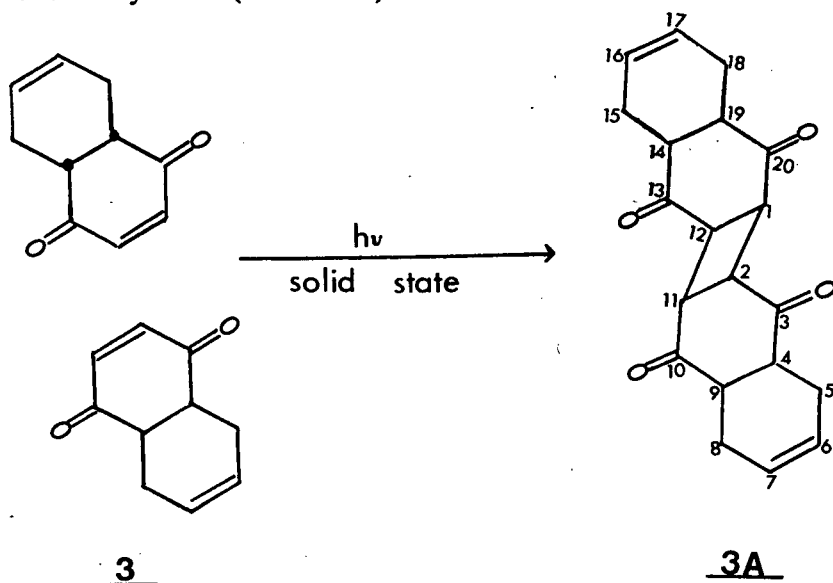


Table VI. Product Yields for the 3 \rightarrow 3A Conversion

<u>Reaction Temperature</u>	<u>% Conversion</u>	<u>% Yield</u>
Ambient	16	86
Ambient	19	80
Ambient	36	100
Ambient	77	75
0.0 - 4.3°	94	92

Dimer 3A crystallized from chloroform solution as colorless flakes, the infrared spectrum of which was identical to that of the crude product and also to that of a photolyzed KBr pellet containing 3. It correctly analyzed for the dimer $C_{20}H_{20}O_4$.

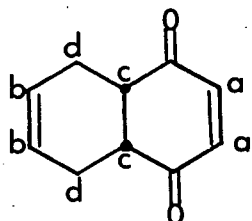
Since the crystals obtained from chloroform were unsuitable for X-ray structure determination, the dimeric structure 3A was deduced from spectroscopic data.

In the infrared, cyclobutane ring vibrations are not as well defined as are those of cyclopropanes⁵⁰. Derfer and coworkers⁵¹ reported that seven substituted cyclobutanes which they investigated absorbed in the $920-910\text{ cm}^{-1}$ region. Reid and Sack⁵² followed up with a report that when all the cyclobutane ring carbons are substituted, the absorptions are shifted to the $888-868\text{ cm}^{-1}$ region. More recently, Dekker and coworkers⁵³ reported absorptions in the $1000-850\text{ cm}^{-1}$ region which they attributed to the cyclobutane ring vibrations in the $920-850\text{ cm}^{-1}$ region which may be taken as indicative of the presence of a four-membered ring. The carbonyl chromophore absorbed at 5.85μ .

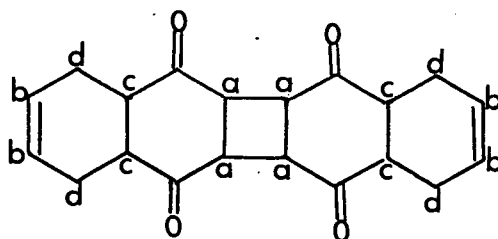
In the Raman, cyclobutanes are reported⁵⁰ to have a characteristic C-C stretch at 933 cm^{-1} . Dimer 3A had an absorption at 935 cm^{-1} in the Raman.

The nuclear magnetic resonance spectrum was informative. A singlet at $\delta 3.64$ was assigned to the cyclobutane ring protons. This is in good agreement with δ values of 3.47 and 3.64 for the cyclobutane protons of 1A and 2A respectively. The other assignments

which are given below compare well with the absorptions of corresponding protons in the monomer.



3



3A

Proton type	Absorptions	
	Monomer <u>3</u>	Dimer <u>3A</u>
	δ	
a	6.57(s)	3.64(s)
b	5.63(m)	5.70(m)
c	3.15(m)	3.20(m)
d	2.28(m)	2.30(m)

All the spectroscopic data summarised above and the elemental analysis led to the identification of the dimer as pentacyclo[10.8.0.0^{2,11}.0^{4,9}.0^{14,19}]eicosa-6,16-dien-3,10,13,20-tetrone, 3A of as yet unassigned stereochemistry.

In attempts to obtain crystals of 3A which are suitable for X-ray structure determination, 3A was crystallized from a number of solvents including glacial acetic acid and acetonitrile.

The infrared spectrum of crystals obtained from glacial acetic acid was identical to that obtained by crystallizing from

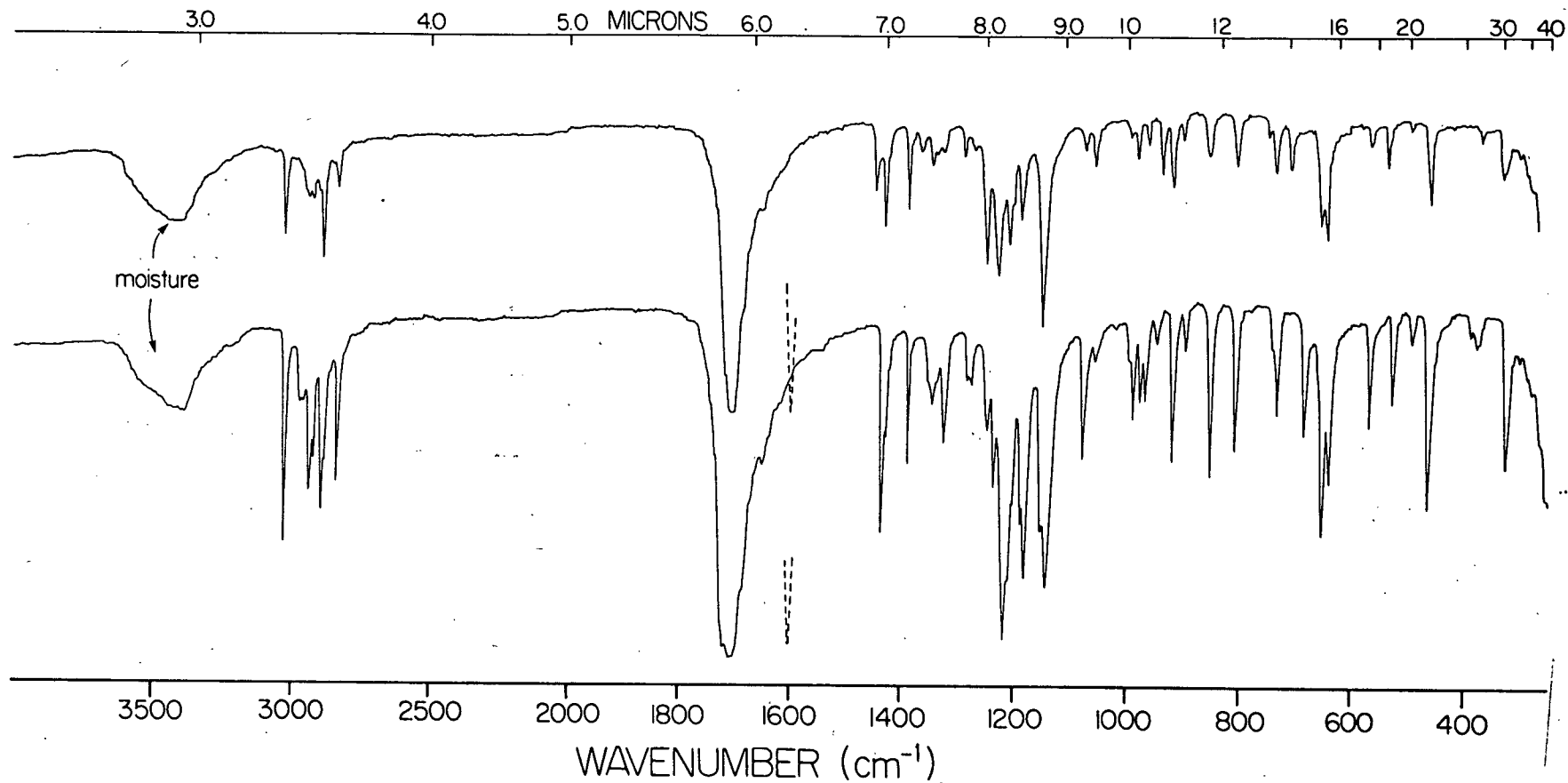


Figure 10. Infrared spectra of KBr pellets containing 4-5% by weight of Dimer 3A (Top) and Dimer 3B (Bottom). Ordinates have been shifted for clarity.

acetonitrile. These crystals are judged to be identical and will be subsequently referred to as 3B. As Figure 10 shows the infrared spectrum of 3B greatly resembles that of the initial dimer 3A. Nevertheless, the two spectra are not identical.

The absorption spectra of 3A and 3B crystals in the Raman were also different. The characteristic cyclobutane C-C stretch in 3B was at 931 cm^{-1} .

The nuclear magnetic resonance spectrum of 3B was however, identical to that of 3A. The 3B crystals correctly analyzed for the dimer $\text{C}_{20}\text{H}_{20}\text{O}_4$.

One of the 3B crystals obtained as colorless, sparkling little rods and measuring $0.50 \times 0.30 \times 0.30\text{ mm}$ was used for X-ray structure determination. Accurate cell constants were obtained from 2 θ values of 15 manually centred reflections and refined by the least-squares refinement method. Intensity data from 1488 independent reflections were collected and treated as described^{47b}. The R value after refinements was 0.037.

Crystal Data^{47b}

$\text{C}_{20}\text{H}_{20}\text{O}_4$, monoclinic, space group $\text{P2}_1/\text{c}$ with $a=11.7302(5)$, $b=6.4142(2)$, $c=10.9331(5)\text{ \AA}$, $\beta=114.624(3)^\circ$ and $Z=2$. Figure 11 is a stereo diagram of dimer 3B.

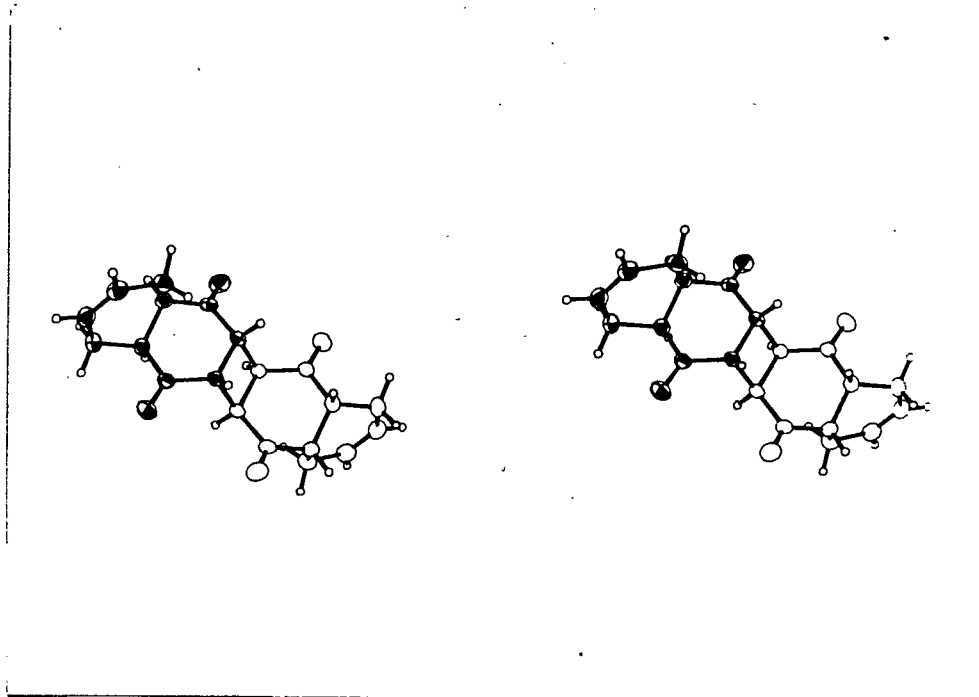
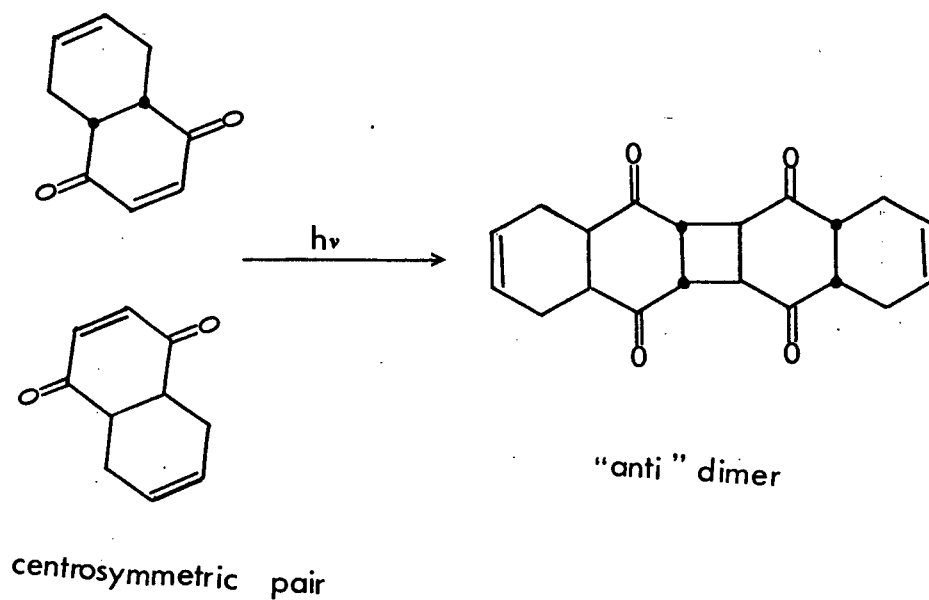
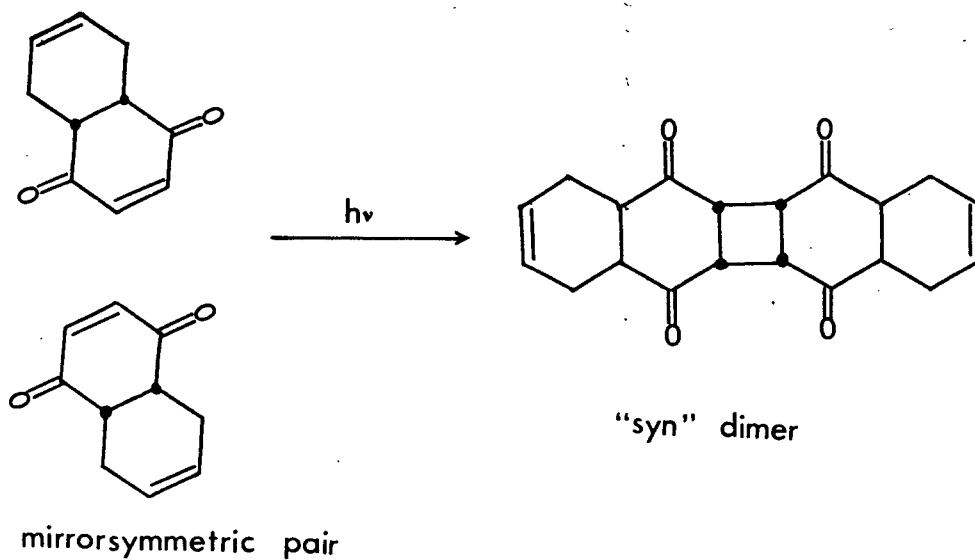


Figure 11. Stereo diagram of the 3B molecule. Non-hydrogen atoms are shaded for one of the monomer units and open for the other monomer unit for clarity.

The vital question is whether or not the centrosymmetric dimer 3B is the original product of the photodimerization of crystals of 3. Because of reports^{53,54} of syn→anti isomerizations of cyclobutanes and other small rings by acidic reagents such as sulfuric and phosphoric acids, it was suspected, at first, that 3A and 3B might be stereoisomers.

If one allows that no isomerization about the decalin ring junction occurs during the dimerization, then the number of

possible stereoisomers of the dimer is only two - one of these, the "syn" isomer, arises when monomer pairs are oriented in a mirror-symmetric fashion and the other, the "anti" isomer arises from a



centrosymmetric pair of monomer units. The assumption made above is justified by the previously described dimerizations (1 → 1A and 2 → 2A) in which configurations about the decalin bridgeheads are maintained during the reaction and also because such isomerizations proceed via the enolate ions and require basic catalysts⁵⁵.

Since 3B crystals have been shown by the X-ray structure to be the "anti" isomer, attempts were made to establish whether or not the original dimer 3A was the "syn" isomer. The method of choice was the joint use of infrared and Raman spectroscopy as described by Ziffer and Levin⁵⁶ for use in differentiating dimers having centres of symmetry, C_i , from their non-centrosymmetric isomers.

In this scheme, for a given sample, absorptions in the Raman and infrared which occur at the same frequency, $\pm 5 \text{ cm}^{-1}$, are termed coincidences. For a molecule possessing a C_i symmetry element, the infrared and Raman absorptions are mutually exclusive i.e. a vibration which is infrared active is Raman inactive and vice-versa. So, for a C_i and a non- C_i isomeric pair, there will be, in general, more coincidences for the non- C_i member than for the centrosymmetric isomer. For example, Ziffer and Levin⁵⁶ found that the head-to-head dimer of cyclopentenone which lacks a centre of symmetry had 84% of its Raman lines coinciding within $\pm 5 \text{ cm}^{-1}$ with its infrared lines while the centrosymmetric head-to-tail dimer had only 25%. As molecular size increases, however, the number of "accidental" coincidences also increases so that the differentiation by this method

becomes less clear-cut. For example, the non- C_1 and C_1 isomers of the dimer of 1-indenone had 67% and 38%, respectively, of their Raman lines coinciding with their infrared lines. Although, the 29% difference here is not as startling as in the previous example, it was thought sufficient for a preliminary differentiation if indeed 3A and 3B are mirrorsymmetric and centrosymmetric, respectively. Dimer 3A had, by this analysis, 45% of its Raman lines coinciding with its infrared lines while the centrosymmetric dimer 3B had 39%. The 6% difference here is really too small to ascribe to mirror-symmetric, centrosymmetric configurational isomers. On the other hand, if one assumes that dimer 3A is also centrosymmetric, then one is left to explain the differences in the infrared spectra of 3A and 3B.

Given the supposition that 3A and 3B are identical, the differences between the two infrared spectra can be due to contamination of the two samples by different impurities and/or different intermolecular coupling effects⁵⁷. The first of these possibilities is unlikely since different batches of crystals obtained from the same solvent from different sources had identical spectra. Furthermore, the infrared spectra of these crystallizing solvents revealed that the crystals were not contaminated by any of them. This leaves one with the likelihood that the infrared spectral differences merely reflect different orientations of the individual molecules within the crystal. There is ample documentation of these crystal packing

effects in the infrared absorption spectra of solids⁵⁷. To prove that the absorption differences are due to intermolecular effects, one would normally need to record the infrared spectrum of a solution or melt where such effects are absent or less pronounced. Unfortunately, the insolubility of 3A and 3B crystals in addition to their thermal instabilities near their melting points led to the failure of these methods. Nevertheless, examples of pronounced intermolecular effects in solid state infrared absorptions make the supposition of 3A being identical to 3B a tenable one. For example, the spectra of gaseous and solid benzene (Figure 12) taken from reference 57 illustrate the sort of differences which can arise from intermolecular interactions. The gaseous state represents the "free"

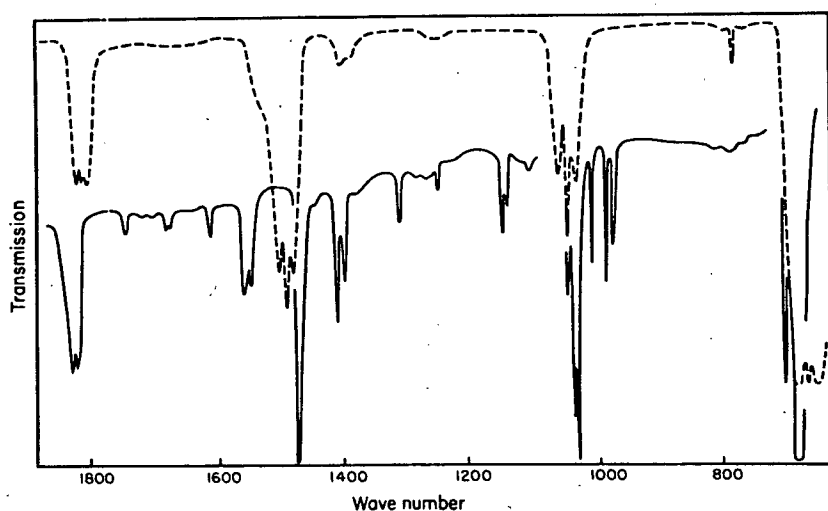


Figure 12. Part of the absorption spectrum of benzene: --- is gas and — is solid. Ordinates are shifted for clarity.

state in which the observed absorptions are purely those of the isolated molecule. For the crystal, there are absorptions arising from coupling between the vibrations of adjacent molecules in addition to those due to intramolecular vibrations. The intermolecular component of the absorption spectrum depends on the relative orientations of molecules within the crystal and hence, such factors as degree of crystallinity will affect the spectrum. This is manifest in the infrared spectra of polymer samples in which differing degrees of crystallinity can be achieved by crystallization. The effects of crystallization on the spectra of such samples have been reported^{57,58}. Dows and others^{59,60} report other incidences of differing infrared absorptions in the solid state which illustrate intermolecular coupling effects. In one of such examples, Dows and coworkers⁵⁹ report that ammonium azide solid obtained by sublimation represents a disordered crystal which becomes ordered on warming. The infrared spectra of the disordered and ordered crystals were similar but different.

Crystals of 3A and 3B may, therefore, represent different crystal modifications of the same compound and the differences in the infrared spectra of these two crystals dispersed in KBr matrices may merely be due to different intermolecular interactions within each of these two crystals. Owing to the negligible solubility of the dimer in chloroform, it is likely that the crystals formed from it form quickly and are disordered. This is especially true since

the infrared spectrum of these crystals is identical to that of the crude product and there are indications from the packing diagram of the monomer (below) that the dimer molecules as they first form are at best only semi-oriented.

The monomer, 3, crystallized from a solvent mixture of petroleum ether and diethyl ether as well-formed, yellow needles. Owing to the instability of the crystal in the X-ray beam, the collection of data for the structure determination required two pieces of crystal measuring 0.80 x 0.30 x 0.20 mm each which had been cut from larger crystals. The X-ray data^{47c} were obtained and treated as in previous cases. Accurate unit cell constants were obtained by least-squares refinement of 2 θ values of 16 manually centered reflections. The intensity data were obtained from 2496 independent reflections and refined by the full-matrix least-squares procedure. The final R value was 0.060.

Crystal Data^{47c}

$C_{20}H_{20}O_2$, monoclinic, space group $P2_1/c$ with $a=5.266(1)$, $b=24.267(5)$, $c=14.506(4)$ Å, $\beta=114.50(2)^\circ$ and $Z=8$.

The packing diagram of monomer 3 (Figure 13) revealed two crystallographically independent types of molecules in the unit cell. These have been labelled A and B, respectively, in Figure 13. As can be seen from this diagram, layers of the A type alternate with those of the B type. Molecules of the A type form an axial repeat

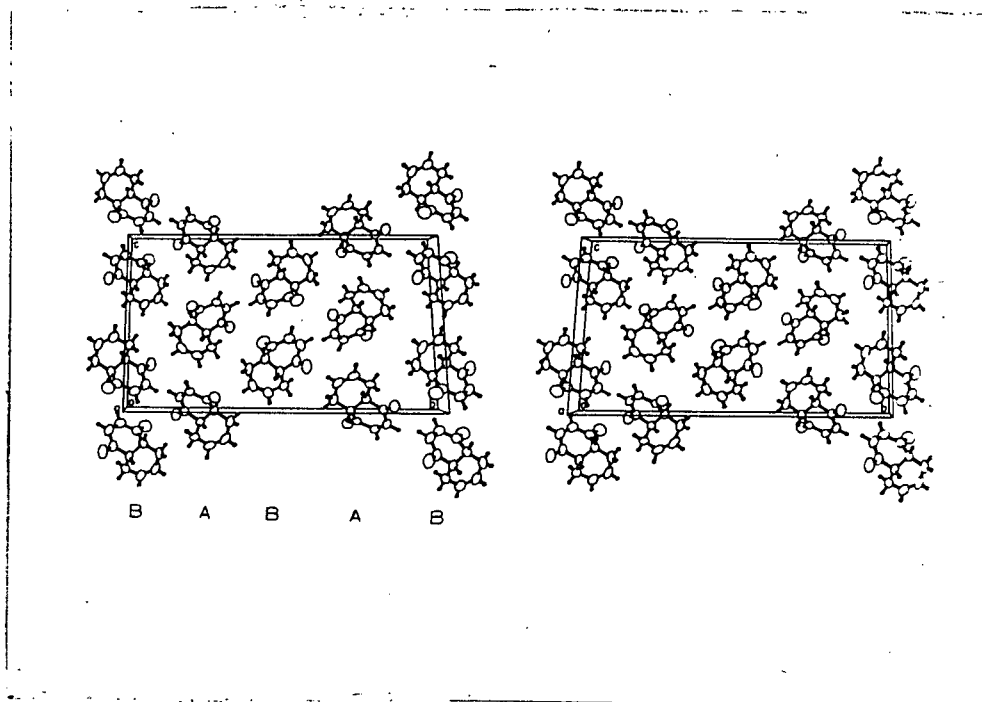


Figure 13. Stereo diagram of the contents of the unit cell for compound 3.

pattern, i.e., each molecule is related to its nearest neighbour by a cell translation of 5.266 \AA . This latter distance, therefore, also measures the intermolecular distance between the mid-points of the C2, C3 and C2', C3' double bonds. Furthermore, as can be seen from the stereo diagram of adjacent molecules of the A type (Figure 14), there is no overlap of these two π systems. On the other hand, molecules of the B type occur in pairs related by a centre of symmetry denoted by X in Figure 15. In this arrangement, the C3, C2 and C2', C3' double bonds of adjacent molecules are parallel but offset with the C2 of one molecule directly above the C2' of the other. The C2 to C2' contact is the shortest intermolecular distance and measures 3.351 \AA . The centre-to-centre separation of the

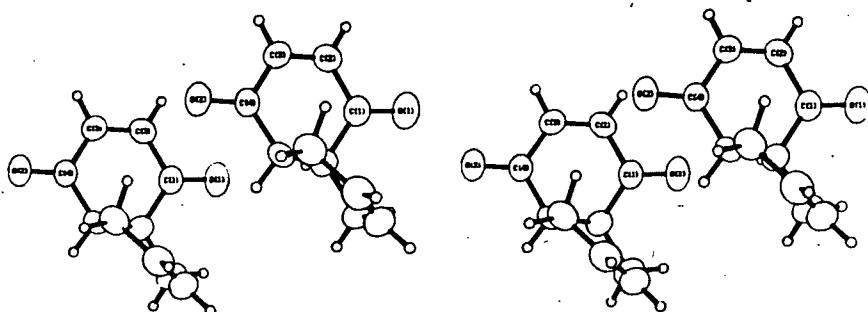


Figure 14. Stereo diagram of molecule type A and its nearest neighbour related by a simple cell translation.

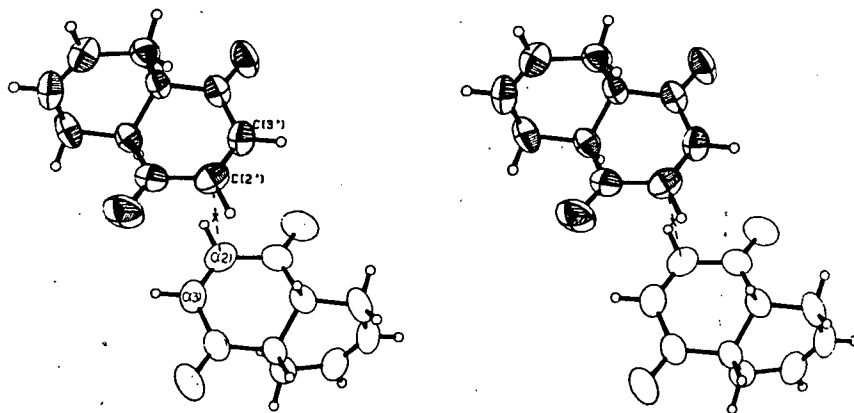


Figure 15. Stereo diagram of a type B molecule (shaded ellipsoids) and its nearest neighbour (unshaded ellipsoids) related by a centre of symmetry, X.

two double bonds is 3.755 \AA in this case. This is also the separation between C2 and C3' and between C3 and C2'. With the aid of a stereo viewer, the overlap of the two double bonds can be appreciated. The arrangement of molecules of the B type are analogous to that found in crystals of monomer 1 which as previously shown, dimerized to the centrosymmetric dimer 1A.

By analogy to the 1 \rightarrow 1A conversion, the centrosymmetric dimer 3B results from a topochemically controlled dimerization in the B stack with C2, C3 of one monomer linking up with C3', C2', respectively of its nearest neighbour (Figure 15). The centre-to-centre separation, d , of the two double bonds involved in this dimerization is 3.755 \AA which is shorter than the corresponding separation in monomer 1 crystals and should make dimerization in this stack relatively more facile. Also this distance, $d=3.755 \text{ \AA}$, falls within the range $4.2 > d > 3.5 \text{ \AA}$ experimentally established for similar photodimerizations in the solid state^{12b,61}.

On the basis of the large separation of 5.266 \AA between the two double bonds of adjacent pairs of molecules of the A type, no dimerization is expected to occur in this stack. However, as shown by monomer conversions in excess of 50% (Table VI) this is not the case. Dimerization, most likely, originates in the B stack giving rise to centrosymmetric dimers intercalated into the lattice of the monomer. The boundaries between the reacted and unreacted regions of the crystal are akin to dislocation sites since molecules

here may have different orientations from those located elsewhere in the crystal lattice. These boundaries may be sites for further reaction in the crystal. The lack of formation of the mirror-symmetric ("syn") dimer when molecules in the A stack eventually react may merely reflect an energetically unfavorable process of forming a sterically crowded dimer.

As mentioned earlier in the Introduction, Cookson and coworkers²³ reported the formation of a dimer of 3 of unknown stereochemistry during their photolysis of 3. They reported that facile internal oxidation-reduction occurred when they tried to dehydrogenate the dimer to the dimer of naphthoquinone. They speculated that this might indicate that the dimer had a syn-configuration about the cyclobutane ring. Since the authors irradiated ethyl acetate solutions of 3 rather than the pure crystals, it cannot be said with any certainty that their dimer and the one reported in this work have the same stereochemistry nor is it certain that their 'dimer' is not actually a mixture of stereoisomeric dimers of 3 since such dimerizations in solution often produce a mixture of syn-, and anti-configured cyclobutane derivatives^{62,63}.

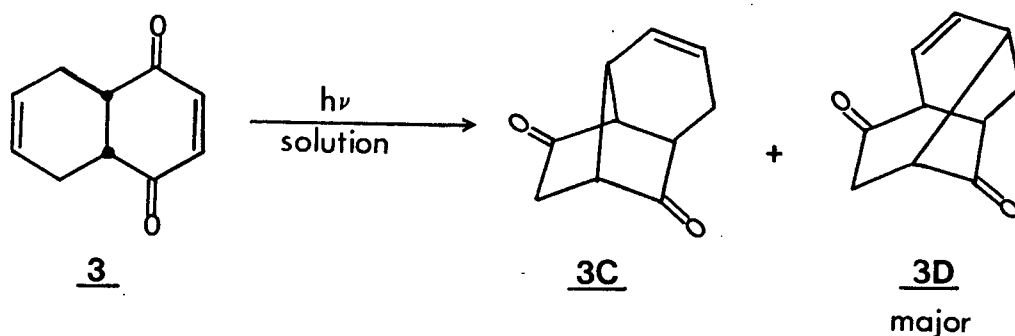
An attempt was made recently by Dekker and coworkers⁶⁴ to assign the stereochemistry about the cyclobutane rings of dimers of 3 and 2 by comparing their rates of cleavage with those of naphthoquinone dimers of known stereochemistry using zinc and zinc chloride reagent. Their results were interpreted as indicative of a syn-configuration

about the cyclobutane ring for both dimers, but as the authors themselves cautioned, such a conclusion would be risky since little is known about the mechanism of the ring cleavage reaction by zinc and zinc chloride and about the effects of the aromatic ring on one hand and the olefinic bond on the other. As the X-ray crystal structure shows (Figure 9) the dimer of monomer 2 is centrosymmetric and, therefore, has the anti- and not the syn-configuration about the cyclobutane ring. This does not rule out the possibility of the syn dimer being formed in the irradiation of 2 in solution and since it is not clear from Dekker's report whether the dimers were prepared by irradiating solutions or crystals of 3 and 2 respectively, one cannot say whether the dimers they isolated were the same as the ones reported here.

Irradiation of 3 in Solution

In the solution photochemistry of 3, the presence of a polymeric material in the reaction mixture was indicated^{24a}. This, no doubt, partially accounted for the low yield of 10%, of the identified products. It was, therefore of interest to find out if this unidentified polymeric material contained dimer(s) of 3. To do this, benzene solutions of 3 were irradiated. The amount of solid deposited during the reaction varied from run to run but never exceeded 49% of total recovered material. The infrared spectrum of the crude solid deposit showed both OH and C=O absorptions. The presence of the OH group was further confirmed by NMR. Mass spectral

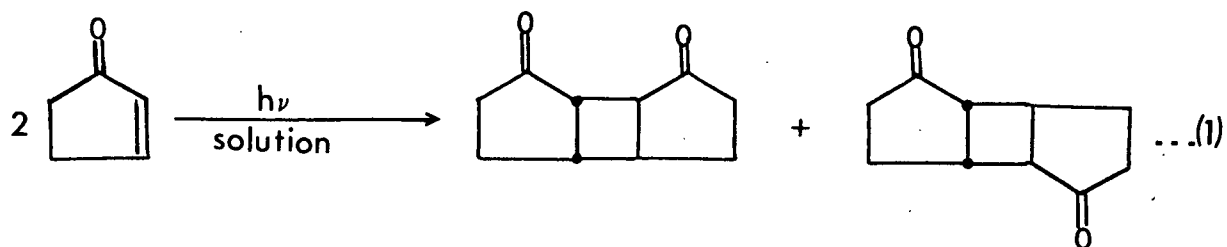
analysis of the solid showed peaks up to 495 as compared to 324 for the dimer of 3. These spectral characteristics coupled with the solubility of the solid in CHCl_3 and acetone show that whatever the structure of this "polymeric" material, it contains very little of the dimer of 3. Preparative GLC of the benzene soluble portion of the reaction mixture confirmed earlier results^{24a}. These are summarised in the equation below.



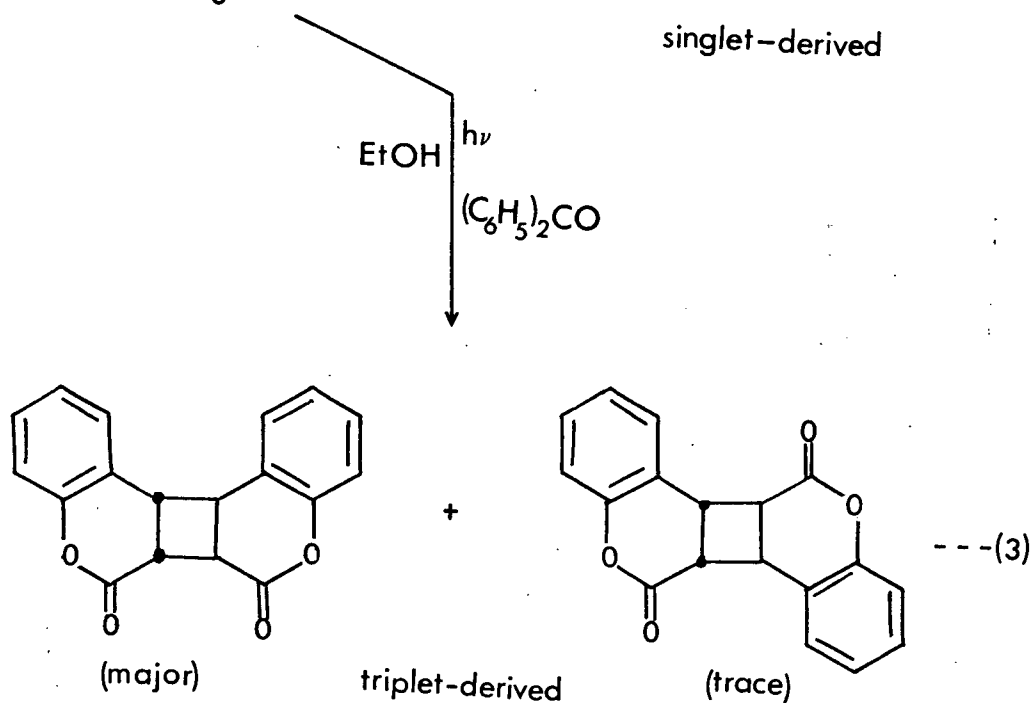
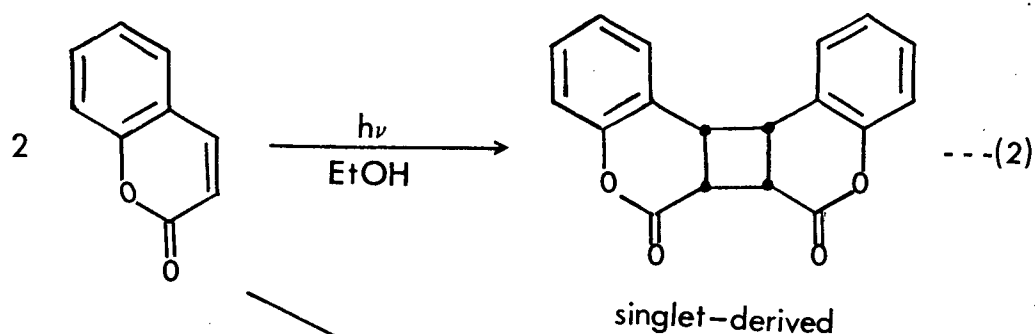
Reactive State and Mechanism for the Photodimerization Reactions

Although no mechanistic investigations have been carried out for the photodimerizations of substrates 1, 2 and 3, analogy can be drawn from numerous examples of such reactions both in the solid state⁶¹ and in solution^{62,63}.

For example, the dimerization of 2-cyclopentenone in solution has been shown by quenching studies to be triplet derived⁶². So are a number of photodimerizations of α,β -unsaturated cyclic ketones^{62,63}. Nevertheless, a number of photodimerizations both in the solid state and in solution are known to occur from the singlet



state^{61,65}. The solution photodimerization of coumarin, equations 2 and 3 below, has been shown to occur from either the singlet or the triplet depending on the reaction conditions⁶⁵. Very interestingly,



thymine photodimerizes from the triplet in solution but the equivalent solid state reaction occurs from the singlet state⁶⁶. This and Schmidt's generalization that the majority of solid-state photodimerizations occurs from the first excited singlet⁶¹ would seem to indicate that solid state photodimerization proceeds via a reactive state which is different from that which obtains in solution. Given the narrow energy separation between the n, π^* singlet, the n, π^* and the π, π^* triplets in some of these α, β -unsaturated ketones, it might very well be that no generalization can be made about the nature of the reactive excited species involved in the photodimerizations of 1, 2 and 3.

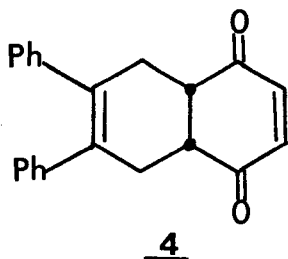
Whatever the nature of the excited species, there is general agreement that the reaction involves the union of an excited monomer and a ground state monomer. This has been experimentally demonstrated for both solid state⁶¹ and fluid media⁶² photodimerizations. Although the two new bonds to be formed in this reaction have been shown to occur in a stepwise fashion for dimerizations in solution^{62,63}, the concerted $[\pi_2^s + \pi_2^s]$ mechanism cannot be ruled out for reactions occurring from the singlet manifold for which no spin pairing process is necessary before ring closure. The stereospecificity of the solid state reactions of substrates 1, 2 and 3 in no way identifies the reaction mechanism, however, since the formation of a biradical which is frozen in the conformation of its monomer units by the crystal lattice could still give a stereospecific product.

In conclusion, the topochemical principle has been well demonstrated by the UV induced dimerization of 4a β ,5,8,8a β -tetrahydro-1,4-naphthoquinone and two of its dimethyl derivatives. The stereochemistry of each of the dimers has been unambiguously determined for the first time using single crystal X-ray diffraction methods.

2. Intramolecular Hydrogen Abstraction

6,7-Diphenyl-4a β ,5,8,8a β -tetrahydro-1,4-naphthoquinone, 4

Compound 4 crystallized out of a solvent mixture of acetone and hexane as well-formed yellow needles. One of these crystals



measuring 0.47 x 0.43 x 0.70 mm was used for X-ray structure determination.

The method and data treatments are the same as for previously reported structure determinations. Unit cell parameters were refined from 2 θ values of 19 reflections. Intensity data were collected from 3365 independent reflections. The R value after refinements was 0.053.

Crystal Data⁶⁷:

C₂₂H₁₈O₂, monoclinic, space group P2/c with a=27.092(4), b=6.527(2), c=22.112(3) Å, β =120.562(9)° and Z=8. The conformation of the molecule is twisted such that the bridgehead hydrogens are staggered with a torsion angle of 62°. Bond lengths and angles are normal. A stereo diagram of the molecule is shown in Figure 16.

Intermolecular distances mostly correspond to van der Waals contacts except one notable distance, namely, the distance between O(2)

of one unit and the H(3) of the nearest molecule. This distance is 2.39 Å compared to a normal van der Waals contact of about 2.6 Å⁶⁸.

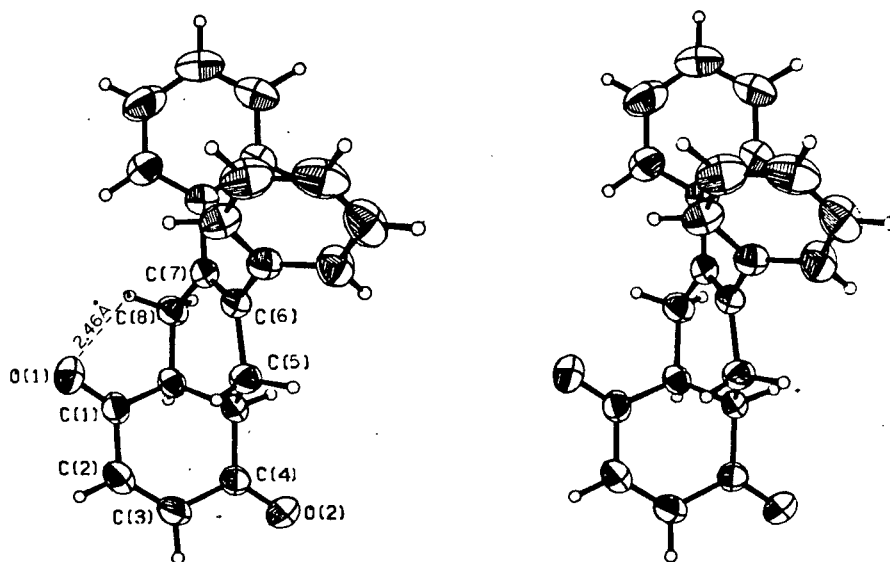
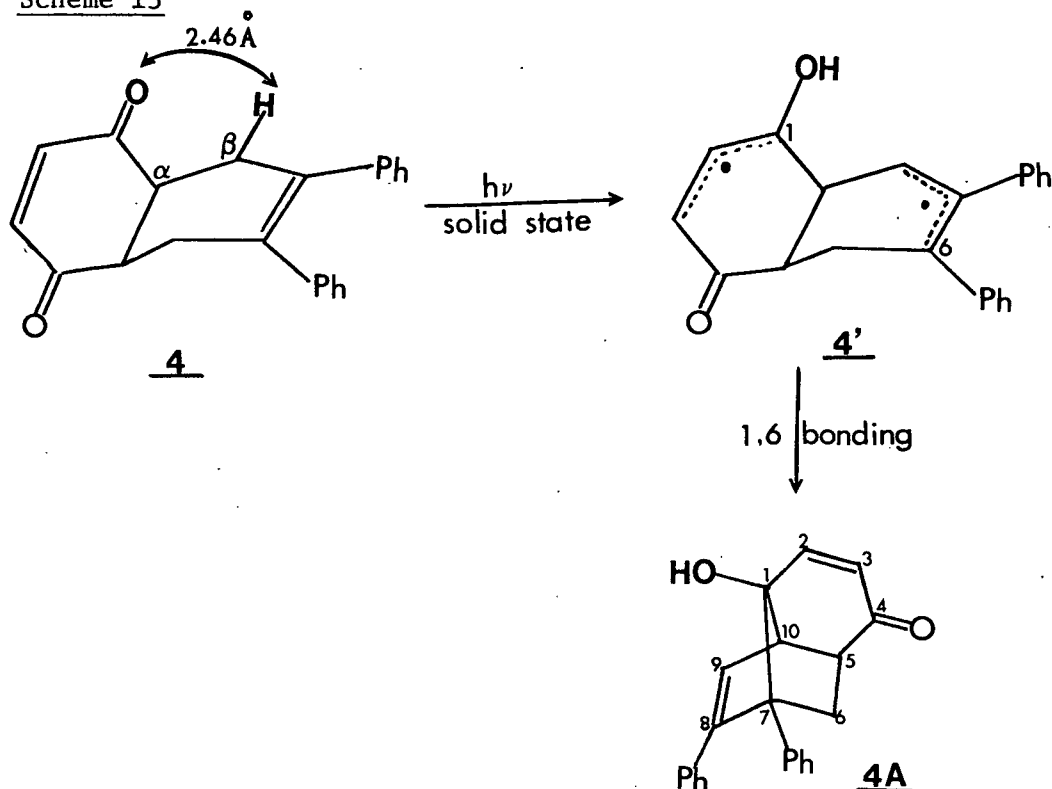


Figure 16. Stereo diagram of compound 4.

Irradiation of 4 both in KBr and as the pure solid in vacuo below the eutectic temperature (151.3°) gave the enone-alcohol 4A expected from the abstraction of a β -hydrogen by oxygen (Scheme 13). As the stereo diagram in Figure 16 shows, one of the oxygens, namely, O(1) is located near and coplanar with one of the C8 hydrogens, H(8B). The abstraction most likely involves these two atoms. The interatomic

Scheme 13



distance involved in the abstraction is 2.46 \AA . The diradical **4'** resulting from β -hydrogen abstraction is most likely frozen in the conformation of its precursor. In that conformation, radical centres 1 and 6 are only 3.51 \AA apart as compared to distances of $>4 \text{ \AA}$ for C3, C6 and C3, C8 separations, respectively. Closure of biradical **4'** between centres 1 and 6 gives the observed enone alcohol product **4A**. The latter was easily identifiable by its infrared and NMR spectra. The carbonyl absorption of the six-membered ring enone came at 5.97μ (cf. 5.92 and 5.95μ for **4**). The OH absorbed broadly but moderately at 2.92μ . In the NMR of all previously encountered enone alcohols of this general structure, the C10 bridgehead proton absorbed in the range

3.24 - 2.87 δ^{24} . This has become diagnostic for the enone alcohol structure. In 4A, this methine appeared as a doublet, $J=3$ Hz, at 3.45 δ . The shift downfield is likely due to the deshielding effect of the neighbouring aromatic ring. The hydroxyl proton resonated as a singlet at 2.73 δ and was easily exchanged for deuterium when D_2O was added.

In experimental runs in which conversion of starting material to product(s) was carried to >17%, a second product, 4B was also isolated. That this product arose from a secondary photolysis of the primary photoproduct was borne out by the following experimental facts: (i) at low conversions, 4A was the sole product isolated; (ii) the formation of 4B led to diminished yields of 4A (Table VII); (iii) during the photolysis of KBr pellets of 4, depletion of 4

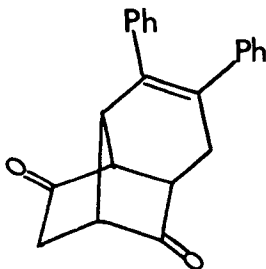
Table VII. Product Yields for the $4_{(s)} \rightarrow 4A + 4B$ Conversion

<u>Reaction Temperature</u>	<u>% Conversion</u>	<u>% Yields</u>	
		<u>4A</u>	<u>4B</u>
-10.4 to -9.8°	17	67	None
18.5 to 22.0	66	47	8
17.3 to 18.5	>90	33	15

and formation of 4A preceded the appearance of 4B as shown by infrared spectra recorded at 10 minute intervals during the irradiation; (iv) 4A dispersed in KBr or as the pure solid was converted to 4B under

reaction conditions identical to those used for the 4 → 4A transformation.

Photoproduct 4B correctly analyzed for $C_{22}H_{18}O_2$ and was characterised as 2,3-diphenyltricyclo[5.3.0.0^{5,10}]deca-2-ene-6,9-dione on the basis of its infrared, NMR and mass spectra.



4B

It had a carbonyl absorption at 5.73μ which is characteristic of the infrared absorption of compounds of similar structure having the five-membered ring ketone²⁴. In the NMR spectrum the following assignments were made: $\delta 7.23 - 6.87$ (m, 10H, aromatic), 3.23 (m, 2H, C7 and C10 methines), 3.07 (m, 1H, C5 methine), 2.83 (m, 3H, C1 and C4 protons), calcd⁶⁹ 2.57 (dd, $J=20$ and 5 Hz 1H, C8 exo), calcd⁶⁹ 2.20 (dd, $J=20$ and 1.5 Hz, C8 endo). The assignment of the C8 exo and endo protons was based on the disappearance of the $\delta 2.57$ resonance upon deuterium exchange in basic deuterium oxide and the concomitant collapse of the doublet of doublets at calcd. $\delta 2.20$ to a broad singlet at $\delta 2.21$. The facile exchange of this exo hydrogen in bicyclo[2.2.1]-heptanone systems has been reported in the literature⁷⁰. The NMR absorption pattern of compound 4B is very similar to that of the previously reported^{24a} analog compound 2C (Figures 17a and 17b). For

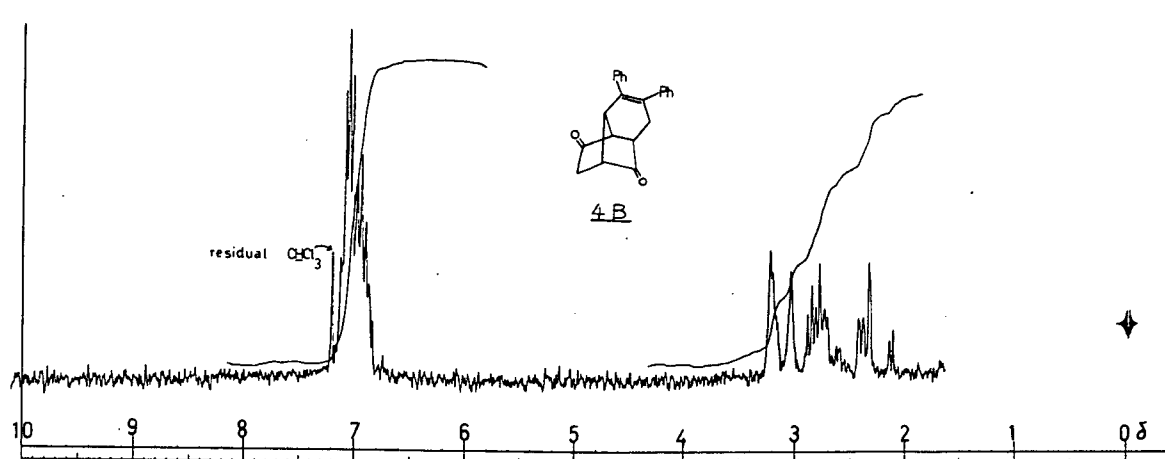


Figure 17a. A 100 MHz PMR Spectrum of 2,3-Diphenyltricyclo[5.3.0.0^{5,10}]-deca-2-ene-6,9-dione, **4B**.

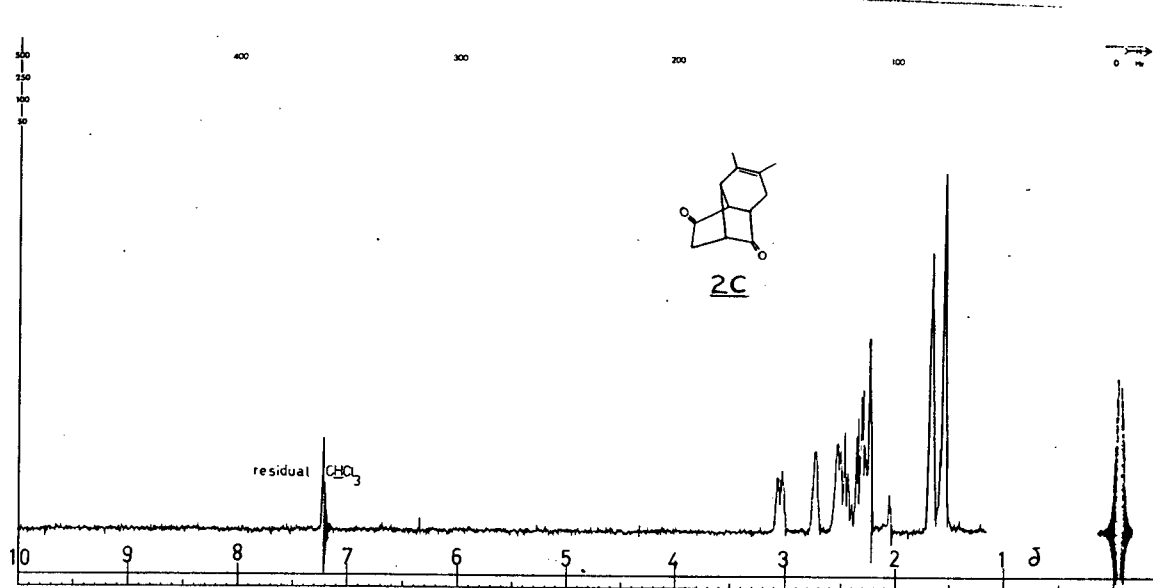


Figure 17b. A 100 MHz PMR Spectrum of 2,3-Dimethyltricyclo[5.3.0.0^{5,10}]-deca-2-ene-6,9-dione, **2C**.

example, the exo and endo protons at C8 each resonated as a doublet of doublets at calcd. δ 2.47 and 2.19 in 2C. In photoproduct 4B these protons also resonated each as a doublet of doublets at calcd. δ 2.57 and 2.20, respectively.

Since the photochemical behaviour of substrate 4 has, hitherto, not been studied in solution, photolyses of it in benzene were also carried out to ascertain if its reactivity in solution differed from the solid state photoreactivity. These results are summarised in equation 4 below.

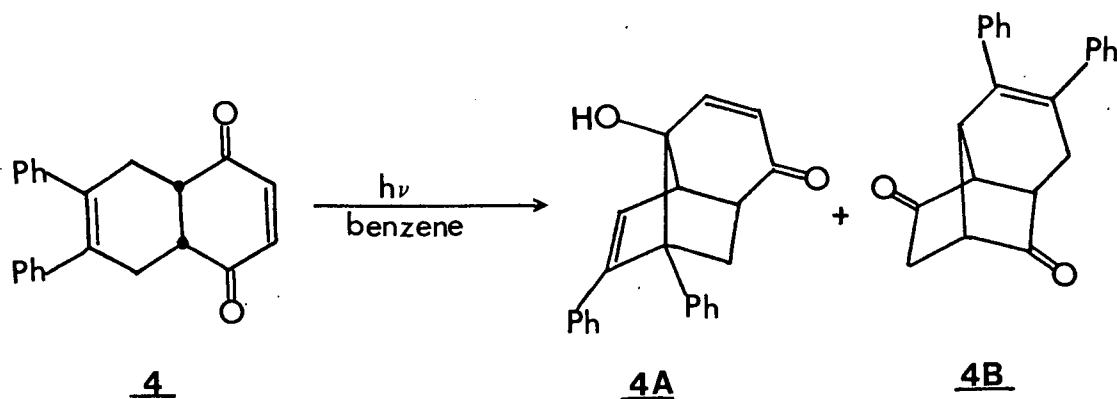
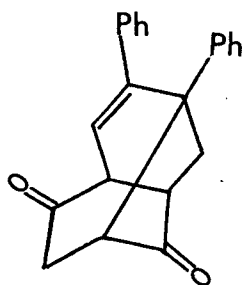


Table VIII. Product Yields for the 4(solution) \rightarrow 4A + 4B Conversion

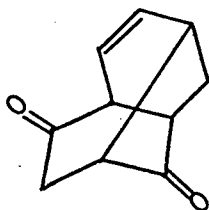
<u>Duration of Irradiation</u>	<u>Product Ratios</u> <u>4A:4B</u>
3.0 hours	3:1
3.1 "	3:2
3.9 "	1:2

Unlike the solid state reaction, product 4B is formed concomitantly with 4A as determined by following the reaction at 0.1 hour intervals using infrared spectroscopy. As in the solid state reaction, photoproduct 4A was again found to be photolabile as shown by (i) the varying ratio of 4A:4B as the reaction proceeds (Table VIII); (ii) independent photolysis of 4A under the same reaction conditions as for the 4 → 4A conversion gave 4B and a compound having 5.68 and 5.80 μ carbonyl stretches in the infrared. Although this latter compound was not investigated further, it probably has the assigned structure 4C since previous investigations²⁴ of the photochemistry of these tetrahydro-1,4-naphthoquinones in solution have shown that only photoproducts of this structure absorb at ~ 5.70 and 5.80 μ . Examples of this are given below:



4C

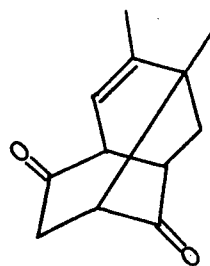
5.68, 5.80



3D

C=O, μ

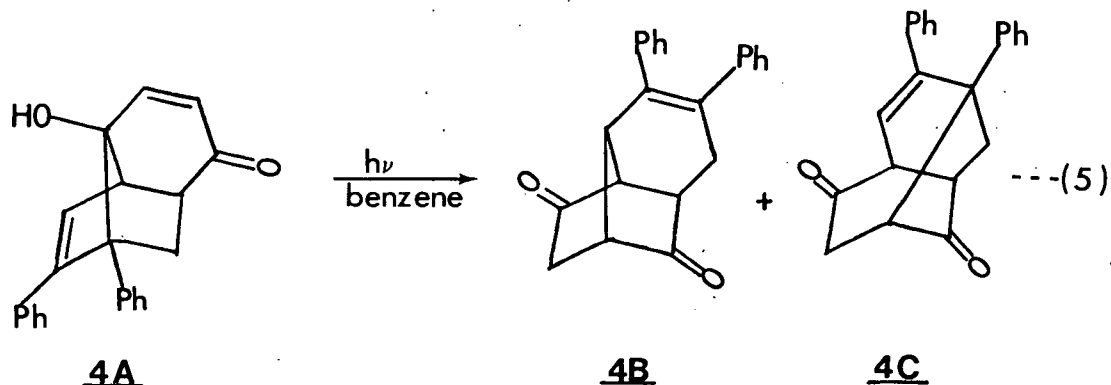
5.68, 5.80



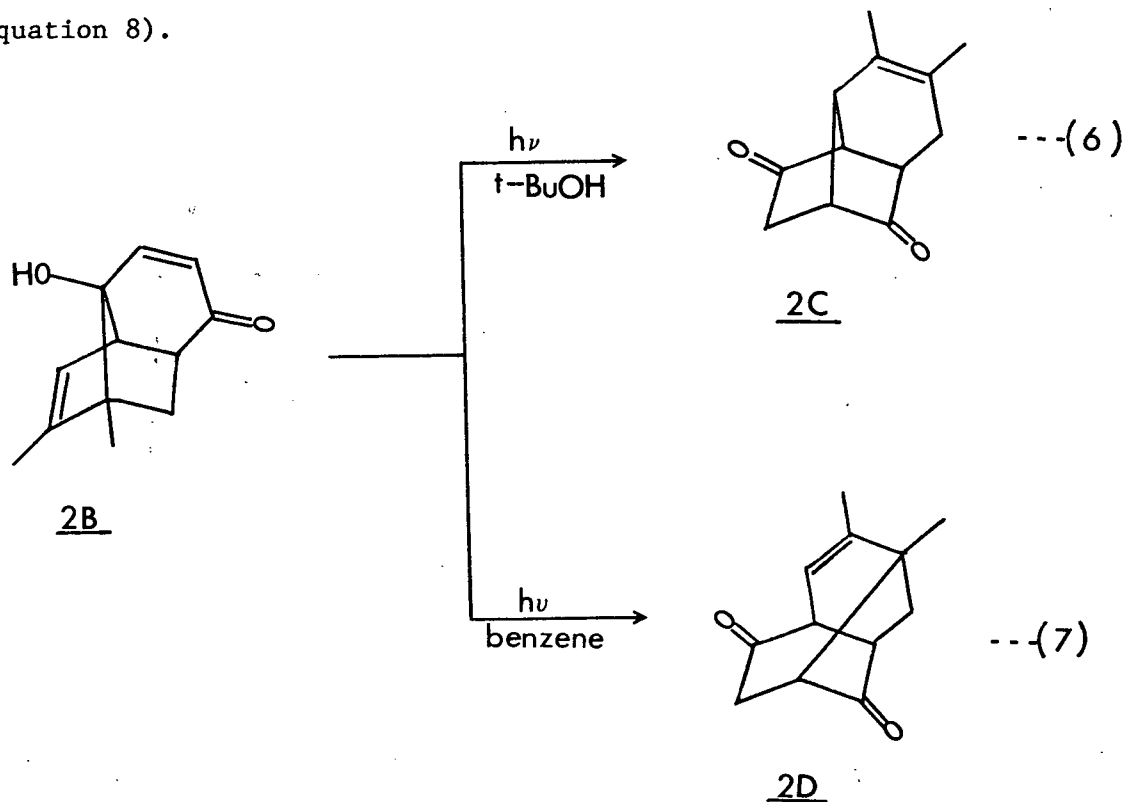
2D

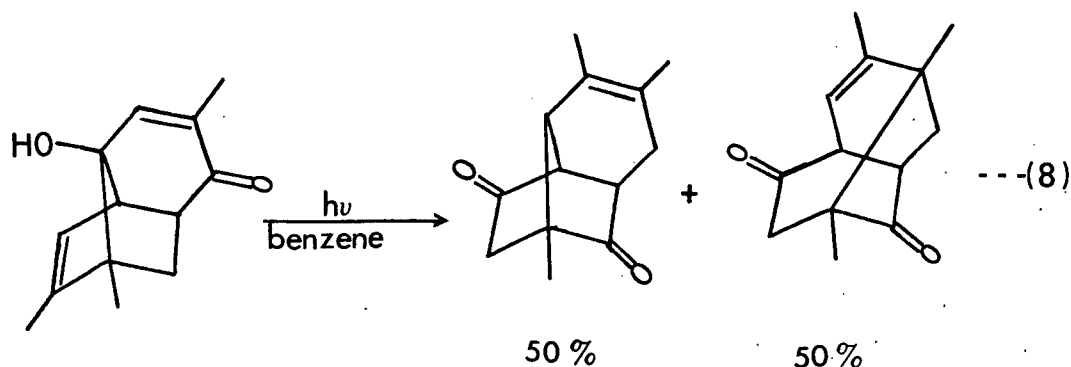
5.69, 5.81

The formation of ene-diones 4B and 4C from enone alcohol 4A is not novel. Scheffer and coworkers^{24a} reported the conversion of the



dimethyl enone-alcohol 2B to the ene-dione 2C in tert-butyl alcohol and 2B to 2D in benzene (equation 6 and 7). The conversion of an enone-alcohol to both ene-diones in benzene was also later reported⁷¹ (equation 8).

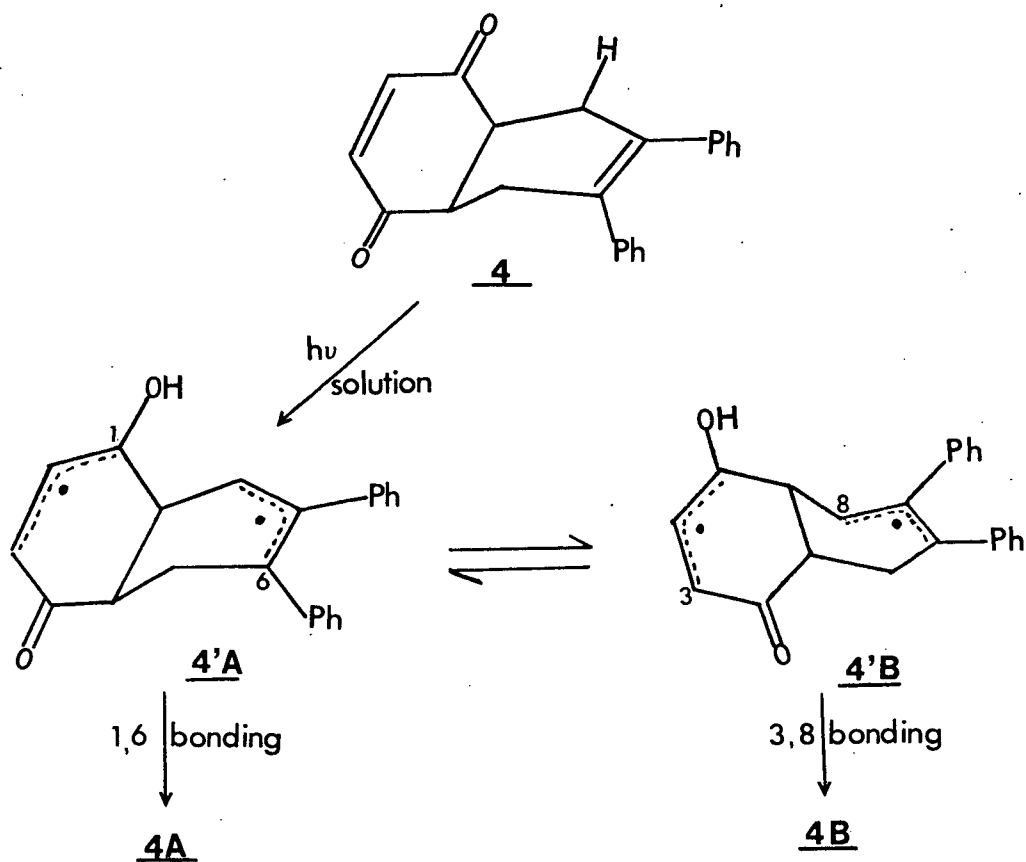




The photochemical formation of 4B from 4A is formally a disallowed [3,3] suprafacial-suprafacial sigmatropic rearrangement⁷² and is, therefore, likely, a non-concerted reaction. On the other hand, the 4A → 4C conversion is a [1,3] suprafacial sigmatropic shift which is photochemically allowed. It can, therefore, but need not be, concerted. In both the solid state and in solution, photoproduct 4B was photostable under the reaction conditions.

Turning now to the primary reaction, namely, the 4 → 4A + 4B reaction in benzene, analogy is drawn to earlier systems studied in our laboratory in which both product types were formed as primary products^{24,71}. The formation of both of these products can be explained by postulating the same diradical intermediate 4' which was used earlier to explain the formation of 4A from 4 in the solid state. As can be seen from Scheme 14, photoproducts 4A and 4B probably arise from different conformers of the biradical intermediate 4'. The reason behind this stipulation comes from the X-ray data as well as the solid state results. Photoproduct 4B can only form from biradical 4' of unspecified conformation if bond formation occurs between C3 and C8. This is not likely to happen from conformer 4'A

Scheme 14

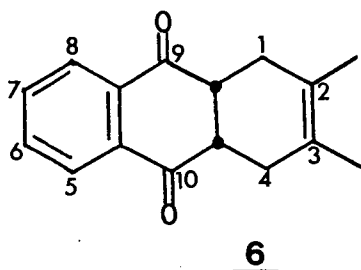


since these centres are greater than 4\AA apart. On the other hand, C1 and C6 are only 3.51\AA apart in substrate 4. Assuming that the conformation in which the molecules crystallize is also the preferred conformation in solution, it can be seen that the biradical intermediate may form and close to the enone-alcohol from this conformation i.e. no gross conformational changes are mandatory for the 4 \rightarrow 4A conversion. The 4 \rightarrow 4B conversion most likely requires a conformational change. Since conformational mobility is possible in fluid media, a

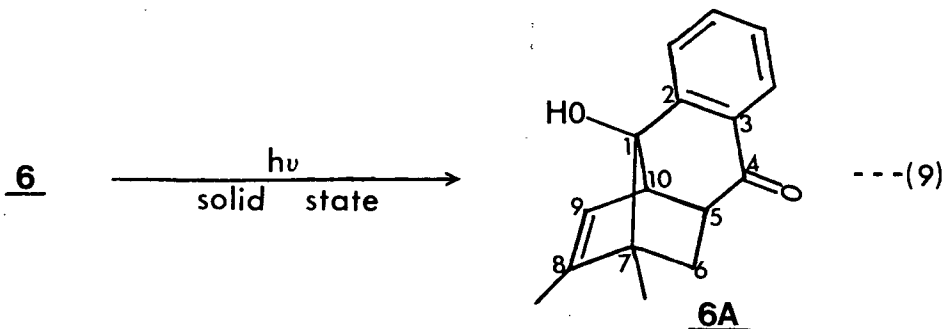
conformer such as 4'B is possible in solution and not in the solid state and the now nearness of the C3 and C8 centres would allow product 4B to be formed. The observation that photoproduct 4B is the minor product of the primary reaction in solution is most likely a reflection of the conformational change necessary to allow for its formation.

2,3-Dimethyl-1,4-4a β ,9a β -tetrahydro-9,10-anthraquinone, 6

Compound 6 crystallised from acetone solution as colorless



rods. Irradiation of 6 in the solid state below the eutectic temperature (126.0°) gave enone-alcohol 6A (equation 9) in 60%



isolated yield. The structure of 6A follows ultimately from comparison of its spectral data with those of authentic 6A prepared

using the procedure of Scheffer and coworkers^{24a}. The conversion of 6 to 6A involves the abstraction of a β -hydrogen by one of the oxygens of an excited carbonyl chromophore followed by C9 to C3 bonding. The transformation is analogous to the 4 \rightarrow 4A conversion.

A small piece of crystal 6 measuring 1.0 x 0.80 x 0.30 mm was cut from a larger crystal and used for the determination of the X-ray structure⁷³. Unit cell constants were refined by least-squares from the observed 2θ values of 17 reflections. Intensity data from 1313 independent reflections were used for the structure determination. The R value after full-matrix refinements was 0.055.

Crystal Data⁷³

$C_{16}H_{16}O_2$, orthorhombic, space group $Pna2_1$ with $a=15.643(2)$, $b=5.160(1)$, $c=15.568(2)$ Å, $\beta=90^\circ$ and $Z=4$. The structure of the molecule is shown in Figure 18.

The hydrogen abstracted in the 6 \rightarrow 6A conversion is one of the C1 hydrogens. The interatomic separation between this hydrogen and the abstracting atom O(1) is 2.57 Å. The abstraction would give rise to a biradical 6' (Scheme 15). Electron delocalization into the aromatic ring is expected to aid the stabilization of 6'. However, no bond formation involving the aromatic ring carbon atoms is expected since this will result in loss of the stabilization energy associated with the aromatic ring. This leaves only two possible modes of ring closure for biradical 6', namely bonding between C9 and

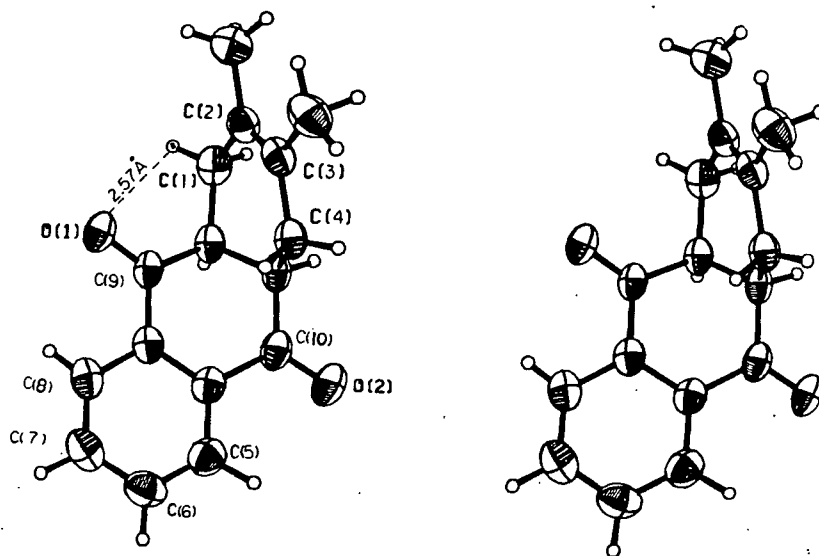
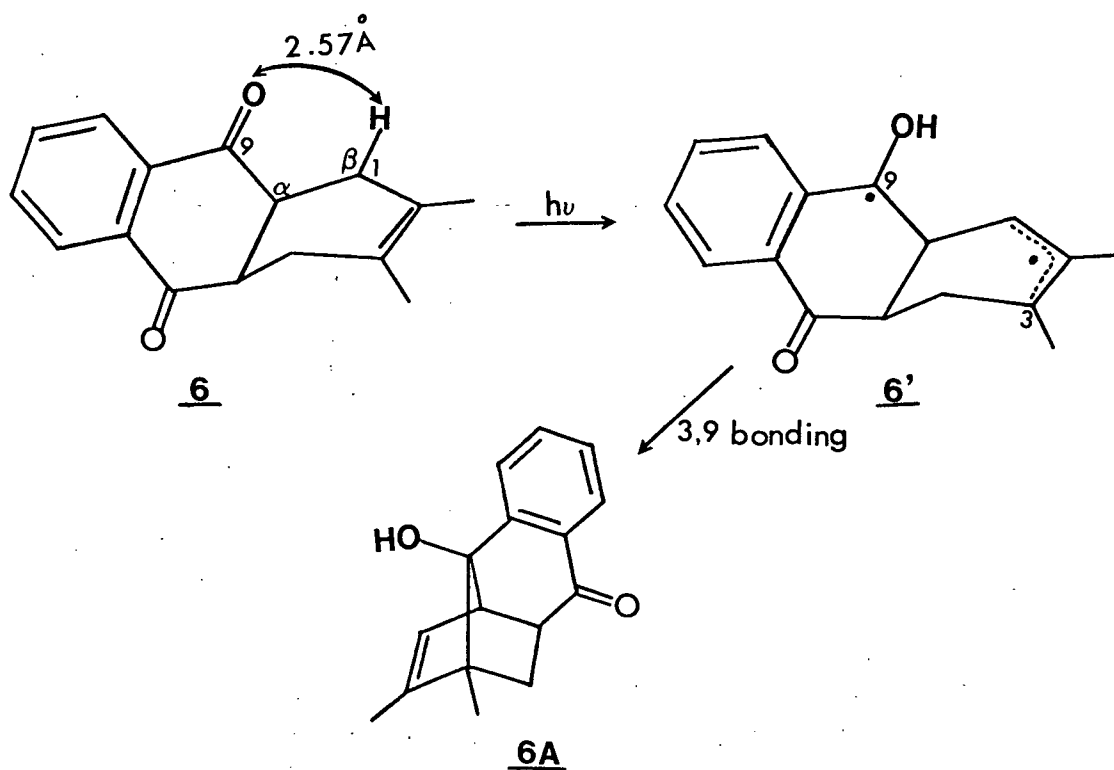


Figure 18. Stereo diagram of compound 6.

Scheme 15

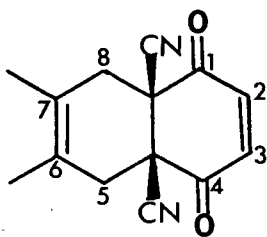


C1 and between C9 and C3. As already mentioned in the Introduction, the formation of a cyclopropane ring in these already rigid polycyclic systems is unlikely and has to date not been observed. Bond formation between C3 and C9 gives rise to the observed product 6A. In substrate 6 the interatomic separation between C3 and C9 is only 3.46 Å so here as in the 4 → 4A transformation, the biradical can form and collapse to the observed product without any gross changes in conformation.

Not surprisingly, irradiation of degassed solutions of 6 also gave 6A as the only product because as pointed out, the biradical intermediate 6' can only close between C3 and C9.

6,7-Dimethyl-4aβ,8aβ-dicyano-4aβ,5,8,8aβ-tetrahydro-1,4-naphthoquinone, 7

Large, sparkling yellow crystals of 7 were obtained by crystallization from a solvent mixture of acetone and light petroleum ether.



7

One crystal measuring 0.50 x 0.40 x 0.40 mm was used for X-ray structure determination. Unit cell constants were obtained by least-squares refinement of the observed 2θ values of 23 reflections.

Intensity data from 2445 independent reflections were used to solve the structure. The final R value after refinements was 0.055.

Crystal Data⁷⁴

$C_{14}H_{12}N_2O_2$, monoclinic, space group $P2_1/c$ with $a=8.717(5)$, $b=12.464(2)$, $c=12.783(5)$ Å, $\beta=117.87(3)^\circ$, and $Z=4$. A stereo view of the molecule is given in Figure 19.

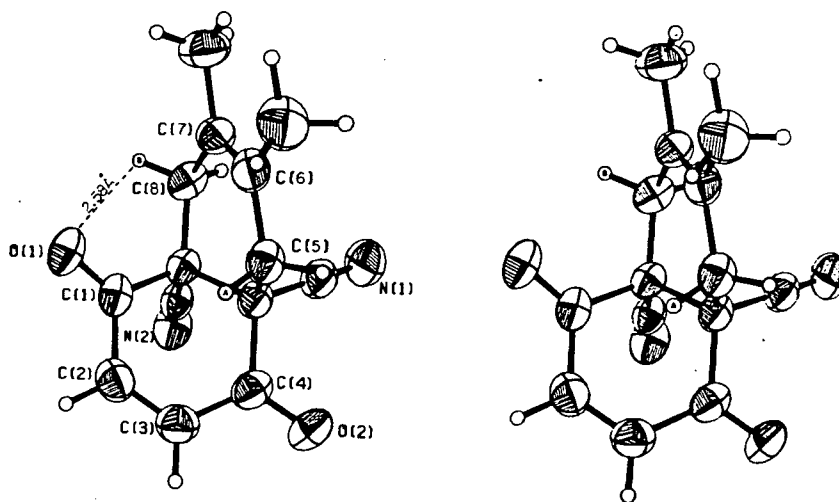
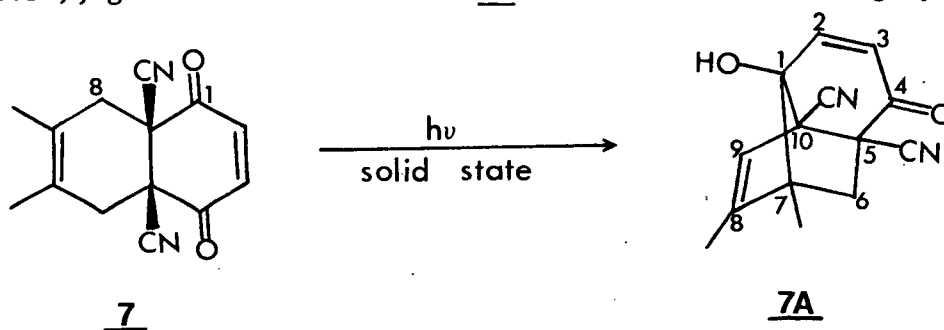


Figure 19. Stereo diagram of compound 7.

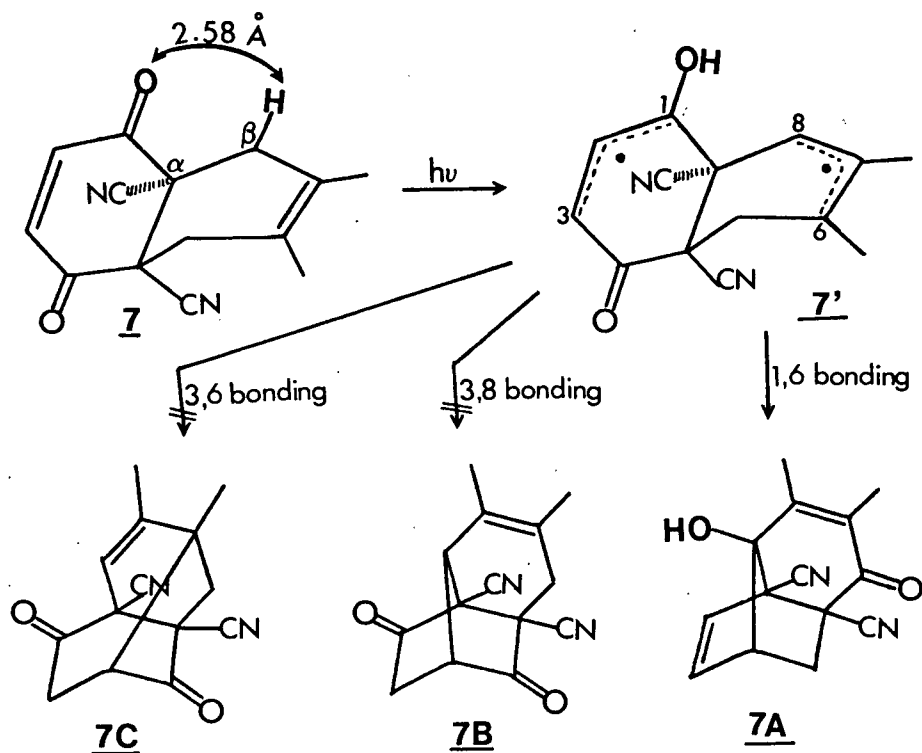
Irradiation of 7, either as a solid dispersed in a KBr matrix or as the pure solid in vacuo below the eutectic temperature (118.5°), gave the enone-alcohol 7A in 92% isolated average yield.



Photoproduct 7A was conclusively identified by comparing its physical and spectral characteristics with those of authentic 7A prepared by the method of Scheffer and coworkers^{24b}.

The formation of 7A formally involves the abstraction of one of the C8 methylene hydrogens, H_β, by O(1) and collapse of the resulting biradical through bond formation between carbons 1 and 6. The H_β...O(1) distance in the crystal is 2.58 Å. The separation of C1 and C6 in the crystal is 3.38 Å. So here as in the two previous examples, the formation of the biradical intermediate in this reaction and its subsequent collapse to enone-alcohol does not require any conformational changes. The only other possible but unobserved bonding modes are between C3 and C6 and between C3 and C8. The separations between these carbons in the crystal are 3.86 and >4 Å, respectively. Not only are these distances longer than the C1, C6 separation in the crystal but the p-orbitals at these centres are directed away from

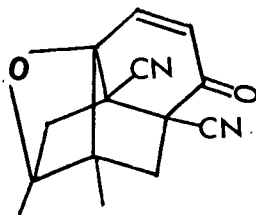
Scheme 16



each other so that overlap between them cannot be achieved.

One might expect that like many of the substrates in this series of tetrahydro-1,4-naphthoquinones, substrate **7** in solution might give the ene-diones **7B** and **7C**. Irradiation of degassed benzene solutions of **7** gave 74% yield of enone-alcohol **7A** and 7% yield of a compound melting at 156 - 158°. The latter compound had the following spectral data: In the infrared it had cyano stretching frequencies at 4.44 and 4.46 μ and a carbonyl stretch at 5.90 μ . The single C=O stretch at 5.90 μ ruled out both ene-diones **7B** and **7C**. In the nuclear magnetic resonance spectrum, it had two doublets, $J_{AB}=10\text{Hz}$, sited at $\delta 7.44$ and 6.41, respectively, which integrated for 1H each. The

rest of the spectrum had δ 2.56 (s, 2H), 2.45 (d, J=15 Hz, 1H), 1.72 (d, J=15 Hz, 1H), 1.56 (s, 3H) and 1.38 (s, 3H). Its mass spectrum showed a parent peak at m/e=240. This product, 7D is tentatively assigned the oxetane structure below:



7D

The absence of ene-diones 7B and 7C has been ascribed to the prevention of conformational changes even in solution as a result of bridgehead substitution.

As an attempt to see if any similarities exist between the geometries of a substrate and its solid state photoproduct, the X-ray structure of enone-alcohol 7A was also determined⁷⁵. A stereo view of the molecule is shown in Figure 20. As can be seen from comparing this diagram with that of the starting crystal 7, the 7 \rightarrow 7A conversion is attended by the conversion of the favorable half-chair conformation of the C5-C10 ring to a boat form. The conformation of the quinone ring remains essentially the same.

During the X-ray structure determination, there were indications that enone-alcohol 7A might be optically active. The molecule itself is chiral, but one would expect that in a biradical

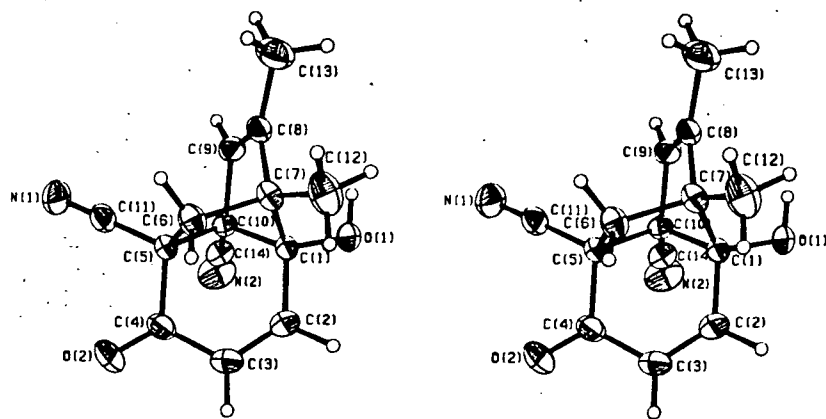


Figure 20. Stereo diagram of enone-alcohol, 7A.

ring closure, both levorotatory and dextrorotatory molecules should form in equal proportions giving racemic 7A. If crystals of 7A were optically active, it meant that a racemic mixture had been formed during crystallization, an uncommon occurrence in organic chemistry. When single crystals as well as clusters of crystals of 7A were used in optical rotation determinations, the results shown in Table IX were obtained.

Table IX. Specific Rotation of Solutions of Crystals of 7A

<u>Description of Crystal</u>	<u>$[\alpha]_D^{25.5^\circ}$</u>
Single	+3.0°
Single	+2.5°
Single	-67.7°
Clusters	-14.5°

The fact that some of the single crystals were levorotatory and others dextrorotatory means that crystallization followed by mechanical separation had effected resolution of the racemic photoproduct. The fact that the specific rotation of the levorotatory single crystal is not equal to that of the dextrorotatory crystal is an indication that the resolution is only partial. Nevertheless, such a spontaneous resolution through crystallization is rare. The historical example of this phenomenon was reported by Louis Pasteur^{76a} who allowed a solution of sodium ammonium tartrate to crystallize by slow evaporation below 27° and was subsequently able to separate the two enantiomers by mechanically picking them apart. Since then, very few examples of this occurrence have been reported. Among these are the spontaneous crystallization of active material from dl solutions of (i) 3,3-diethyl-5-methyl-2,4-diketopiperidine^{76b}, (ii) narcotine^{76c}, (iii) laudanosine^{76c} and (iv) methyl-ethyl-allyl-anilinium iodide^{76d}.

The crystal packing diagram revealed that compound 7 represents the crossover from inter to intra-molecular reactivity in

this series of tetrahydro-1,4-naphthoquinones. Figure 21 shows portions of adjacent molecules within a crystallographic cell. The π overlap of the ene-dione double bonds which is necessary for dimerization is not achieved due to a slight tilt of the C2, C3 plane

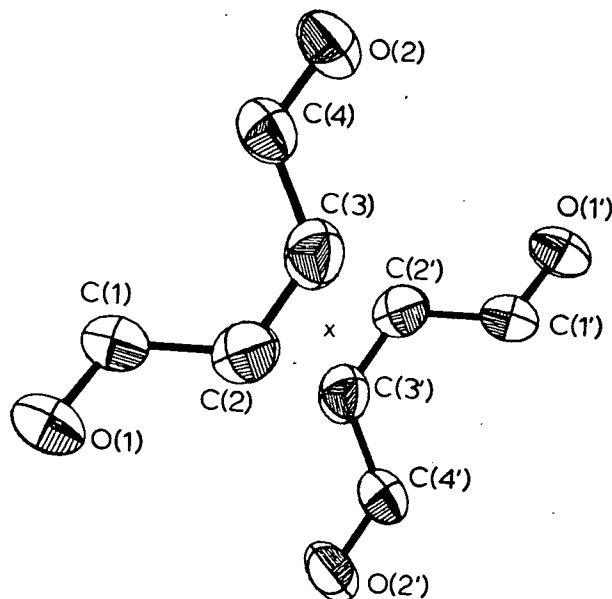
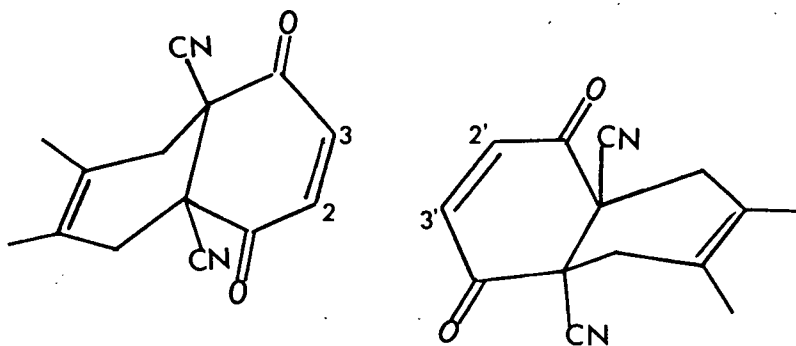


Figure 21. Neighbouring ene-dione systems of a pair of molecules of 7 viewed perpendicular to the C(1), C(2), C(3) plane.

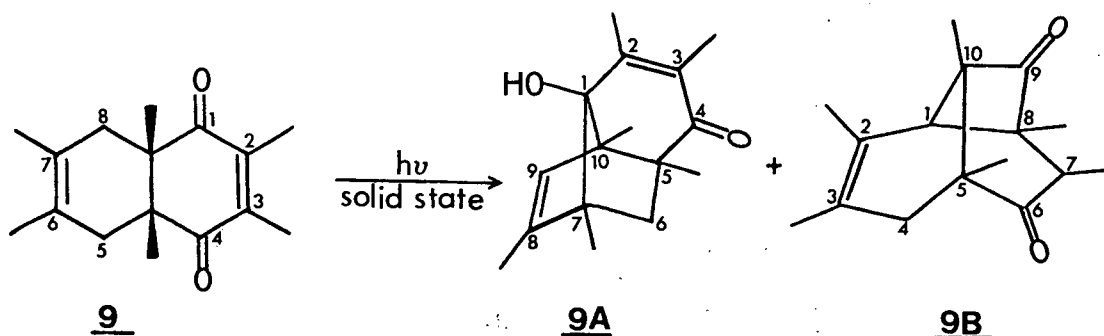
of the molecule above the plane of the paper relative to the C2', C3' plane of the molecule below it (Figure 21). The intermolecular contacts are also much longer than the corresponding distances for substrates 1, 2 and 3. For example the C2 to C2' distance is 4.37Å. Because of the tilt of the C2, C3 plane of one of the molecules of the pair mentioned previously, the C2--C2' distance does not represent the shortest intermolecular contact. The latter turns out to be the C2 to C3' distance of 4.09Å which still exceeds the sum of the van der Waal's radii⁶⁸ of the two atoms by 0.69Å. The centre-to-centre



separation of the double bonds is 4.1\AA , and so not only are the orbitals not-aligned for intermolecular overlap but the limit of double bond separation necessary for photodimerization in the crystalline state^{12b,61} has also been reached. Consequently, no photochemical dimerization was observed when crystals of 7 were irradiated.

2,3,4a β ,6,7,8a β -Hexamethyl-4a β ,5,8,8a β -tetrahydro-1,4-naphthoquinone, 9

Large, pale yellow crystals of 9 were obtained by crystallizing from petroleum ether. Smaller but better-formed crystals for crystallographic purposes were obtained by crystallizing from acetone. Crystals obtained from either solvent reacted in identical fashion



both in KBr and as the pure solid. Thus, one may assume that the crystal form is not changed as a result of change of crystallizing solvent. UV irradiation of 9 below the eutectic temperature (-16.0°) led to the formation of enone-alcohol 9A and the ene-dione 9B in the ratio 2:3. This ratio was invariant below the eutectic at varying conversions (Table X) as one would expect from a reaction in

Table X. Product Ratios and Combined Yields for the $9 \rightarrow 9A + 9B$
Conversion, in the Solid State

Reaction Temperature	% Conversion	% Recovery	Combined GLC Yields	Ratio <u>9A:9B</u>
-34.3° to -33.5°	41	91	77%	2:3
-34.7° to -32.5°	54	94	88%	2:3
-33.5° to -30.3°	68	63	46%	2:3
-25.6° to -23.1°	77	71	62%	2:3
-25.3° to -23.4°	88	78	75%	2:3

which both products are primary products. Yields are quite high provided the recovery of reaction mixture from the reactor is high. The structures of 9A and 9B were confirmed by comparing their physical and spectral data with those of 9A and 9B obtained previously and reported in the literature²⁴. As mentioned in the Introduction, 9A and 9B are thought to derive from different excited states, enone

alcohol 9A from an n, π^* singlet and ene-dione 9B from a π, π^* triplet. This being the case, it was of interest to repeat the solution photochemistry, which has hitherto been done only at ambient temperature, at temperatures below the eutectic to see if the ratio of 9A:9B was the same for the solution photolysate as for the solid state reaction at similar temperatures. Table XI summarizes results of the conversion 9 \rightarrow 9A + 9B in anhydrous ether below the eutectic. In terms of percentages, this ratio differs

Table XI. Product Ratios for the 9 \rightarrow 9A + 9B Conversion in Solution

$$\underline{9} \xrightarrow[h\nu]{\text{ether}} \underline{9A} + \underline{9B}$$

Reaction Temperature	% Conversion	Ratio <u>9A:9B</u>
-33.0° to -31.5°	21	1:2
-31.5° to -29.0°	25	1:2
-32.5° to -31.5°	52	1:2
-31.5° to -29.5°	63	1:2

from the solid state products ratio by only 7%, a difference too small to warrant explaining especially in view of the fact that product ratios in solution may be solvent dependent²⁴.

The X-ray structure of 9 was solved by direct methods as described⁷⁷. The crystal dimensions were 0.15 x 0.20 x 0.20 mm. Unit cell constants were obtained by least-squares refinement of the observed

2 θ values of 15 reflections. The intensity data of 2786 independent reflections were used in the structure determination. The R value after refinements was 0.088.

Crystal Data⁷⁷

C₁₆H₂₂O₂, monoclinic, space group P2₁/c with a=7.312(3), b=11.540(4), c=16.674(3) Å, β =92.26(3)° and Z=4. Figure 22 gives a stereo view of the molecule.

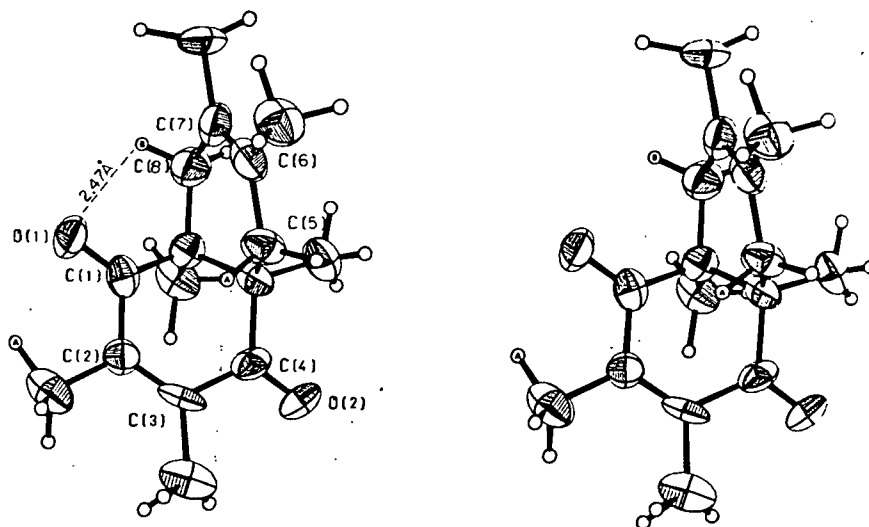
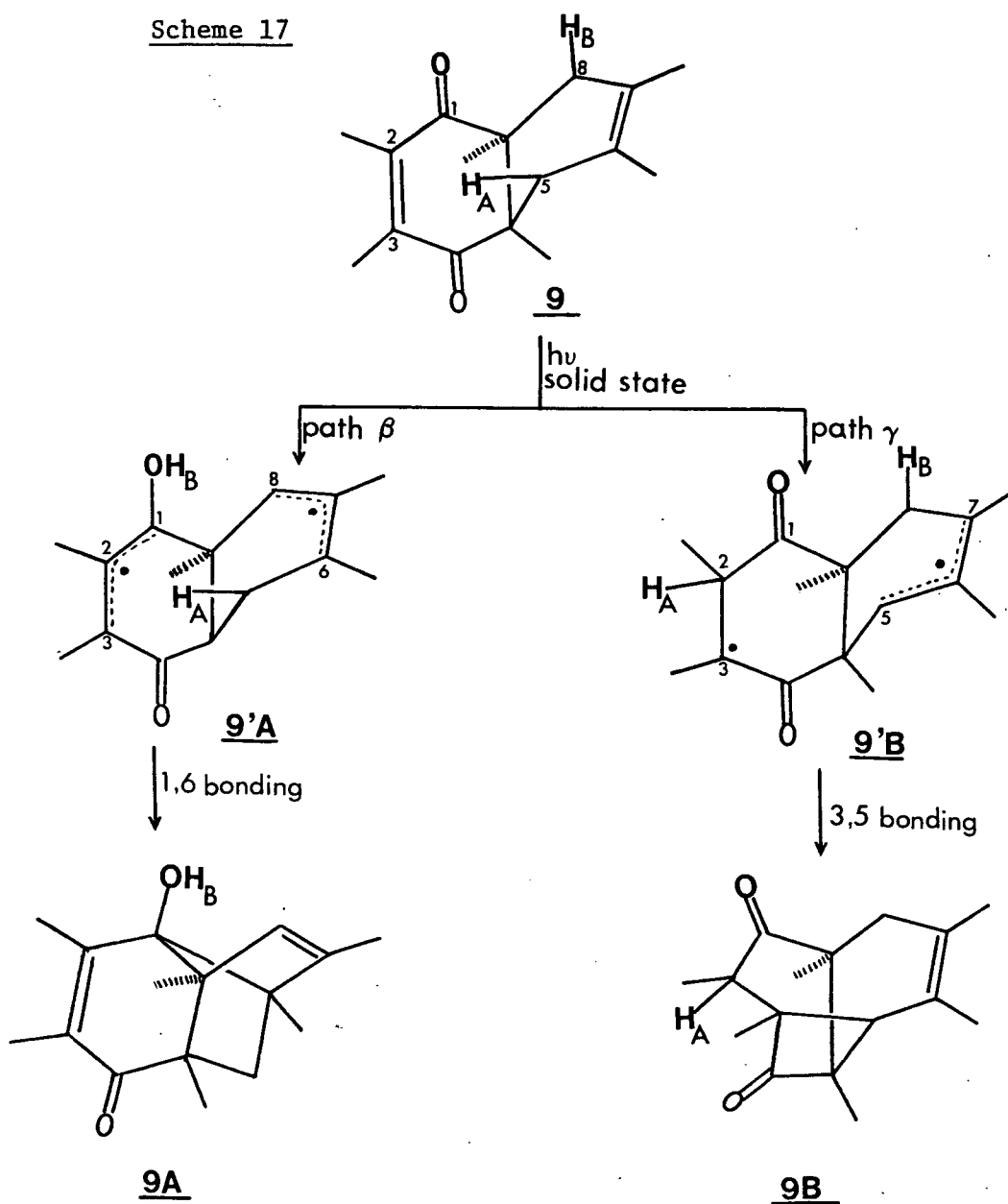


Figure 22. Stereo diagram of substrate, 9.

Scheme 17



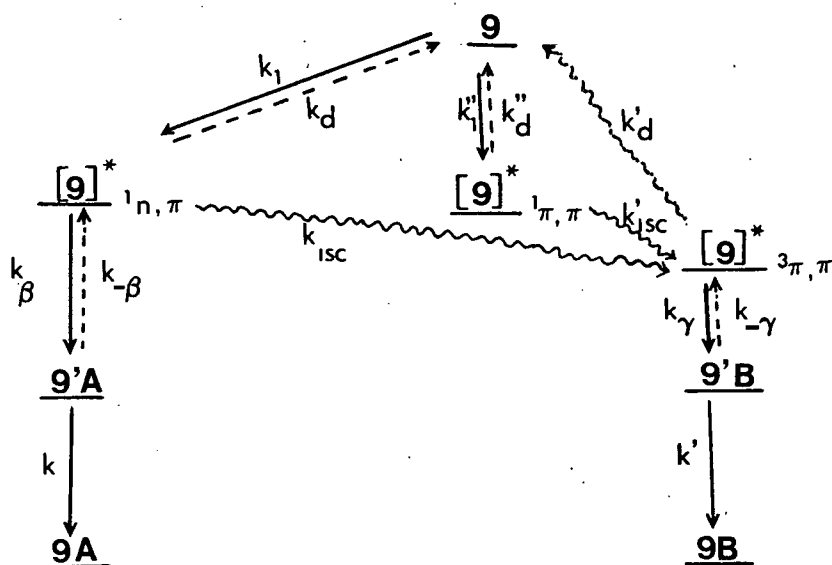
Photoproduct **9A** is the enone-alcohol product arising from the abstraction of H_B , one of the C8 hydrogens, by O(1) followed by bond formation between C1 and C6 radical centres (Scheme 17). The H_B to

O(1) distance is 2.47\AA and the C1 to C6 distance is 3.35\AA . The unobserved bonding modes of biradical 9'A, namely C3 to C6 and C3 to C8 were both $>4\text{\AA}$ in the crystal of 9.

The ene-dione product, 9B, formally arises from the abstraction of one of the C5 hydrogens, namely, H_A , by C2 giving biradical 9'B which then closes by bonding C3 to C5. The distance between the abstractable hydrogen and the abstracting carbon, namely $H_A \cdots C2$ is 2.89\AA in the starting material 9. As in previous cases, if there are no gross changes in conformation attending the reaction, one could approximate interatomic separations in the biradical intermediate to the corresponding interatomic distances in the substrate. The C3, C5 separation is thus only 3.17\AA . Not only is the interatomic separation favorable but the geometry of the molecule has the p orbitals at these centres directed towards each other thus promoting interaction and ultimately bond formation (Scheme 17). As in the case of biradical 9'A, the unobserved bonding mode in biradical 9'B, namely C3 to C7, would have involved bringing together carbon centres which are $>4\text{\AA}$ in the crystal of the substrate to closer proximity, a process which is likely to entail conformational changes impermissible by the lattice of the host.

The 3:2 ratio for photoproducts 9B and 9A does not reflect the relative rates for γ - vs β -hydrogen abstraction. As the kinetic scheme below suggests, the rates of formation of products 9A and 9B depend on a number of factors. For example, the relative population of the

Scheme 18

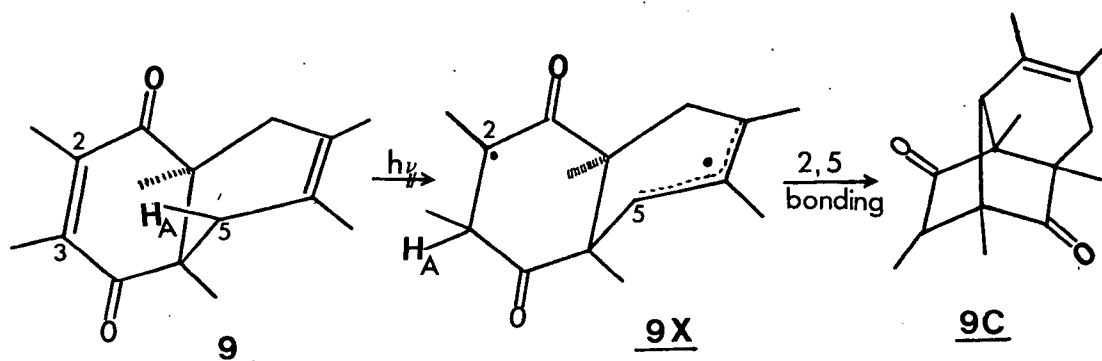


$1_{n,\pi}^*$ and $3_{\pi,\pi}^*$ states, the rates of decay of these two excited states and the rates of biradical closure relative to reverse hydrogen transfer will all be reflected in the overall rates of formation of these two products.

One interesting revelation from the crystallographic data is that the hydrogen which is abstracted by enone carbon is quite distinct from the hydrogen which is abstracted by oxygen, i.e. the β -carbon of the enone system and the oxygen do not compete for the same hydrogen in this reaction, a fact which is not evident from the chemical structure of **9** because of the symmetry of the molecule.

Another interesting point to be noted is that from the X-ray crystal structure, H_A can, in principle, be abstracted by either C2

or C3, being 2.89Å from C2 and 2.80Å away from C3. Abstraction by C3 would have given biradical 9X which can close to 9C, an unobserved

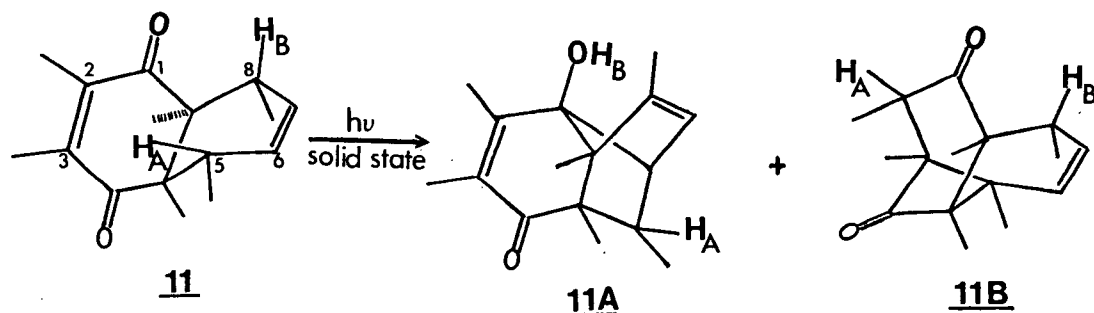


photoproduct, by bonding centres, C2 and C5. Such an abstraction would have proceeded via a five-membered transition state as opposed to the six-membered transition state that gives rise to the observed photoproduct 9B. That 9C is not formed may mean that the well-known order $1,5 > 1,6 \gg 1,4$ for rates of hydrogen abstraction in acyclic systems holds for this rigid system as well, the preference here being a 1,5 over a 1,4 hydrogen abstraction.

2,3,4a β ,5 β ,8 β ,8a β -Hexamethyl-4a β ,5,8,8a β -tetrahydro-1,4-naphthoquinone, 11

This adduct was studied in spite of the dismal yields (<5%) of its preparation because it is the only substrate other than 9 which has been reported to date to undergo γ -hydrogen abstraction by enone carbon in solution^{24b}. The study of its structure and reactivity in the solid state was desirable if for no other reason than to ensure that the solid state reactivity of 9 was not an isolated case and thus provide a firmer ground for any conclusions which may be drawn from this reaction.

Compound 11 was obtained as pale yellow rods from petroleum ether as the crystallizing solvent. It reacted in KBr and as the pure solid below the eutectic temperature (60.5°) to give enone-alcohol 11A and ene-dione 11B in a combined isolated yield of 85%. Of the two



photoproducts the ene-dione 11B was favored 2:1 over the enone-alcohol 11A. The 11A:11B ratio was shown to be invariant at varying conversions of the starting material (Table XII) which is to be expected in a reaction in which both products are primary products and are photostable

Table XII. Product Yields and Ratios for the 11 \rightarrow 11A + 11B Conversion

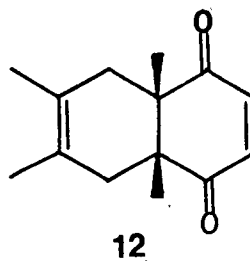
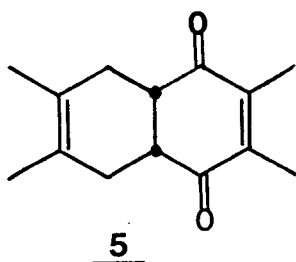
<u>Reaction Temperature</u>	<u>% Conversion</u>	<u>Combined Yields</u> <u><u>11A</u> + <u>11B</u></u>	<u><u>11A:11B</u></u>
-32.4° to -31.7°	100%	85%	1:2
-31.6° to -27.3°	100%	86%	1:2
-32.1° to -31.5°	56%	81%	1:2
-32.0° to -30.9°	57%	95%	1:2
-31.9° to -31.6°	29%	93%	1:2

under the reaction conditions. That these products are photostable was substantiated by irradiating a KBr pellet containing these two primary products for one hour. The recorded infrared spectrum showed neither new peaks nor changes in peak intensities. Pure crystals of 11A were also irradiated in a KBr matrix for 2 hours. The infrared spectrum of the irradiated pellet was identical to that of pure 11A.

The structural assignments for the two products, 11A and 11B, were made on the basis of their spectral data which were identical to those reported for compounds of identical structure isolated from the photolysate of compound 11 in benzene by Scheffer and coworkers^{24b}.

The formation of these two products is analogous to the $\underline{9} \rightarrow \underline{9A} + \underline{9B}$ conversion discussed earlier. The yields and product ratios are comparable for the two cases. By analogy to the $\underline{9} \rightarrow \underline{9A} + \underline{9B}$ transformation, photoproduct 11A most likely arises from the $^1_{n,\pi^*}$ state while the ene-dione photoproduct 11B most probably forms from the $^3_{\pi,\pi^*}$ state. As mentioned in the Introduction, methyl substitution on the ene-dione double bond and the bridgehead positions seems to be required for the observation of the $^3_{\pi,\pi^*}$ derived γ -hydrogen abstraction by carbon in this series of tetrahydro-1,4-naphthoquinones. It is understandable that the substitution of electron donating groups such as alkyl groups on the ene-dione double bond should lower the $^3_{\pi,\pi^*}$ energy level since the promotion of a π electron to a π^* level leaves the carbon(s) of the π system electron deficient. It is, however, clear

that substitution on the ene-dione double bond alone is not sufficient for the observation of γ -hydrogen abstraction by carbon since substrate 5 does not undergo γ -hydrogen abstraction by carbon in solution^{24a}. It



has not yet been determined whether methyl substitution on the bridge-head positions alone suffices for the observation of this $^3\pi, \pi^*$ reaction. The substrate necessary to decide this is compound 12 which cannot be obtained by the Diels-Alder addition of 2,3-dimethylbenzoquinone to 2,3-dimethylbutadiene (which gives exclusively 5). Substrate 12 has not been studied thus far because of this synthetic problem.

Substrate 11 not only has the same substitution pattern as 9 but the X-ray structure⁹⁷ also shows that it has the prerequisite geometry for both β -hydrogen abstraction by oxygen and γ -hydrogen abstraction by carbon.

The crystal structure was determined using a crystal measuring $0.30 \times 0.30 \times 0.70$ mm. Unit cell and intensity data were measured on a Datex-automated G.E. XRD 6 diffractometer with Cu K_α technique. Unit cell parameters were obtained by a least-squares refinement of the observed 2θ values of 16 reflections. The structure was solved using intensity data of 2051 independent reflections. Unlike the previously described X-ray structures, the structure of 11

could not be solved by direct methods⁴⁶. It was solved by a symbolic addition and tangent refinement procedure⁷⁹. The final R value was 0.070.

Crystal Data⁷⁹

$C_{16}H_{22}O_2$, monoclinic, space group $C2/c$ with $a=24.930(7)$, $b=7.795(3)$, $c=14.472(5)$ Å, $\beta = 101.13(3)^\circ$ and $Z=8$. Like all the tetrahydro-1,4-naphthoquinones, the molecule is twisted such that the bridgehead groups are staggered. Figure 23 is a stereo diagram of the molecule.

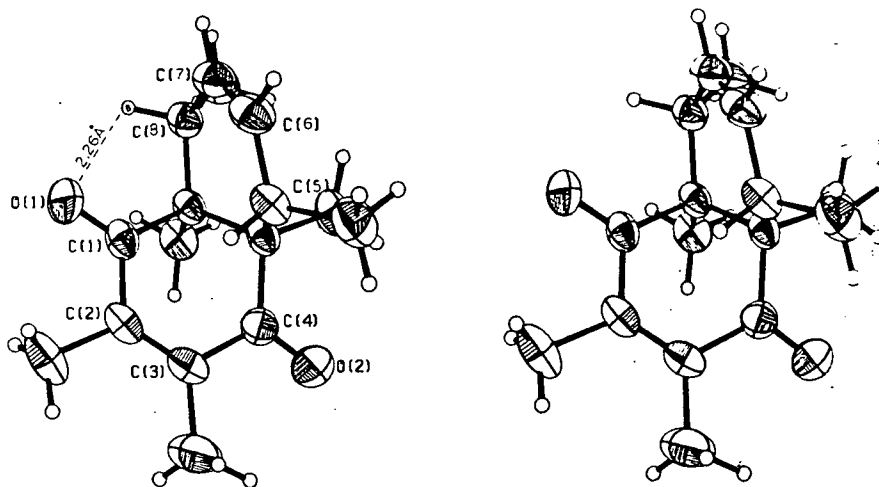
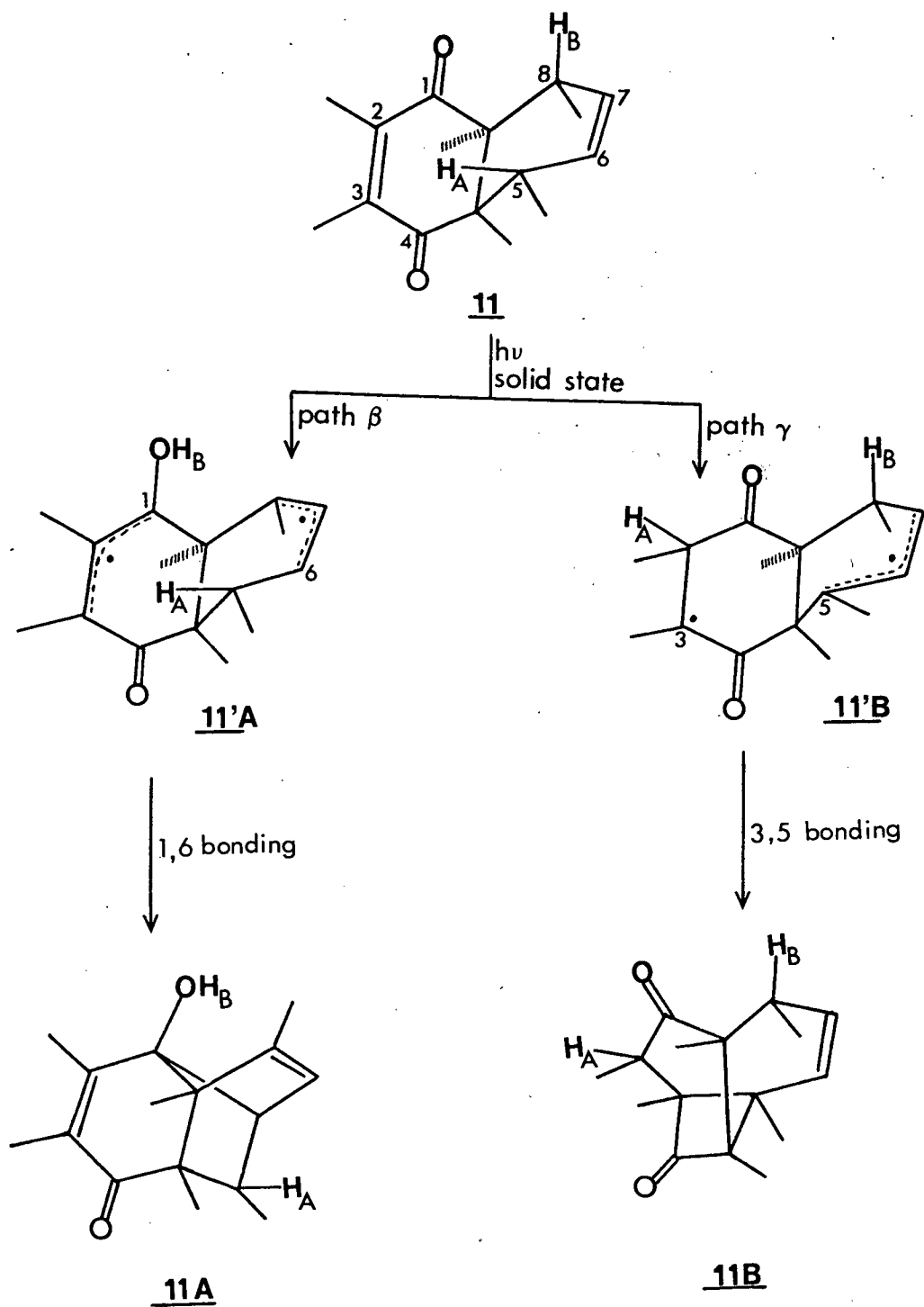


Figure 23. Stereo diagram of substrate 11.

Scheme 19



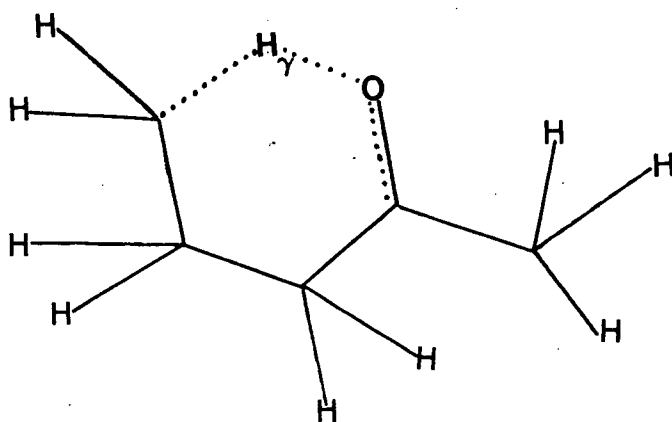
As in previous cases, the enone-alcohol product 11A arises from the abstraction of the C(8) hydrogen by O(1) followed by bond formation between carbons 1 and 6 (Scheme 19). It can be seen from the stereo diagram (Figure 23) that the C(8) hydrogen is in the plane of the C(1)=O(1) group. The H to O separation in the crystal is 2.26 \AA which is a reduction of 0.21 \AA over the corresponding distance in substrate 9. It is, in fact the shortest H $_{\beta}$ to O distance observed in this series of tetrahydro-1,4-naphthoquinones. This should facilitate β -hydrogen abstraction. Furthermore, the C(1) to C(6) separation is 3.33 \AA which is short enough for a van der Waals interaction. (The sum of the van der Waal's contact radius for the two carbons is 3.40 \AA based on \bar{r}_w values compiled by Bondi⁶⁸.) Thus the biradical intermediate 11'A (Scheme 19) can bond between C(1) and C(6) to form stable product 11A without prior conformational changes.

The formation of ene-dione 11B arises from the abstraction of the C5 hydrogen by carbon 2 followed by ring closure between C3 and C5. The C5 hydrogen is almost equidistant from C2 and C3, being 2.70 \AA from C2 and 2.66 \AA away from C3. The situation is completely analogous to the case of molecule 9 where this hydrogen is 2.89 \AA and 2.80 \AA , respectively from C2 and C3. The relatively shorter hydrogen to carbon separations in 11 should result in a comparatively faster abstraction process. The comparatively shorter irradiation times for the complete conversion of 11 to products may be a manifestation of the nearness of both the C(8) hydrogen and the C(5) hydrogen to the

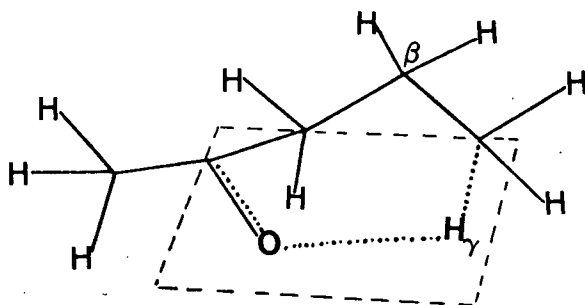
abstracting atoms. As in the case of substrate 9, the abstraction of the C(5) hydrogen by C(3) through a five-membered transition state is not observed. Photoproduct 11B arises from the abstraction of the C(5) hydrogen by C(2). The resulting biradical 11'B then closes its radical centres by bonding C(3) to C(5). The C(3) to C(5) separation in the crystal is a short 3.17Å and so here, as in all previous cases, the biradical intermediate can close to product from the conformation in which it is formed, i.e. no conformational changes are required for the conversion of substrate 11 to stable photoproducts.

The Geometry of the Transition State for β - and γ^C -Hydrogen Abstractions

Ever since the publication by McLafferty and coworkers⁴³, of the molecular orbital calculations on the transition state geometry for γ -hydrogen abstraction in 2-pentanone, a number of investigators have probed the geometric requirements not only for the McLafferty rearrangement but also for the photochemical Norrish Type II reaction. In the original paper cited, Boer, Shannon and McLafferty examined a number of conformations for the six-membered cyclic transition state including non-planar ones and found that the energy barrier to abstraction has a minimum when the abstractable hydrogen is in the plane of the carbonyl group. They cited two geometries which have this arrangement:- one of these, shown below, has all the ring atoms of the six-membered transition state in the same plane with a favorable H_Y-O distance of 1.1Å but unfavorable eclipsing of the methylene hydrogens;



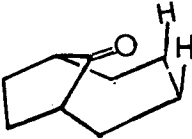
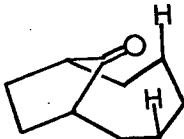
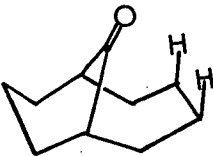
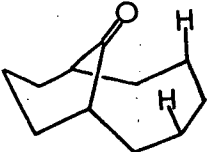
the second geometry, a non-planar one which has all the hydrogens staggered, is shown below. Its calculated energy was roughly the same as that of the planar one previously discussed. In this latter



conformation all six atoms of the six-membered cyclic transition state except C_β are in the same plane. With normal bond distances and angles assumed, McLafferty and coworkers found the $H_\gamma-O$ distance to be a considerably longer, 1.81\AA , compared to the 1.1\AA for the planar conformation. Since the McLafferty rearrangement had earlier been shown to occur only when the $H_\gamma-O$ distance was 1.8\AA or less^{41,80}, McLafferty and coworkers⁴³ concluded that the transition state geometry

for γ -hydrogen abstraction was most likely planar. What happens, then, in rigid systems where planarity cannot be achieved? Does the rearrangement still occur? To answer these questions, Henion and Kingston⁴² investigated a bicyclononanone, two bicyclodecanones and a bicycloundecanone. Using Dreiding molecular models, they measured the distance $H_{\gamma}-O$ and the angle τ which the approaching hydrogen makes with the plane of the carbonyl group at the position of its closest approach to the oxygen. They then investigated their mass spectra. Their results are summarised in Table XIII.

Table XIII. Effects of Structure on the McLafferty Rearrangement

<u>Ketone</u>	<u>H_{γ} to O distance, Å</u>	<u>τ°</u>	<u>Occurrence of the McLafferty Rearrangement</u>
	1.6	80	No
	1.6	50	Yes
	2.0	80	No
	1.5	50	Yes

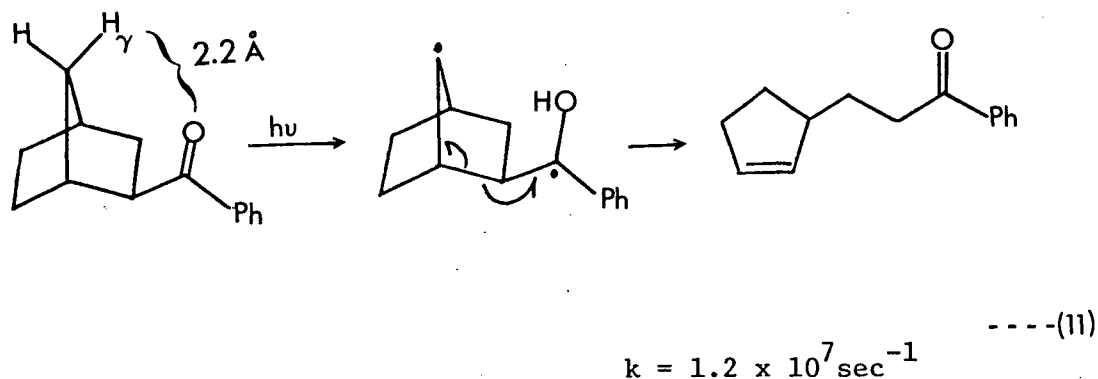
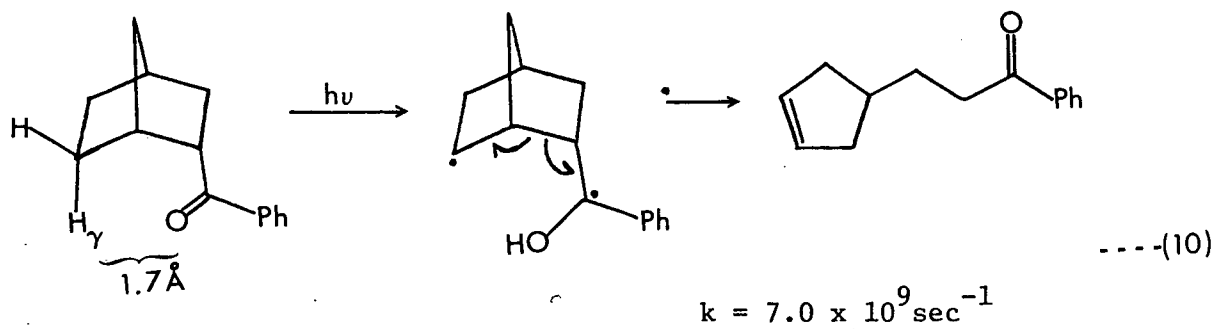
In the earlier calculations⁴³ the transition state geometry in which $\tau=45^\circ$ has an estimated energy which is 76.3 kcal above that of the planar transition state geometry. Table XIII clearly shows that while a planar six-membered ring may be the most favorable geometry energetically for flexible molecules, it is not by any means a sine qua non for the occurrence of the McLafferty rearrangement.

Turning now to photochemical hydrogen abstractions, it is important to note that both the Norrish Type II reaction and the McLafferty rearrangement require an electron-deficient carbonyl system. In the McLafferty rearrangement, this is attained by electron removal during ionization while the photochemical system relies on the promotion of an electron from an n orbital into an antibonding π^* orbital. The net effect of electron promotion is to leave an electron-deficient oxygen. It is, therefore, not surprising that the photochemical abstraction reaction has a few characteristics in common with the thermal McLafferty rearrangement. For example, for both reactions γ -hydrogen abstraction is more facile for secondary hydrogens than for primary hydrogens. However, there are some differences worth noting when discussing the geometries of the activated complex for these reactions.

In the ground state, the carbonyl carbon is sp^2 hybridized and the C=O bond length is approximately 1.2\AA . In the excited state, the carbonyl carbon of formaldehyde and presumably other saturated ketones and aldehydes is sp^3 hybridized and the C=O bond is longer than it is in the ground state by about 0.1\AA ^{81a}. In addition, the C=O bond

of the excited molecule is out of plane of the CH_2 group by 27° and 35° for the singlet and triplet n, π^* states respectively^{81a}. Overall, the geometric change is one of a planar ground state molecule becoming pyramidal in the excited state. Such is, however, not true for conjugated carbonyl compounds as revealed by the spectroscopic studies of a number of investigators⁸¹. There are two important consequences of conjugation. First, it has been established⁸¹ that conjugation stabilizes the planar geometry relative to the pyramidal one. For example, the analyses of the n, π^* absorption spectra of propenal^{81c} and propynal^{81d} have shown that the C-C-O angle changes by only 3° and 5° , respectively, from the ground state values. This is in sharp contrast to the reported change of $20\text{--}27^\circ$ for formaldehyde^{81a,e}. The second effect of conjugation is that excitation is no longer confined to the carbonyl group^{81a} and both the C=C and C=O bonds in propenal undergo bond lengthening although the latter's increase is more pronounced. For propenal and propynal the C=O bond lengthens by 0.08\AA ^{81c} and 0.095\AA ^{81d} respectively as a result of n, π^* excitation. In summary, α, β -unsaturated carbonyl chromophores are expected to retain their planar configuration upon n, π^* excitation in contrast to their saturated analogs which are planar in their ground state but pyramidal in the excited state. This difference in geometry has to be borne in mind when discussing transition state geometries for photochemical hydrogen abstraction reactions. There are indications that although the Norrish II reaction and the McLafferty rearrangement both involve the

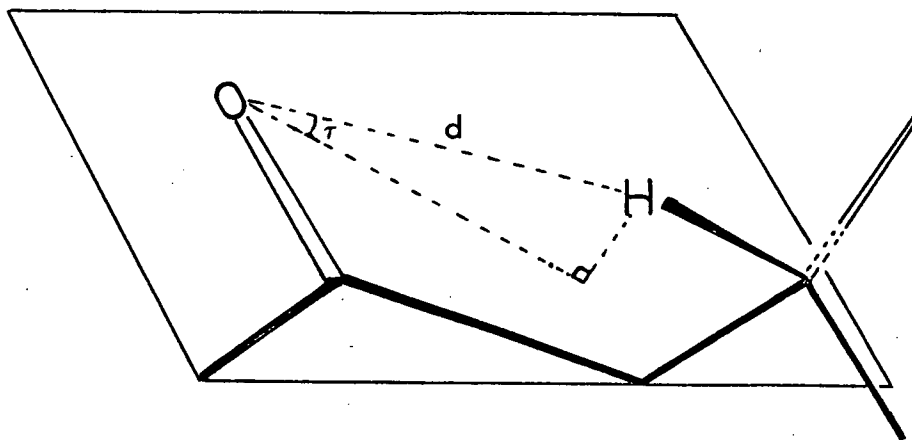
abstraction of a γ -hydrogen via a six-membered transition state, the two transition states have different geometries. For example, Lewis and coworkers⁴⁴ found that both endo- and exo-2-benzoylnorbornane undergo the Norrish II photoelimination reaction. Their molecular models revealed that the abstractable hydrogen, H_γ , comes within 1.7\AA of the carbonyl oxygen in the endo isomer. The corresponding closest approach H_γ to O distance in the exo isomer was, however, a relatively long 2.2\AA . Although this greater H_γ to O distance was reflected by the ~ 600 fold difference in the rates of hydrogen abstraction for the two substrates (equation 10 and 11), the fact that the exo-



isomer reacted at all shows that for photochemical hydrogen abstraction reactions the H_Y-O distance is not limited to the 1.8\AA maximum established for the McLafferty rearrangement. Perhaps a better guide for the H_Y to O distance requirement should be the sum of the van der Waals radii, r_w , of the two atoms involved, namely, hydrogen and oxygen. Van der Waals radii differ widely depending on the method of their calculation. For instance, the van der Waals radii, r_b , calculated by Pauling's approximation for H and O are 1.06 and 1.42\AA , respectively⁶⁸. Use of these values would give the maximum H-O contact distance of 2.5\AA reported by Winnik and coworkers⁸². However, as pointed out by Bondi⁶⁸ and Edward⁸³ the "best" values for the van der Waals radii of various elements which are compatible with X-ray crystallographic data and are best suited for volume calculations are those designated \bar{r}_w . If one depicts the interaction between the two atoms involved in the abstraction reaction as two colliding spheres of radii $\bar{r}_w(O)$ and $\bar{r}_w(H)$ respectively, then the contact distance between the two atoms will be the sum of these two radii. Using $\bar{r}_w(O)$ and $\bar{r}_w(H)$ values from the recent calculations of Bondi yields a sum of 2.72\AA . This value represents an upper limit on the distance requirements for the abstraction of a hydrogen by oxygen. The lower limit will be represented by the length of the OH bond itself⁸⁴. Thus, for the observation of hydrogen abstraction by oxygen, the H to O separation, d , must be such that $2.72\text{\AA} \geq d > 0.96\text{\AA}$. This condition is calculated for ground state atoms but should hold for n, π^* state hydrogen

abstractions by oxygen. The abstraction involves the half-filled n orbital of oxygen which is included in the ground state atomic radius, \bar{r}_w . The analogous distance requirement, d , for hydrogen abstraction by carbon will be $2.90\text{\AA} \geq d > 1.07\text{\AA}$ using the sum of the \bar{r}_w^{68} for C and H for the upper limit and the length of the C-H bond⁸⁴ as the lower limit.

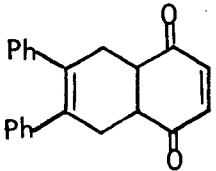
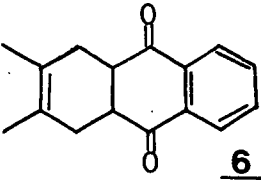
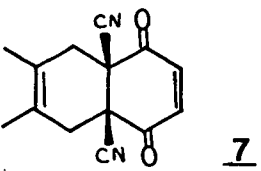
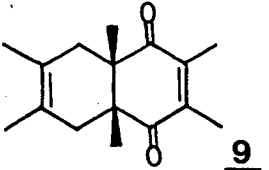
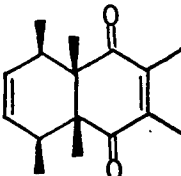
The second parameter which has been used to define the geometry of the transition state is the angle τ defined as the angle that the itinerant H makes with the plane of the carbonyl group. This angle is shown diagrammatically below. The H_β to O distances and the τ



values for the substrates found to undergo β -hydrogen abstraction are tabulated in Table XIV below. Also given in this table are the H_γ to C distances and τ' values for the substrates for which γ -hydrogen

abstraction by carbon was observed. For β -hydrogen abstraction, all the $H_{\beta}O$ interatomic separations were below the stipulated maximum

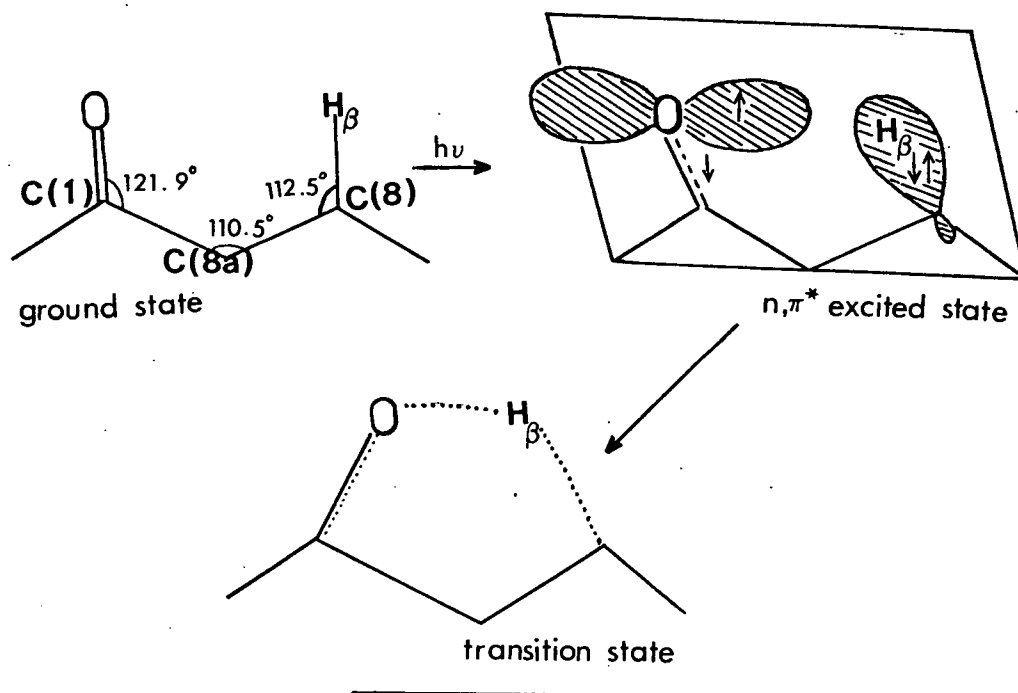
Table XIV. Interatomic Distances, Å, and Approach Angles for Hydrogen Abstraction

Substrate	H_{β} to O ($H_B(5)$ to O(1))	H_{γ} to C ($H_A(5)$ to C(2))	τ°	τ'°
 <u>4</u>	2.46	-	3°	-
 <u>6</u>	2.57	-	5°	-
 <u>7</u>	2.58	-	8°	-
 <u>9</u>	2.47	2.89	0°	52°
 <u>11</u>	2.26	2.66	1°	50°

separation. The distance requirement is, therefore, well met. Also as the τ values indicate, in all cases the hydrogen to be abstracted is also in the plane of the carbonyl group, the out of plane angle being $\leq 8^\circ$ in every case. Substrate 9 affords the ideal case with $\tau=0^\circ$ i.e. the hydrogen lies exactly in the plane of the carbonyl group. Using the X-ray data for this substrate⁷⁷, some important information can be glimpsed about the geometry of the transition state.

The transformation leading to the biradical precursor of enone-alcohol 9A and all enone-alcohols, in general, most likely involves the abstraction of one of the C8 hydrogens by the half-filled n-orbital of O(1). The hydrogen which is abstracted is the one which is closest to and in the plane of the C(1)=O(1) group. This is evident from the lack of enone-alcohol formation in irradiated crystals of 10 in which the C(8) hydrogen is remote and out of plane with the C(1)=O(1) group. In substrate 9, atoms O(1), C(1), C(8a) and the hydrogen to be abstracted all lie in the same plane. The C(8) atom is calculated to be only 16° above the plane of these four atoms. The bond angles (Scheme 20) are also in excellent agreement with the expected values of 120° and 109.5° for sp^2 and sp^3 hybridized carbon, respectively. Since the angle for planar cyclopentane is 108° , there will be some angle strain at the transition state if, as is expected, C(1) remains sp^2 hybridized. Although, a planar cyclopentane-like transition state for substrate 9 has undesirable eclipsing of its C(8a) bridgehead methyl and the unabstracted C(8) hydrogen, it must be

Scheme 20



borne in mind that this strain is present in the substrate rather than introduced at the transition state. Turning now to the γ -hydrogen abstraction by carbon, the H_γ -C separation, d , for substrates 9 and 11 are 2.89 and 2.66 Å, respectively. Both distances satisfy the interatomic separation requirement stipulated for this reaction. Unlike the case of β -hydrogen abstraction, the approach angle τ deviates significantly from zero. As Table XIV shows, the hydrogen approaches the plane of the C2, C3 double bond at angles of 50° and 52° respectively for substrates 9 and 11. Interestingly, this is the same as the approach angle, τ , estimated from molecular models by Henion and Kingston⁴² for the McLafferty rearrangement of bicyclo[5.2.1]decan-10-one

and bicyclo[5.3.1]undecan-11-one. The only transition state geometry compatible with the X-ray structure of substrates 9 and 11 turns out to be a boat (Figure 24) not a chair-like cyclohexane ring as suggested by Wagner and coworkers⁷⁸ for acyclic substrates. Since the boat-like conformation is forced on the transition state, no doubt,

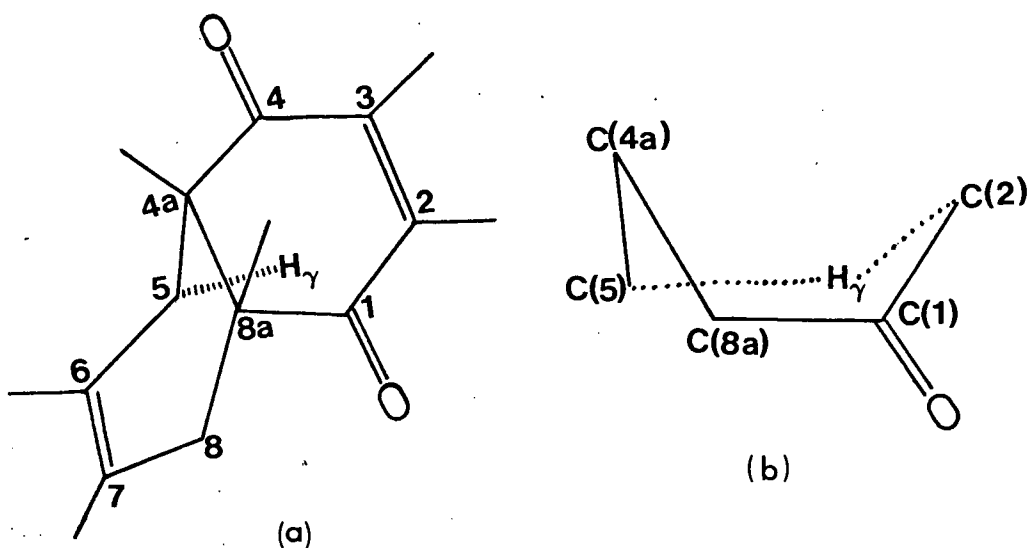


Figure 24. (a) Ground state geometry of substrate 9 and (b) the proposed transition state geometry for the 9 → 9B conversion.

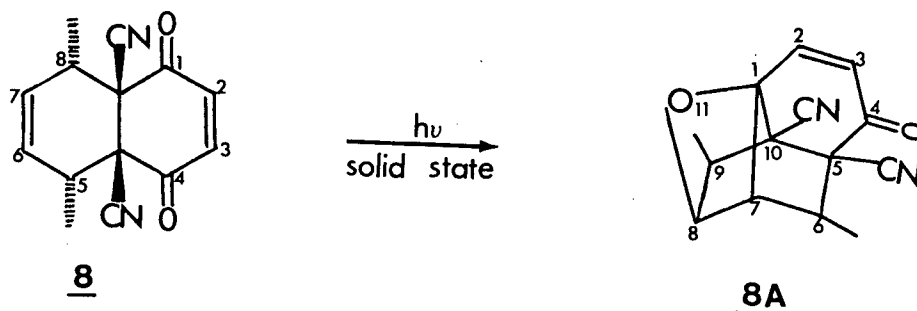
by the decalin ring structure of 9 and 11, the possibility of a chair-like transition state for mobile systems cannot be ruled out. It does mean however that the conformation of the transition state for these hydrogen abstraction reactions is not required to be a strain-free chair.

The abstraction of a γ -H by carbon in substrates 9 and 11 most likely involves the half-filled π orbital of C(2). As mentioned earlier, quenching studies^{24b} have shown the reaction to involve a triplet excited state, most likely a $^3\pi, \pi^*$. In contrast to the β -hydrogen abstraction discussed earlier, the hydrogen abstracted does not lie in the plane of the reactive chromophore, namely the C(2)=C(3) π system. Rather, it approaches C(2) from above the C(2), C(3) plane at an angle of 52° . The suggested six-membered transition state is in a boat conformation.

3. Intramolecular Oxetane Formation

4a β ,8a β -Dicyano-5 α ,8 α -dimethyl-4a β ,5,8,8a β -tetrahydro-1,4-naphthoquinone, 8

Well-formed, pale yellow crystals of 8 were obtained by crystallizing from acetone-hexane. Irradiation of 8 both in a KBr matrix and as the pure solid below the eutectic temperature (123.5°) led to the formation of 5,10-dicyano-6,9-dimethyl-11-oxatetracyclo-[6.2.1.0.^{1,7}0^{5,10}]undec-2-ene-4-one 8A as the sole product. Irradiation of solutions of 8 also give oxetane 8A as the sole photoproduct^{24b}.



Ultimate proof of the product structure came from comparing its spectra with those of authentic 8A prepared by photolysis of 8 in benzene. The X-ray structure of 8A prepared by this latter method has been determined.

The 8 \rightarrow 8A conversion is an intramolecular [$\pi_2^s + \pi_2^s$] addition of a carbonyl functionality to an olefinic moiety. Recent studies on this type of intramolecular photocyclization show that the reaction can occur from the n, π^* singlet as well as from the π, π^*

triplet depending on the intersystem crossing efficiency of the substrate²⁸. The initial interaction of the excited carbonyl chromophore with the isolated double bond is believed to yield an exciplex which may eventually yield an oxetane. In order for the carbonyl group to interact with the olefinic π system, the two π systems must be close enough and aligned so as to have interaction between their p-orbitals. Schmidt and Rabinovich⁸⁵ found, for example, that short intermolecular $C=O \cdots C=C$ contacts of 3.49 and 3.62 Å in the two stacks of 2,5-dimethyl-p-benzoquinone and a parallel arrangement of the two π -systems favored oxetane formation upon irradiation.

X-ray structure determination was carried out⁸⁷ on a single crystal of 8 measuring 0.50 x 0.30 x 0.30 mm. Unit-cell parameters were refined by least squares from the observed 2 θ values of 14 reflections. The structure was solved by direct methods⁴⁶ using intensity data of 2419 independent reflections. The final R value was 0.046.

Crystal Data⁸⁷

$C_{14}H_{12}N_2O_2$, orthorhombic, space group Pbcn with $a=15.915(6)$, $b=11.525(4)$, $c=13.157(5)$ Å, $\beta=90^\circ$ and $Z=8$. A stereo diagram of the molecule is shown in Figure 25.

The formation of oxetane 8A arises from a [$\pi 2 + \pi 2$] cycloaddition between $C(1)=O(1)$ and $C(6)=C(7)$. The centre-to-centre separation, d , of these two π systems is only 3.20 Å which is shorter than the intermolecular $C=O$ to $C=C$ contacts encountered by Schmidt

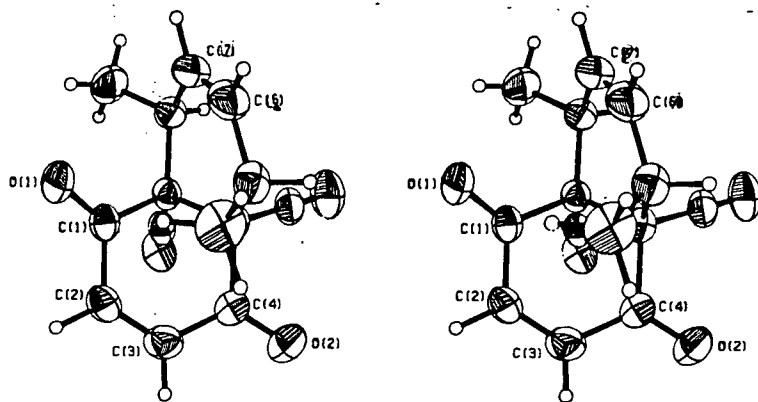


Figure 25. Stereo diagram of substrate 8.

and Rabinovich⁸⁵. But unlike their systems, the intramolecular C=O and C=C bonds involved in the 8 → 8A conversion are not parallel. The orientation of these two double bonds can be appreciated by viewing Figure 25 through a stereo viewer. The direction of the p-orbitals are along the normals to the C(1)=O(1) and C(6)=C(7) planes. The angle between these normals is 99°. This near-orthogonal arrangement of the two π systems which is diagrammatically represented below (Figure 26) promotes interaction and ultimately bond formation.

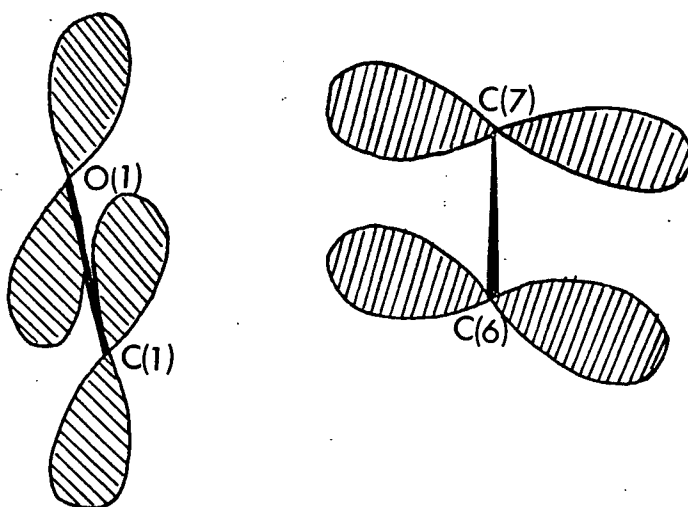


Figure 26. Approach geometry of the C(1)=O and C(6)=C(7) π bonds.

The addition involves the bonding of C(1) to C(6) and O(1) to C(7). These distances are 3.37 and 3.20 Å respectively in the crystal. Using 1.70 and 1.52 Å for the mean van der Waals radii, \bar{r}_w , for C and O respectively⁶⁸, the carbon to carbon van der Waal's contact radius is 3.40Å and that of carbon to oxygen 3.22Å. These distances are almost exactly the distances separating the potential bonding centres in substrate 8. Because of the favorable alignment of the two double bonds and the short interatomic contacts the 8 → 8A conversion can occur without major conformational changes. As the X-ray structure of 8A (Figure 27) shows, the reaction is attended by

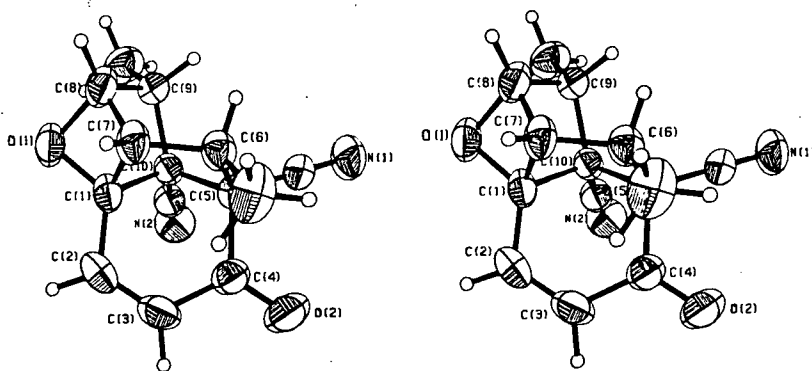


Figure 27. Stereo diagram of oxetane 8A.

very little change in the quinone ring and only shifts in the positions of C(6) and C(7) of the cyclohexene portion of the molecule.

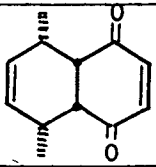
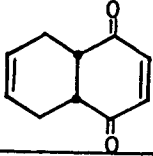
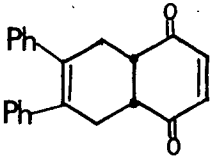
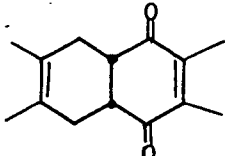
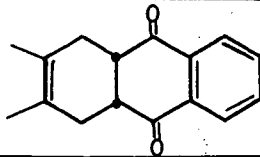
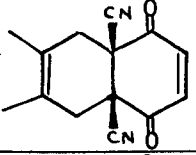
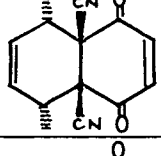
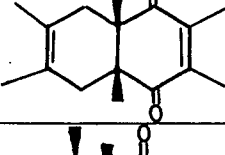
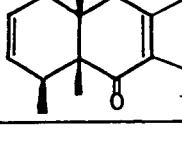
The X-ray data on photoproduct 8A were obtained and treated as in previous structure determination. The dimensions of the crystal used in the determination were 0.70 x 0.50 x 0.20 mm. Unit-cell parameters were obtained by least-squares refinement of the observed 2 θ values of 15 reflections. The structure was solved from treatment of intensity data from 1433 independent reflections. The final R value was 0.048.

Crystal Data⁸⁶

C₁₄H₁₂N₂O₂, orthorhombic, space group P2₁2₁2₁ with a=18.701(6), b=7.274(2), c=9.005(2) Å, β =90° and Z=4. The geometry of the molecule closely resembles that of its precursor 8. The oxetane ring is very distorted with all internal torsion angles greater than 30°.

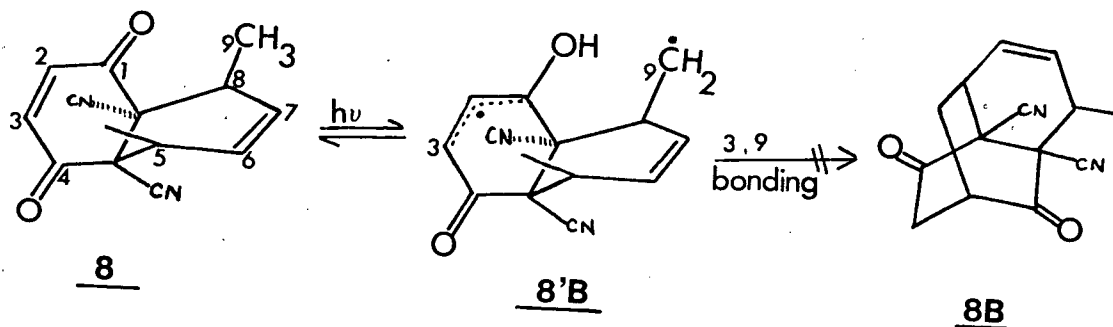
Intramolecular oxetane formation in these tetrahydro-1,4-naphthoquinones seems to be a less preferred reaction than the cyclobutane forming dimerization and the hydrogen abstraction reactions because all the substrates studied have roughly the same orientation of the C(1)=O(1) and C(6)=C(7) double bonds as does 8 and in addition have short contacts between these bonds (Table XV) and yet oxetane formation did not compete with either the dimerization or the hydrogen abstraction reactions. Arnold⁸⁸ has noted a similar trend earlier.

Table XV. Intramolecular Bond Contacts and Orientation

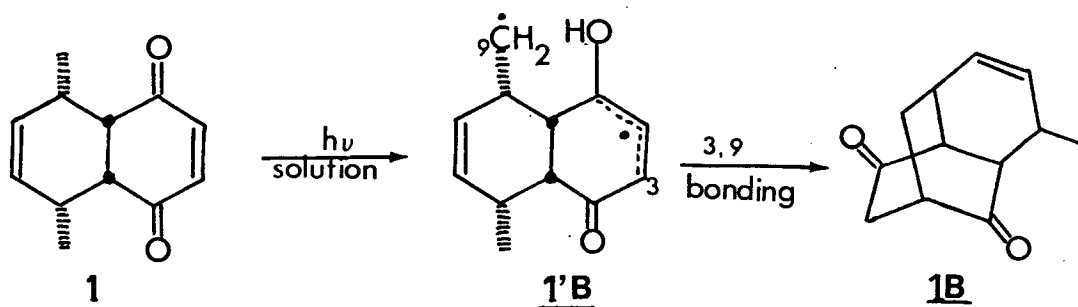
Substrate	Intramolecular C(1)=O(1)...C(6)=C(7) contact, Å (centre to centre)	Angle between normals to the C=O and C=C planes (angle between the p orbital)
 <u>1</u>	3.37	92.4°
 <u>3</u>	3.35 (Type A) 3.40 (Type B)	90.3° (Type A) 88.5° (Type B)
 <u>4</u>	3.45	87.1°
 <u>5</u>	3.41	89.5°
 <u>6</u>	3.39	89.8°
 <u>7</u>	3.26	97.3°
 <u>8</u>	3.20	99.2°
 <u>9</u>	3.29	95.1°
 <u>11</u>	3.38	91.8°

He finds that, in general, whenever a hydrogen is easily accessible to an excited carbonyl group, hydrogen abstraction becomes so important as to exclude oxetane formation.

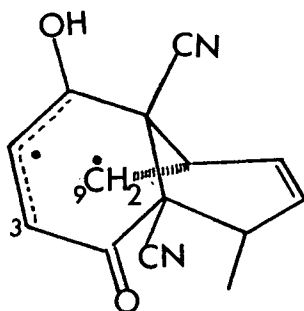
Substrates 8 and 1 are two substrates which one might expect to undergo the Norrish Type II reaction since they have abstractable γ -hydrogens. Substrate 1 did undergo the Type II reaction in solution but not in the solid state because favorable intermolecular contacts in the crystalline state permitted a much preferred dimerization to occur. With unfavorable intermolecular contacts, substrate 8 might be expected to undergo the Type II reaction, especially since the γ -hydrogen to oxygen distance is only 2.41\AA which compares favorably with H-O distances of 2.58\AA or less for the observance of hydrogen abstractions discussed earlier. However, in order for a substrate to give stable products arising from hydrogen abstraction, it has to be able to not only abstract the hydrogen but also close its radical centres. For substrate 8 this means forming a bond between carbons 3 and 9 in the biradical 8'B without gross changes in conformation. These centres are $>4\text{\AA}$ apart in the crystal of 8.



Thus, Norrish Type II products cannot form from the conformations in which these tetrahydro-1,4-naphthoquinones crystallize. The formation of the Type II product 1B during the solution photochemistry of 1 must then be seen as a manifestation of biradical 1B''s ability



to change conformation to one which permits ring closure between carbon centres 3 and 9. For biradical 8'B the change from its original conformation to one such as shown below which permits C3 to C9 bonding, requires that the bridgehead cyano groups be moved,



first, towards each other, then be eclipsed and finally past each other. The final conformation is, probably, as good as the initial one but the process of attaining it is energetically unfavorable

because of dipole-dipole repulsion between the cyano groups. So the difference in reactivity between 1 and 8 in solution is most likely due to the ability of biradical 1'B and not 8'B to change conformation.

4. Unreactive Substrates

2,3,6,7-Tetramethyl-4a β ,5,8,8a β -tetrahydro-1,4-naphthoquinone, 5

Colorless needles of this compound were obtained by crystallizing from petroleum-ether. One of these crystals measuring 0.25 x 0.10 x 0.10 mm was used for X-ray structure determination. Unit cell parameters were obtained by least-squares refinement of the observed 2θ values of 19 reflections. The structure was solved using intensity data of 2442 independent reflections. The final R value was 0.072.

Crystal Data⁸⁹

$C_{14}H_{18}O_2$, monoclinic, space group $P2_1/c$ with $a=5.245(2)$, $b=29.452(7)$, $c=8.278(5)$ Å, $\beta=106.44(4)^\circ$ and $Z=4$. A stereo view of the molecule is shown in Figure 28.

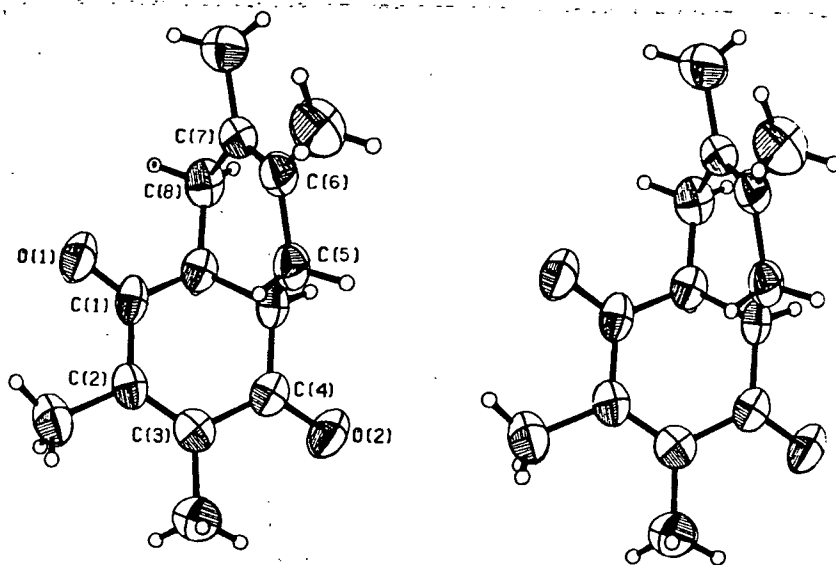
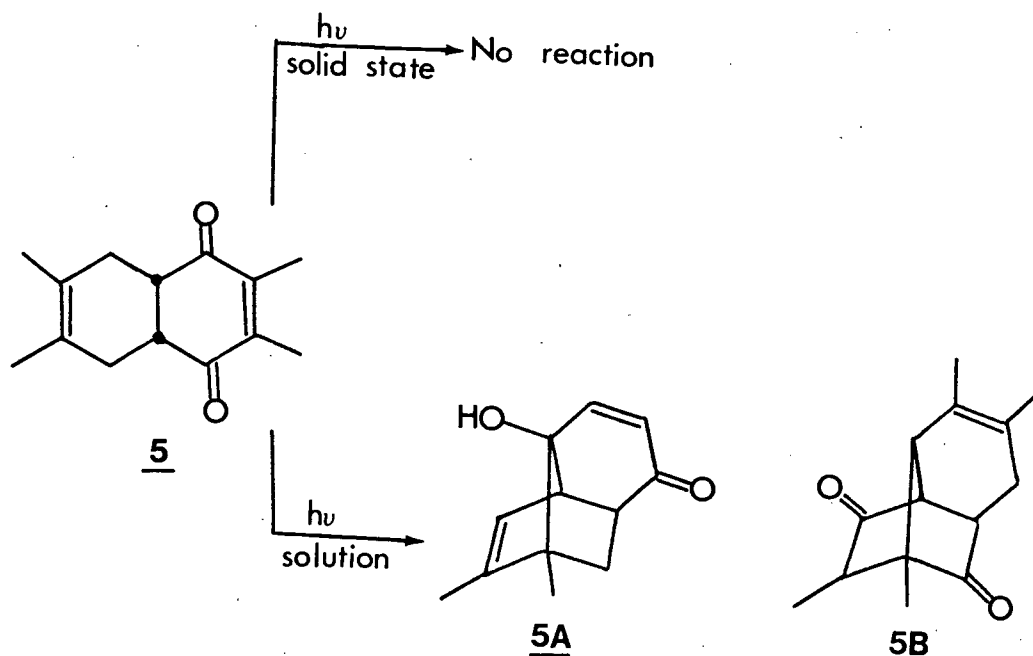


Figure 28. Stereo diagram of substrate 5.

Irradiation of crystals of 5 either in a KBr matrix or as the pure solid in vacuo led to no detectable reaction. In solution, however, this substrate is reported to give photoproducts 5A and 5B



both arising from β -hydrogen abstraction by oxygen.

The X-ray data showed that 5 had the conformational requirements to undergo β -hydrogen abstraction. The O(1) to H_β distance is 2.42\AA and the C(1) to C(6) separation is 3.49\AA . So, one would expect O(1) to abstract H_β upon UV irradiation with subsequent bond formation between C(1) and C(6) to give enone-alcohol 5A. As in previous examples, photoproduct 5B is not expected to form in the irradiation of 5 in the solid state. The inertness of 5 to irradiation is particularly surprising since compound 4 in which the H_β to O(1) distance is 2.46\AA and the C(1) to C(6) separation was

3.51Å did react to give the expected enone-alcohol. These inter-atomic separations are almost exactly equal to the H_β to O(1) and C(1) to C(6) separations in substrate 5. A possible explanation for 5's inertness resides in the crystal packing. Figure 29 shows two adjacent molecules within a crystallographic cell. The C(1)=O(1)

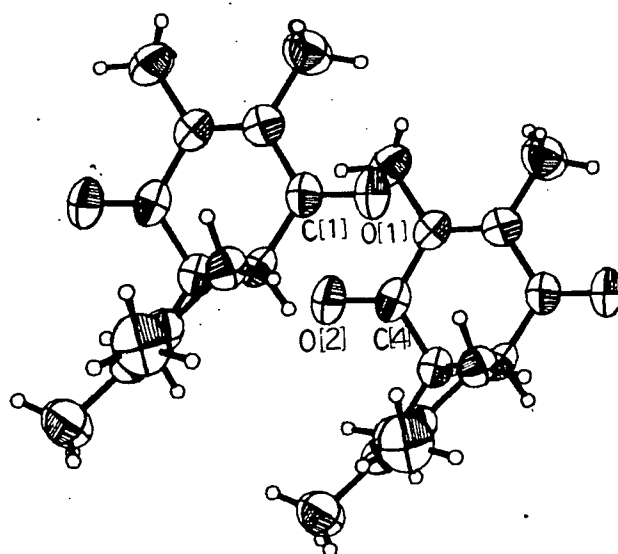


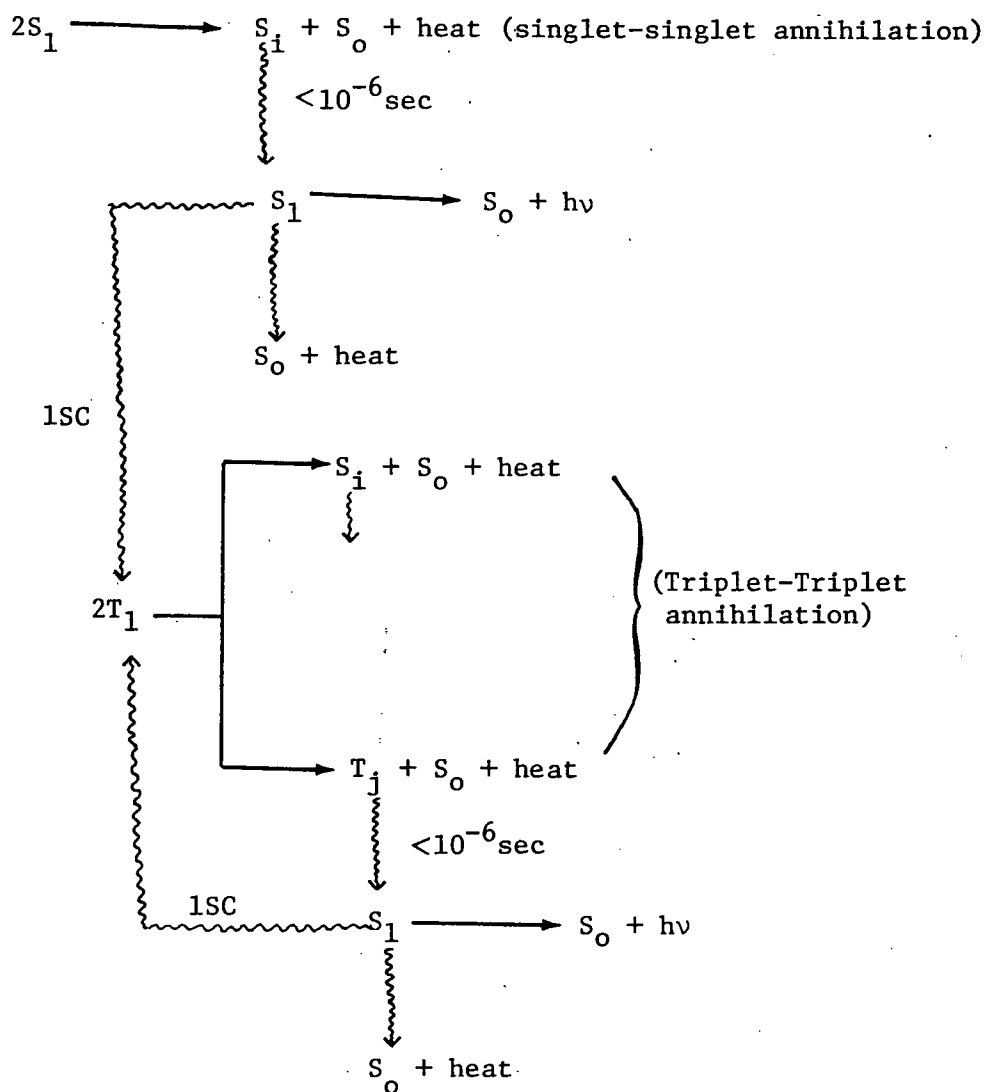
Figure 29. Two adjacent molecules of 5 within a crystallographic cell.

carbonyl group of one molecule lies above the C(4)-O(2) carbonyl group of a second molecule. The angle between the normals to the planes of the two carbonyl groups is only 16.4°. So they are almost in a parallel orientation and the two π systems should interact provided they are close enough to each other. The centre-to-centre double bond separation for these two carbonyl groups is 3.65Å which is certain to promote a strong interaction between these two chromophores. Of the two carbonyl groups only C(1)=O(1) is conformationally capable

of β -hydrogen abstraction upon irradiation. From a crystallographic viewpoint, there are two possible reasons for the photostability of 5 in the solid state but not in solution. The short intermolecular separation of the two carbonyl groups may be giving rise to (i) exciton migration and self-quenching and/or (ii) an interaction between an excited molecule and an unexcited neighbour giving rise to an excimer which subsequently decays and dissociates to two ground state molecules. In connection with the first of these two possibilities, it has already been mentioned in the Introduction that both singlet and triplet migrations are known to occur in crystals and the wandering of the triplet is usually more extensive than that of the singlet partly as a result of the longer lifetime of the triplet state. During migration, the excitation energy is frequently scattered by lattice vibrations until it decays optically or thermally. In addition, migration also promotes the interaction between two excitons. The interaction can be between two singlet excitons or two triplet excitons, the latter interaction is more frequently encountered than the former again because the triplet state lives longer, wanders more extensively and, therefore, has more probability of interacting with another triplet exciton than the singlet. During this intermolecular exciton interaction, one member of the pair comes off with a higher excitation energy than it initially had and the other molecule is deexcited to the ground-state. The electronic energy of the excited partner is usually less than the combined energies of the two excited states since some of the electronic energy

is lost to the lattice as heat during the interaction. The process is known as singlet-singlet annihilation⁹⁰ when the excitons involved are singlets and referred to as triplet-triplet annihilation⁹⁰ when two triplets are involved. The 'new' excitons, S_i and T_j (Scheme 21) cascade down to the lowest singlet which may continue its migration

Scheme 21

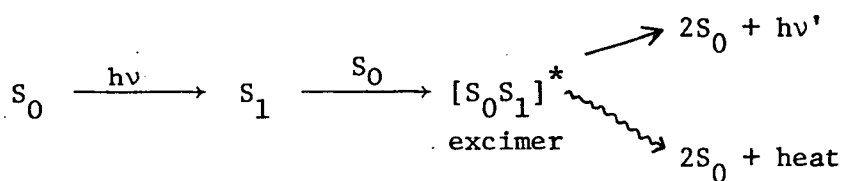


till another annihilation sets in or until it thermally or optically loses its excitation energy. In the quenching of irradiated crystals of 5, host-sensitization²¹ in which the lattice rather than impurities play the major role of transmitting the excitation energy from one part of the crystal to another, is most likely to be the key deactivation pathway. Nevertheless, the possibilities of dislocations and impurities also playing a role cannot be ruled out.

The second possible major path for deactivation, namely, excimer or σ -bond formation and decay requires an association between one excited molecule and one unexcited molecule. The interaction, may or may not entail σ bond formation between the two partners. In the case where the interaction does not entail bond formation, the excited species will resemble an intermolecular exciplex. Since the intermolecular C(1)=O(1) to C(4)=O(2) distance of 3.65Å in 5 is almost equal to the 3.62Å contact of C=O to C=C which permitted oxetane formation in 2,5-dimethyl-p-benzoquinone⁸⁵, the formation of a 1,3-dioxetane as a transient intermediate during the irradiation of crystals of 5 is at least conceivable. To date, no 1,3-dioxetanes have been reported in the literature. Nonetheless, its formation as a transient intermediate followed by facile decomposition to two carbonyl fragments would closely parallel the behaviour of known 1,2-dioxetanes. So that, whatever the nature of the excimer, $(S_0S_1)^*$, it readily decays thermally or photochemically to two ground state molecules. This second mode of deactivation of excited molecules of

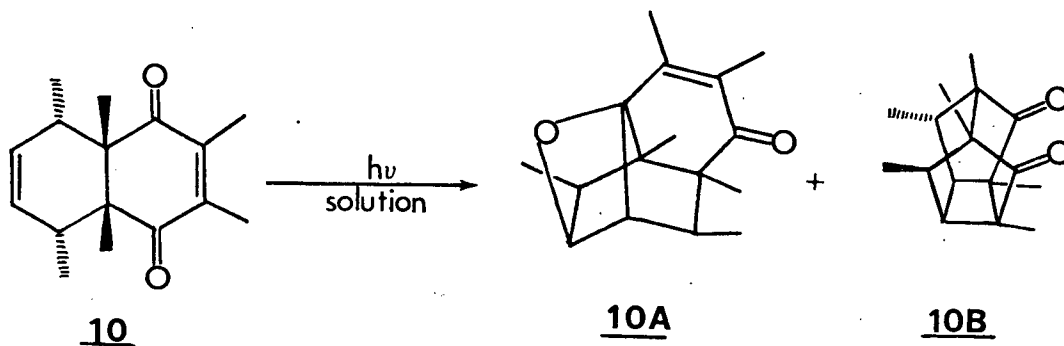
5 in the solid state is summarised in Scheme 22 where S_0 denotes the substrate 5 in its ground state and S_1 denotes 5 in its first excited state.

Scheme 22

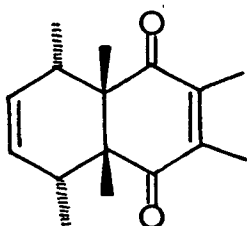


2,3,4a β ,5 α ,8 α ,8a β -Hexamethyl-4a β ,5,8,8a β -tetrahydro-1,4-naphtho-quinone, 10

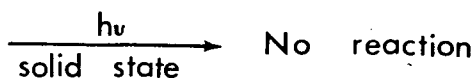
This adduct crystallized out of hexane as low melting rods (mp 52-54°). The X-ray structure of this molecule is not yet available. Nevertheless, its behaviour under UV irradiation in the solid state was studied because it was reported^{24b} to give photolabile oxetane 10A and the caged compound 10B when irradiated in solution. Given the conformation in which all the tetrahydronaphthoquinones so far



studied crystallize, one does not expect 10B to be formed in a lattice-controlled solid state reaction, but 10A might be expected to form by analogy to the 8 \rightarrow 8A conversion previously described. Irradiation of 10 in a KBr matrix gave no reaction in up to 2 hours of irradiation. In the infrared spectrum recorded after 6 hours of irradiation, broadening in the 5.67-5.78 μ region was observed. After 17 hours two new carbonyl absorptions at 5.70 and 5.76 μ became prominent. These absorptions could be due to the caged isomer, the carbonyl absorptions of which have been reported^{24b} at 5.68 and 5.75 μ . Oxetane 10A could also be present but undetected in the infrared since its carbonyl absorption at 6.04 μ coincides with the absorption of residual 10 at 6.00 μ . The long induction period for the appearance of these product(s) and the fact that the KBr pellet was irradiated at room temperature with no provision for preventing the pellet from heating up strongly suggested that the reaction was occurring from the melt and not from the solid. To further substantiate this, pure crystals of 10 were irradiated in vacuo at lower and controlled temperatures to ensure that it stayed solid. Irradiation at 0.03 torr at temperatures between -9.9° and -9.1° for 14 hours gave 95% of recovered material which was shown by thin layer chromatography, infrared and NMR to be identical to the



10



starting material 10. Another trial run at 0.03 torr and slightly higher temperatures (-1.4° to -0.5°) for 13 hours also led to no reaction.

As mentioned earlier, the 4a,5,8,8a-cis-tetrahydro-1,4-naphthoquinones which have thus far been studied seem to prefer cyclobutane ring forming dimerization and hydrogen abstraction to intramolecular oxetane formation. But as has been shown by the 8 → 8A conversion, when none of these preferred reactions is possible, oxetane formation can be observed. The formation of oxetane 10A in solution but not in the solid state may mean that excited 10 crystals have some efficient means of deactivating to ground state which the molecules in solution do not have. But without the X-ray structure, it cannot be ascertained whether this is a crystal packing effect as in the case of substrate 5 or some other conditions peculiar to the crystalline state.

In summary, the four reaction types encountered during UV irradiation of a number of tetrahydro-1,4-naphthoquinones in the solid state can be rationalised in terms of the principle of least motion also known as the topochemical principle^{12,45}. Cohen^{13a} has recently elaborated on this principle. He defined a "reaction cavity" as the space occupied by a reactant molecule or molecules as the case may be. The size and shape of this cavity is determined by the structure and geometry of the molecules of the substrate(s). The topochemical principle is then interpreted to mean that a lattice-controlled transformation proceeds with minimal distortion of the

surface of the reaction cavity. Within this interpretation, extrusions from the cavity as well as the creation of voids within the cavity as a result of a reaction are energetically unfavorable. Figure 30 is a diagrammatic representation of a favorable and unfavorable solid state transformation. As reaction proceeds a point is

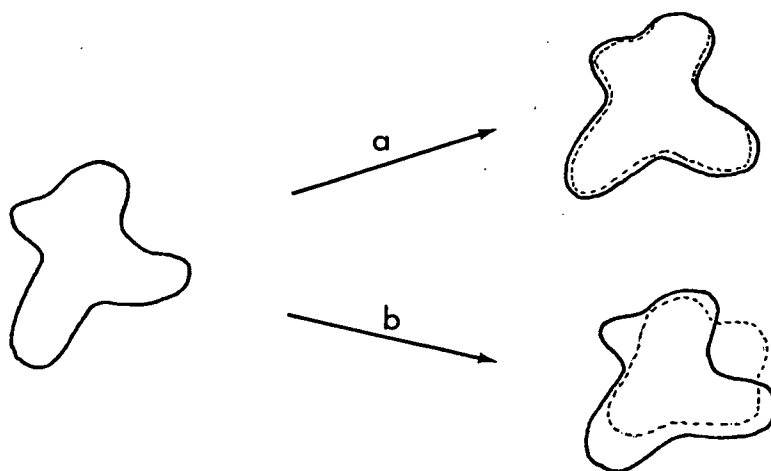


Figure 30. The reaction cavity before reaction (full line) and in the transition state (broken line) for energetically a) favorable process, b) unfavorable process.

reached when the restrictions imposed on the conformation of product molecules is relaxed and the latter then crystallize out in their own conformation. But until this stage is reached, products which have shapes most resembling those of reactant molecules or alternatively those with readily deformable structures will be easily accommodated by the host lattice. The ideal solid state transformation will be one which yields a product which is crystallographically isomorphous with the starting material. Such reactions should

proceed essentially to completion without any distortion of the crystal lattice. Wegner and coworkers⁹¹ reported one such solid state reaction.

In the reactions presented in this publication, it has been shown consistently from the X-ray data of the substrates that the transition state could be reached with hardly any change in the conformation of the substrate. Furthermore, it has been shown that only stable products which can be formed without major changes in the substrates' conformations do form in the solid state reactions.

This conformational control has permitted the estimation of certain useful reaction parameters;-

a) The cyclobutane ring forming $[\pi^2_s + \pi^2_s]$ dimerization has been shown to occur from a centre-to-centre double bond separation, d , of 4.04\AA or less and the two double bonds approach each other in a parallel orientation which allows for maximum overlap of their p-orbitals. The situation here is completely analogous to the dimerization of α -cinnamic acid crystals^{12,59}.

b) Intramolecular oxetane formation has been observed at a centre-to-centre $C=O$ to $C=C$ separation, d , of 3.20\AA . The approach of the two double bonds is such that the p-orbitals are almost at right angles. This near-orthogonal approach is also a good geometry for overlap. The distance separating the two double bonds is short compared to the corresponding separation in intermolecular oxetane forming reactions reported by Schmidt and coworkers⁸⁵. The short

contact would tend to promote a stronger interaction and ultimately ring closure.

c) The abstraction of a hydrogen β to a carbonyl group by the carbonyl oxygen has been shown to occur from a distance ranging from 2.26Å to 2.58Å.

d) The abstraction of a γ -hydrogen by the carbon of an excited enone system occurred from distances of 2.66Å and 2.89Å respectively in two substrates. The longer separation between the abstractable hydrogen and the abstracting atom here as compared to (c) above is a reflection of the larger van der Waals volume of carbon relative to that of oxygen. In both types of hydrogen abstraction, the O to H and C to H separations were less than or equal to the sum of the van der Waals radii of the two atoms involved in the abstraction.

The retention of gross conformation during the abstractions has also made it possible to define the geometry of the transition state more precisely than has hitherto been possible. The abstraction of a hydrogen β to an excited carbonyl group by the carbonyl oxygen has been shown to occur through a planar five-membered transition state. The corresponding abstraction of γ -hydrogen by carbon of an excited enone chromophore has a non-planar six-membered cyclic transition state which is, however, not in the torsion-free chair conformation proposed by McLafferty and coworkers⁴³ but rather in a boat-shaped conformation.

Overall, intermolecular effects have been found to play an important role in the photochemical behaviour of crystals of the tetrahydro-1,4-naphthoquinones studied only when intermolecular contact between unsaturated centres in adjacent molecules is $\leq 4.04\text{\AA}$. When this distance is exceeded, intramolecular processes predominate.

Lastly, the possibility of dislocations and/or defects playing a role in some of these systems cannot be overlooked especially in the 3 \rightarrow 3B conversion and in explaining the behaviour of substrates 5 and 10 in the solid state.

After the commencement of the investigations presented here, a report on gold-catalysed rearrangement of strained small ring hydrocarbons appeared in the literature⁹². There is no indication, however, that the gold metal surface on which the crystals of 1-11 were studied catalysed any of the reactions observed. This conclusion is based on the fact that all the reactions studied in the reactor were also studied in KBr matrices. The reactivity of each compound by both methods was identical.

EXPERIMENTAL

General

Eutectic Temperature

Eutectic temperatures were determined by differential thermal analyses (DTA) using a Perkin Elmer DSC-1B. In each case, the following mixtures were analysed until a sharp melting transition was observed: i) crude reaction mixture, ii) varying compositions of crude reaction mixture and added starting material. Each eutectic mixture was ground into a fine powder. In certain cases, thorough mixing was accomplished by dissolving the mixture in acetone or chloroform, removing the solvent and drying the sample in vacuo. Sample sizes used ranged from 5 to 10 milligrams. The sample was placed in an aluminum planchette and covered with an aluminum lid. Both of these accessories are available as Perkin Elmer Sample Pan Kit No. 219-0041. The lid was firmly pressed against the sample without crumpling or creasing the lid. Scanning for eutectic transitions above ambient temperature was carried out at a slope setting of 510, a differential temperature setting of 485, an average temperature setting of 522 and a scanning rate of 10°/min. Low temperature transitions were determined at slope setting 500, differential temperature setting 491, average

temperature setting 430 and a scanning rate of 5°/min. A transition was recorded as the first departure from base line i.e. at the beginning of a peak. Low temperature transitions were corrected using a calibration graph obtained by scanning for the melting transitions of n-octane (m.p. -56.8°) and ethylene glycol (m.p. -11.5°). All other temperature read-outs were corrected using a calibration graph obtained by scanning melting point standard samples. Each calibration was carried out at the appropriate instrumental settings cited above.

Melting point (m.p.)

All melting points except those indicated by asterisk(s) were taken on a Fischer-Johns hot stage melting apparatus and are uncorrected.

Melting point* (m.p.*)

The melting point of a compound found to melt at about ambient temperature was determined by sealing the sample in a capillary tube, then repeatedly freezing it in liquid nitrogen and thawing it till the walls of the tube became evenly coated with the solid. The capillary tube was then immersed in a stirred dry ice-acetone mixture which was consequently allowed to warm to room temperature. An alcohol thermometer which had been calibrated against a copper-constantan thermocouple in the region 20° to -40° was used to note the temperature of melting. The reported m.p.* was corrected using the calibration graph.

Melting point** (m.p.**)

The melting points of compounds which decompose during normal melting point determinations were carried out by the DTA method. Instrumental settings reported for eutectic temperature determinations above ambient temperature were used.

Infrared

All infrared spectra were recorded on a Perkin-Elmer 457 spectrophotometer. For solids, KBr pellets containing 1-2 mg of the sample per 250 mg of KBr were made using a Perkin-Elmer Potassium Bromide Evacuatable Die 186-0002 and a Carver Laboratory Press Model B. The pressing load was generally 20,000 lbs per square inch. Infrared spectra of liquids were recorded neat.

Nuclear Magnetic Resonance (NMR)

Spectra of starting materials 1-11 and quantitative NMR analyses were taken on a Varian T-60 instrument by the author. Spectra of photoproducts 1A-11B were recorded on either a Varian HA-100 or XL-100 by the departmental spectroscopists, Mr. W.B. Lee and Dr. O. Chan. In all cases, tetramethylsilane (TMS) was added as an internal standard.

Quantitative NMR Analysis⁹³

This was the method of choice for the determination of the extent of reaction for compounds which did not come off the GLC columns tried.

An aliquot, usually 0.3 ml, of a standard solution containing 228.3 mg of CH_3NO_2 per 10.0 ml of CDCl_3 solution was added to an accurately weighed reaction mixture using a 2 ml pipette graduated in 0.01 ml. Sample sizes used ranged from 32.5 to 101.0 mg to ensure good signal to noise ratio. The mixture was shaken well to dissolve. The solution was transferred into an NMR tube. The sample vial was washed with a few drops of CDCl_3 and the washings added to the contents of the NMR tube. The resonance used in each analysis was well resolved and removed from other resonances. The chosen resonance used in each such analysis is indicated in the Experimental. This chosen resonance and that of the internal standard were electronically integrated 4 times.

Since the H signal strength is proportional to the number of magnetic nuclei⁹³, the sample's chosen resonance strength, x , is given by

$$x \propto \frac{w_s}{M_s} \cdot a_s$$

and that of the internal standard's resonance is given by

$$y \propto \frac{w}{M} \cdot b$$

whence
$$\frac{x}{y} = \frac{w_s}{w} \cdot \frac{a_s}{b} \cdot \frac{M}{M_s}$$

and
$$w_s = \frac{M_s}{a_s} \cdot \frac{b}{M} \cdot w \cdot \frac{x}{y}$$

where w_s = milligrams of residual starting material present in the NMR mixture

M_s = molecular weight of starting material

a_s = no. of protons in the integrated resonance of the starting material

b = no. of protons in the integrated resonance of the internal standard (=3 for CH_3NO_2)

M = molecular weight of the internal standard (=61.04)

w = milligrams of internal standard in the NMR sample

x = average electronic integration of the compound's resonance

y = average electronic integration of the internal standard's resonance

The extent of reaction \equiv % conversion =
$$\frac{W - w_s}{W} \quad \text{..... (1)}$$

where W = weight of the reaction mixture used in the analysis.

In the case of the reaction of compound 6, where none of the resonances of the starting material were well resolved from the product resonances, a well resolved resonance of the product,

6A, was used instead. In this case, the substitution,

milligrams of product 6A in the NMR sample = $W - w_s$

was made into equation (1). This equality was valid in this case because the consumption of 6 resulted in the production of only 6A.

Mass Spectra

All mass spectra reported in this work are low resolution spectra obtained on a direct inlet Varian Atlas MAT CH 4-B or AEI MS-9 at 70eV and operated by the departmental analysts, Dr. G. Eigendorf, Mr. G.D. Gunn and Mr. J. Nip.

Elemental Analyses

Elemental analyses were performed by the departmental microanalyst, Mr. P. Borda.

Thin Layer Chromatography (TLC)

Thin layer chromatography carried out for analytical purposes was done on strips of aluminum-backed silica gel 60F-254 (thickness 0.2 to 0.25 mm) available from E. Merck. The developing solvent used in each instance is indicated in parentheses elsewhere in the Experimental. Preparative TLC was carried out on 20x20 cm glass plates coated with silica gel GF-254 (thickness 0.7 to 0.8 mm) which had been dried in air and then at 45-50° overnight.

Column Chromatography

Two types of adsorbents were used: silica gel 60 (particle size less than 0.063 mm) from E. Merck and Woelm's neutral aluminum oxide activity grade 1. The adsorbent and eluent used in each instance are indicated in parentheses.

Gas Liquid Chromatography (GLC)

GLC separations were carried out on either Varian Aerograph 90-P or a Varian Autoprep A-700 instruments connected to Honeywell Elektronik 15 strip chart recorders. The carrier gas in all cases was helium. The column size and packing material as well as the column temperature and helium flow rate through the column are indicated in parentheses where applicable.

Quantitative GLC Analysis

Peak areas used in calculations represent averages of peak areas measured for four or more injections.

Detector Response Factor, k:

The detector response factor, k, for a compound, X, was determined by analysing a solution containing an accurately weighed amount of X and an aliquot of a standard stock solution of an internal standard. Peak areas were calculated using the formula

$$\text{Area} = (\text{peak width at half-height}) \times (\text{height}) .$$

The detector response factor is then given by

$$k = \frac{w_x}{w_s} \cdot \frac{A_s}{A_x}$$

where w_x = weight of compound x

w_s = weight of internal standard

A_s = average peak area of internal standard

A_x = average peak area of compound x

Weight Calculations:

The analysis of a reaction mixture consisted of adding an aliquot of the same internal standard solution as that used for the detector response factor determination, to a weighed amount of the reaction mixture. The resulting solution was then analysed by GLC. The weight of a component, w_i , in the solution is given by the equation

$$w_i = w_s k_i \frac{A_i}{A_s} \quad (2)$$

where w_s = weight of the internal standard used

k_i = the detector response factor for component i

A_i = average peak area for component i

A_s = average peak area for the internal standard

Using equation (2) the weight of residual starting material in a reaction mixture was calculated. As in the case of the NMR analysis

$$\% \text{ conversion} = \frac{W - w_s}{W}$$

where W = weight of the reaction mixture used in the analysis

and w_s = weight of residual starting material in the mixture .

Solvents

All solvents were distilled through a fractionating column. Unless otherwise indicated, the petroleum ether used was the fraction boiling $\geq 68^\circ$.

Optical Rotations, α , for Enone-alcohol 7A were taken on a Perkin-Elmer 141 Polarimeter operated at the sodium D line (589 nm). Single crystals for this purpose were grown from acetone-petroleum ether and checked under a polarizing microscope to determine which crystals were single and which were twinned or clustered. Crystal sizes ranged from 2.4 to 8.7 mg. A solution of known concentration was made up by dissolving a weighted single crystal in distilled acetone to make 1.0 ml of solution. A one-decimeter cell holding ~ 0.8 ml of solution was filled with pure acetone and used to zero the instrument. The cell was then filled with the sample solution and the rotation, α , read. For each sample, four readings were made, and the average reading used in the calculation below. The temperature was also noted. α was also determined for a cluster of crystals (11.9 mg). Specific rotations, $[\alpha]^{t^\circ}$, reported were calculated from the equation below:

$$[\alpha]^{t^\circ} = \frac{\alpha}{l \cdot c}$$

where α = the observed rotation at $\lambda=589$ nm and $t=25.5^\circ$

l = the cell length in decimeters (=1)

c = the concentration of the solution in grams per ml of solution.



Figure 31. Apparatus for Irradiations in the Solid State. (a) Part A; (b) Part A being inserted into Part B.



Figure 31(c). The Assembled Apparatus for Irradiations in the Solid State.

The reactor consisted of two main parts, A and B (Figure 31 above). Part A consisted of a double-walled cylindrical brass drum soldered onto a flat-face half-drum. An inlet and outlet provided for the circulation of coolant through this unit. At the flat surface of the half-drum was a gold-plated circular groove where crystals to be irradiated were grown. The temperature at the reaction site was measured by a copper-constantan thermocouple one junction of which was soldered onto the edge of the golden groove. An aluminum foil roof was positioned over this junction to shield it from direct radiation. The second junction of the thermocouple served as a reference junction and was kept in an ice-slurry during operations. Part B was essentially a brass casing for part A and had the following provisions: a Pyrex window which allowed for the irradiation of the sample externally; a groove with an O-ring to make the system air-tight after the insertion of part A into B; and a vacuum takeoff to an oil-pump for the evacuation of the reactor. The rest of the apparatus consisted of an Ultra Kryomat K-80 DW for the cooling and circulation of coolant through the reactor, a digital microvoltmeter (DMV) the reading of which is convertible to °C using a copper-constantan calibration table⁹⁴, an air-cooled glass filter (Corning 7380 for $\lambda \geq 340$ nm or Corning 3850 for $\lambda \geq 355$ nm) positioned between the Pyrex window and the lamp and finally a water-cooled 450-Watt Hanovia lamp connected to a power source.

In a typical run, crystals of the compound to be studied were weighed and dissolved in 3-5 ml of the solvent(s) of crystallization. Using a disposable pipette, the solution was slowly dropped

on the groove and allowed to slowly evaporate and crystallize overnight. A covering of aluminum foil protected the sample from light and dust particles during this stage.

The Kryomat was set at the temperature chosen for a reaction. The coolant was 50% (V/V) aqueous ethylene glycol for temperatures down to -28° and CHCl_3 for lower temperatures. While the coolant was being cooled to the desired temperature, the floor of the reactor was lined with filter paper. This served to catch any solids which might flake off from the groove during the reaction. Part A was then inserted into B and the two were secured together by screws. The inlet and outlet leads of part A were secured to the appropriate leads of the Kryomat. The reference junction of the thermocouple was inserted into a dewar of ice-slurry and the two terminals connected to the DMV. The reactor was then evacuated and held under vacuum for a minimum of 15 minutes before the circulation of the coolant through the reactor was begun. After the DMV reading indicated the desired temperature, a further 15 minutes were allowed for the system to equilibrate and stabilize. Meanwhile, the filter and lamp were aligned with the Pyrex window. The lamp was positioned about 5" from the Pyrex window which, in turn, was about 4" from the sample. Water circulation through the lamp jacket was begun at this time. A steady jet of air was directed onto the glass filter to prevent it from overheating and cracking. A reflector was placed behind the lamp to minimize dissipation of the light to

the environment, and the lamp was switched on. The DMV reading, the pressure reading of the McLeod gauge attached to the vacuum line, and the time of switching on the lamp were recorded. For reactions lasting 2 hours or less, the reaction temperature was recorded at 10-15 minute intervals. Temperatures of reactions lasting longer than 2 hours were recorded at longer time intervals. The entire temperature range of any run is indicated in the appropriate section of the Experimental Section. The vacuum attained is also given. The longest continuous run was 13.00 hours. Irradiations lasting longer than this were carried out discontinuously over a period not exceeding 3 days.

At the end of a run, the cooling was stopped and the system allowed to reach room temperature before the vacuum was released to prevent condensation of moisture on the reaction mixture. Part A was taken out and laid horizontally. Using disposable pipettes and either acetone or CHCl_3 , the sample was washed off the groove. The solvent was removed and the sample dried in vacuo. The % recovery of material from the reactor is indicated for each run in the appropriate section of the Experimental.

Apparatus and Procedure for Irradiations in Benzene

Photolyses carried out in benzene at room temperature were done using a conventional external irradiation apparatus. Interposed between the water-cooled 450-Watt Hanovia lamp and the solution was an

air-cooled Corning glass filter which was either No. 7380 transmitting $\lambda \geq 340$ nm or No. 3850 transmitting $\lambda \geq 355$ nm. All solutions were thoroughly deoxygenated for about 0.5 hour prior to irradiation and photolysed under Argon of <5 ppm oxygen content available from Canadian Liquid Air.

Apparatus and Procedure for Low Temperature Irradiations in Solution

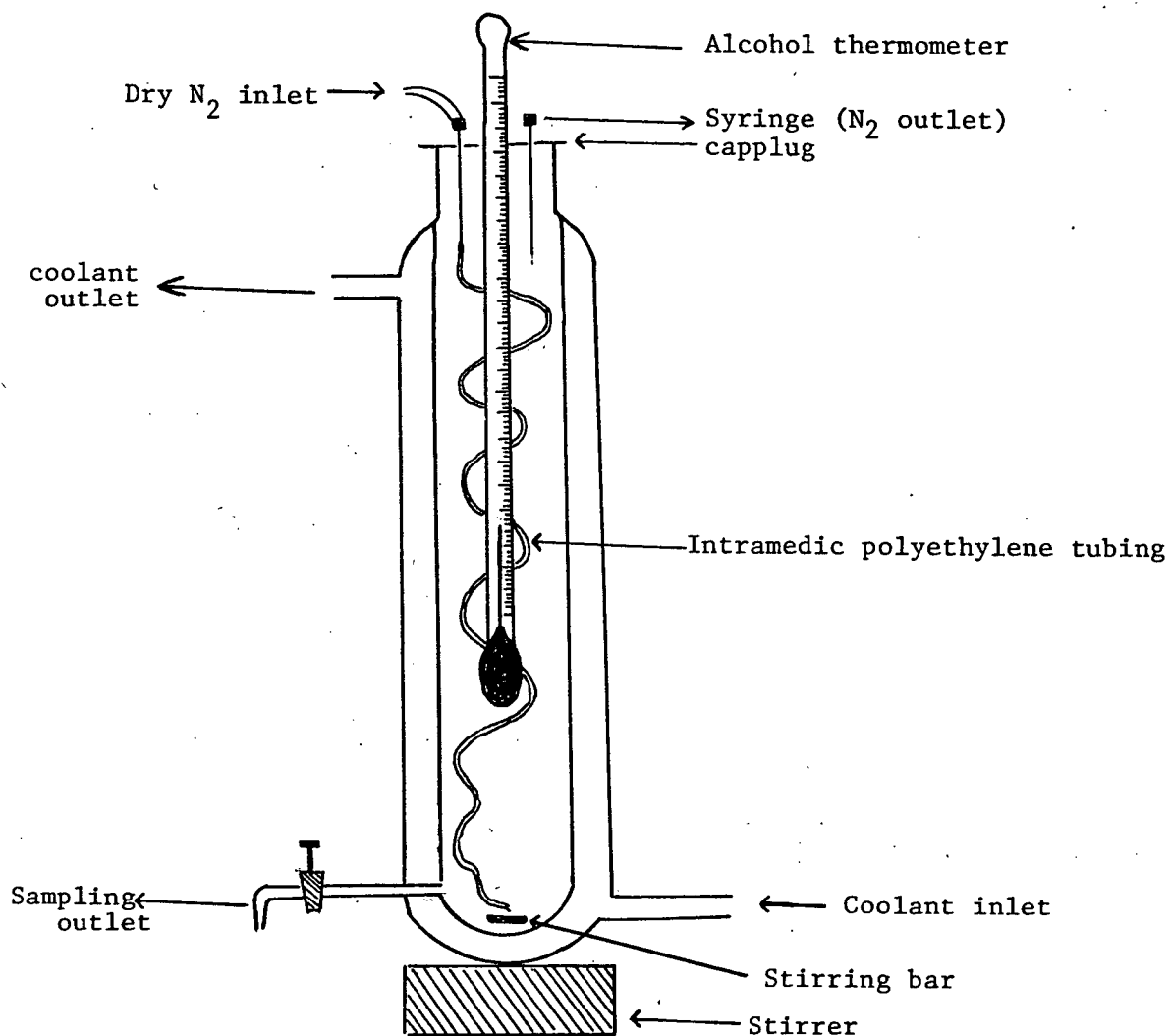


Figure 32. Apparatus for Low Temperature Irradiations in Solution.

The apparatus consisted of a double-walled Pyrex vessel with an inlet and outlet from the outer wall to allow for circulation of coolant. The apparatus also had an outlet with a Teflon stopcock from its innerwall for easy sampling of the reaction mixture at intervals during the course of a reaction. Solutions were deoxygenated and photolysed under L grade high purity nitrogen which was first passed through a tower of Drierite. Gas inlet and exit into the solution were through hypodermic needles inserted through an otherwise airtight capplug stopper equipped with an alcohol thermometer precalibrated against a copper-constantan thermocouple. Solutions were magnetically stirred. Moisture condensation and its subsequent freezing on the apparatus were mimimized by directing a fast current of air over the sides of the reactor. Irradiations were discontinuous but were completed within two days. As in the case of all other modes of irradiation, the light source was a 450-Watt Hanovia lamp, and an air-cooled filter (Corning No. 7380 for $\lambda \geq 340$ nm and No. 3850 for $\lambda \geq 355$ nm) was placed in between lamp and reactor.

Wavelength of Irradiations

Compounds 1 through 8 and substrate 10 were studied at $\lambda \geq 340$ nm. Compounds 9 and 11 were irradiated at $\lambda \geq 355$ nm. These are the same wavelengths at which these compounds have been studied in solution in earlier work²⁴.

Preparation of 5 α ,8 α -Dimethyl-4 $\alpha\beta$,5,8,8 $\alpha\beta$ -tetrahydro-1,4-naphtho-quinone⁹⁵, 1

A slurry of 3.04 g (0.028 mole) of p-benzoquinone in 5.29 g of trans,trans-2,4-hexadiene was heated under reflux at 62° with stirring until all of the quinone had dissolved. Heating was continued for a further 15 minutes. The mixture was then left stirring at room temperature for 3 hours. Removal of the excess diene in vacuo left 5.03 g (94%) of a bright yellow solid. Crystallization twice from ether-petroleum ether gave yellow rods of 1.

Mp 55-56° (lit.⁹⁵ 58-59.5°).

Ir (KBr), 5.92, 5.98 (C=O), 6.24 (conj. C=C) μ .

NMR (CCl₄) δ , 6.62 (s, 2H, C2 and C3 vinyl), 5.53 (s, 2H, C6 and C7 vinyl), 3.25 (m, 2H, 4 $\alpha\beta$ and 8 $\alpha\beta$ methines), 2.50 (m, 2H, C5 and C8 methines), 1.12 (d, J=7 Hz, 6H, methyls).

Irradiation of Adduct 1 in KBr

Irradiation of a 0.5% KBr pellet of 1 for 1.5 hours led to complete disappearance of the 6.24 μ absorption of 1. The infrared in addition, showed new C=O absorptions at 5.82 and 5.90 μ .

Irradiation of 1 in the Solid State

A solution of 114.9 mg of 1 in petroleum ether was slowly evaporated on the reactor's groove and left overnight. The

resulting crystals were irradiated at 0.03 torr between -2.0° and -1.5° for 1 hour. The recovery was 98%. The resulting solid was washed thrice with petroleum ether and the washings stripped of solvent and dried in vacuo to give 43.2 mg of solid which was shown by TLC, NMR and ir to be residual starting material 1. The insoluble product was dried in vacuo. This gave 67.9 mg (95% yield) of 1A. The extent of reaction calculated from weight of unrecovered 1 was 62%. Yields of 1A at other conversions are tabulated in the text. An infrared spectrum of the crude product was taken. Following this, the crude material was crystallized from CHCl_3 -hexane to give sparkling colorless plates suitable for single crystal X-ray structure determination.

Mp** 265.0° with decomposition.

Ir (KBr), 5.82 and 5.90 (C=O) μ .

NMR (CDCl_3) δ , 5.83 (s, 4H, vinyls), 3.47 (s, 4H, cyclobutane ring methines), 3.22 (dd, $J=3$ and 2 Hz, 4H, C4, C9, C14 and C19 methines), 2.50 (m, 4H, C5, C8, C15 and C18 methines), 1.10 (d, $J=7$ Hz, 12H, methyls).

Mass spectrum m/e parent 380

Anal. Calcd. for $\text{C}_{24}\text{H}_{28}\text{O}_4$: C, 75.76; H, 7.42.

Found : C, 75.48; H, 7.42.

Preparation of 6,7-Dimethyl-4 α ,5,8,8 α -tetrahydro-1,4-naphthoquinone⁹⁶, 2

Recrystallized p-benzoquinone (3.14 g, 0.03 mole) was suspended in 4.65 g of 2,3-dimethyl-1,3-butadiene and heated at 65°

under reflux for 2 hours. Removal of excess diene in vacuo gave 2.92 g (93%) of crude 2 which was dissolved in ether and filtered. Removal of ether followed by crystallization once from ethanol and twice from petroleum ether gave pale yellow crystals of 2.

Mp 115-116° (lit.⁹⁶ 115-117°).

Ir (KBr), 5.93 (C=O), 6.24 (conj. C=C) μ .

NMR (CDCl₃) δ , 6.58 (s, 2H, C2 and C3 vinyls), 3.10 (m, 2H, C4a and C8a methines), 2.20 (m, 4H, C5 and C8 methylenes), 1.63 (s, 6H, methyls).

Irradiation of Adduct 2 in KBr

A 0.5% KBr pellet of 2 was irradiated ($\lambda \geq 340$ nm) and the reaction monitored by ir. After 5 hours of irradiation, the 6.24 μ absorption of 2 was completely gone. In addition, the 5.93 μ C=O stretch of 2 had been replaced by a 5.85 μ C=O absorption.

Irradiation of 2 in the Solid State

Crystals of compound 2 (93.0 mg) were irradiated in a covered Pyrex petri dish for 0.4 hour. The resulting solid was washed three times with chloroform and the washings concentrated and analyzed by TLC (silica gel; chloroform). With the exception of a base spot, the TLC showed only residual 2. The dry weight of recovered 2 was 55.8 mg. The solid product 2A was dried in vacuo. The crude yield was 36.1 mg (97%). The extent of reaction (% conversion)

calculated from unrecovered 2 was 40%. Yields of 2A from other runs at varying conversions are given in the text. The infrared spectrum of the crude product was recorded. Crystallization from chloroform afforded tiny, sparkling, colorless plates of 2A.

Mp** 264.7° with decomposition.

Ir (KBr), 5.85 (C=O) μ .

NMR (CDCl₃) δ , 3.64 (s, 4H, cyclobutane ring methines), 3.18 (m, 4H, C4, C9, C14 and C19 methines), 2.22 (m, 8H, methylenes), 1.66 (s, 12H, methyls).

Mass spectrum m/e parent 380.

Anal. Calcd. for C₂₄H₂₈O₄: C, 75.76; H, 7.42.

Found : C, 75.61; H, 7.29.

Notes of 2A Crystal Used for X-ray Structure Determination

The crystals obtained by crystallizing from chloroform were too small for use in the X-ray structure determination. Larger single crystals for this purpose were obtained by crystallizing crude 2A from acetonitrile. The ir of this batch of 2A crystals was identical in every respect to the ir of crude 2A as well as to the 2A that had been crystallized from chloroform.

Preparation of 4a β ,5,8,8a β -Tetrahydro-1,4-naphthoquinone⁵⁵, 3

A solution of 1,4-benzoquinone which had been crystallized twice from acetone-petroleum ether was made by dissolving 13.0 g

(0.12 mole) in 200 ml of benzene in a hydrogenation bottle. The solution was cooled to 0°, and 18 ml of 1,3-butadiene which had been condensed to liquid using dry-ice acetone was added and the bottle firmly stoppered and replaced in its shield. The stopper was secured by screws in a rocker of a hydrogenation apparatus and the solution mechanically rocked for 21 days. The resulting yellow solution was stripped of solvent and excess diene leaving an oil which solidified on cooling in ice. It was crystallized once from petroleum ether and twice from ether-petroleum ether. The yield after the three crystallizations was 61%.

Mp 53.5-54° (lit.⁵⁵ 52-54°).

Ir (KBr), 5.97 (C=O), 6.24 (conj. C=C) μ .

NMR (CCl₄) δ , 6.57 (s, 2H, C2 and C3 vinyls), 5.63 (m, 2H, C6 and C7 vinyls), 3.15 (m, 2H, 4a,8a methines), 2.28 (m, 4H, C5 and C8 methylenes).

Irradiation of 3 in KBr

A 0.7% KBr pellet of 3 was irradiated ($\lambda \geq 340$ nm) for 3 hours. Ir of the irradiated pellet showed complete disappearance of the conjugated C=C stretch at 6.24 μ . The C=O absorption had also shifted from 5.97 to 5.88 μ .

Irradiation of 3 in the Solid State

Crystals of compound 3 (135.5 mg) were irradiated at 0.01 torr between 4.3° and 0.0° for 1 hour. The solid was washed off the

reactor's cavity with acetone and chloroform. Removal of solvents and drying in vacuo left 124.0 mg of solid ($\approx 92\%$ recovery). It was redissolved in chloroform and suction filtered. The filtrate was concentrated and checked by TLC (silica gel; chloroform). Apart from a base spot, the only other spot was that of starting material, 3. The chloroform soluble portion was 8.2 mg. The chloroform insoluble solid was 117.6 mg (92% yield). Infrared spectra of the crude solid and also of the recovered starting material were recorded. The latter was confirmed to be residual 3. The product was crystallized from refluxing chloroform. The crystals thus obtained were colorless, sparkling flakes. The ir of the crystallized material was identical to that of the crude product, 3A. Yields of 3A from other runs are given in the text. Compound 3A had M_p^{**} $280^\circ \pm 2^\circ$ with decomposition.

Ir. (KBr), 5.85 (C=O) μ .

NMR ($CDCl_3$) δ , 5.70 (m, 4, vinyls), 3.64 (s, 4H, cyclobutane ring methines), 3.20 (m, 4H, C4, C9, C4 and C19 bridgehead methines), 2.30 (m, 8H, methylenes).

Mass spectrum m/e parent 324.

Anal. Calcd. for $C_{20}H_{20}O_4$: C, 74.06; H, 6.22.

Found : C, 73.88; H, 6.15.

Notes on 3B Crystal Used for X-ray Structure Determination

The crystals of 3A obtained from crystallizing from chloroform

were too small and thin for single crystal X-ray structure determination. Larger crystals for this purpose were obtained by crystallizing from acetonitrile. The infrared spectrum of this material (3B) is discussed in the text. Its NMR was identical to that of 3A crystallized from chloroform.

Irradiation of Adduct 3 in Benzene

A solution of 406.0 mg of compound 3 in 200 ml benzene was degassed and photolysed for 24.2 hours. The resulting milky solution was filtered and the solid component dried and weighed. Its weight was 165.0 mg. Ir of the crude material showed a broad OH at 2.90μ and a C=O absorption at 5.87μ . The absorptions were generally very broad especially in the fingerprint region.

NMR ($(\text{CD}_3)_2\text{CO}$) δ , 6.80 (s), 5.07 (br,m), 2.51 (br,s, broadens on adding D_2O), 1.53 (m).

Mass spectrum: highest observed m/e = 495.

The filtrate was concentrated and separated by GLC (5' x $\frac{1}{4}$ " of 20% DEGS on 60/80 Chromosorb W at 150° and 150 ml/min). Two peaks with retention times of 4 and 6 minutes, respectively were obtained. They were subsequently identified as 3C and 3D by comparing their ir's with those of authentic samples. Of the two, 3D, retention time = 6 minutes, was the major.

Preparation of 6,7-Diphenyl-4a β ,5,8,8a β -tetrahydro-1,4-naphthoquinone⁹⁷, 4

This was a four-step synthesis comprising

- (a) The preparation of benzil dihydrazone from benzil^{97a},
- (b) the conversion of the benzil dihydrazone to diphenylacetylene^{97a},
- (c) the conversion of the diphenylacetylene to 2,3-diphenyl-1,3-butadiene^{97b}, and
- (d) the Diels-Alder reaction between the diene from part (c) and p-benzoquinone to give 4^{97c}.

(a) A solution of 105.1 g (0.5 mole) of benzil and 76.0 g of 85% hydrazine hydrate in 325 ml of n-propyl alcohol was refluxed for 61.5 hours. The resulting red solution was first cooled to room temperature and then cooled in an ice-bath for one hour. The benzil dihydrazone was filtered, washed with a total of 200 ml of ethanol in portions and then dried in vacuo for one hour. This gave 100.4 g of benzil dihydrazone.

(b) The benzil dihydrazone was transferred to a one-litre three-necked flask fitted with a reflux condenser and a mechanical stirrer and 480 ml of benzene added. Yellow HgO (240 g) was added in small amounts to the suspended mixture over a period of 1.5 hours with stirring and gentle heating over a steam bath. After the addition, the mixture was further stirred for 1.5 hours during which time a vigorous reaction accompanied by frothing occurred. It was kept under control by cooling in an ice bath. The mixture was left at room temperature overnight and then filtered. The residue was washed with 100 ml of benzene and the washings added to the filtrate. The latter

was dried over anhydrous Na_2SO_4 , filtered and stripped of solvent. The residue was distilled at 0.02 torr and 125° . This gave 62.1 g of pale yellow solid diphenylacetylene.

Crystallization from 95% ethanol gave 53.7 g of diphenylacetylene, m.p. $56-58^\circ$ (lit.^{97a} $60-61^\circ$).

(c) A 500 ml three-necked round-bottomed flask was fitted with a sealed mechanical stirrer, a reflux condenser and a thermometer. A T-joint was attached to the top of the condenser. The remaining two arms of the T-joint were connected to a source of pure nitrogen and a bubbler respectively. The flask was flushed with nitrogen and 5 g of dry sodium hydride and 120 ml of anhydrous dimethyl sulfoxide introduced into the flask. The mixture was heated to 75° under N_2 with stirring for 40 minutes. The flask was then cooled to 30° using a water-bath. The thermometer was replaced by a dropping funnel containing 17.8 g (0.1 mole) of diphenylacetylene in 80 ml of anhydrous dimethyl sulfoxide. This latter solution was added dropwise to the grey contents of the flask. Following the addition, the dropping funnel was replaced by the thermometer and the mixture heated to and maintained at 70° for 2.5 hours. It was subsequently cooled to room temperature and the reddish-brown mixture slowly poured over ice with stirring and left at room temperature until all the ice had melted. The crude mixture was extracted five times with 200 ml portions of ether and the combined ethereal extracts washed with 300 ml of water and then dried over anhydrous sodium sulfate.

Removal of the ether in vacuo left 16.4 g of a reddish-brown oil which was divided into two portions. Each portion was chromatographed on 200 g columns of neutral alumina using as eluents benzene-hexane, (1:7) and then (1:3). The pale yellow fractions were combined and stripped of solvents in vacuo to give 12.0 g of impure 2,3-diphenyl-1,3-butadiene as an oil. It was used in the procedure described below without further purification.

(d) All of the oil from part (c) and 3.0 g (0.03 mole) of p-benzoquinone were dissolved in 80 ml of benzene and refluxed for 18 hours. The mixture was cooled to room temperature and stripped of solvent. Hexane was added in small portions until precipitation had ceased. The precipitate was filtered and washed twice with cold hexane. It was dried in air to give 3.9 g of compound 4 as a greenish-yellow solid (45% yield based on p-benzoquinone). It was crystallized twice from acetone-hexane to give pale yellow needles.

Mp 163-164.5° (lit.^{97c} 163°).

Ir (KBr), 5.92 and 5.95 (C=O), 6.24 (conj. C=C) μ .

NMR (CDCl₃) δ , 7.10 (s, 10H, aromatic), 6.68 (s, 2H, C2 and C3 vinyls), 3.47 (m, 2H, C4a and C8a methines), 2.77 (m, 4H, C5 + C8 methylenes).

Irradiation of 4 in KBr

The irradiation, $\lambda \geq 340$ nm, of a 0.4% KBr pellet of 4 for twenty minutes led to its complete depletion as shown by the disappearance of a moderately intense peak ($\sim 46\%$ of the absorbance of the C=O peak) at 11.52 μ .

In the carbonyl region, the 5.92 and 5.95 μ absorptions due to 4 had been replaced by a single C=O absorption at 5.97 μ . In addition, a broad but distinct OH absorption at 2.91 μ was noted.

The ir recorded after further irradiation indicated a new product formation after a total irradiation time of 0.5 hour. This new product had a 5.72 μ C=O. It increased in intensity at the expense of the 5.97 μ C=O absorption of the primary product till it eventually became the most intense of the two carbonyl peaks after 6 hours.

Irradiation of 4 in the Solid State

Crystals of compound 4 (50.0 mg) were irradiated at 0.05 torr between -10.4° and -9.8° for 15 minutes. 94% of material was recovered. Preparative TLC (silica gel; 15% ethyl acetate-benzene) of the mixture gave 41.3 mg of residual 4 and 5.8 mg of the product 4A. The extent of reaction, based on recovered starting material, was 17% and the yield of product 67%.

In another run, 136.7 mg of 4 was irradiated at 0.02 torr between 18.5° and 22.0° for 2 hours. Preparative TLC as before gave 46.4 mg of residual 4, 7.1 mg of 4B and 41.2 mg of 4A. The yields of 4B and 4A were, thus, 8% and 47% respectively.

Lastly, irradiation of 83.0 mg of 4 at 0.01 torr between 17.3° and 18.5° for 11 hours followed by preparative TLC gave 6.2 mg of residual 4, 11.7 mg of 4B and 25.7 mg of 4A. The yields of these

two products were, therefore, 15% and 33% respectively.

The products 4A and 4B were crystallized from acetone-hexane; 4A was white, feathery needles.

Mp 189.5°-190.0°.

Ir (KBr), 2.92 (OH), 5.97 (C=O) μ .

NMR (CDCl₃) δ , 7.17 (m, 10H, phenyls), 6.44 (d, J=10 Hz, 1H, C2 vinyl), 6.30 (d, J=3 Hz, 1H, C9 vinyl), 6.01 (dd, J=10 and 2 Hz, 1H, C3 vinyl), 3.45 (d, J=3 Hz, 1H, C10 methine), 2.73 (s, 1H, disappears on adding D₂O, OH), 2.65 (m, 2H, C6 methylenes), 2.13 (dd, J=14 and 9 Hz, 1H, C5 methine).

Mass spectrum m/e parent 314.

Anal. Calcd. for C₂₂H₁₈O₂: C, 84.05; H, 5.77.

Found : C, 84.06; H, 5.87.

Product 4B crystallized as colorless needles.

Mp 170.5°-171.5°

Ir (KBr), 5.73 (C=O); 6.25 (conj. C=C) μ .

NMR (CDCl₃) δ , 7.23-6.87 (m, 10H, aromatic), 3.23 (m, 2H, C7 and C10 methines), 3.07 (m, 1H, C5 methine), 2.83 (m, 3H, C1 methine and C4 methylenes), calcd.⁶⁹ 2.49 (dd, J=20 and 5 Hz, 1H, C8 exo), calcd.⁶⁹ 2.30 (dd, J=20 and 1.5 Hz, C8 endo).

Mass spectrum m/e parent 314.

Anal. Calcd. for C₂₂H₁₈O₂: C, 84.05; H, 5.77.

Found : C, 83.95; H, 5.71.

Base-Catalyzed Deuterium Exchange of Ene-Dione 4B

Six drops of a 2N solution of KOH in D₂O were added to the NMR sample of 4B. The tube was periodically shaken. A spectrum recorded after 12 hours showed no changes. However, after 4.5 days, the 2.49 δ resonances attributed to the C8 exo proton had disappeared, the doublet of doublet resonances due to the C8-endo proton had collapsed to a broad singlet at 2.31 δ and the small splitting of the multiplet at 3.23 δ was no longer present. The remainder of the spectrum remained unchanged.

Photolysis of 4 in Benzene

A solution of 214.9 mg of compound 4 in 100 ml of benzene was degassed and irradiated, for 3.0 hours. The solvent was removed in vacuo and the resulting mixture separated by preparative TLC (silica gel; 15% ethyl acetate-benzene). This gave 31.0 mg of 4B and 85.2 mg of 4A. (Combined yields = 54%. Ratio of 4A:4B = 3:1.)

In another run, 100.0 mg of 4 in 100 ml of benzene was degassed and photolysed for 3.1 hours. Treatment of this mixture as above gave 8.2 mg of residual 4, 24.8 mg of 4B and 34.1 mg of 4A. (Combined yield of products = 64%. Ratio of 4A:4B = 3:2.) Finally, photolysis of a solution of 159.7 mg of 4 in 100 ml of benzene for 3.9 hours followed by preparative TLC gave 57.1 mg of 4B and 26.3 mg of 4A. (Combined yields = 52%. Ratio of 4A:4B = 1:2.)

The m.p.'s and spectra of products 4A and 4B were identical to those reported for the solid state photolysis products.

Analytical Run:- A solution of 23.0 mg of adduct 4 in 10 ml of benzene was degassed and irradiated. Aliquots were withdrawn at 0.1 hour intervals, and used for analyses by TLC (silica gel; 15% ethyl acetate-benzene) and ir. After 0.1 hour of irradiation, a peak at 8.42μ characteristic of enone-alcohol product, 4A, had begun to develop in the ir. The presence of 4A was further confirmed by TLC. Also in this ir, a broadening was observed in the 5.70μ region indicating the presence of the ene-dione, 4B. In the ir of the sample withdrawn after 0.2 hour of irradiation, the 2.97μ OH stretch attributable to 4A became apparent. In subsequent spectra of samples withdrawn after 0.3, 0.4 and 0.5 hour of irradiation respectively, peaks due to 4A and 4B steadily increased. In none of the five samplings was the starting material, 4, depleted. This was shown by the persistence of the moderately intense peak at 11.52μ due to 4. (Its intensity \approx 46% the absorbance of the C=O peak.) This was confirmed by TLC.

Irradiation of Photoproduct 4A in the Solid State

Crystals of the enone-alcohol photoproduct, 4A (17.0 mg) were photolysed at 0.05 torr between 17.5° and 18.2° for 12 hours. Ir of the residue showed a 5.73μ C=O characteristic of the ene-dione 4B.

Photolysis of Photoproduct 4A in Benzene

A solution of 24.4 mg of photoproduct 4A in 20 ml of benzene was degassed and photolysed. The reaction was monitored by TLC (silica gel; 15% ethyl acetate-benzene). After 0.6 hour of irradiation, two spots were detected in addition to that of 4A. The reaction was stopped after 2.1 hours of total irradiation. Ir of the crude mixture showed broad C=O stretches at 5.65, 5.75 and 5.90 μ . The mixture was separated by preparative TLC. The uppermost spot had 5.68 and 5.80 μ C=O stretches in the ir and was assigned structure 4C. The middle spot had a 5.73 μ C=O characteristic of 4B, and the lower spot had a 2.92 μ OH and a 5.90 μ C=O and was consequently identified as residual 4A.

Irradiation of Photoproduct 4B in KBr

The irradiation of a 0.4% KBr pellet of 4B was followed by ir at hourly intervals up to 11.1 hours of total irradiation. There was no change in the ir.

Irradiation of Photoproduct 4B in Benzene

A solution of 10.0 mg of ene-dione 4B in 10 ml of benzene was degassed and irradiated for 2 hours. The ir of the irradiated sample was identical to that of 4B.

Preparation of 2,3,6,7-Tetramethyl-4a β ,5,8,8a β -tetrahydro-1,4-naphthoquinone⁹⁸, 5

(a) 2,3-Dimethyl-1,4-benzoquinone.

The procedure is that described by Fieser^{98a} for the preparation of quinones. A two-liter flask having a long neck was set up for steam distillation. The condenser from this flask was connected by means of an adapter to a two-liter, round-bottomed, short-necked flask which served as the receiver. This latter was submerged in a bucket of ice slurry and was equipped with a second condenser clamped in a vertical position. These measures were taken to prevent loss of the volatile quinone. Water was started running through both condensers and the reaction flask disconnected. Dry, well powdered 3-amino-o-xylene sulfate (12.63 g) was introduced into the reaction flask. Concentrated H₂SO₄ (45 ml) was diluted with 200 ml of H₂O, cooled, and added to the contents of the flask. Powdered MnO₂ (20.44 g) was added next and the flask quickly swirled to mix the contents and then immediately connected to the rest of the apparatus. The contents were steam distilled. Occasionally, the condenser between the reaction flask and the receiver became clogged with the quinone and it became necessary to temporarily stop the water running through this condenser to allow the quinone to distill into the receiver. After 1 hour, the distillation was ended. A small amount of the quinone lodged in the condenser was washed into the receiver with ether.

An additional 100 ml of ether was added to the quinone and the resulting ethereal solution dried over anhydrous Na_2SO_4 for a few hours. The ether was removed in vacuo and the o-xyloquinone so produced used in the next step without further purification.

(b) 2,3,6,7-Tetramethyl-4 α ,5,8,8 α -tetrahydro-1,4-naphthoquinone^{98b}, 5

All of the quinone prepared above was dissolved in 10 ml of ethanol in a 50 ml round-bottomed flask. Three ml of 2,3-dimethyl-1,3-butadiene was added and the mixture refluxed for 8.5 hours. It was subsequently stripped of solvent in vacuo and the resulting solid crystallized from petroleum ether using Norit to decolorize. A further recrystallization gave crystals of 5.

Mp 104.0-104.5° (lit.^{98b} 105-106.5°).

Ir (KBr), 5.95 and 5.98 (C=O), 6.18 (conj. C=C) μ .

NMR (CCl_4) δ , 3.07 (m, 2H, C4a and C8a methines), 2.13 (m, 4H, C5 and C8 methylenes), 1.97 (s, 6H, C2 and C3 methyls), 1.63 (s, 6H, C6 and C7 methyls).

Irradiation of 5 in KBr

A 0.7% KBr pellet of 5 was irradiated discontinuously for a total of 12 hours. Ir recorded at hourly intervals showed no new peaks.

Irradiation of 5 in the Solid State

Crystals of compound 5 (35.8 mg) were irradiated at 0.03 torr between 8.0° and 9.3° for a total of 30.3 hours. The recovery was 86%. TLC (silica gel; 15% ethyl acetate-benzene) showed a single spot with an R_f identical to that of 5. The ir and NMR of the irradiated sample were also identical to those of 5.

Preparation of 2,3-Dimethyl-1,4,4a β ,9a β -tetrahydro-9,10-anthraquinone⁹⁹, 6

A solution of 8.0 g (0.05 mole) of 1,4-naphthoquinone and 8.0 g (0.1 mole) of 2,3-dimethyl-1,3-butadiene in 100 ml of ethyl alcohol was refluxed for 5 hours. On cooling to room temperature, the mixture solidified. It was left in the refrigerator overnight. The solid was broken up with a spatula and sucked dry. It was washed three times with 15 ml portions of cold ethanol and dried in vacuo for 3 hours. The yield was 10.9 g (91%). It was crystallized from acetone with Norit to remove colored impurities. This gave 7.7 g of sparkling colorless crystals. During a subsequent recrystallization from acetone, two distinct crystals were formed, one (the major) was colorless rods of the desired adduct, 6; the other was bright yellow plates which darkened on exposure to air for prolonged periods. The ir and NMR of this latter compound suggested it might be 2,3-dimethyl-1,4-dihydro-9,10-anthraquinone formed by partial air oxidation of 6. Adduct 6 had mp 148.0-148.5° (lit.⁹⁹ 150.0°).

Ir (KBr), 5.92 (C=O), 6.26 (conj. C=C) μ .

NMR (CDCl₃) δ , 8.23-7.56 (m, 4H, phenyl), 3.38 (m, 2H, C4a and C9a methines), 2.31 (m, 4H, C1 and C4 methylenes), 1.68 (s, 6H, methyls).

Irradiation of 6 in KBr

A 0.4% KBr pellet of 6 was irradiated ($\lambda \geq 340$ nm) and the reaction monitored by ir. The ir taken after 26.4 hours of irradiation showed an OH peak at 2.90 μ . The C=O absorption of 6 at 5.92 μ was unchanged but the intensity of the conjugated C=C absorption at 6.26 μ was reduced relative to the C=O absorption.

Irradiation of 6 in the Solid State

Crystals of compound 6 (132.4 mg) were irradiated in vacuo (0.02 torr) between 8.3° and 10.0° for a total of 30.8 hours. A pale yellow solid (131.9 mg \equiv 100% recovery) was obtained. Preparative TLC (silica gel; 15% ethyl acetate-benzene) of the reaction mixture gave 58.3 mg of residual 6 and 44.6 mg of product 6A (60% yield). Small amounts (~5% each) of the quinol and the dihydro analog of 6 were also isolated. The product, 6A, was washed with hexane, dried and sublimed at 103° and 0.03 torr. Subsequent crystallization from acetone-benzene gave colorless crystals of 6A.

Mp: 124.5-125.5°, (lit.^{24a} 126.0-126.5°).

Ir (KBr), 2.90 (OH), 5.93 (C=O), 6.23 (conj. C=C) μ .

NMR (CDCl₃) δ , 8.00-7.25 (m, 4H, aromatic), 5.74 (m, 1H, C9 vinyl),

3.22 (d, J=3 Hz, 1H, C10 methine), 2.79 (s, 1H, disappears on adding D₂O, OH), 2.54 (dd, J=8 and 3 Hz, 1H, C5 methine), 1.83 (d, J=1.5 Hz, 3H, C8 methyl), 1.58 (dd, J=13 and 3 Hz, 1H, C6 endo), 1.34 (dd, J=13 and 3 Hz, 1H, C6 exo), 1.01 (s, 3H, C7 methyl).

Mass spectrum m/e parent 240.

Irradiation of 6 in the Solid State. Calculation of Extent of Reaction

Crystals of compound 6 (161.0 mg) were irradiated at 0.03 torr between 8.1° and 9.5° for 31.5 hours. The amount of material recovered from the reactor was 149.4 mg (≅93% recovery). A portion of this mixture (101.0 mg) was analyzed by NMR using 0.4 ml of a stock solution of nitromethane containing 228.3 mg of nitromethane per 10 ml of CDCl₃ solution as the internal standard. The NMR integration of the C9 vinyl of the product 6A was used for the analysis. The calculated extent of reaction was 28.5%. (For method of calculation see under General in the Experimental Section.)

Photolysis of 6 in Benzene

A solution containing 116.6 mg of 6 in 100 ml of benzene was degassed and irradiated for 30.1 hours. Removal of solvent in vacuo, left a thick yellow oil. Preparative TLC of this material gave 39.3 mg of residual 6 and 49.7 mg (64% yield) of the alcohol, 6A. The latter was washed with hexane, dried and sublimed at 0.04 torr and 104°. Subsequent crystallization from acetone-hexane gave colorless

plates of 6A.

Mp 125.0°-126.0° (lit.^{24a} 126.0-126.5°).

Ir and NMR were identical to those reported for 6A isolated in the solid state photolysis of 6.

Preparation of 2,3-Dicyano-1,4-benzoquinone¹⁰⁰

Commercial 2,3-dicyanohydroquinone (8.1 g, 0.05 mole) was suspended in 50 ml of CCl₄ in a 250 ml flask. Nitrogen dioxide (as nitrogen tetroxide) was condensed in a receiving tube cooled by liquid nitrogen. The condensed liquid was added in small portions to the suspension of the quinol with stirring. The addition was continued until brown fumes of nitrogen oxides persisted for several minutes. Stirring was continued for a further 1 hour after which excess oxides of nitrogen were removed by a stream of nitrogen gas. The resulting mixture was filtered to give a yellow solid which was crystallized from CHCl₃-benzene to afford 6.9 g (87% yield) of golden crystals of 2,3-dicyano-1,4-benzoquinone.

Mp 181-182° (lit.¹⁰⁰ 178-180°).

Preparation of 4a β ,8a β -Dicyano-6,7-dimethyl-4a β ,5,8,8a β -tetrahydro-1,4-naphthoquinone¹⁰¹, 7

Crystals of 2,3-dicyano-1,4-benzoquinone (4.0 g, 0.025 mole) and 100 ml of a solvent mixture of acetone-benzene (1:1 V/V) were introduced into a 250 ml three-necked flask equipped with a

condenser. The mixture was warmed and magnetically stirred until the quinone dissolved. The solution was cooled to room temperature and 3.7 g (0.05 mole) of 2,3-dimethyl-1,3-butadiene added. The mixture was stirred at room temperature for 22 hours and then stripped of solvents and excess diene. This left a thick oil which precipitated upon addition of light petroleum (30°-60°). The flask was cooled in ice for 30 minutes and the resulting golden yellow solid was filtered; washed with petroleum-ether (30°-60°) and dried. This gave 5.9 g (98%) of compound 7. It was crystallized twice from acetone-petroleum ether to give large, sparkling, yellow plates of 7.

Mp 156.5°-157.5° (lit.¹⁰¹ 157°-158°).

Ir (KBr), 4.44 (C≡N), 5.79 and 5.86 (C=O), 6.24 (conj. C=C) μ .

NMR (CDCl₃) δ , 6.88 (s, 2H, C2 and C3 vinyl), 2.71 (s, 4H, C5 and C8 methylenes), 1.73 (s, 6H, methyls).

Photolysis of 7 in KBr

A 0.4% KBr pellet of 7 was irradiated. After 0.3 hour of irradiation, a new broad but intense peak was observed at 2.91 μ (OH). In the carbonyl region, the 5.79 μ peak had decreased relative to the 5.86 μ peak. After 0.5 hour of irradiation, a new absorption began to develop at 5.62 μ . This peak increased at the expense of the 2.91 and 5.86 μ absorptions until it became the more intense of the two carbonyl peaks after a total of 18 hours of irradiation.

Irradiation of Compound 7 in the Solid State

Crystals of compound 7 (230.4 mg) were irradiated at 0.01 torr between 19.3° and 19.7° for 1.5 hours. The reaction mixture which was retrieved from the reactor weighed 195.2 mg (85% recovery).

To 22.0 mg of the reaction mixture, 0.2 ml of a stock solution of benzophenone (internal standard) in chloroform was added. GLC analysis of this mixture was carried out on a 5' x $\frac{1}{4}$ " 10% OV-210 column at 175° and a flow rate of 160 ml/min. The detector response factor for 7 under identical conditions was determined to be 1.34. The calculated % conversion of 7 from the GLC analysis of the reaction mixture was 34%. (For method of calculation, see under General in the Experimental Section). The rest of the reaction mixture (172.5 mg) was separated by preparative TLC (silica gel; 10% acetone-chloroform). This gave 109.2 mg of residual 7 and 57.3 mg of 7A (91% yield). The yields from three other runs were 98%, 94% and 87% at conversions of 19%, 30% and 26% respectively. The product from all the runs was combined and crystallized from acetone-hexane to give colorless crystals of 7A.
Mp. 195-196° (reported^{24b} 188-190°).

Ir (KBr), 2.93 (OH), 4.41 and 4.45 (C≡N), 5.87 (C=O), 6.15 (conj. C=C) μ .

NMR (CDCl₃-acetone d₆) δ , 7.00 (d, J=10 Hz, 1H, C2 vinyl), 6.22 (d, J=10 Hz, 1H, C3 vinyl), 5.79 (d, J=1.5 Hz, 1H, C9 vinyl), 2.80 (s, 1H,

OH, disappears on adding D₂O), 2.16 (d, J=13.5 Hz, 1H, one of the C6 methylenes), 1.92 (d, J=13.5 Hz, 1H, the other C6 methylene), 1.91 (d, J=1.5 Hz, 3H, C8 methyl), 1.21 (s, 3H, C7 methyl).

Mass spectrum m/e parent 240.

Anal. Calcd. for C₁₄H₁₂N₂O₂: C, 69.99; H, 5.04; N, 11.66.

Found : C, 69.99; H, 5.00; N, 11.54.

Irradiation of Product 7A in KBr

The irradiation of a 0.4% KBr pellet of 7A for 2.5 hours led to new carbonyl absorptions at 5.61 and 5.76 μ . After 8.4 hours, the 5.61 μ C=O was the most intense of the three carbonyl peaks.

Irradiation of 7 in Benzene

A solution of 242.0 mg of compound 7 in 150 ml of benzene was degassed and photolysed for 0.5 hour. Preparative TLC (silica gel; 10% acetone-chloroform) gave 121.4 mg of residual 7, 89.8 mg of product 7A (74% yield) and 8.3 mg of compound 7B (7% yield). The mp and spectra of 7A were identical to those of 7A isolated from the solid state photolysis of 7. Compound 7B had m.p. 156-158°.

Ir (KBr), 4.44 and 4.46 (C \equiv N); 5.90 (C=O) μ .

NMR (CDCl₃) δ , 7.44 (d, J=10 Hz, 1H, C2 vinyl), 6.41 (d, J=10 Hz, 1H, C3 vinyl), 2.56 (s, 2H, C6 or C9 methylenes), 2.45 (d, J=15 Hz, 1H, one of the C9 or C6 methylenes), 1.72 (d, J=15 Hz, the other C9 or C6 methylene), 1.56 (s, 3H, C8 methyl), 1.38 (s, 3H, C7 methyl).

Mass spectrum m/e parent 240.

A possible structure for 7B is discussed in the text.

Preparation of 4a β -8a β -Dicyano-5 α ,8 α -dimethyl-4a β ,5,8,8a β -tetrahydro-1,4-naphthoquinone^{24b}, 8

A solution of 1.5 g (0.009 mole) of 2,3-dicyano-1,4-benzoquinone was dissolved in 60 ml of benzene-acetone (1:1) and 1.5 g of trans,trans-2,4-hexadiene added. The mixture was magnetically stirred at room temperature for 21 hours. The resulting yellow solution was stripped of solvents and residual diene. The solid was crystallized from acetone-hexane to give 1.4 g (65% yield) of sparkling, pale yellow crystals.

Mp 153°-154° (lit.^{24b} 155°-156°).

Ir (KBr), 4.45 (C \equiv N), 5.78 and 5.88 (C=O), 6.24 (conj. C=C) μ .

NMR (CDCl₃) δ , 6.94 (s, 2H, C2 and C3 vinyls), 5.62 (s, 2H, C6 and C7 vinyls), 3.09 (q, J=8 Hz, 2H, C5 and C8 methines), 1.29 (d, J=8 Hz, 6H, C5 and C6 methyls).

Irradiation of 8 in KBr

A 0.4% KBr pellet of 8 was irradiated. The ir taken after 1.3 and 4.3 hours, respectively showed no new peaks. However, after 24 hours of total irradiation, the 5.87 μ C=O had grown in intensity relative to the 5.78 μ C=O.

A. Irradiation of Adduct 8 in the Solid State

Crystals of adduct 8 (172.0 mg) were photolysed discontinuously at 0.02 torr between 7.2° and 8.3° for a total of 35 hours. Recovery of material from the reaction stage was 166.1 mg (97%). Preparative TLC (silica gel, 30% ethyl acetate-benzene) gave 130.3 mg of residual 8, and 27.0 mg (75% yield) of a thick oil which solidified on standing. The yields from two other runs were 74% and 65% respectively. The product from all runs was combined and crystallized twice from ether-petroleum ether with a few drops of acetone. The resulting colorless crystals, 8A, had mp 138-139° (lit.^{24b} 137.5°-139°).

Ir (KBr), 4.45 (C≡N), 5.90 (C=O), 6.28 (conj. C=C) μ .

NMR (CDCl₃) δ , 7.54 (d, J=10 Hz, 1H, C2 vinyl), 6.27 (d, J=10 Hz, 1H, C3 vinyl), 4.77 (d, J=3.5 Hz, 1H, C8 methine), 3.18 (d, J=3.5 Hz, 1H, C7 methine), 2.88 (q, J=7 Hz, 1H, C6 or C9 methine), 2.64 (q, J=8 Hz, 1H, C6 or C9 methine), 1.39 (d, J=7 Hz, 3H, C6 or C9 methyl), 0.94 (d, J=8 Hz, 3H, C6 or C9 methyl).

Mass spectrum m/e parent 240.

B. Irradiation of 8 in the Solid State and Determination of the Extent of Reaction

Crystals of 8 (147.5 mg) were irradiated discontinuously as in A above at a vacuum of 0.03 torr and temperatures between 7.5° and 9.0° for a total of 31 hours. (The reactor was positioned

at the same distance from the lamp as in A). The recovery of material from the reactor was 94%. A 0.3 ml aliquot of a stock solution of nitromethane containing 228.3 mg of CH_3NO_2 per 10 ml of deuteriochloroform solution was added to 32.5 mg of the reaction mixture. This mixture was analysed quantitatively by NMR using the integrations of the C2 and C3 Hs of 8 at 6.94 δ relative to those of the methyl resonance of nitromethane, the internal standard. Using the method outlined under General in the Experimental Section, the residual 8 in the 32.5 mg of mixture was found to be 26.0 mg. The extent of reaction was thus 20%.

To check the accuracy of the method, 33.2 mg of authentic 8 and 0.3 ml of the internal standard stock solution were analysed as above. The amount of 8 as calculated from the NMR analysis was 33.1 mg. The accuracy of this method was thus >99%.

Irradiation of Adduct 8 in Benzene

A solution containing 131.7 mg of compound 8 in 100 ml of benzene was degassed and photolysed, discontinuously for 3 hours. The reaction was followed by TLC (silica gel; 30% ethyl acetate-benzene).

The irradiated solution was concentrated and subjected to column chromatography (silica gel; 30% ethyl acetate-benzene). Combination of the first six fractions followed by removal of solvents gave 20.0 mg of residual 8. Fractions 7-14 gave 67.8 mg (60% yield)

of a pale yellow oil, 8A, which was crystallized twice from ether-petroleum ether with a few drops of acetone.

Mp 141.5°-142.5° (lit.^{24b} 137.5°-139°).

Its ir and NMR were identical to those of solid state product 8A.

Preparation of 2,3,4a β ,6,7,8a β -Hexamethyl-4a,5,8,8a-tetrahydro-1,4-naphthoquinone¹⁰², 9

A mixture of 2.0 g (0.024 mole) of 2,3-dimethyl-1,3-butadiene, 1.61 g (0.098 mole) of duroquinone and a few crystals of hydroquinone were heated in a sealed Pyrex tube at 197° for 23 hours. The contents of the tube were washed out with chloroform. Subsequent removal of the solvent and excess diene left a solid which was crystallized thrice from petroleum ether (68°). This gave 1.36 g (56% yield) of large, pale-yellow crystals of 9.

Mp 113-114° (lit.¹⁰² 115-117°).

Ir (KBr), 5.97 (C=O), 6.15 (conj. C=C) μ .

NMR (CCl₄) δ , 2.70-1.50 (m, 4H, C5 and C8 methylenes), 1.86 (s, 6H, C6 and C7 methyls), 1.60 (s, 6H, C2 and C3 methyls), 1.10 (s, 6H, C9 and C10 methyls).

Irradiation of 9 in KBr

A 0.4% KBr pellet of 9 was irradiated and the reaction followed by ir. After 3 hours of irradiation, the spectrum showed a new broad peak at 2.90 μ indicative of OH and two new carbonyl absorptions at 5.64 and 5.83 μ respectively.

Irradiation of 9 in the Solid State

In a series of reactions, 50-80 mg of 9 were irradiated at 0.03-0.05 torr between -26° to -23° for periods ranging from 1.5 to 24 hours. The recovery of material from the reactor in all cases was >78%. All the reaction mixtures were combined and separated by column chromatography (silica gel; 8% ethyl acetate-benzene). The order of elution was 9, 9B, and 9A. Compound 9 was crystallized from petroleum ether and shown by m.p. ir and NMR to be residual starting material. Product 9B was purified by short path vacuum distillation at 0.01 torr and 65-70° using a Kugelrohr.

Mp* 24.5-26.0°.

Ir (KBr), 5.67, 5.84 (C=O) μ .

NMR (CCl₄) δ , 2.44 (q, J=7.5 Hz, 1H, C7 methine), 2.02 (m, 3H, C1 methine and C4 methylenes), 1.68 (m, 6H, vinyl methyls), 1.21 (s, 3H, methyl), 1.03 (s, 3H, methyl), 1.03 (d, J=7.5 Hz, 3H, C7 methyl), 0.95 (s, 3H, methyl).

Product 9A crystallized from petroleum ether as colorless crystals.

Mp 101.0-102.0° (lit.^{24a} 101.0-102.0°).

Ir (KBr), 2.87 (OH), 6.03 (C=O) μ .

NMR (CCl₄) δ , 5.38 (m, 1H, C9 vinyl), 2.24 (s, 1H, disappears on adding D₂O, OH), 1.85 (d, J=2 Hz, 3H, C3 methyl), 1.76 (d, J=13 Hz, 1H, one of the C6 methylenes), 1.08 (s, 3H, methyl), 0.97 (d, J=13 Hz, 1H, the other C6 methylene), 0.85 (s, 3H, methyl), 0.80 (s, 3H, methyl).

The above spectra reported for 9A and 9B were identical to authentic samples prepared by photolysis of adduct 9 in benzene.

Authentic Samples of Products 9A and 9B

Samples of 9A and 9B for comparative purposes and for the determination of the detector response factors (below) were kindly supplied by Mr. J.P. Louwerens to whom the author is grateful.

Irradiation of 9 in the Solid State. Quantitative GLC Analyses

Analyses were carried out on a 5' x $\frac{1}{4}$ " column of 20% DEGS on 60/80 Chromosorb W operated at 150° and 150 ml/min. Retention times were 16.4, 19.0 and 22.0 minutes for 9B, 9 and 9A respectively. The detector response factors for 9B, 9, and 9A were determined to be 1.5, 1.2 and 1.3 respectively, using a solution containing weighed amounts of the three compounds and an aliquot of a stock solution of biphenyl as the internal standard. (For method of calculations, see under General in the Experimental Section).

Crystals of 9 (49.3 mg) were irradiated between -34.0° and -33.5° for 8 hours. A 0.5 ml aliquot of the stock solution of biphenyl (173.2 mg per 10 ml of benzene solution) was added to the reaction mixture and the mixture analysed by GLC. Results of this and other runs are tabulated in the text under Results and Discussion.

Photolysis of 9 in Diethyl Ether Below the Eutectic Temperature

These reactions were carried out in the apparatus for low temperature solution reactions described under General in the Experimental Section.

A solution containing 86.8 mg of 9 in 40 ml of anhydrous diethyl ether was degassed and photolysed, between -31.5° and -29.0° for 6.5 hours. The reaction mixture was analyzed by GLC using biphenyl as internal standard. For the results of this and other runs, see text.

Preparation of 2,3,4a β ,5 α ,8 α ,8a β -Hexamethyl-4a β ,5,8,8a β -tetrahydro-1,4-naphthoquinone^{24b}, 10

A mixture of 1.6 g (9.7 millimole) of duroquinone, 2.0 g of trans,trans-2,4-hexadiene and a few crystals of hydroquinone were heated in a sealed Pyrex tube at 143° for 46 hours. After cooling, the solid was washed out with acetone. The mixture was stripped of solvent and approximately 100 ml of petroleum ether added. The mixture was warmed with swirling and then filtered. The off-white solid portion (0.611 g) was sublimed at 0.03 torr and 150° and subsequently identified by m.p., ir and NMR to be durohydroquinone. The filtrate was concentrated and cooled first to room temperature and then in ice. This gave 250.3 mg of residual duroquinone. The mother liquor was chromatographed on 30 g of silica gel (<0.08 mm) using benzene as eluent. Fractions were checked by GLC.

(7' x 1/4" column of 20% DEGS on 60/80 Chromosorb W at 170° and 200 ml/min.). The fractions containing duroquinone and 10 were concentrated and separated by GLC. This gave 311.3 mg (15% yield) of 10 as a pale yellow oil. It was crystallized twice from hexane to give material melting at 52-54° (reported^{24b} 47-50°).

Ir (KBr), 5.91 and 6.00 (C=O), 6.13 (conj. C=O) μ .

NMR (CDCl₃) δ , 5.44 (s, 2H, C6 and C7 vinyls), 2.02 (q, J=8 Hz, C5 and C8 methines), 1.91 (s, C2 and C3 methyls), 1.27 (s, 6H, C4a and C8a methyls), 1.01 (d, J=8 Hz, 6H, C5 and C8 methyls).

Irradiation of 10 in KBr

A 0.4% KBr pellet of 10 was irradiated. The ir of the pellet was recorded at hourly intervals for the first 2 hours and then at longer intervals up to 17 hours total time of irradiation. There were no changes in the spectrum for the first 2 hours. However, after 6 hours of total irradiation, broadening in the 5.6-5.78 μ region became apparent. The ir recorded after 17 hours of irradiation showed two new carbonyl stretches at 5.70 and 5.76 μ .

Irradiation of 10 in the Solid State

A solution containing 56.6 mg of 10 in acetone-hexane was slowly evaporated on the reaction stage and left overnight. It was observed that no crystallization had occurred. The apparatus was assembled as for a normal run except that the sample was neither

cooled nor irradiated. It was left under vacuum thus for an hour. The reaction stage was subsequently cooled down to -9.5° and the sample kept under vacuum and at this temperature for 6 hours. It was subsequently left under vacuum overnight. This procedure allowed 10 to crystallize out on the reaction stage. The sample was irradiated at 0.03 torr between -9.9° and -9.1° for a total of 14 hours. The material which was recovered from the reactor weighed 53.4 mg (95% recovery).

The irradiated sample was checked by TLC (silica gel; 15% ethyl acetate-benzene), GLC (7' x $\frac{1}{4}$ " column of 20% DEGS on 60/80 Chromosorb W, at 170° and 150 ml/min.), ir and NMR. All analyses showed the presence of only 10.

In a similar procedure 43.2 mg of 10 evaporated from petroleum ether was irradiated at 0.04 torr and -1.4° to -0.5° for 13 hours. Analyses as above again showed no reaction had occurred.

Preparation of 2,3,4a β ,5 β ,8 β ,8a β -Hexamethyl-4a,5,8,8a-tetrahydro-1,4-naphthoquinone^{24b}, 11

A mixture of 3.20 g (19.5 millimoles) of duroquinone, 4 g of trans,trans-2,4-hexadiene and a few crystals of hydroquinone was heated at 185° in a sealed Pyrex tube for 22.4 hours. The resulting dark-brown mixture was washed out with chloroform. An insoluble solid (1.6 g) was filtered and purified by sublimation (150° , 0.03 torr). It had mp $228-229^{\circ}$ and was identified by infrared, NMR and

elemental analysis to be durohydroquinone, mp⁸⁴ 233°. The mother liquor was concentrated and subjected to column chromatography on 64 g of neutral alumina activity grade 1 from M. Woelm. It was eluted first with benzene and approximately 110 ml collected and shown by GLC (5' x ¼" stainless steel, 20% DEGS on 60/80 Chromosorb W; 130°, 180 ml/min) to contain none of the desired Diels-Alder adduct. The eluting solvent was changed to 15% ethyl acetate-benzene and subsequent fractions checked by GLC. The fractions containing adduct 11 were combined and stripped of solvents. The resulting oil solidified on standing to give 160 mg (3% yield) of compound 11. It was crystallized twice from petroleum-ether to give pale-yellow rods of 11 melting at 104-105° (lit.^{24b} 103-104°).

Ir (KBr) 5.99 (C=O), 6.12 (conj. C=C) μ .

NMR (CDCl₃) δ , 5.42 (s, 2, vinyls), 2.85 (q, J=7 Hz, 2, C5 and C8 methines), 1.97 (s, 6, C2 and C3 methyls), 1.13 (s, 6, C4a and C8a methyls), 0.93 (d, J=7 Hz, 6, C5 and C8 methyls).

Irradiation of Compound 11 in KBr

A 0.4% KBr pellet of compound 11 was irradiated ($\lambda \geq 340$ nm) and the reaction monitored by infrared. After 0.5 hour, the reaction was complete as judged by the disappearance of a moderately intense peak of 11 at 7.98 μ . A fairly sharp and intense peak had developed at 2.88 μ . In addition, there were new carbonyl absorptions at 5.67, 5.85 and 6.05 μ , respectively. Further irradiation up to 1.5 hours of

total irradiation time produced no further changes in the spectrum.

A. Irradiation of Compound 11 in the Solid State

Crystals of compound 11 (56.9 mg) were irradiated ($\lambda \geq 355$ nm) at 0.005 torr and between -32.4 and -31.7° for 5.6 hours. The reaction mixture was washed off the reactor's cavity with chloroform, stripped of solvent and dried in vacuo. The recovered material weighed 49.2 mg (86% recovery). A small amount of this mixture (5 mg) was used in GLC analysis (5' x $\frac{1}{4}$ " stainless steel column of 20% DEGS on A/W Chromosorb W; 60/80 mesh) at 150° and 100 ml/min. It showed two peaks with retention times of approximately 16 and 22 minutes, respectively. The rest of the reaction mixture (44.2 mg) was subjected to preparative TLC (silica gel; 8% ethyl acetate-benzene). This gave 11.6 mg of a white solid (lower band) and 25.9 mg of an oil. The infrared and NMR spectra of these two samples showed that the solid was enone-alcohol 11A and the oil ene-dione 11B. The starting material 11 which has the same R_f (TLC) and the same GLC retention time as product 11B was found to be absent from the NMR sample of 11B. The conversion of starting material to photoproducts is thus complete. The combined isolated yield of the two products is 85% and the 11A:11B ratio is 1:2.

In another run, 70.4 mg of crystals of adduct 11 were irradiated at 0.005 torr and between -31.6° and -27.3° for 5 hours. The recovered material from the reactor weighed 60.8 mg (86% recovery).

A portion of this material (29.0 mg) was set aside for GLC analysis. The rest of the reaction mixture was separated by preparative TLC (silica gel; 8% ethyl acetate-benzene) and shown by NMR to contain only photoproducts 11A and 11B.

An aliquot (0.2 ml) of a stock solution of internal standard (173.2 mg of biphenyl in 10 ml of benzene) was added to the 29.0 mg of reaction mixture and the resulting solution analyzed by GLC (5' x 1/4" column of 20% DEGS at 150° and 150 ml/min). The peak areas for biphenyl, 11B and 11A were calculated for each of 4 injections. The relative areas (area of sample peak/area of biphenyl peak) were calculated and the average relative area for each of the two peaks found. The detector response factors for 11B and 11A under identical GLC conditions were 1.9 and 1.7, respectively. Using these values, the average relative areas and the weight of internal standard in the GLC mixture, the weight of each of the two products was calculated as outlined under General in the Experimental Section. This analysis showed that the 29.0 mg sample of reaction mixture contained 8.4 mg of enone-alcohol 11A and 16.7 mg of ene-dione 11B. The combined GLC yield of the two products is thus 86% and the 11A:11B ratio is 1:2.

B. Low Conversions of Adduct 11

Since the starting material 11 and one of its photoproducts, namely 11B could not be separated by GLC or TLC under the conditions

tried, the analyses of reaction mixtures containing 11, 11A and 11B were carried out as follows: the reaction mixture was first separated by TLC into two fractions, one containing solely 11A and the other containing product 11B and residual starting material 11. The 11 + 11B mixture was then analyzed by quantitative NMR using the integrated peak area of the C2 and C3 methyl resonance of 11 at δ 1.97 and the peak area of the resonances of added biphenyl as internal standard. This analysis allowed for the calculation of the weight of residual 11 in the reaction mixture. The yield of photoproduct 11B is then easily found by subtracting the calculated weight of residual 11 from the 11 + 11B mixture. Below is one of the low conversion runs which was analyzed by this method.

Crystals of compound 11 (53.6 mg) were irradiated at 0.005 torr between -32.1° and -31.5° for 2 hours. The weight of recovered reaction mixture from the reactor was 49.1 mg (92% recovery). Preparative TLC (silica gel; 8% ethyl acetate-benzene) gave 6.4 mg of enone-alcohol 11A and an upper band material of 29.5 mg. Crystallized biphenyl (8.4 mg) was added to the upper band material to serve as the internal standard. The mixture was dissolved in chloroform-d and analyzed quantitatively by NMR. The ten protons of biphenyl integrated for 39.5 and the six protons of 11 integrated for 26. Using the formula given under General in the Experimental Section, the residual starting material 11 in the sample was calculated to be 15.8 mg. The conversion of 11 to products is thus 56% and the weight of product 11B is 13.7 mg. The combined yield

of products 11A and 11B by this analysis is 81% and the 11A:11B ratio is again 1:2. The results of similar runs are given in the text.

The enone-alcohol product from all the runs was combined and crystallized from petroleum-ether to give colorless rods of 11A melting at 158-159° (lit.^{24b} 156.5-157°C).

Ir (KBr) 2.94 (OH), 6.04 (C=O) and 6.15 (conj. C=C) μ .

NMR (CDCl₃) δ , 5.92 (m, 1, vinyl), 2.63 (dd, $J_{6,7}=3$ Hz, $J_{7,8}=3$ Hz, 1, C7 methine), 2.57 (s, 1, OH, disappears on adding D₂O), 2.23 (m, 1, C6 methine), 1.91 (d, $J_{<2}$ Hz, 3, C3 methyl), 1.82 (d, $J_{<2}$ Hz, 3, C2 methyl), 1.78 (d, $J_{<2}$ Hz, 3, C9 methyl), 0.87 (s, 3, C5 methyl), 0.77 (s, C10 methyl), 0.75 (d, $J=7$ Hz, C6 methyl).

Mass spectrum m/e parent 246.

The above spectra were identical to those of 11A isolated from the photolysis of adduct 11 in benzene^{24b}.

All the upper band materials from preparative TLC were combined and photolysed for 0.3 hours to photolyse residual 11. The resulting mixture was separated by preparative TLC (8% ethyl acetate-benzene). The oil (upper band material) was assigned the structure 11B based on the following spectra data:

Ir (Film), 5.64 and 5.83 (C=O) μ .

NMR (CDCl₃) δ , 6.04 (dd, $J_{2,3}=10$ Hz, $J_{3,4}=5.5$ Hz, 1, C3 vinyl), 5.59 (dd, $J_{2,3}=10$ Hz, $J_{2,4}=1.5$ Hz, 1, C2 vinyl), 2.82 (q, $J=7.5$ Hz, 1, C7 methine), 2.26 (m, 1, C4 methine), 1.15 (s, C8 methyl), 1.15 (d, $J=7.5$ Hz, C7 methyl), 1.13 (s, C1 methyl), 1.11 (d, $J=7.5$ Hz, C4 methyl), 1.09 (s, methyl), 1.04 (s, methyl).

Mass spectrum m/e parent 246.

The infrared and NMR spectra were identical to those of 11B isolated from the photolysate of 11 in benzene^{24b}.

Irradiation of Enone-Alcohol 11A in KBr

A 0.4% KBr pellet of photoproduct 11A was irradiated ($\lambda \geq 355$ nm) continuously for 2 hours. The infrared spectrum of the irradiated pellet was identical to that of 11A.

BIBLIOGRAPHY

- (1) (a) J.C.D. Brand and J.C. Speakman, "Molecular Structure", Edward Arnold Publishers Ltd., London, 1964, p. 210.
(b) G.H. Stout and L.H. Jensen, "X-ray Structure Determination", Macmillan Co., New York, N.Y. 1960.
(c) M.J. Buerger, "Crystal Structure Analysis", Wiley and Sons, New York, N.Y. 1960.
- (2) (a) J.M. Thomas and J.O. Williams, "Progress in Solid State Chemistry", Vol. 6, H. Reiss and J.O. McCaldin, Ed., Pergamon Press, Oxford, 1961, p. 119-154.
(b) J.M. Thomas, Adv. Catal., 19, 202 (1969).
(c) J.M. Thomas, Chem. Brit. 6, 60 (1970).
(d) J.M. Thomas, Phil. Trans. R. Soc. Lond., A, Vol. 277, 251 (1974).
(e) I.C. Paul and D.Y. Curtin, Accounts Chem. Res., 6, 217 (1973) and references 22b, 30, 32 and 40 therein.
- (3) D. Hull, "Introduction to Dislocations", Pergamon Press, New York, N.Y., 1965.
- (4) H.G. van Bueren, "Imperfections in Crystals", Interscience, New York, N.Y., 1960.
- (5) W. Dekeyser, "Reactivity of Solids", J.H. de Boer, W.G. Burgers, E.W. Gorter, J.P.F. Huese and G.C.A. Schuit, Ed., Elsevier Publishing Co., New York, N.Y., 1961, p. 376.
- (6) "Physics and Chemistry of the Organic Solid State", Vol. 1, D. Fox, M.M. Labes and A. Weissberger, Ed., Interscience, New York, N.Y., 1963, ch. 3, 4 and 5.

- (7) J.N. Sherwood and S.J. Thomson, Trans. Faraday Soc., 56, 1443 (1960).
- (8) (a) D.K. Ghosh and D.H. Whiffen, Mol. Phys., 2, 285 (1959).
(b) W.E. Gibbs and R.L. Van Deusen, J. Polymer Sci., 54, 51 (1961).
(c) I. Miyagawa and W. Gordy, J. Chem. Phys., 30, 1590 (1959).
(d) H.M. McConnell, C. Heller, T. Cole and R.W. Fessenden, J. Am. Chem. Soc., 82, 766 (1960).
- (9) (a) I. Norman and G. Porter, Proc. Roy. Soc. (London), A230, 399 (1955).
(b) J.W. Breitenbach and H. Frittm, J. Polymer Sci., 29, 565 (1956).
- (10) J.P. McCullough, H.L. Finke, J.F. Messerly, S.S. Todd, T.C. Kincheloe, and G. Waddington, J. Phys. Chem., 61, 1105 (1957).
- (11) M.D. Cohen, R. Cohen, M. Lahav and P.L. Nie, J. Chem. Soc. Perkin Trans. II, 1095, (1973).
- (12) (a) M.D. Cohen and G.M.J. Schmidt, J. Chem. Soc., 1996 (1964).
(b) G.M.J. Schmidt, "Reactivity of the Photoexcited Organic Molecule", Interscience, New York, N.Y. 1967, p. 227.
- (13) (a) M.D. Cohen, Angew. Chem. Int. Ed. Engl., 14, 388 (1975).
(b) E.J. Baum, "Excited State Chemistry", J.N. Pitts, Jr., Ed, Gordon and Breach, New York, N.Y. 1970, p. 121.
- (14) D. Goode, Y. Lupien, W. Siebrand, D.F. Williams, J.M. Thomas and J.O. Williams, Chem. Phys. Lett., 25, 308 (1974).
- (15) (a) J.O. Williams and J.M. Thomas, Trans. Faraday Soc., 63, 1720 (1967).
(b) J.M. Thomas and J.O. Williams, Chem. Commun., 432 (1967).

- (16) (a) D.P. Craig and P. Sarti-Fantoni, Chem. Commun., 742 (1966).
(b) M.D. Cohen, Z. Ludmer, J.M. Thomas and J.O. Williams, Proc. Roy. Soc. (London), A324, 459 (1971).
(c) M.D. Cohen, Z. Ludmer, J.M. Thomas and J.O. Williams, Chem. Commun., 1172 (1969).
(d) M.D. Cohen and B.S. Green, Chem. Brit., 9, 490 (1973).
- (17) G.C. Nieman and G.W. Robinson, J. Chem. Phys., 37, 2150 (1962).
- (18) M.A. El-Sayed, M.T. Wauk and G.W. Robinson, Mol. Phys., 5, 205 (1962).
- (19) G. Schuster and N.J. Turro, Tetrahedron Lett., 2261 (1975).
- (20) (a) O. Simpson, Proc. Roy. Soc., (London), A238, 402 (1956).
(b) D.C. Northrop and O. Simpson, ibid., A234, 136 (1956).
- (21) D.L. Dexter, J. Chem. Phys., 21, 836 (1953).
- (22) O. Diels and K. Alder, Chem. Ber., 62, 2362 (1929).
- (23) R.C. Cookson, E. Crundwell, R.R. Hill, and J. Hudec, J. Chem. Soc., 3062 (1964).
- (24) (a) J.R. Scheffer, K.S. Bhandari, R.E. Gayler and R.A. Wostradowski, J. Am. Chem. Soc., 97, 2178 (1975) and reference 2 therein.
(b) J.R. Scheffer, B.M. Jennings and J.P. Louwerens, J. Am. Chem. Soc., 98, 7040 (1976).
(c) J.R. Scheffer and B.M. Jennings, Chem. Commun., 609 (1975).
- (25) (a) A. Padwa and R. Gruber, J. Am. Chem. Soc., 92, 107 (1970).
(b) A. Padwa and W. Eisenhardt, ibid., 93, 1400 (1971).
(c) R.A. Cormier, W.L. Schreiber and W.C. Agosta, J. Am. Chem. Soc., 95, 4873 (1973).

- (d) R.A. Cormier and W.C. Agosta, ibid., 96, 618 (1974).
- (e) T. Hasegawa, H. Aoyama and Y. Omote, Tetrahedron Lett., 1901 (1975).
- (26) (a) P.J. Wagner, Accounts Chem. Res., 4, 168 (1971) and references therein.
- (b) P.J. Wagner and G.S. Hammond, "Advances in Photochemistry", Vol. 5, W.A. Noyes, Jr., G.S. Hammond, and J.N. Pitts, Jr., Ed., Interscience, New York, N.Y., 1968, p. 21-156 and references therein.
- (27) (a) W. Herz and M.G. Nair, J. Am. Chem. Soc., 89, 5474 (1967).
- (b) S. Wolff, W.L. Schreiber, A.B. Smith, III, and W.C. Agosta, ibid., 94, 7797 (1972).
- (c) A.B. Smith, III, and W.C. Agosta, J. Am. Chem. Soc., 95, 1961 (1973).
- (d) A. Marchesini, U.M. Pagnoni and A. Pinetti, Tetrahedron Lett., 4299 (1973).
- (28) R.R. Sauers, A.D. Rousseau and B. Byrne, J. Am. Chem. Soc., 97, 4947 (1975) and references 2-21 therein.
- (29) (a) R.C. Cookson, E. Crundwell and J. Hudec, Chem. Ind. (London), 1003 (1958).
- (b) P. Yates and P.E. Eaton, Tetrahedron Lett., 5 (1960).
- (c) P.E. Eaton and T.W. Cole, Jr., J. Am. Chem. Soc., 86, 962, 3157 (1964).
- (30) R.C. Cookson, R.R. Hill and J. Hudec, J. Chem. Soc., 3043 (1964).
- (31) P.J. Wagner, A.E. Kempainen and H.N. Schott, J. Am. Chem. Soc., 95, 5604 (1973).

- (32) G. Porter and P. Suppan, Trans. Faraday Soc., 61, 1664 (1965).
- (33) H. Morrison, V. Tisdale, P.J. Wagner and K.-C. Liu, J. Am. Chem. Soc., 97, 7189 (1975).
- (34) (a) I. Kochevar and P.J. Wagner, J. Am. Chem. Soc., 94, 3859 (1972).
(b) R.A. Caldwell, G.W. Sovocool and R.P. Gajewski, J. Am. Chem. Soc., 95, 2549 (1973).
- (35) S.G. Cohen, A. Parola and G.H. Parsons, Jr., Chem. Rev., 73, 141 (1973) and references therein.
- (36) K. Watanabe, T. Nakayama and J. Mottl, J. Quart. Spectry. Radiative Transfer, 2, 369 (1962).
- (37) K. Furukawa and E.A. Ogryzlo, J. Photochem., 1, 163 (1972/73).
- (38) (a) D. Bellus, D.R. Kearns and K. Schaffner, Helv. Chim. Acta., 52, 971 (1969).
(b) T. Kobayashi, M. Kurono, H. Sato and K. Nakanishi, J. Am. Chem. Soc., 94, 2863 (1972).
- (39) R.L. Cargill, W.A. Bundy, D.M. Pond, A.B. Sears, J. Saltiel and J. Winterle, Mol. Photochem., 3, 123 (1971) and references therein.
- (40) (a) J.C. Dalton, K. Dawes, N.J. Turro, D.S. Weiss, J.A. Barltrop and J.D. Coyle, J. Am. Chem. Soc., 93, 7213 (1971).
(b) K. Dawes, J.C. Dalton and N.J. Turro, Mol. Photochem., 3, 71 (1971).
- (41) (a) D.H. Williams, J.M. Wilson, H. Budzikiewicz and C. Djerassi, J. Am. Chem. Soc., 85, 2091 (1963).
(b) D.H. Williams and C. Djerassi, Steroids, 3, 259 (1964).
(c) C. Djerassi, G. von Mutzenbecher, J. Fajkos, D.H. Williams and H. Budzikiewicz, J. Am. Chem. Soc., 87, 817 (1965).

- (d) C. Djerassi and L. Tökés, ibid., 88, 536 (1966).
- (e) L. Tökés, R.T. LaLonde and C. Djerassi, J. Org. Chem., 32, 1020 (1967).
- (42) J.D. Henion and D.G.I. Kingston, J. Am. Chem. Soc., 96, 2532 (1974).
- (43) F.P. Boer, T.W. Shannon and F.W. McLafferty, J. Am. Chem. Soc., 90, 7239 (1968).
- (44) F.D. Lewis, R.W. Johnson and R.A. Ruden, J. Am. Chem. Soc., 94, 4292 (1972).
- (45) (a) H.W. Kohlshütter, Z. Anorg. Allg. Chem., 105, 121 (1918).
(b) H.W. Kohlshütter, Naturwissenschaften, 11, 865 (1923).
(c) E. Hertel, Z. Electrochem., 37, 536 (1931).
- (46) R.E. Long, Ph.D. Thesis, University of California, Los Angeles, 1965.
- (47) (a) S.E.V. Phillips and J. Trotter, Acta Crystallogr., B33, in press.
(b) S.E.V. Phillips and J. Trotter, Acta Crystallogr., B33, in press.
(c) S.E.V. Phillips and J. Trotter, Acta Crystallogr., B33, in press.
- (48) R.C. Cookson, D.A. Cox and J. Hudec, J. Chem. Soc., 1717 (1962).
- (49) G.W. Griffin, A.F. Velluro and K. Furukawa, J. Am. Chem. Soc., 83, 2725 (1961).
- (50) L.J. Bellamy, "The Infrared Spectra of Complex Molecules", 3rd Ed., Chapman and Hall Ltd., 1975, p. 33.
- (51) J.M. Derfer, E.E. Pickett and C.E. Boord, J. Am. Chem. Soc., 71, 2482 (1949).
- (52) E.B. Reid and M. Sack, J. Am. Chem. Soc., 73, 1985 (1951).
- (53) J. Dekker, P.J. van Vuuren and D.P. Venter, J. Org. Chem., 33, 464 (1968).

- (54) R. Criegee, J. Dekker and H.A. Brune, Ber. Deut. Chem. Ges., 96 2368 (1963).
- (55) E.E. van Tamelin, M. Shamma, A.W. Burgstahler, J. Wolinsky, R. Tamm and P.E. Aldrich, J. Am. Chem. Soc., 91, 7324 (1969).
- (56) H. Ziffer and I. Levin, J. Org. Chem., 34, 4057 (1969).
- (57) D.A. Dows in "Physics and Chemistry of the Organic Solid State", Vol. 1, D. Fox, M. Labes and A. Weissberger, Ed., Interscience, New York, N.Y., 1963, ch. 11 and references therein.
- (58) C.Y. Liang, S. Krimm and G.B.B.M. Sutherland, J. Chem. Phys., 25 543, 549 (1963).
- (59) D.A. Dows, E. Whittle and G.C. Pimentel, J. Chem. Phys., 23, 1475 (1955) and references 11 and 12 therein.
- (60) (a) J.K. Brown and N. Sheppard, Discuss. Faraday Soc., 9, 144 (1950).
(b) J.K. Brown and N. Sheppard, Trans. Faraday Soc., 50, 535 (1954).
- (61) G.M.J. Schmidt, Pure Appl. Chem., 27, 647 (1971).
- (62) P.E. Eaton, Accounts Chem. Res., 1, 50 (1968) and references therein.
- (63) P. de Mayo, Accounts Chem. Res., 4, 41 (1971) and references therein.
- (64) J. Dekker, F.J.C. Martins, J.A. Kruger and A.J. Goosen, Tetrahedron Lett., 3721 (1974).
- (65) (a) G.S. Hammond, C.A. Stout and A.A. Lamola, J. Am. Chem. Soc., 86, 3103 (1964).
(b) H. Morrison, H. Curtis and T. McDowell, ibid., 88, 5415 (1966).
- (66) (a) A.A. Lamola, Photochem. Photobiol., 7, 619 (1968).
(b) R. Lisewski and K.L. Wierzchowski, ibid., 11, 327 (1970).

- (67) S.E.V. Phillips and J. Trotter, Acta Crystallogr., B32, 3098 (1976).
- (68) A. Bondi, J. Phys. Chem., 68, 441 (1964).
- (69) (a) D.H. Williams and I. Fleming, "Spectroscopic Methods in Organic Chemistry", 2nd Ed., McGraw-Hill (UK) Ltd., Maidenhead, Berkshire, England, 1973, p. 96.
- (b) R.M. Silverstein and G.C. Bassler, "Spectroscopic Methods in Organic Chemistry", 2nd Ed., John Wiley and Sons Inc., New York, N.Y., 1967, p. 118.
- (70) N.H. Werstiuk and R. Taillefer, Can. J. Chem., 48, 3966 (1970).
- (71) B.M. Jennings, Ph.D. Thesis, University of British Columbia, 1975.
- (72) R.B. Woodward and R. Hoffman, "The Conservation of Orbital Symmetry", Academic Press, New York, N.Y. 1970.
- (73) S.E.V. Phillips and J. Trotter, Acta Crystallogr., in press.
- (74) S.E.V. Phillips and J. Trotter, Acta Crystallogr., B32, 3101 (1976).
- (75) S.E.V. Phillips and J. Trotter, Acta Crystallogr., in press.
- (76) (a) L. Pasteur, Ann. Chim. et phys., 24, 442 (1848).
- (b) K. Vogler and M. Kofler, Helv. Chim. Acta., 39, 1387 (1956).
- (c) R.C. Ferreira, Nature, 171, 39 (1953).
- (d) E. Havinga, Biochim. et Biophys. Acta, 13, 171 (1954).
- (77) S.E.V. Phillips and J. Trotter, Acta Crystallogr., B32, 3088 (1976).
- (78) P.J. Wagner, P.A. Kelso, A.E. Kemppainen and R.G. Zepp, J. Am. Chem. Soc., 94, 7500 (1972) and references 2-4 and 8 therein.
- (79) S.E.V. Phillips and J. Trotter, Acta Crystallogr., B32, 3091 (1976).
- (80) A.F. Thomas and B. Willhalm, Helv. Chim. Acta., 50, 826 (1967).

- (81) (a) J.C.D. Brand and D.G. Williamson, Advan. Phys. Org. Chem., 1, 365 (1963) and references therein.
- (b) J.C.D. Brand and D.G. Williamson, Discuss. Faraday Soc., 35, 184 (1963).
- (c) D.A. Haner and D.A. Dows, J. Mol. Spectrosc., 34, 296 (1970).
- (d) C.T. Lin and D.C. Moule, ibid., 38, 136 (1971).
- (82) (a) M.A. Winnik, A. Lemire, D.S. Saunders and C.K. Lee, J. Am. Chem. Soc., 98, 2000 (1976).
- (b) M.A. Winnik, S.N. Basu, C.K. Lee and D.S. Saunders, ibid., 98, 2928 (1976).
- (83) J.T. Edward, J. Chem. Educ., 47, 261 (1970).
- (84) "Handbook of Chemistry and Physics", 52nd Ed., Chemical Rubber Co., Cleveland, Ohio, 1971-1972.
- (85) D. Rabinovich and G.M.J. Schmidt, J. Chem. Soc., B., 144 (1967).
- (86) S.E.V. Phillips and J. Trotter, Acta Crystallogr., in press.
- (87) S.E.V. Phillips and J. Trotter, Acta Crystallogr., B32, 3095 (1976).
- (88) D.R. Arnold, "Advances in Photochemistry", Vol. 6, W.A. Noyes, Jr., G.S. Hammond and J.N. Pitts, Jr., Ed., Interscience, New York, N.Y., 1968, p. 301.
- (89) S.E.V. Phillips and J. Trotter, Acta Crystallogr., B32, 3095 (1976).
- (90) H. Sternlicht, G.C. Nieman and G.W. Robinson, J. Chem. Phys., 38, 1326 (1963).
- (91) J. Kaiser, G. Wegner and E.W. Fischer, Isr. J. Chem., 10, 157 (1972),
- (92) L.-U. Meyer and A. de Meijere, Tetrahedron Lett., 497 (1976).

- (93) (a) D.J. Pasto and C.R. Johnson, "Organic Structure Determination", Prentice-Hall Inc., Englewood Cliffs, N.J., 1969, p. 207.
- (b) J.A. Pople, W.G. Schneider and H.J. Bernstein, "High Resolution Nuclear Magnetic Resonance", McGraw-Hill Inc., 1959, ch. 19 and references therein.
- (94) H. Schenker, J.I. Lauritzen, Jr., R.J. Corriccini and S.T. Lonberger "Reference Tables for Thermocouples", National Bureau of Standards Circular, 561 (1955), U.S. Government Printing Office, Washington, D.C., p. 35.
- (95) H.V. Euler, H. Hasselquist and A. Glaser, Ark. Kemi, 3, 49 (1951).
- (96) A. Mandelbaum and M. Cais, J. Org. Chem., 27, 2245 (1962).
- (97) (a) A.C. Cope, D.S. Smith and R.J. Cotter, Org. Syntheses Coll. Vol. 4, 377 (1963).
- (b) I. Iwai and J. Ide, Org. Syn., 50, 62 (1970).
- (c) C.F.H. Allen, C.G. Eliot and A. Bell, Can. J. Res. (B), 17, 87 (1939)
- (98) (a) L.F. Fieser, "Experiments in Organic Chemistry", 2nd Ed., D.C. Heath and Co., Boston, Mass., 1941, p. 228.
- (b) L.F. Fieser and F.C. Chang, J. Am. Chem. Soc., 64, 2048 (1942).
- (99) C.F.H. Allen and A. Bell, Org. Syn., 22, 37 (1942).
- (100) A.G. Brook, J. Chem. Soc., 5040 (1952).
- (101) M.F. Ansell, B.W. Nash and D.A. Wilson, J. Chem. Soc., 3023 (1963).
- (102) M.F. Ansell, B.W. Nash and D.A. Wilson, J. Chem. Soc., 3027 (1963).

APPENDIX

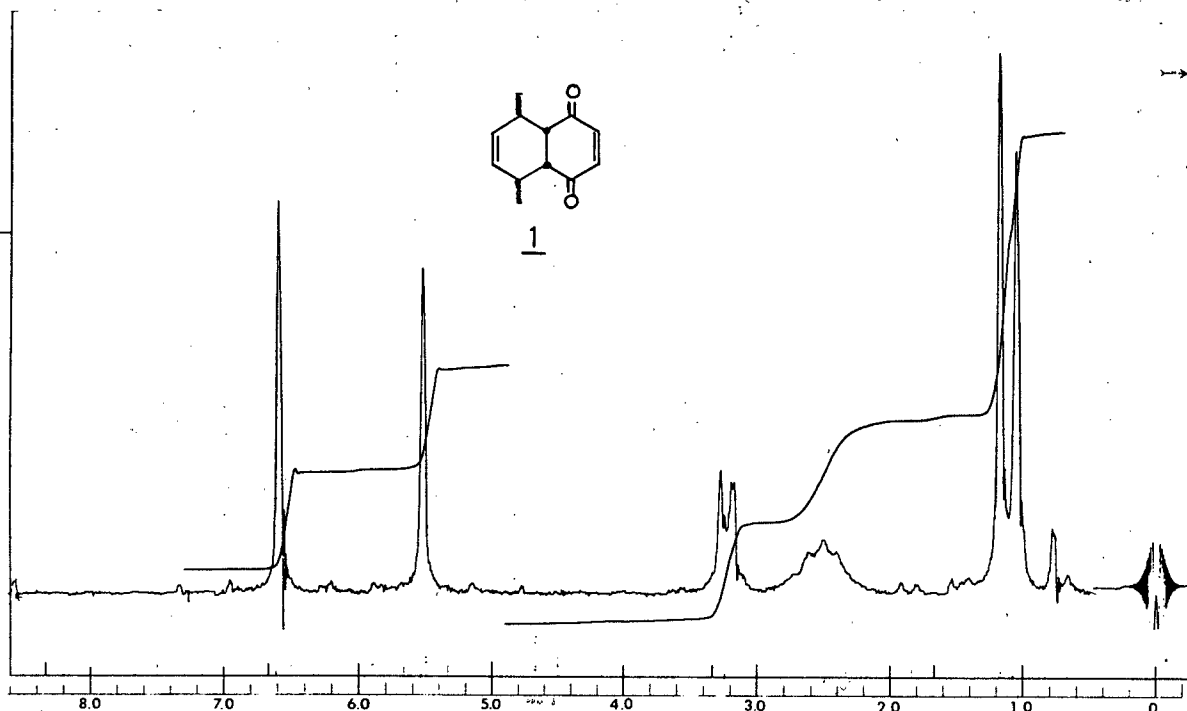


Figure 33. A 60 MHz PMR Spectrum of 5 α ,8 α -Dimethyl-4 α β ,5,8,8 α β -tetrahydro-1,4-naphthoquinone, **1**.

* = CDCl₃ impurity (see Figure 55)

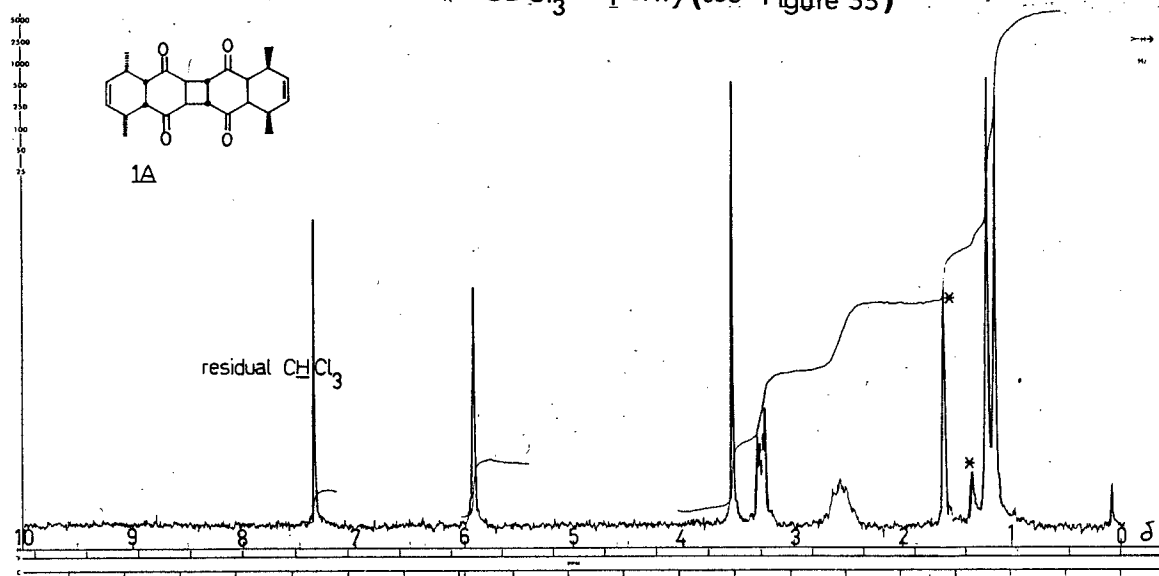


Figure 34. Fourier Transform 100 MHz PMR Spectrum of 5,8,15,18-Tetramethylpentacyclo[10.8.0.0²,11.0⁴,9.0¹⁴,19]eicosa-6,16-dien-3,10,13,20-tetrone, **1A**.

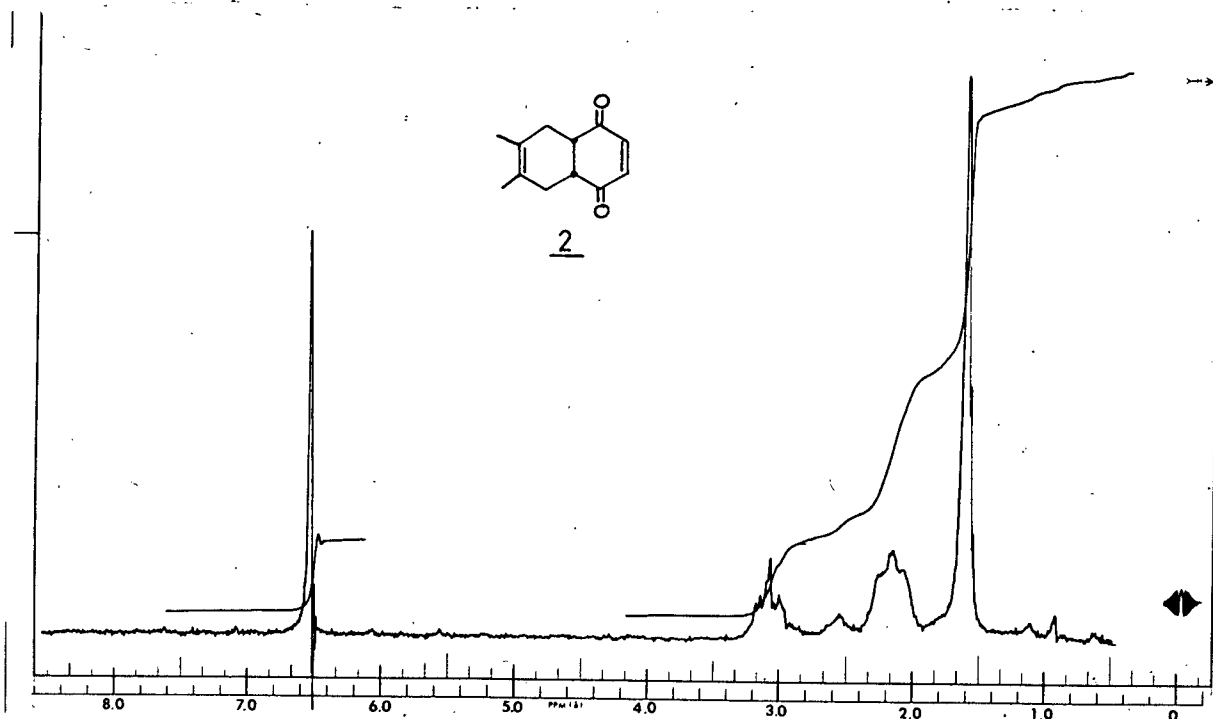


Figure 35. A 60 MHz PMR Spectrum of 6,7-Dimethyl-4aβ,5,8,8aβ-tetrahydro-1,4-naphthoquinone, **2**.

*=CDCl₃ impurity (see Figure 55)

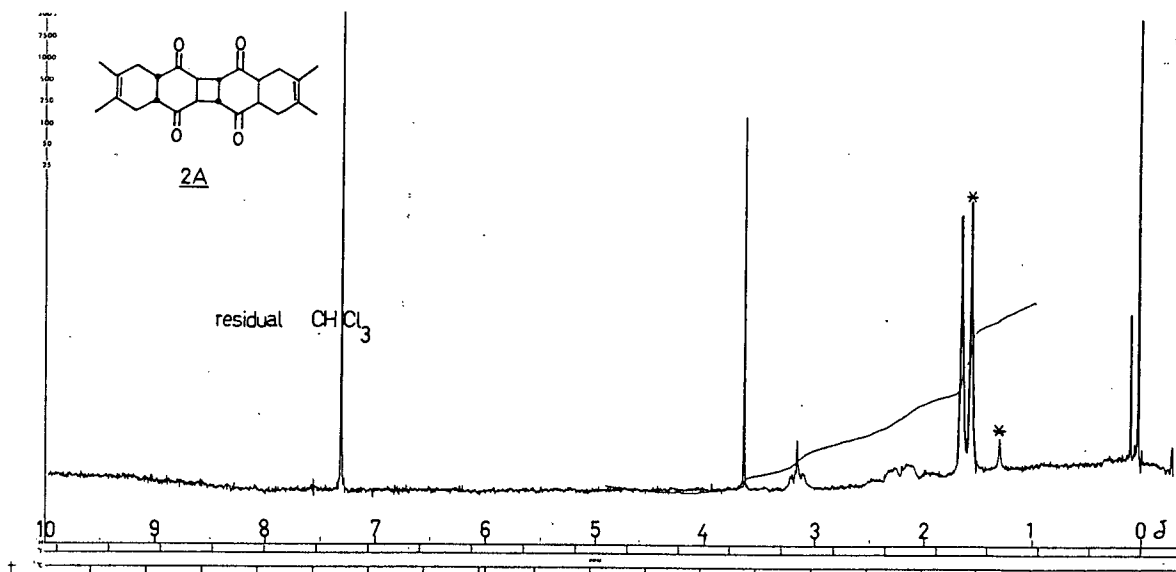


Figure 36. Fourier Transform 100 MHz PMR Spectrum of 6,7,16,17-Tetramethylpentacyclo[10.8.0.0^{2,11}.0^{4,9}.0^{14,19}]eicosa-6,16-dien-3,10,13,20-tetrone, **2A**.

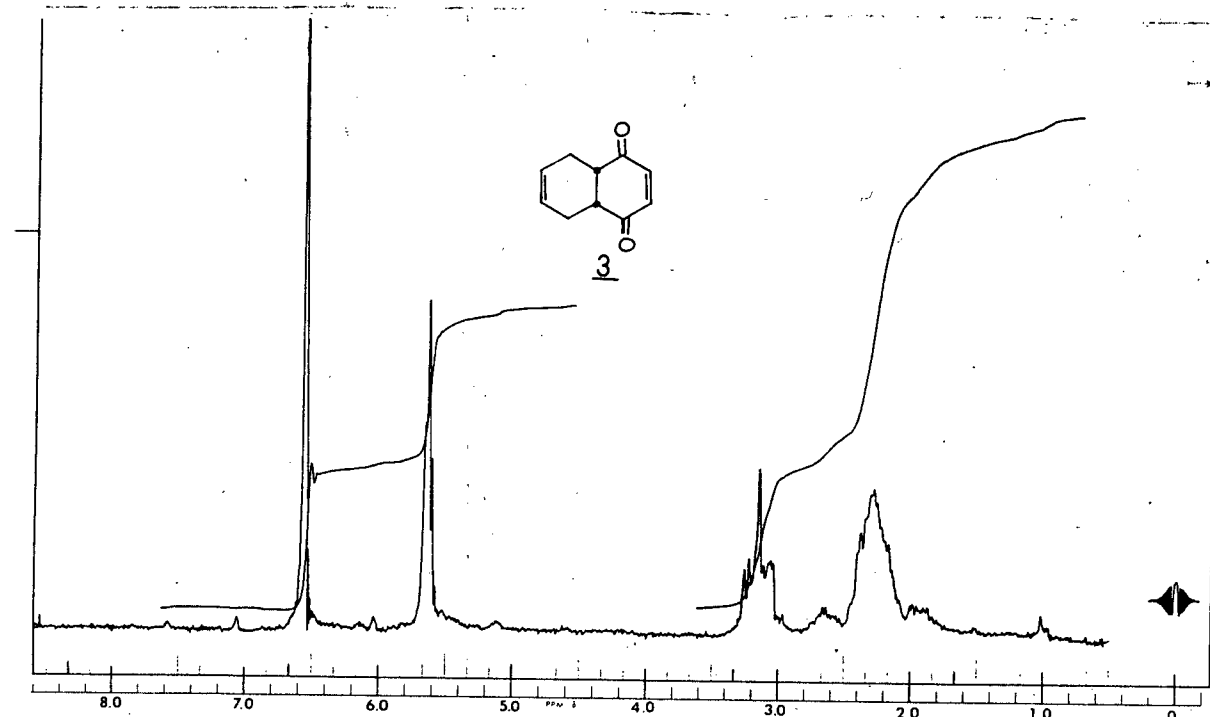


Figure 37. A 60 MHz PMR Spectrum of 4aβ,5,8,8aβ-Tetrahydro-1,4-naphthoquinone, 3.

* = CDCl_3 impurity { see Figure 55 }
 ** = noise spike

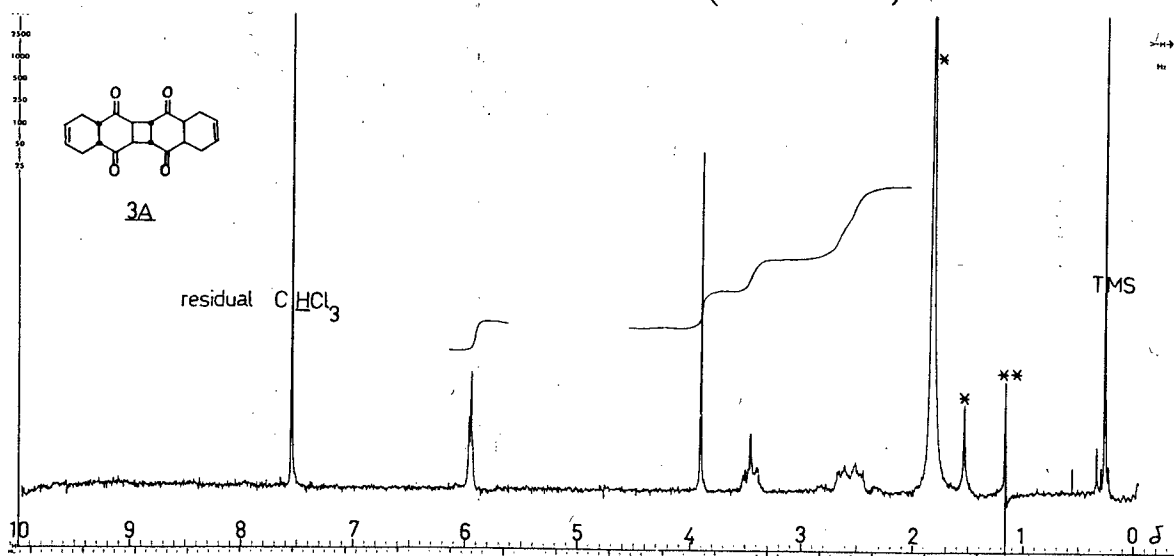


Figure 38. Fourier Transform 100 MHz PMR Spectrum of Pentacyclo-[10.8.0.0^{2,11}.0^{4,9}.0^{14,19}]eicosa-6,16-diene-3,10,13,20-tetrone, 3A.

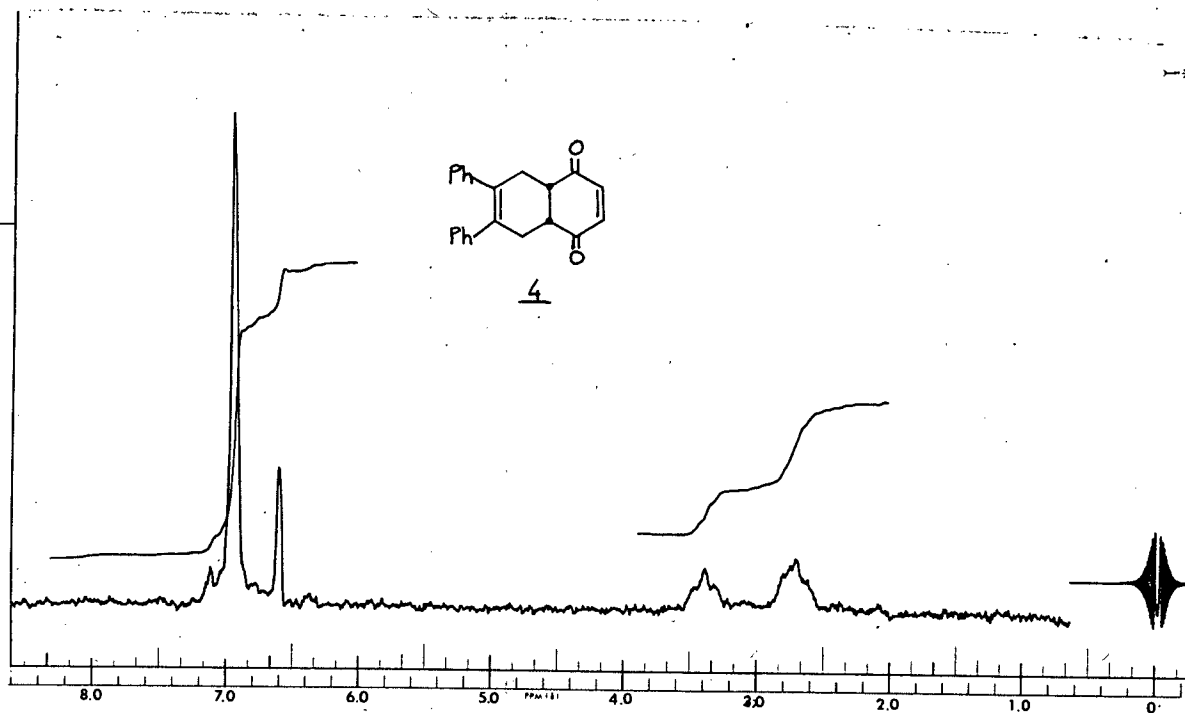


Figure 39. A 60 MHz PMR Spectrum of 6,7-Diphenyl-4aβ,5,8,8aβ-tetrahydro-1,4-naphthoquinone, 4.

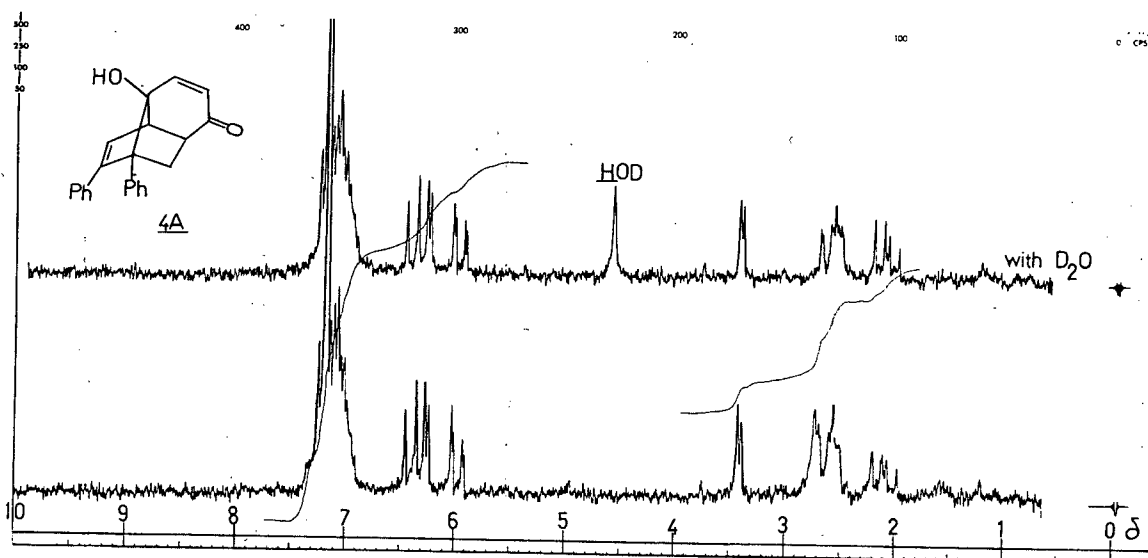


Figure 40. A 100 MHz PMR Spectrum of 1-Hydroxy-7,8-diphenyltricyclo[5.3.0.0^{5,10}]deca-2,8-dien-4-one, 4A.

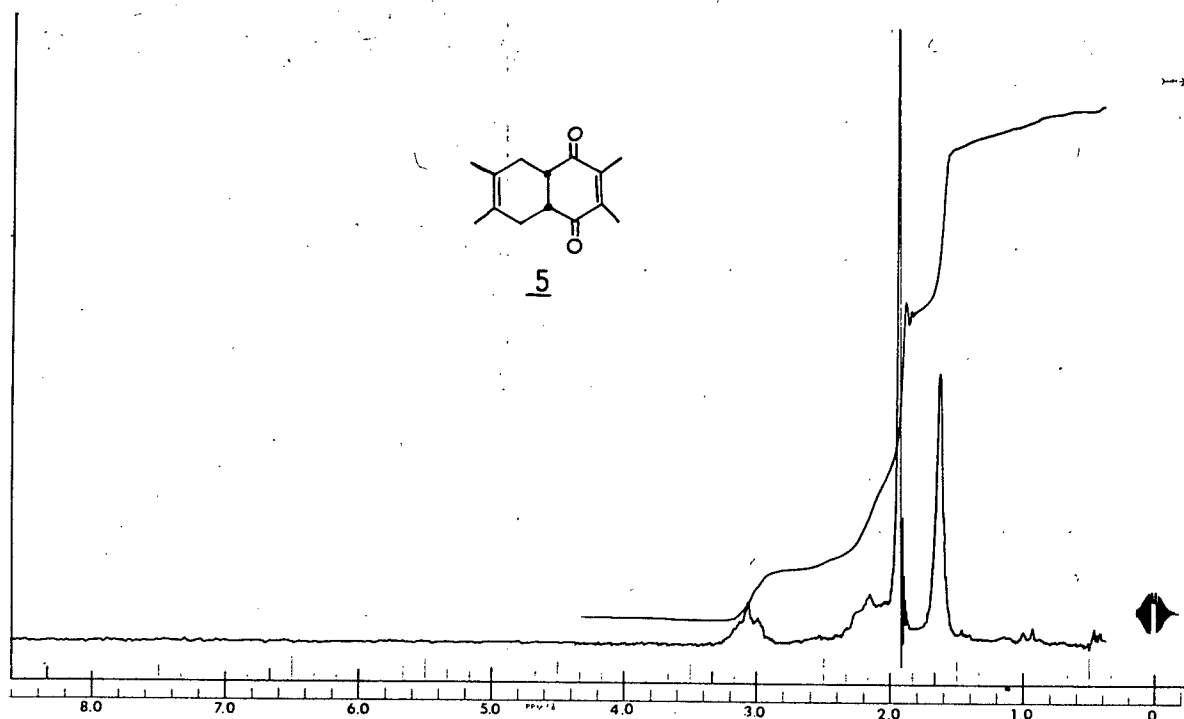


Figure 41. A 60 MHz PMR Spectrum of 2,3,6,7-Tetramethyl-4a β ,5,8,8a β -tetrahydro-1,4-naphthoquinone, 5.

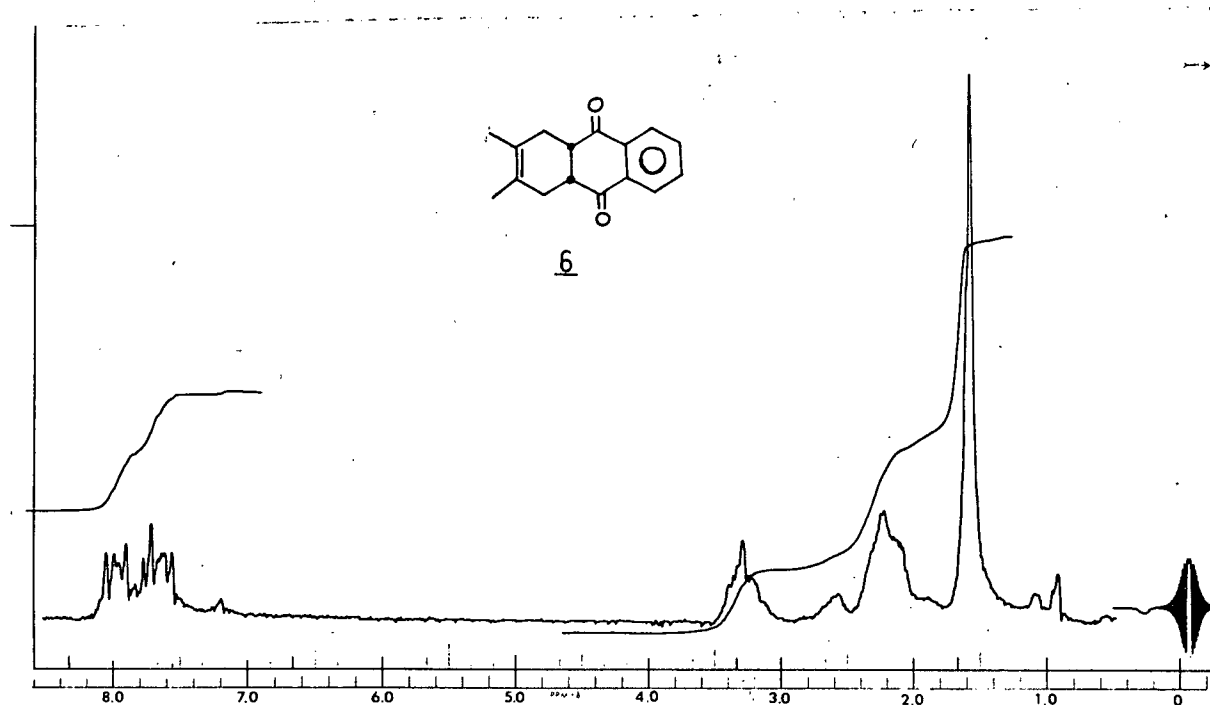


Figure 42. A 60 MHz PMR Spectrum of 2,3-Dimethyl-1,4,4a β ,9a β -tetrahydro-9,10-anthraquinone, **6**.

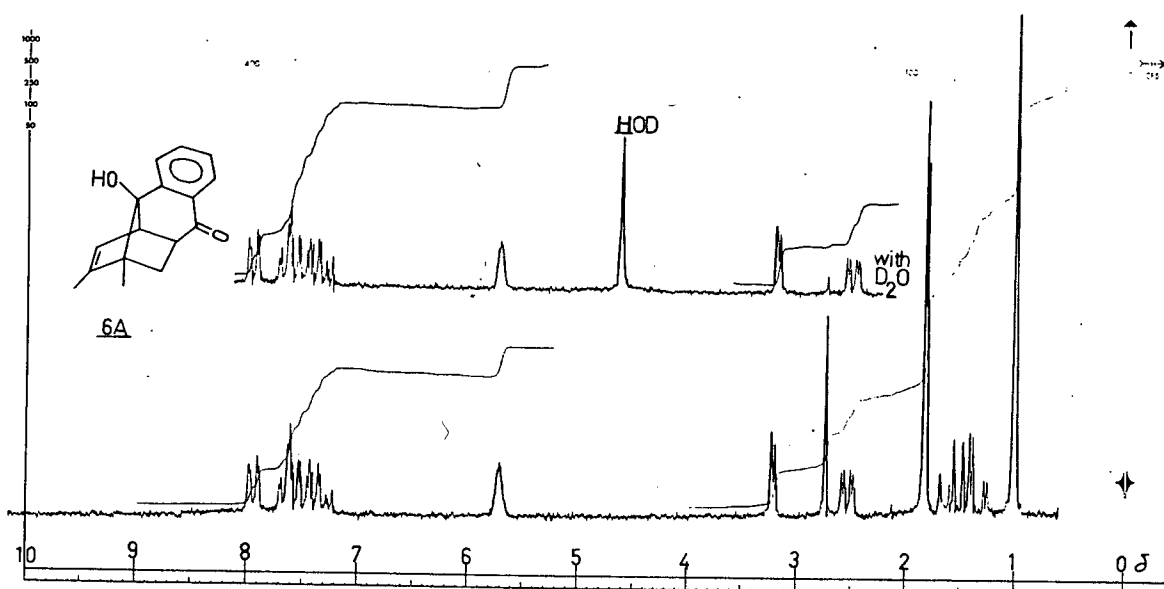


Figure 43. A 100 MHz PMR Spectrum of 1-Hydroxy-2,3-benzo-7,8-dimethyltricyclo[5.3.0.0^{5,10}]deca-8-ene-4-one, **6A**.

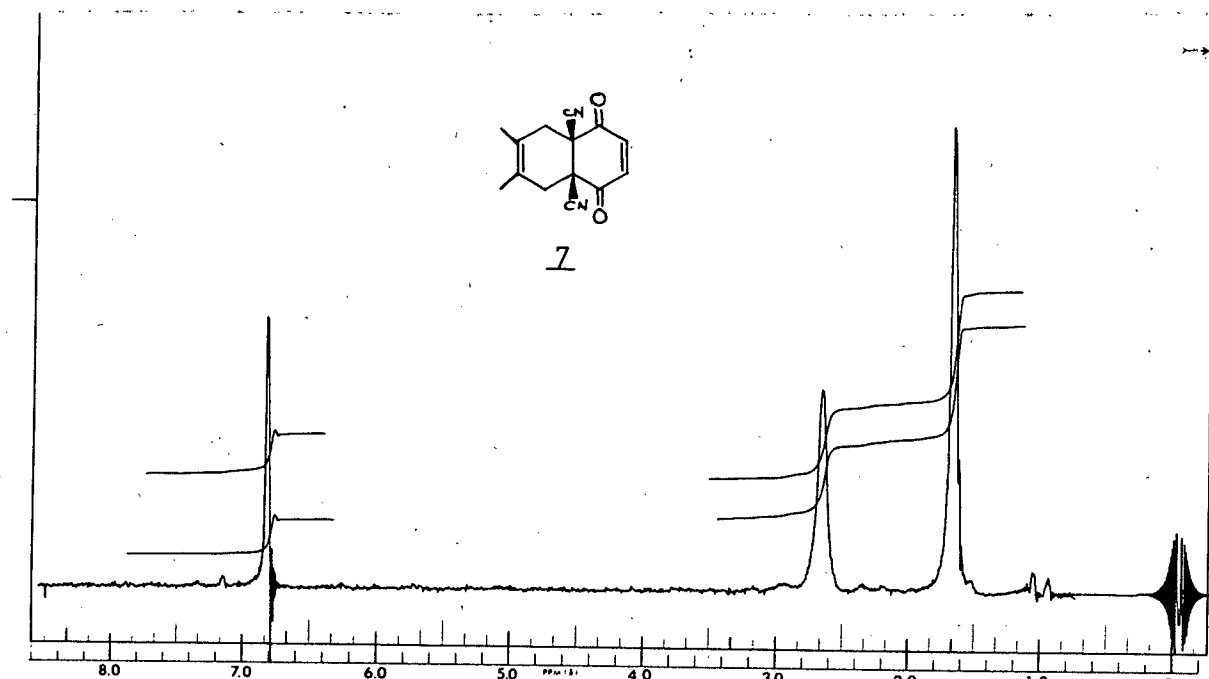


Figure 44. A 60 MHz PMR Spectrum of 4a β ,8a β -Dicyano-6,7-dimethyl-4a β ,5,8,8a β -tetrahydro-1,4-naphthoquinone, **7**.

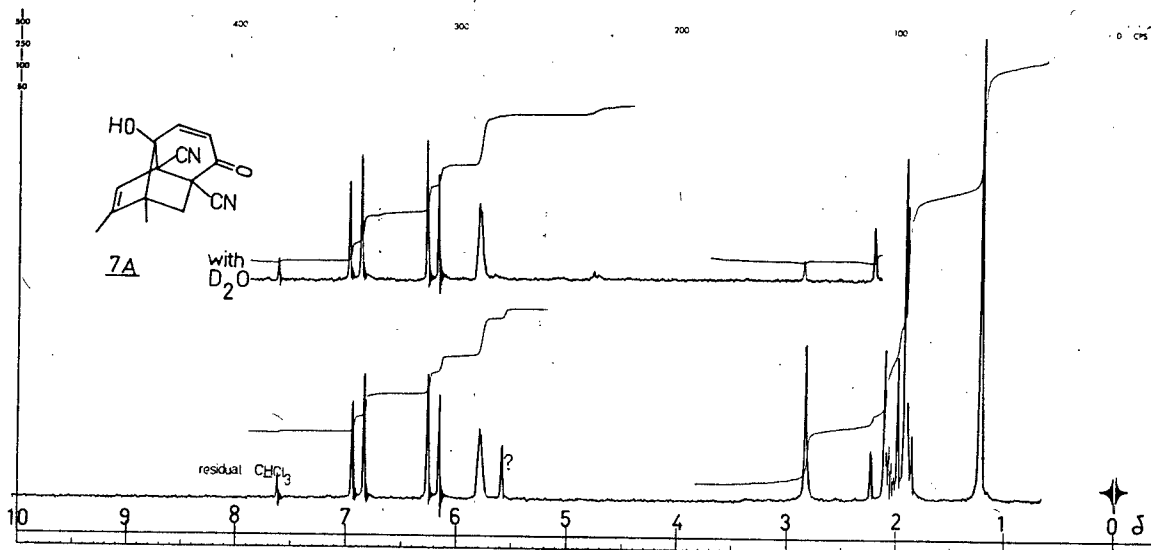


Figure 45. A 100 MHz PMR Spectrum of 1-Hydroxy-5,10-dicyano-7,8-dimethyltricyclo[5.3.0.0^{5,10}]deca-2,8-dien-4-one, **7A**.

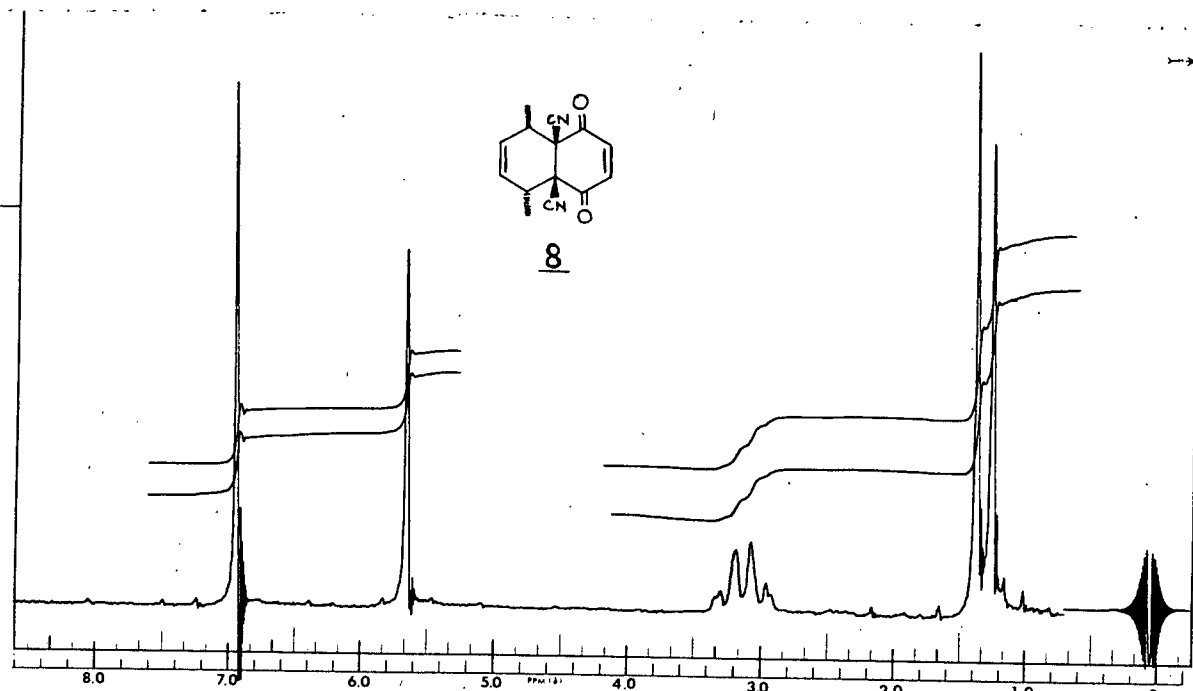


Figure 46. A 60 MHz PMR Spectrum of 4aβ,8aβ-Dicyano-5α,8α-dimethyl-4aβ,5,8,8aβ-tetrahydro-1,4-naphthoquinone, **8**

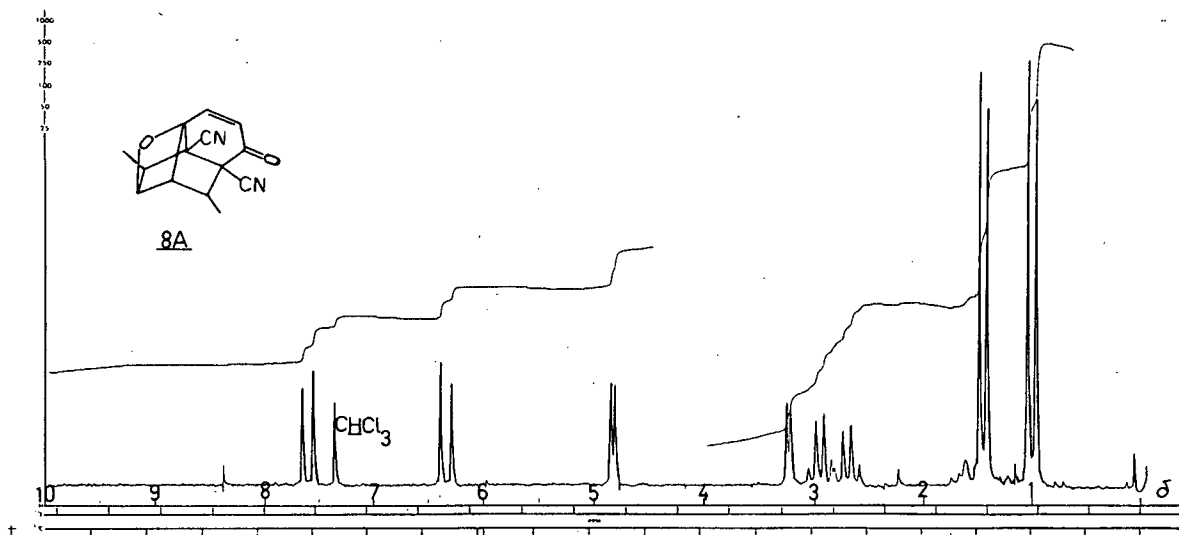


Figure 47. A 100 MHz PMR Spectrum of 5,10-Dicyano-6,9-dimethyl-11-oxatetracyclo[6.2.1.0^{1,7}.0^{5,10}]undec-2-ene-4-one, **8A**.

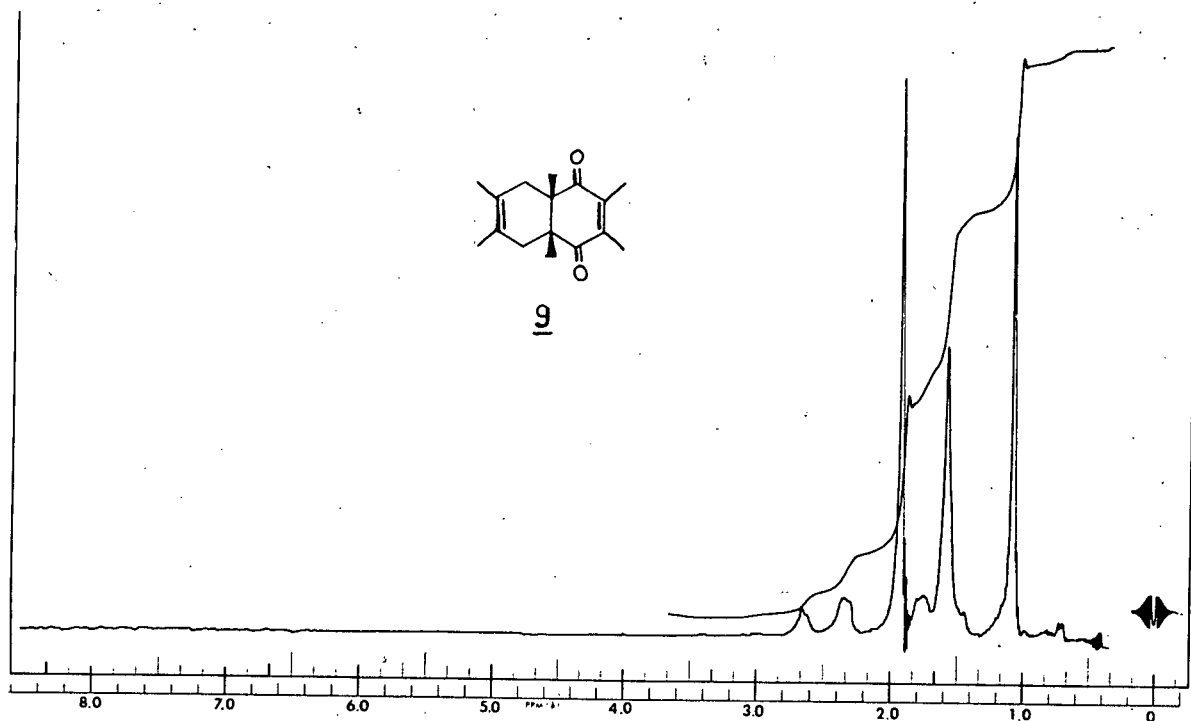


Figure 48. A 60 MHz PMR Spectrum of 2,3,4a β ,6,7,8a β -Hexamethyl-4a β ,5,8,8a β -tetrahydro-1,4-naphthoquinone, **9**.

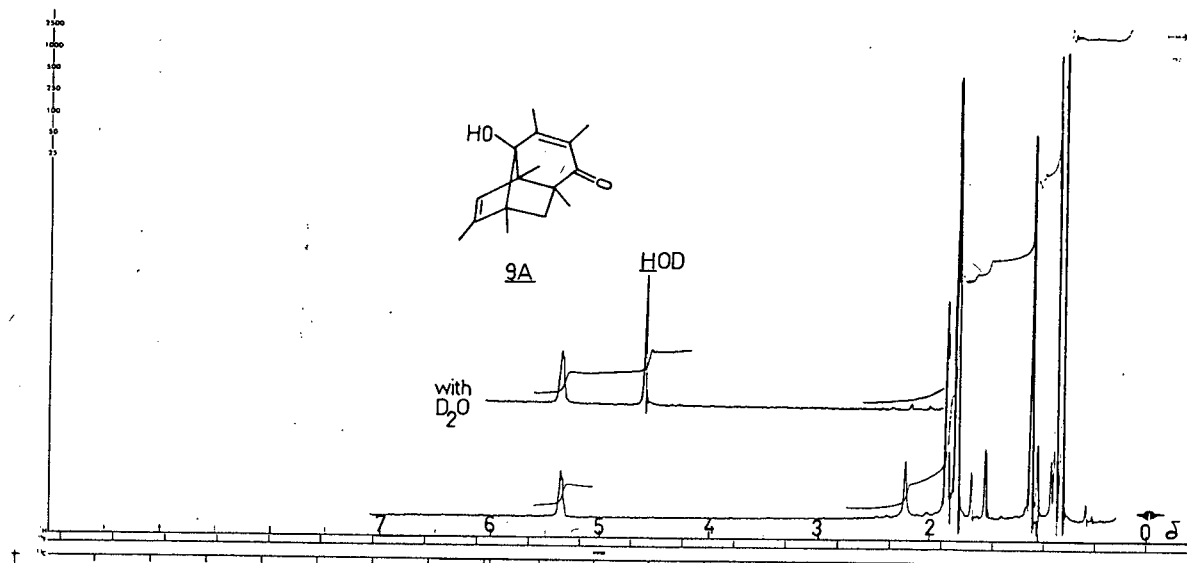


Figure 49. A 100 MHz PMR Spectrum of 1-Hydroxy-2,3,5,7,8,10-hexamethyltricyclo[5.3.0.0^{5,10}]deca-2,8-dien-4-one, **9A**.

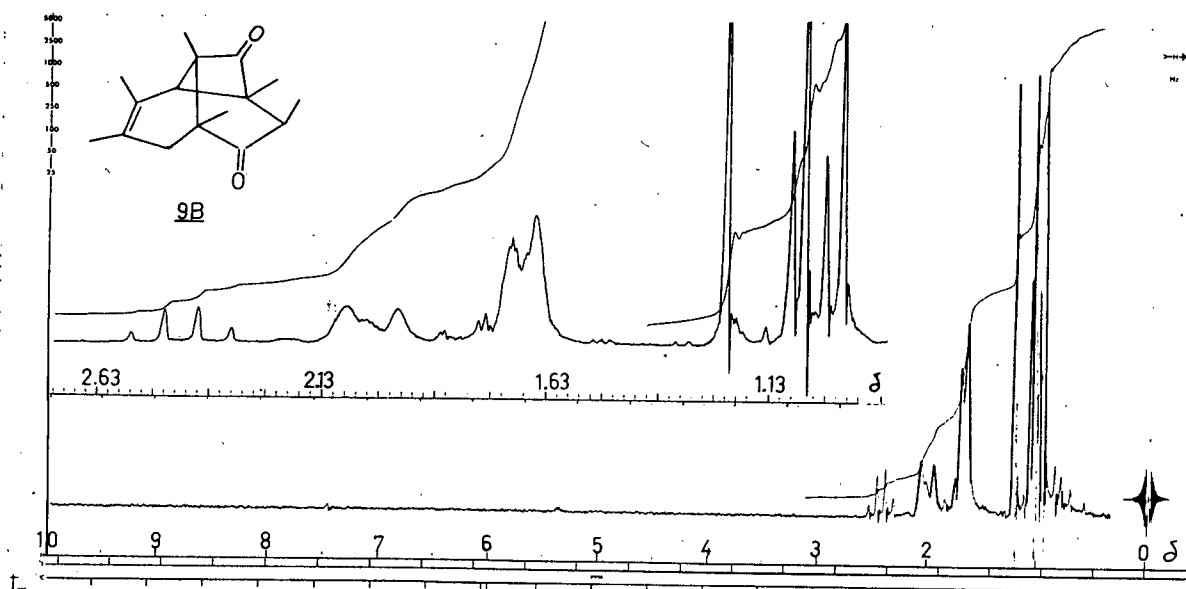


Figure 50. A 100 MHz PMR Spectrum of 2,3,5,7,8,10-Hexamethyl-tricyclo[6.2.0.0^{5,10}]deca-2-en-6,9-dione, 9B.

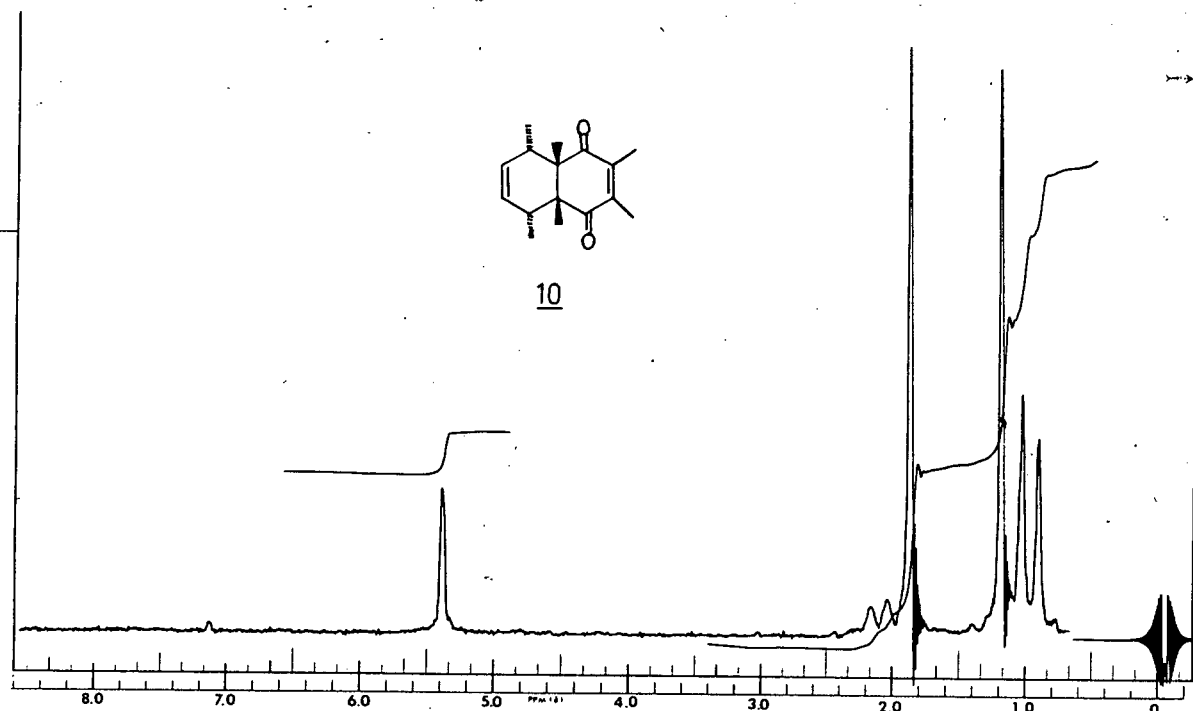


Figure 51. A 60 MHz PMR Spectrum of 2,3,4aβ,5α,8α,8aβ-Hexamethyl-4aβ,5,8,8aβ-tetrahydro-1,4-naphthoquinone, 10.

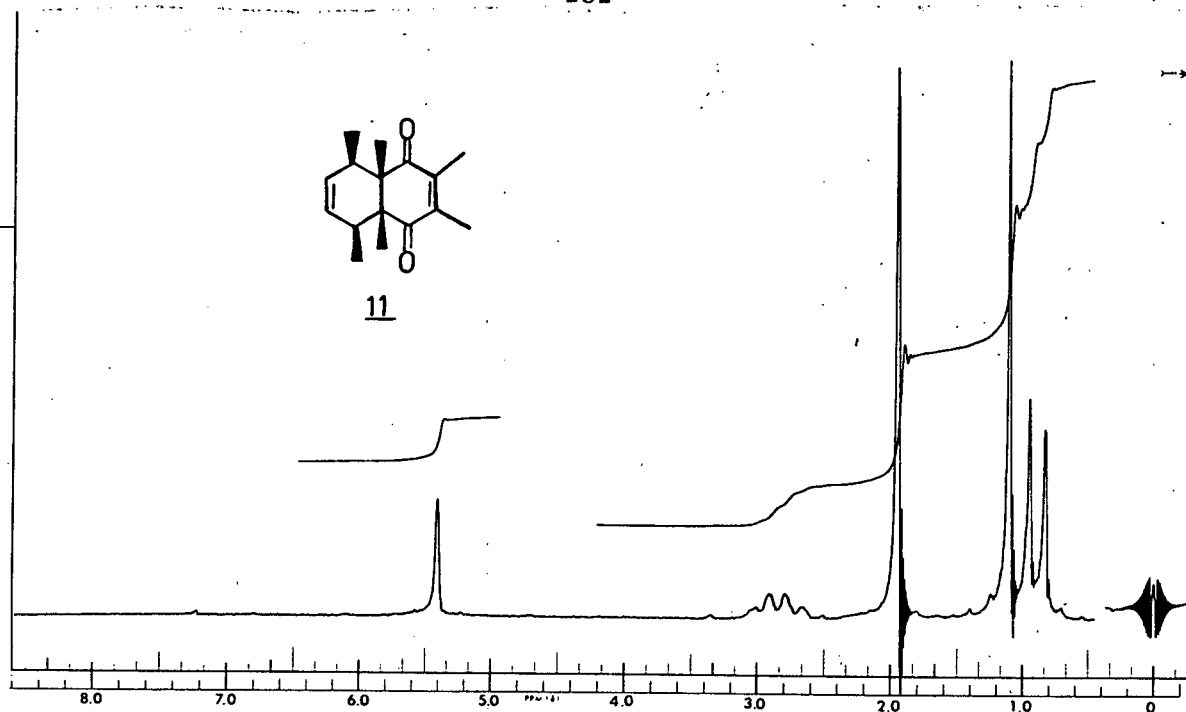


Figure 52. A 60 MHz PMR Spectrum of 2,3,4a β ,5 β ,8 β ,8a β -Hexamethyl-4a β ,5,8,8a β -tetrahydro-1,4-naphthoquinone, 11.

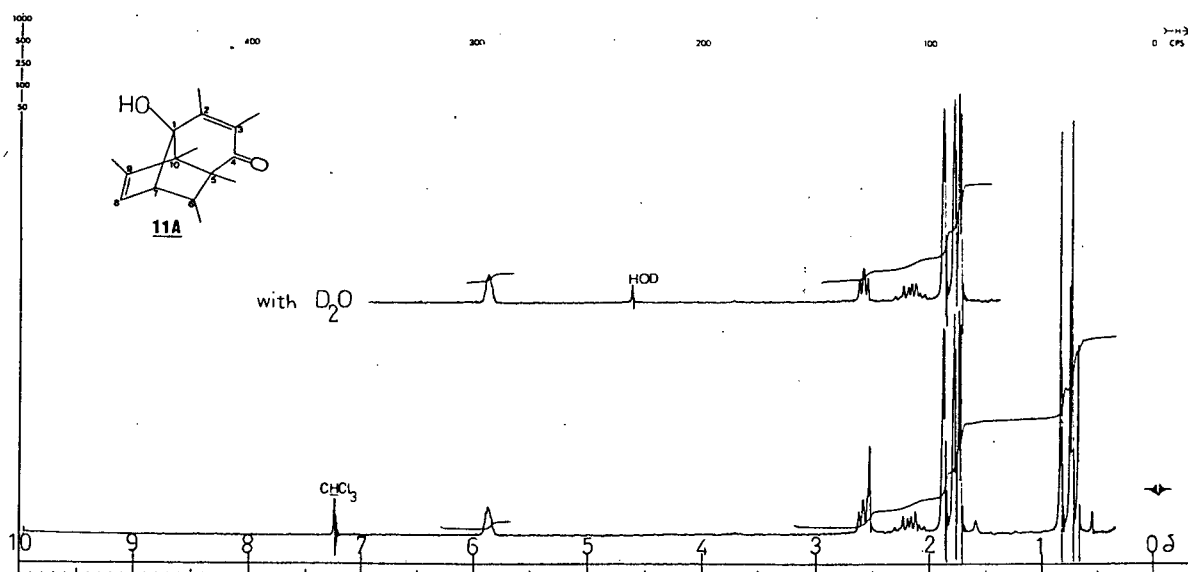


Figure 53. A 100 MHz PMR Spectrum of 1-Hydroxy-2,3,5,6,9,10-hexamethyltricyclo[5.3.0.0^{5,10}]deca-2,8-dien-4-one, 11A.

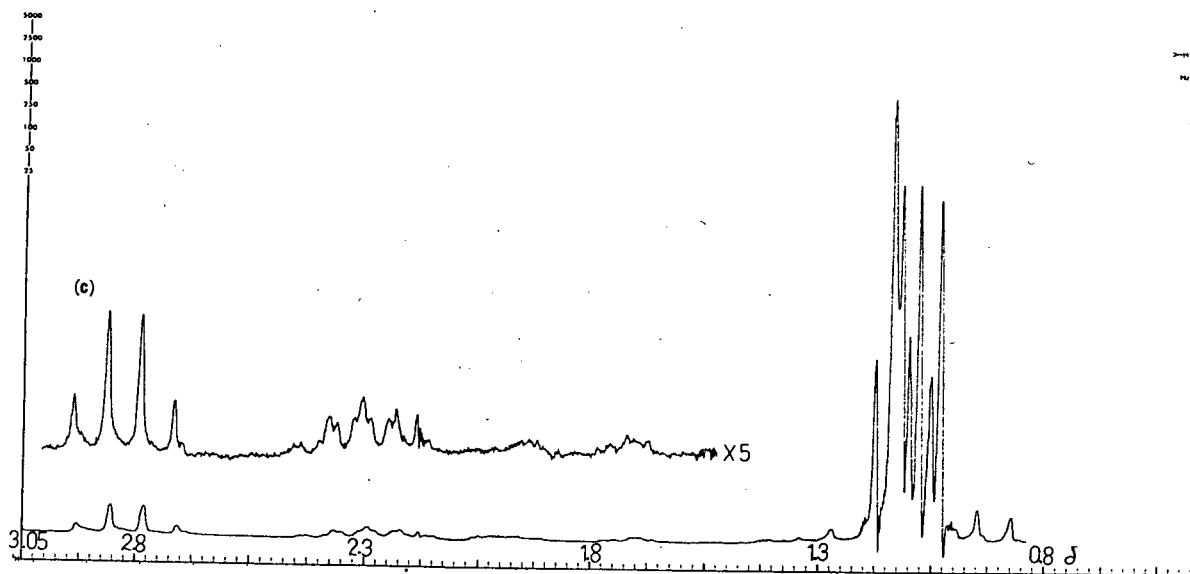
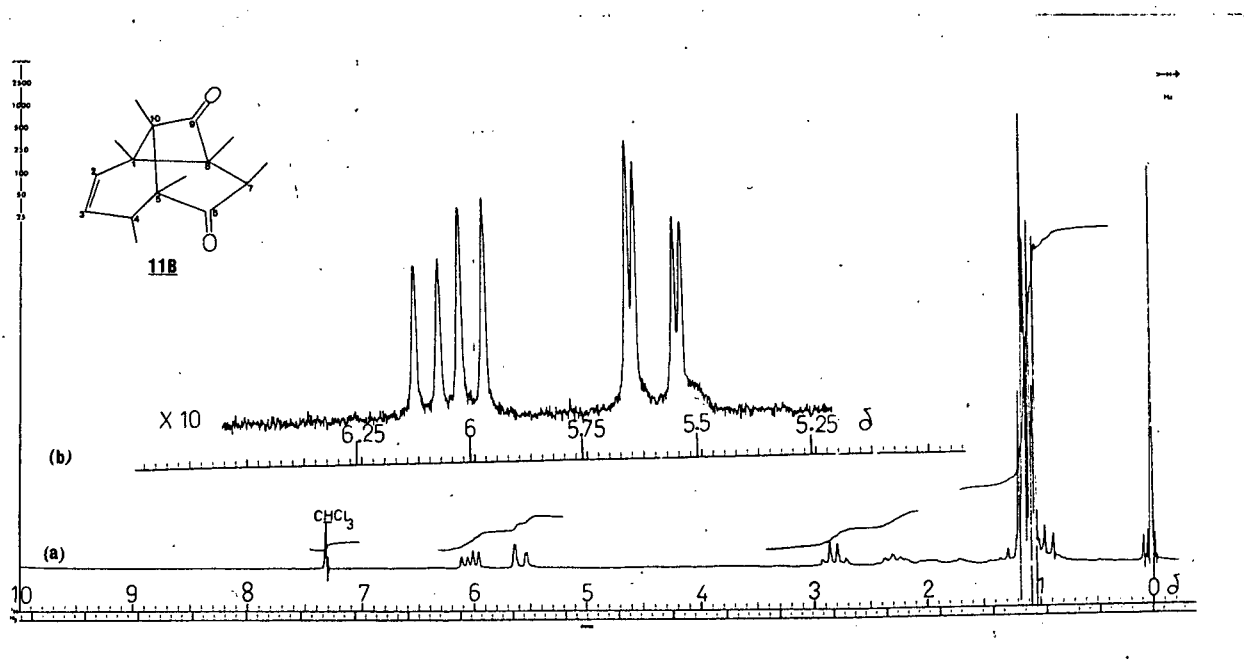


Figure 54. A 100 MHz PMR Spectrum of 1,4,5,7,8,10-Hexamethyltricyclo[6.2.0.0^{5,10}]deca-2-en-6,9-dione, **11B**; (a) 1000 Hz sweep width; (b) 250 Hz sweep width of the 6.5 - 5.25 δ region with amplitude magnification of x10; (c) 250 Hz sweep width of the 3.05 - 0.8 δ region.

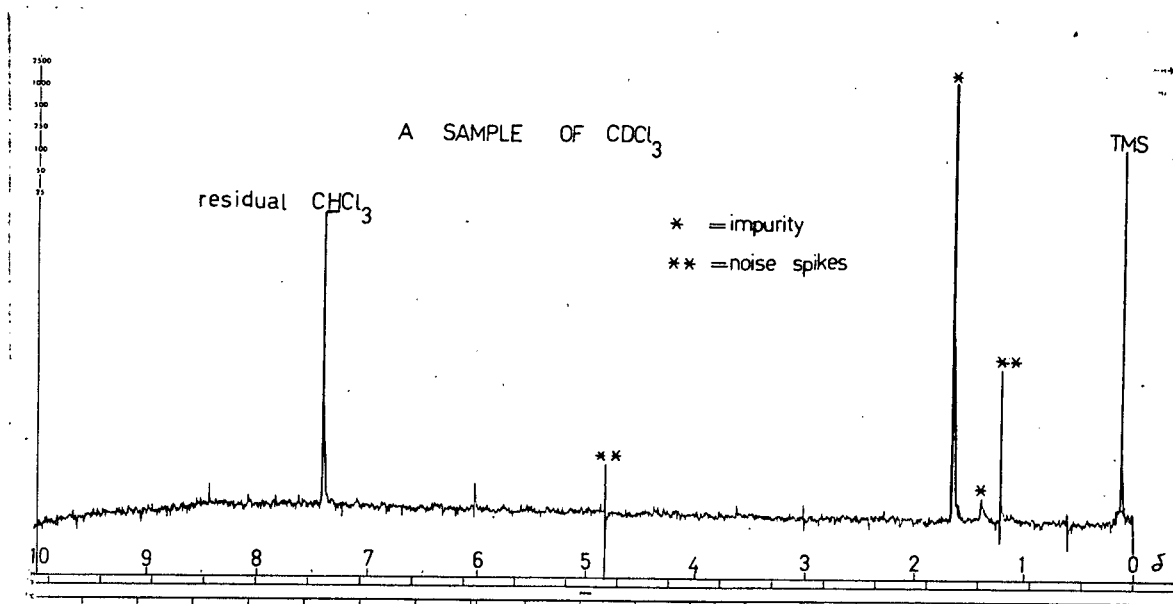


Figure 55. Fourier Transform 100 MHz PMR Spectrum of CDCl_3 from Merck Sharp & Dohme Canada Limited, Kirkland, Quebec.

UV Absorption Spectra of Substrates 1-11

All the tetrahydro-1,4-naphthoquinones which have been studied in this investigation show two principal absorptions in the UV. The absorption due to the π, π^* transition reminiscent of α, β -unsaturated ketones occurs in the range 225 - 280 nm and is the more intense of the two bands. The absorption at longer wavelength, ≥ 340 nm, is due mostly to a forbidden n, π^* transition and its extinction coefficient for all substrates was ≤ 150 . The intensity of this latter absorption may be enhanced through mixing with the allowed π, π^* transition³⁰. Absorptions for the individual compounds are given in Table XVI.

Table XVI* UV Absorption Spectra of Substrates 1-11

<u>Compound</u>	<u>Band I</u>	<u>Band II</u>
	$\lambda_{\max}, \text{nm}(\epsilon)$	
<u>1</u> (benzene)		371 (68)
<u>2</u> (MeOH)	226 (8.7×10^3)	370 (70)
<u>3</u> (benzene)	280 (7.5×10^3)	370 (63)
<u>4</u> (MeOH)	280 (7.5×10^3)	342 (72)
<u>5</u> (MeOH)	225 (9.4×10^3)	330 (115)
<u>6</u> (MeOH)	250 (1.1×10^4) 296 (1.9×10^3)	340 (150)
<u>7</u> (MeOH)	225 (8.9×10^3)	340 (93)
<u>8</u> (MeOH)	240 (6.2×10^3)	352 (64)
<u>9</u> (MeOH)	251 (1.1×10^4)	280-400 ($\epsilon_{340}=146$)
<u>10</u> (benzene)		350 (83)
<u>11</u> (MeOH)	251 (8.7×10^3)	340 (70)

* (Compiled from Reference 24).

As mentioned in the text, the irradiations of these substrates in the solid state were carried out at the same wavelengths as reported for the irradiations in solution²⁴, i.e., $\lambda \geq 340$ nm. This has allowed for a more valid comparison of reactivity differences in the two phases than would have been possible otherwise. With regard to earlier investigations of substrate 3 using sunlight²² and Pyrex-filtered UV light²³, respectively, the results presented here would seem to indicate a wavelength dependence for these reactions. Thus, it is very likely that tar formation as earlier observed^{22,23} is promoted by excitation of all the chromophores while a more selective excitation (mostly n, π^*) leads cleanly to dimer formation when intermolecular separation and geometry favor it or to intramolecular processes when the former process is blocked.